THE ROLE OF DOPAMINE D1 AND D2 RECEPTOR-EXPRESSING STRIATAL NEURONS IN THE CORTICOSTRIATAL CIRCUITRY OF ALCOHOL USE DISORDER

A Dissertation

by

YIFENG CHENG

Submitted to the Office of Graduate and Professional Studies of
Texas A&M University
in partial fulfillment of the requirements for the degree of

DOCTOR OF PHILOSOPHY

Chair of Committee,	Jun Wang
Committee Members,	William H. Griffith
	Ursula H. Winzer-Serhan
	Rachel Smith
Head of Program,	Warren E. Zimmer

December 2018

Major Subject: Medical Sciences

ABSTRACT

Alcohol use disorder (AUD) changes glutamatergic and γ-aminobutyric acidergic (GABAergic) neurotransmission in many neuronal populations. The dorsomedial part of the striatum (DMS) and its critical glutamatergic input, prefrontal cortex (PFC), have been strongly associated with AUD. The DMS contains two types of medium spiny neurons (MSNs): dopamine D1 receptor- and D2 receptor-expressing MSNs (D1-MSNs or D2-MSNs), which have been shown oppositely control the reward-seeking behavior. It is unclear how alcohol affects glutamatergic and GABAergic neurotransmission onto D1- and D2-MSNs and how these types of neurons control alcohol-related behavior. Thus, I first examined the effect of adult alcohol drinking on D1- and D2-MSNs and their contributions to the alcohol-drinking behavior of mice. Then, we investigated the causality between synaptic plasticity and alcohol-seeking behavior in adult rats. Lastly, we further tested prenatal alcohol exposure (PAE)-evoked glutamatergic changes in DMS D1-MSNs of adult mice.

In this dissertation study, I first found that adult alcohol exposure distinctly facilitated glutamatergic inputs in D1-MSNs and GABAergic transmission D2-MSNs. I further discovered that *in vivo* chemogenetic excitation of D1-MSNs or inhibition of D2-MSNs increased voluntary alcohol consumption, whereas inhibition of D1-MSNs or excitation of D2-MSNs reduced this behavior. Then, we found that optogenetically induced long-term potentiation (LTP) at DMS corticostriatal (especially at mPFC→D1-MSNs) synapses produced a long-lasting increase of alcohol-seeking and -drinking behavior in rats, whereas long-term depression (LTD) induction caused a long-lasting decrease on this behavior. Lastly, I found hyperactivity in both juvenile and adult

offspring. Furthermore, I showed that PAE potentiated glutamatergic transmission onto D1-MSNs and increased the dendritic complexity of D1-MSNs in those hyperactive adult offspring. Taken together, my graduate study suggests that adult alcohol exposure selectively strengthens glutamatergic activity in D1-MSNs and enhances GABAergic activity in D2-MSNs. This alcohol-mediated alternation of D1- and D2-MSNs, in turn, contributes to alcohol-drinking behavior. This cell type-specific regulation on alcohol-drinking behavior may due to the fact that glutamatergic synaptic plasticity between mPFC→D1-MSNs controls alcohol-seeking and -taking behavior. Lastly, PAE affects glutamatergic transmission onto D1-MSNs, indicating a potential mechanism underlying PAE-induced hyperactivity.

ACKNOWLEDGMENTS

I would like to thank my committee chair, Dr. Jun Wang, and my committee members, Dr. William H. Griffith, Dr. Ursula H. Winzer-Serhan, and Dr. Rachel Smith for their guidance and support throughout the course of this research.

Thanks also go to my friends (Dr. Xijun Shi, Ms. Xuan Zhou, Mr. Tian Lan, Ms. Tian Su, Ms. Lijun Duan, Dr. Shuo Wang, and Mr. Zheren Zhou) and colleagues (especially Dr. Tengfei Ma, Dr. Cathy Huang, Dr. Emily Roltsch Hellard, Ms. Jiayi Lu, Ms. Xuehua Wang, Ms. Katherine A. Rees, Mr. Xueyi Xie, Mr. Sebastian Melo, Ms. Britton Barbee, Mr. Jared Jerger) and the department faculty (Dr. Rajesh C. Miranda and Dr. Laura Smith) and staff for making my time at Texas A&M University a great experience.

Finally, thanks to my mother (Ms. Yuzhi Qian) for her encouragement and to my fiancée (Ms. Bizhu He) for her patience and love.

CONTRIBUTORS AND FUNDING SOURCES

Contributors

This work was supervised by a dissertation committee consisting of Assistant Professor Jun Wang [advisor], Professor William H. Griffith, and Associate Professor Ursula H. Winzer-Serhan of the Department of the Department of Neuroscience and Experimental Therapeutics and Assistant Professor Rachel Smith of the Department of Psychology.

The electrophysiology experiments for Chapter II were provided by Dr. Tengfei Ma, Cathy C.Y. Huang, and Ms. Jiayi Lu. The western blot experiments for Chapter II was assisted by Dr. Xiaoyan Wei. The electrophysiology experiments for Chapter IV was provided by Dr. Tengfei Ma. The behavior experiments for Chapter IV was assisted by Dr. Emily Roltsch Hellard. The biochemical experiments were conducted in part by Ms. Jiayi Lu and Dr. Xinsheng Gao of the Department of Molecular and Cellular Medicine. All experimental animals were bred by Ms. Xuehua Wang.

All other work conducted for the dissertation was completed by the graduate student, Mr. Yifeng Cheng, independently.

Funding Sources

Graduate study was supported by [NIH/NIAAA] under Grant Number [R01AA021505] (JW), [U01AA025932] (JW), R01AA024659 (RM) and by Texas Research Society on Alcoholism (TxRSA) (YC).

NOMENCLATURE

AUD	Alcohol Use Disorder
AMPA	α-amino-3-hydroxy-5-methyl-4-isoxazolepropionic acid
ADH	Alcohol Dehydrogenase
CDC	Centers for Disease Control and Prevention
CINs	Cholinergic Interneurons
CNO	Clozapine-N-oxide
CPP	Condition Place Preference
DA	Dopamine
DAT	Dopamine Transporter
DREADDs	Designer Receptors Exclusively Activated by Designer Drugs
DLS	Dorsolateral Striatum
DMS	Dorsomedial Striatum
eCB	Endocannabinoid
EP	Entopeduncular Nucleus
FASD	Fetal Alcohol Spectrum Disorder
FSIs	Fast-spiking Interneurons
GABA	γ-aminobutyric Acid
GRIK	G-protein-coupled inwardly rectifying K^+ channel
GP	Globus Pallidus
GPe	External part of Globus Pallidus
GPi	Internal part of Globus Pallidus

GSK3β	Glycogen Synthase Kinase-3β
HFS	High-Frequency Stimulation
IGF1	Insulin-like Growth Factor 1
LOFC	Lateral Orbitofrontal Cortex
LTD	Long-term Depression
LTP	Long-term Potentiation
LTSIs	Low-threshold Spiking Interneurons
L1-CAM	L1 Cell Adhesion Molecule
MSNs	Medium Spiny Neurons
mPFC	Medial Prefrontal Cortex
mEPSCs	Miniature Excitatory Postsynaptic Currents
mIPSCs	Miniature Inhibitory Postsynaptic Currents
NMDA	N-methyl-D-aspartate receptors
NAc	Nucleus Accumbens
nAChRs	Nicotinic Acetylcholine receptors
NSDUH	National Survey on Drug Use and Health
oPSD	Optogenetic Postsynaptic Depolarization
PAE	Prenatal Alcohol Exposure
PFC	Prefrontal Cortex
RPE	Reward Prediction Error
SNc	Substantia nigra, pars compacta
SNr	Substantia nigra, par reticulata
TH	Tyrosine Hydroxylase

VTA	Ventral Tegmental Area
VS	Ventral Striatum

TABLE OF CONTENTS

Page

LIST OF FIGURES

Page

CHAPTER I

INTRODUCTION AND LITERATURE REVIEW

1.1 Overview

Alcohol is an addictive substance and alcohol use disorders (AUDs) is a very common and severe psychiatric disease (World Health Organization, 2014; Center for Behavioral Health Statistics and Quality, 2015). Alcohol-addictive individuals lose their control over alcohol consumption and continue to drink despite the negative effect on their family, their career, and even their health. According to a report from World Health Organization in 2014 on alcohol and health, inappropriate use of alcohol causes approximately 3.3 million deaths globally per year (equal to 5.9% of total deaths), and 5.1% of the global burden of alcohol use-related diseases (World Health Organization, 2014). Globally, it has also been reported that about 16% of aged 15 years or older alcohol drinker are exposed to repeated and excessive episodic drinking (Enoch and Goldman, 2002). More importantly, the harmful use of alcohol also imposes significant social and economic costs on society globally (World Health Organization, 2014). For example, alcohol-related problems cost about 125 billion euros in the European Union in 2003 (Anderson and Baumberg, 2006), and in the Republic of South Africa, the estimated costs nearly reached 12% of the 2009 gross domestic product (Matzopoulos et al., 2014). In American, it has been diagnosed in about 17 million American adults as alcoholics and costs the United States about 250 billion of dollars resulting in a significant economic and social burdens (Whiteford et al., 2013; Glantz et al., 2014; World Health Organization, 2014). Based on the report from Centers for Disease Control and Prevention (CDC) and National Survey on Drug Use and Health (NSDUH), AUD is ranked at top number two for the prevalence of disease and cost to society (National Drug Intelligence Center, 2011; National Center for Health Statistics, 2013; Warren et

al., 2014; Health et al., 2016). Recently, in the year 2016, US Surgeon General also issued their first alcohol-related report to highlight alcoholism and addiction (U.S. Department of Health and Human Services (HHS), 2016). Given this huge social impact, there is a strong need for understanding how alcohol affects the brain and hijack our behavior. Unfortunately, only a limited number of therapeutics are available to treat AUD due to unclear mechanisms underlying it.

The distribution of ethanol, a main chemical component in the alcohol, is similar to water and can reach an equilibration throughout organs and cells within a few minutes of drinking (Cederbaum, 2012). After alcohol drinking, ethanol is mainly absorbed by the gastrointestinal tract and metabolized in the liver (> 90%), and the metabolism rate of blood alcohol is dose-dependent (DiPadova et al., 1987; Kalant, 1996). Meanwhile, ethanol can easily penetrate through the brain blood barrier and concentrate in the brain (Kalant, 1996). The alcohol reaches peak concentration in the brain after 30 to 60 minutes from oral administration, and the level of alcohol is about 70-80% of blood alcohol concentration (Kalant, 1996). Ethanol as a non-specific pharmacological agent has many molecular targets in the brain (Ron and Barak, 2016; Abrahao et al., 2017). For example, acute alcohol administration potentiates γ-aminobutyric acid receptors ($GABA_A$ receptors), nicotinic acetylcholine receptors (nAChRs), and inhibits N-methyl-D-aspartate receptors (NMDARs) (reviewed in (Abrahao et al., 2017)). In contrast, chronic alcohol administration facilitates NMDARs activity (Wang et al., 2007). Thus, the neuronal circuitry mechanism underlying AUD behavior seems complicated.

Dopamine (DA) plays an essential role in the modulation of synaptic plasticity. The DA neurons and its major targets, such as the striatum and prefrontal cortex (PFC) are major targets of drugs and alcohol (Luscher and Malenka, 2011). Despite the diversity of chemical structure

and the molecular target, all addictive drugs and alcohol can increase DAergic neuron firing and DA release through different mechanisms. For example, nicotine can activate α4β2-containing nAChRs and increase firing of DA neurons (Maskos et al., 2005), whereas cocaine can block DA transporter (DAT) on the presynaptic terminal of DA neurons and increase the DA concentration in the synaptic cleft (Volkow et al., 1997). Depends on the pattern of drinking, alcohol has distinct effects on these neuronal transmission systems. For example, acute alcohol consumption can cause an increase of DA release, whereas long-term alcohol consumption produces a hypodopaminergic state in the brain, (Bassareo et al., 2003; Barak et al., 2011). The dorsal striatum is also another major target of midbrain DAergic neurons. The dorsal striatum can be further divided into two part: the dorsomedial striatum (DMS) and the dorsolateral striatum (DLS). The DLS mainly controls habitual behavior, whereas the DMS mainly controls goal-directed behavior (Voorn et al., 2004).

Although how alcohol exposure impacts individual brain regions has been extensively studied (Sun and Rebec, 2005; Wang et al., 2007; Belin and Everitt, 2008; Wang et al., 2010; Wang et al., 2012; Barker et al., 2013; Bock et al., 2013; Land et al., 2014; Wang et al., 2015; Cheng et al., 2017), a major question that still remains is how alcohol exposure causes synaptic plasticity within a specific circuit and the behavioral outcome of this circuit.

1.2 Alcohol Metabolism

Alcohol is mainly absorbed by the gastrointestinal tract and reach the maximum concentration in the blood in about 20 min, and the metabolism rate of blood alcohol is dose-dependent (DiPadova et al., 1987; Kalant, 1996). Alcohol is mainly metabolized in the liver (> 90%). In the liver, there are mainly three pathways for alcohol metabolism (Lieber, 2000, 2005): 1, alcohol dehydrogenase (ADH) pathway; 2, the microsomal alcohol oxidizing system; 3,

catalase. Each of these pathways is located in the different subcellular compartment and will generate different metabolic products (Lieber, 2000).

The ADH pathway locates in the cytosol (Lieber, 2000). In this pathway, alcohol will be oxidized to acetaldehyde with loss of H, which reduces NAD to NADH. Increasing NADH will facilitate the fat accumulation and cause hyperlipemia, hypoglycemia and so on (Lieber, 1992). Acetaldehyde can be future metabolized into acetate. Both acetate and acetaldehyde are toxic to the body. ADH is a very critical enzyme in the ADH pathway. Human liver ADH is a zinc metalloenzyme, which can be classified into five different forms (Lieber, 2000), and the expression of human ADH is controlled by five-gene loci of *ADH*, *ADH1* through *ADH5* (Bosron et al., 1993). ADH class I-III mainly locate in hepatocyte, among which I and II mainly contribute to alcohol oxidization. ADH class III has low affinity with alcohol. ADH class IV can metabolize alcohol outside of hepatocyte, e.g., gastric cells (Yokoyama et al., 1996). More importantly, polymorphism occurs at two loci, *ADH2* and *ADH3*, which belong to ADH class I. As a result, genetic polymorphism of ADH controls individual differences in the rate of alcohol metabolism and influence the severity of alcohol-induced liver disease (Lieber, 2000).

The second pathway is through the microsomal ethanol-oxidizing system (MEOS), which located in the endoplasmic reticulum (Lieber, 2000). This system can be found in liver microsomes and is inducible by chronic alcohol drinking (Lieber and DeCarli, 1968). In MESO, ethanol also will be oxidized to acetaldehyde via an ethanol-inducible cytochrome P4502E1 enzyme (CYP2E1)(Lieber, 2000). This induction contributes to metabolic tolerance to alcohol with other P450 cytochromes (CYP1A2, CYP3A4) possibly involved (Salmela et al., 1998). However, clinically, higher CYP2E1 will increase the vulnerability of the alcoholic due to the high capacity of CYP2E1 to convert xenobiotics to highly toxic metabolites (Lieber, 2000).

Meanwhile, CYP2E1 also generates lots of active oxygen ($O_2^{\cdot-}$, $OH^{\cdot}$ or other free radicals), which decrease the level of GSH and promote injury and cell death(Lieber, 2000). Polymorphism of CYP2E1 was found in the 5'-flanking regions of the human cytochrome *2E1* gene (Hayashi et al., 1991). Two nucleotide exchanges in restriction sites (*Pst*I and *Rsa*I) that contributes to the polymorphism of *2E1* gene (Hayashi et al., 1991). Based on this, *2E1* gene can be classified into three types (Hayashi et al., 1991). Type A is homozygous with normal alleles, *c1*,*c1*. Type C is homozygous for nucleotide exchange, *c2*;*c2*. Type B is heterozygous having a normal and a mutated allele, *c1*;*c2*. A *C2* allele is a rare mutant allele with lacking-*Rsa*I site, which contributes to higher transcriptional activity, protein level, and enzyme activity than wild-type *c1*. More importantly, the frequency of the *c2* allele varies in different populations (Stephens et al., 1994). The highest frequency has been reported in the Taiwanese and Japanese, while in African Americans, European Americans and Scandinavians, the frequency is much lower (Stephens et al., 1994). The variety of frequency of c2 allele causes the difference in alcohol tolerance and its relative toxicity among different human populations. In another word, the risk of drinking alcohol is different among distinct populations.

The third pathway is catalase, which locates in the peroxisomes (Lieber, 2005). Catalase oxidizes alcohol into acetaldehyde with the presence of H_2O_2 (Lieber, 2005). However, there is a limited amount of H_2O_2 in the liver under physiologic condition (Lieber, 2005). Thus, catalase system plays no major role in ethanol oxidation.

1.3 Alcohol and Direct Molecular Targets

Alcohol is a non-specific pharmacological chemical, which targets on many neurotransmitter receptors and ion-channels including NMDAR, $GABA_AR$, glycine receptor, nAChRs, L-Ca_v, potassium channels (Vengeliene et al., 2008), but also alter cell signaling

systems. The detailed actions of alcohol on ion-channels and cell signaling systems are described below.

NMDARs: NMDARs are very important for learning and memory. Lovinger et al. found that acute bath application of 5-200 mM ethanol inhibited NMDAR activity and 50 mM ethanol produces about 61% inhibition of NMDAR-induced current (Lovinger et al., 1989). This ethanol-induced inhibition of NMDARs involves the N-terminal and the 3rd transmembrane domain of the NMDARs (Smothers et al., 2013). Another study showed that the GluN2B-containing NMDAR is more sensitive than GluN2A-containing NMDAR to ethanol inhibition in cultured HEK cells (Smothers et al., 2001). However, during alcohol withdrawal, GluN2B-containing NMDAR activity exhibited long-term facilitation (Wang et al., 2007), which may contribute to alcohol-induced plasticity. As a result, adaptive responses such as enhanced glutamatergic transmission and expression of NMDARs may occur to counterbalance the inhibitory effect of acute alcohol exposure (reviewed in Vengeliene et al., 2008). These *ex vivo* results are also consistent with pharmacological studies which showed that an NMDAR antagonist or GluN2B antagonist reduces alcohol consumption in rats (Bienkowski et al., 1999; Wang et al., 2010).

$GABA_AR$s: The $GABA_AR$ is a chloride permeable channel and mediates inhibitory effects. Alcohol can alter both synaptic and extrasynaptic $GABA_AR$ activity. It has been found that extrasynaptic $\alpha4\beta3\delta$ subunit- and $\alpha6\beta3\delta$ subunit-containing $GABA_AR$s are very sensitive to low concentration of ethanol (1-3 mM) leading to an increase in extrasynaptic α,δ subunit-contained $GABA_AR$-mediated current by 40-50% (Sundstrom-Poromaa et al., 2002; Wallner et al., 2003). Acute administration of ethanol also facilitates synaptic $GABA_AR$ activity, specifically targets $\alpha4$, δ subunits (Diaz et al., 2014; Carlson et al., 2016). More studies have

shown that knockout of α or δ subunits in mice reduces alcohol consumption (Mihalek et al., 2001; Boehm et al., 2004; Crabbe et al., 2006; June et al., 2007). In contrast, chronic alcohol drinking decreases the density of $GABA_A$Rs, and therefore reduces the striatal GABAergic transmission (Golovko et al., 2002; Boehm et al., 2004; Wilcox et al., 2014). The decreased $GABA_A$R activity attenuates GABAergic synaptic strength, which has been reported in the striatum in a recent study (Wilcox et al., 2014). This may reduce the inhibitory tone in the striatum and increase alcohol-drinking behavior.

Glycine receptors: The glycine receptor is also a chloride permeable channel and is composed of α and β subunit (Betz, 1991). Ethanol has been reported to facilitate the homomeric α1 glycine receptor-induced current in a dose-dependent manner (10-200 mM)(Betz, 1991). Mutation of PKC phosphorylation site on α1 subunit decreases the sensitivity to ethanol (Betz, 1991). More studies also provide evidence that 100 mM ethanol greatly potentiates glycine receptor-mediated synaptic transmission in hypoglossal motoneurons (Sebe et al., 2003), lateral orbitofrontal cortex (LOFC) (Badanich et al., 2013) and VTA (Ye et al., 2001), which result in inhibition of neuronal activity.

nAChRs: Neuronal type of nAChRs are either homomeric or heteromeric receptors, which composed by the combination of either α2 - α10 or β2 - β4 subunits (Itier and Bertrand, 2001). The previous study showed that low concentration of ethanol (less than 100 mM) activated α2- or α4-containing nAChRs (reviewed in Vengeliene et al., 2008) and suppressed the activity of α7 nAChRs (Yu et al., 1996). However, higher alcohol concentration activates all types nAChRs (reviewed in Vengeliene et al., 2008). This may contribute to the findings that DA overflow is promoted by ethanol-induced enhancement of nAChR activity and alcohol-induced

DA overflow within the NAc is mediate by nAChR located in the VTA (Larsson et al., 2002; Molander et al., 2005).

Large-conductance Ca^{2+}-activated K^+ channel (BK channel): Much evidence suggests a potential direct interaction of ethanol with BK channels. Dopico et al. (2014) revealed that acute ethanol application enhances BK channel activity leading to inhibition of striatal neuronal activity. Bukiya et al. (2014) also demonstrated that alcohol binds selectively onto a water-accessible site with the presence of calcium leading to activation of channels. In addition, inhibition of BK channel trafficking reduces ethanol-induced hyperactivity and neurotransmitter release in *C. elegans* (Oh et al., 2017).

G-protein-coupled inwardly rectifying K^+ channel (GIRK): Early study reported that ethanol acts on the C-terminal region of GIRK and enhance its function in cerebellar granule cells and direct target on the C-terminal region (Lewohl et al., 1999). And mutation of GIRK1/2 or GIRK3 subunit channels in mice showed an impairment of ethanol-induced analgesia and reduced alcohol conditioned place preference (Kobayashi et al., 1999; Tipps et al., 2016). Recently, more studies demonstrated that alcohol enhances GIRK channel activity (Bodhinathan and Slesinger, 2013; Glaaser and Slesinger, 2017). A biophysical analysis reported that ethanol targeted in a hydrophobic ethanol-binding pocket, which located on the cytoplasmic domains of GIRK (Aryal et al., 2009).

L-type Ca^{2+} channel: In addition to BK and GIRK channels, alcohol also targets L-type calcium channels. Two studies demonstrated that low concentration of ethanol (5-10 mM) significantly inhibits peak amplitudes and the probability of opening L-type Ca^{2+} channels (Mullikin-Kilpatrick and Treistman, 1994; Wang et al., 1994). Note that the activation of L-type Ca^{2+} channels induces LTD at the corticostriatal synapse (Adermark and Lovinger, 2007).

L1 cell adhesion molecule (L1-CAM): L1-CAM is a potential target of alcohol in fetal alcohol spectrum disorder (FASD) and plays crucial roles in synaptic plasticity in adult brain (Maness and Schachner, 2007). A previous biophysics study demonstrated that ethanol molecules have a specific binding site on lg1 domains (Arevalo et al., 2008). It has been reported that ethanol inhibits L1-CAM molecules, which may contribute to the pathogenesis in the development of FASD (Tang et al., 2006).

Insulin-like growth factor 1 (IGF1): IGF1, like insulin, belongs to insulin-like peptides (ILPs) and is very important for plasticity, adult neurogenesis, as well as learning and memory (reviewed in Fernandez and Torres-Aleman, 2012). Ethanol inhibits the IGF1-mediated cell proliferation in a dose-dependent manner (10 – 100 mM) (Resnicoff et al., 1993). Many early studies indicated that this inhibitory effect might be due to inhibition of IGF-1-mediated intracellular signal transduction (Resnicoff et al., 1994; Seiler et al., 2000). Also, ethanol at 100 mM inhibits IGF1 activity and induces apoptosis in cultured cerebellar granule neurons (Zhang et al., 1998).

1.3 Dopamine Neurons and AUD

In 1973, Ahlenius (1973) used a catecholamine-synthesis inhibitor and blocked alcohol-induced talkativeness, enhancement of social interaction and euphoria in human. This was the first time to demonstrate the importance of DA in alcohol-induced reward. DA neurons, mainly located in the VTA and the substantial nigra pars compacta (SNc), play an important role in the processing of reward- and drug-related stimulations (Schultz et al., 1997; Wise, 2008; Volkow and Morales, 2015). DA neurons have two firing modes, tonic mode (1 - 8 Hz) or a transient high-frequency phasic status (500 ms, > 15Hz) (Grace and Bunney, 1983). The tonic mode of DA transmission maintains a basal level of DA, which enables the normal functions of the neural

circuit (Schultz, 2007). The phasic mode results in a sharply increase (phasic burst) or decrease (phasic pause) the firing rates for 100-500 ms, which lead to a dramatic change from the basal level of DA and this change can last for several seconds (Schultz et al., 1997; Schultz, 2007). Traditionally, phasic mode DA release was believed to encode reward value. More recent findings have demonstrated that DA signaling encodes for a reward prediction error (RPE) (Schultz et al., 1997; Bromberg-Martin et al., 2010; Steinberg et al., 2013), which is believed to encode reward learning and adaptive behavior. Dr. Schultz and his colleagues have shown that phasic DA firing mode is time-locked to unexpected or novel reward as well as a reward-related cue to make a reward prediction (Grace et al., 2007). If a reward value is larger than predicted reward, DA neurons will be strongly excited (phasic bursts) and have a large release of DA, whereas if a reward value is smaller than predicted reward or a reward is omitted at its appointed time, DA neurons will be strongly inhibited (phasic paused), which can cause a sharp decrease in DA concentrations. If a reward is cued in advanced and the size of reward can be fully predicted, DA neurons have little or no response and keep tonic firing. The same principle also applies to DA responses to reward-related and predictable cues. For example, DA neurons will have burst firing responding to a cue that informs a bigger reward in the future, whereas DA neurons will have pause firing responding to a cue that informs a smaller reward in the future. Similarly, DA neurons will have little response to cues that carry no reward information.

Although addictive drugs and alcohol exhibit a wide range of molecular structures and actions, they generally share the same principle that induces the phasic DA neuronal firing and results in an increase of striatal DA concentrations (Sulzer, 2011; Volkow and Morales, 2015). Usually, DA levels are generally modulated by three major mechanisms: 1. Increased DA neuronal firing, which is modulated by reward size and environmental cues. 2. Reuptake rate

through the DAT located on presynaptic DA neuronal terminals. 3. The state of DA neuronal terminal, which determines the number, and the size of quantal release and release probability. Thus, addictive drugs and alcohol can use these three major mechanisms to drive abnormal DA release. For examples, nicotine activates nAChRs, resulting in excitation of DA neurons. Additionally, opioids activate μ opioid receptors, resulting in disinhibition of DA neurons (Mifsud, 1989; Johnson, 1992; Chen et al., 2018). The excitation and disinhibition of DA neurons lead to a burst firing of these neurons and increase DA release probability, which may contribute enhancement of reward prediction error (Hart et al., 2014; Chang et al., 2016). Additionally, cocaine and amphetamines can act on DAT to disrupt the normal DA uptake processes and increase extracellular DA level (Giros, 1996; Volkow et al., 2000; Kahlig et al., 2005).

Alcohol, like other addictive substance (e.g., nicotine, opioids or cocaine), has been extensively shown in both preclinical and clinical studies to increase the striatal DA release. In 1988, Engel and his colleagues used *ex vivo* and *in vivo* voltammetry and found that acute administration of alcohol increased DA levels in the NAc of rats (Engel, 1988). Later, more groups found that voluntary oral drinking of alcohol caused DA release in the rat NAc in a dose-dependent manner (Weiss, 1993; Doyon et al., 2003; Ericson et al., 2003; Larsson et al., 2005). More literature also demonstrated a link between alcohol-related environmental cue and DA release. For example, a predictable visual cue (Katner, 1999; Melendez, 2002) and olfactory cue (Katner, 1999) alone (without alcohol being present) increase the DA release in the NAc in rats. To further examine the role of the DA neurons in alcohol consumption, intra-NAc alcohol infusion stimulates DA release in the NAc (Yoshimoto, 1991). Specifically, acute alcohol exposure was reported to increase the release of DA in the shell part of the NAc, but not in the

core part (Bassareo et al., 2003). More importantly, an alcohol-induced increase of striatal dopamine release has also been extensively observed in human clinical studies. In the 1990s, the development of positron imaging technique (PET) and the radiotracer ^{11}C-raclopride enabled us to investigate the real-time change of in vivo dopamine level in humans (Placzek et al., 2016). As a result, a battery of human imaging studies showed that acute and chronic alcohol exposure leads to an increase of dopamine release in the caudate-putamen (or striatum in rodents) (Boileau et al., 2003; Martinez et al., 2005; Urban et al., 2010; Aalto et al., 2015).

In addition to increased striatal dopamine release, acute administration of alcohol increases the firing rates of dopamine neurons in vivo and ex vivo. For example, Gessa used in vivo electrophysiology recording and found that intravenous administration of alcohol increases the firing rates of dopamine neurons in the rat VTA and SNc (Gessa, 1985). However, the ethanol concentration cannot be controlled during in vivo recording and whether the neuronal response results from the direct target of alcohol is also difficult to prove. Thus, ex vivo electrophysiology examination on the effect of ethanol on a DAergic neuron is needed. Brodie did series studies using ex vivo or in vitro electrophysiology to investigate the effect of ethanol on VTA dopamine neurons. In 1990, he developed a method to prepare the VTA-containing brain slices and found that ethanol excited VTA dopamine neuron in rat slices (Brodie, 1990). More importantly, the extent of DA neuron excitation is depended on ethanol concentration. In his later study, he further verified this effect in three different rat strains and further found that serotonin increased the potency of ethanol to excite VTA neurons, which might be one mechanism in ethanol-induced reward behavior (Brodie, 1994). In 1998, Brodie explored more detailed mechanisms underlying the ethanol-induced increase in the firing rate of VTA neurons (Brodie, 1998). He revealed that ethanol not only directly depolarizes VTA neurons but also

reduce the amplitude of the depolarizing phase and after-hyperpolarization of the action potential (Brodie, 1998). Furthermore, ex vivo bath application of ethanol also increases the "sag" amplitude (defined as the difference between the initial and the end of the voltage response) and voltage/current curve. This evidence suggests that ethanol can directly change member potential and the shape of the spike leading to the faster firing. Note that all these ethanol-induced alternations on VTA dopamine neurons are dose-dependent (Brodie, 1998; Brodie, 1999).

The third effect of alcohol on the DA system is that alcohol can also promote DA synthesis. For example, intraperitoneally injection of alcohol in mice yield an increase in DA synthesis, and this ethanol-induced DA synthesis can be blocked by a low dose of dopamine synthesis blocker (Garlsson, 1974). Further study revealed that both acute and chronic alcohol exposure could deplete dopamine stores from terminals and acute alcohol administration can increase dopamine synthesis that prevents dopamine depletion (Fadda, 1980).

Human alcoholism patients usually have a long-time alcohol exposure history. More studies have demonstrated that chronic alcohol intake commonly induces a dopamine deficit state (Barak et al., 2011; Diana, 2011; Koob, 2013). Barak et al. (2011) established a high level of alcohol drinking in rats using an intermittent-access two-bottle choice paradigm. After long-term excessive alcohol intake (> 7 weeks), Barak and his colleagues employed the *in vivo* microdialysis approach and found that 24-h withdrawal from alcohol led to a dramatic decrease of dopamine levels in the NAc (Barak et al., 2011). In addition to decreasing the tonic striatal dopamine level, more studies found that chronic exposure to alcohol decreased the expression of tyrosine hydroxylase (TH) and increased the expression of DAT in the striatum (Rothblat, 2001; Healey et al., 2008). A recent study also found that chronic alcohol exposure in mice resulted in an attenuation of baseline dopamine synthesis (Siciliano et al., 2017). Also, a series of studies

have shown that chronic alcohol exposure reduces tonic- and burst-firing rates of VTA DA neurons in rats (Bailey, 2001; Shen, 2003; Shen et al., 2007). Note that the alternation of DA neuron activity can change the postsynaptic dopamine receptor signaling. For example, densities of DA D2 receptors are reduced in the dorsal and ventral striatum, olfactory tubercle, SNc, and VTA of alcohol-preferring rats (McBride, 1993). Human clinical studies also demonstrated that chronic alcohol exposure decreases the dopamine level with reduction of D2 receptors (Volkow et al., 1996; Martinez et al., 2005; Zandy et al., 2015).

Drug and alcohol-evoked DA release shapes the synaptic plasticity in both the DA system and DAergic neuron-projecting regions such as the PFC and striatum (Wolf, 2002). One major hypothesis linked neuronal plasticity with drug addiction in the involved DA system. In 2001, Ungless found that a single exposure to cocaine-induced long-term excitatory potentiation (LTP) in DA neurons (Ungless et al., 2001). Later, another study demonstrated that drugs of abuse produced short- and long-term modifications of the firing of VTA DA neurons (Bonci et al., 2003). Previous studies further have shown that actively seeking cocaine, morphine or nicotine induce excitatory LTP in the VTA DA neurons (Saal et al., 2003; Chen et al., 2008). In addition, chronic alcohol exposure causes an increase in NMDAR expression levels and α-amino-3-hydroxy-5-methyl-4-isoxazolepropionic acid receptor (AMPAR) activity in the VTA (Ortiz et al., 1995; Stuber et al., 2008).

1.4 Striatum and AUD

DAergic neurons mainly project to the striatum, which is an important brain structure of the basal ganglia and gates all inputs into the basal ganglia. The basal ganglia are highly conserved across all vertebrate species and consist primarily of the globus pallidus (GP) and the striatum. The striatum is an essential nucleus in the basal ganglia, gating major inputs and

integrating information from cortical, thalamic and midbrain afferents (reviewed in Braunlich and Seger, 2013). Commonly, the striatum can be functionally divided into the ventral part (VS) and dorsal part (DS) without a clear difference in cytoarchitecture and chemoarchitecture. Given that inputs to the striatum are organized topographically, the VS and DS can be dissociated based on their distinct connectivity (Voorn et al., 2004).

The striatum has distinct gross anatomy between primates and rodents. The ventral striatum in rodents is the ventral extent of the striatum, corresponding to the ventral putamen and ventral caudate in primates. In a rodent model, the ventral striatum is also termed as nucleus accumbens (NAc). The NAc can be further subdivided into the core and shell regions. The shell part of NAc is associated with expression of goal-directed behaviors, and behavioral sensitization (Corbit et al., 2001; Hernandez et al., 2002; Ito et al., 2004). The shell receives glutamatergic inputs from many cortical and subcortical areas, such as medial regions of the prefrontal cortex (mPFC) (Gunaydin and Kreitzer, 2016), the paraventricular nucleus of the thalamus (Zhu et al., 2016), posterior regions of the basolateral amygdala (MacAskill et al., 2014), the cingulate cortex (Gunaydin and Kreitzer, 2016), OFC (Schilman et al., 2008), ventral subiculum (Bossert et al., 2016), and CA1 region of the hippocampus (MacAskill et al., 2014). The shell part receives DAergic input mainly from the VTA (Adrover et al., 2014; Saunders et al., 2018). The major output target of the NAc shell is the ventral pallidum (VP), the lateral hypothalamus (LH), the SNc and dorsal VTA (Groenewegen et al., 1996). The NAc core is linked with impulsivity (Sesia et al., 2008) and instrumental responding to Pavlovian cues (Floresco et al., 2008). The major glutamatergic inputs to the core are the PFC (Britt et al., 2012; Barrientos et al., 2018), OFC (Barrientos et al., 2018), insular cortex (Barrientos et al., 2018), cingulate cortex (Barrientos et al., 2018), motor cortex (Barrientos et al., 2018), infralimbic

cortex (Barrientos et al., 2018), perirhinal cortex (Barrientos et al., 2018), entorhinal cortex (Barrientos et al., 2018), rostral basolateral amygdala (Britt et al., 2012), paraventricular nucleus of the thalamus (Barrientos et al., 2018), central medial thalamic nucleus (Barrientos et al., 2018), mediodorsal thalamic nucleus (Barrientos et al., 2018), parafascicular nucleus (Barrientos et al., 2018), rhomboid thalamic nucleus (Barrientos et al., 2018), and parahippocampal gyrus (Groenewegen et al., 1996; Floresco et al., 2008; Britt et al., 2012). The NAc core receives DAergic input from both the VTA and SNc (Barrientos et al., 2018; Saunders et al., 2018). The outputs from the NAc core are similar to the shell (reviewed in Smith et al., 2013).

The dorsal striatum in primates is separated into two nuclei, the caudate and putamen. In rodents, the dorsal striatum is contiguous and can be further functionally divided into the medial part (DMS referred to caudate) and the lateral part (DLS referred to putamen). The DLS is associated with habitual behavior (Graybiel et al., 1994; Kreitzer and Malenka, 2008). The major glutamatergic inputs to the DLS are the motor cortex (Rothwell et al., 2015), the sensory cortex (Yin, 2010), lateral part of the OFC (Schilman et al., 2008), insular cortex (Munoz et al., 2018) and parafascicular thalamic nucleus (Parker et al., 2016). The DLS also receives DAergic input from the SNc and GABAergic inputs from the auditory cortex (Rock et al., 2016), the BNST (Smith et al., 2016), and the GPe (Mallet et al., 2008; Gittis et al., 2014; Mallet et al., 2016). In contrast, the DMS controls acquisition of goal-directed behavior (Graybiel et al., 1994; Yin et al., 2005a; Yin et al., 2005b; Kreitzer and Malenka, 2008). The major glutamatergic inputs to the DMS are the mPFC (Gunaydin and Kreitzer, 2016), the OFC (Schilman et al., 2008; Hoover and Vertes, 2011), the cingulate cortex (Gunaydin and Kreitzer, 2016), the secondary motor cortex (Gremel and Costa, 2013a), the BLA, and the parafascicular thalamic nucleus (Brown et al., 2010). In addition, the major GABAergic inputs are from the BNST (Smith et al., 2016), GPe

(Mallet et al., 2008; Gittis et al., 2014; Mallet et al., 2016), and motor cortex (Rock et al., 2016). Similar to the NAc, the DMS also receives DAergic input from both the VTA and SNc (Beier et al., 2015). The outputs of the DLS and the DMS are the GPi, GPe, SNr and the SNc (Lerner et al., 2015).

Increasing evidence suggests that the dorsal striatum plays a vital role in drug and alcohol addiction (Wang et al., 2007; Everitt and Robbins, 2013; Volkow and Morales, 2015). For example, human imaging studies suggest that cocaine cues increase the DA release in the dorsal striatum (Volkow et al., 2006; Wong et al., 2006). Also, inhibition of the dorsal striatal activity decreases cocaine-seeking behavior (Fuchs et al., 2006; See et al., 2007; Belin and Everitt, 2008). For alcohol addiction, a human imaging study revealed that heavy drinkers present a higher activity of the dorsal striatum than that of light drinkers (Vollstadt-Klein et al., 2010). In addition, upregulation of BDNF levels or inhibition of glutamatergic activity in the dorsal striatum attenuates alcohol-drinking and -seeking behaviors (McGough et al., 2004; Wang et al., 2007; Jeanblanc et al., 2009; Wang et al., 2010). Conversely, exposure to drugs of abuse and alcohol potentiates AMPAR- and NMDAR-mediated glutamatergic transmission in the dorsal striatum (Wang et al., 2010; Wang et al., 2012; Corbit et al., 2014). Furthermore, inhibition of striatal glutamatergic activity in the dorsal striatum suppresses operant alcohol self-administration and cocaine relapse (Wang et al., 2010; Wang et al., 2012; Ma et al., 2014; Pascoli et al., 2014). Increasing evidence suggested that the DMS has been strongly implicated in drug and alcohol abuse (Volkow et al., 2006; Wang et al., 2010; Wang et al., 2012; Nam et al., 2013; Wang et al., 2015).

The DMS receives multiple glutamatergic inputs from cortex, thalamus, and amygdala (Hoover and Vertes, 2011; Gremel and Costa, 2013b; Wall et al., 2013; Gunaydin and Kreitzer,

2016; Smith et al., 2016). The connections between the cortex and the DMS are important for the control of goal-directed behaviors such as drug-seeking and -taking (Yin and Knowlton, 2006; Balleine and O'Doherty, 2010; Lovinger, 2010; Everitt and Robbins, 2013), and these circuits are linked to drug and alcohol addiction (Volkow et al., 2006; Wang et al., 2010; Nam et al., 2013; Everitt and Robbins, 2016). The frontal part of the cortex, including the PFC, plays a very crucial role in decision making and goal-directed behavior (Schoenbaum et al., 2006; Lee, 2008; Rushworth and Behrens, 2008; Gremel et al., 2016). The PFC strongly associated with drug and alcohol-related behavior (Volkow et al., 2009; Koob and Volkow, 2010; Luscher and Malenka, 2011; Everitt and Robbins, 2013; McGuier et al., 2015; Volkow and Morales, 2015). For example, self-administration of alcohol increases the c-Fos expression in the mPFC area, which indicated the activation of mPFC neurons following alcohol intake (Dayas et al., 2007). In addition, chronic alcohol exposure increases NMDAR activity in the layer V mPFC neurons, reduce long spine volume after chronic alcohol exposure (Kroener et al., 2012). Also, human imaging studies also indicated an essential role of the PFC in drug and alcohol addiction (Schoenbaum et al., 2006; Rando et al., 2011). For example, the volume of gray matter in the PFC area is significantly smaller in the alcoholism patient than normal people (Rando et al., 2011).

1.5 Striatal Neurons and AUD

The striatum does not contain any glutamatergic neurons, and the majority of neurons are GABAergic neurons (Kreitzer, 2009). The striatal neurons can be anatomically divided into two populations: (1) principal projections neurons and (2) interneurons. The interneurons (< 1 - 3 %) critically regulate striatal activity, plasticity, and output.

The striatal interneurons can be categorized into GABAergic interneurons and cholinergic interneurons (Kreitzer and Malenka, 2008; Kreitzer, 2009). Striatal GABAergic interneurons based on the physiological features can be classified into two populations: fast-spiking interneurons (FSIs), which also express parvalbumin, and low-threshold spiking interneurons (LTSIs), which express somatostatin-nitric-oxide-synthase, neuropeptide-Y-positive cells, and also may express calretinin-positive interneurons (Kreitzer and Malenka, 2008; Kreitzer, 2009). The FSIs are only a small proportion of striatal neurons, but they are crucial for regulating striatal neuronal activity and output. The FSI has relatively low resting membrane potentials (- 60 mv). The deficits of FSI causes impairment of procedural learning deficits in mice (Mallet et al., 2005) and inhibition of striatal GABA signal decreases SNr neuronal firing rate and induce movement deficits (Yoshida et al., 1991; Yamada et al., 1995). FSIs receive glutamatergic inputs also from the cortex and thalamus, and GABAergic inputs from both collateral GABAergic interneurons innervation and MSNs' inputs. Unlike MSNs, the excitation of FSI only requires small numbers of afferents fiber, which usually can form multiple synaptic connections with FSI (Ramanathan et al., 2002). FSIs target extensively proximal dendrites of MSNs and suppress the generation of action potentials in MSNs (Bennett and Bolam, 1994; Koós and Tepper, 1999; Mallet et al., 2005). Thus, modulation of the FSI activity is very important for striatal function. DA can increase FSI activity via D5 receptors that are expressed on the FSI and also via the D2 receptor that is expressed on GABAergic presynaptic terminals onto FSI (Bracci et al., 2002). Besides DA, FSIs also receive modulation from acetylcholine via nAChRs that are located on FSI (Zhou et al., 2002; Centonze et al., 2003). The other type of GABAergic interneuron, LTSIs, has fewer and less dense dendritic branches relative to FSIs. LTSIs may receive different inputs as FSIs and target on MSNs (Straub et al., 2016). The LTSIs

have higher resting membrane potentials relative to FSIs and higher input resistance. However, the physiological roles of LTSIs are not clearly understood.

Cholinergic interneurons (CINs) are another important type of striatal interneurons. Typically, cholinergic neurons have been well characterized to have large cell bodies (20 – 50 μm diameter) and widespread axonal fields. CINs receive glutamatergic inputs mainly from the thalamus and, to a lesser extent, from the cortex (Lapper and Bolam, 1992; Thomas et al., 2000). Unlike other striatal neurons, CINs are peacemaker neurons in the striatum that can fire spontaneously (2 - 10 Hz). A critical feature of CINs is that salient stimuli pause the spontaneous firing, such as environmental change, reward prediction, and reward-related cues (Graybiel et al., 1994). The activity of CINs can also be modulated by DA and ACh signals via D2 and D5 receptor, as well as M2 and M4 receptors (Levey et al., 1993; Hersch et al., 1994; Bergson et al., 1995). Very recently, a study reported that CINs could be subdivided into two types based on co-release GABA and referred to as CGINs and CINs. CGINs have higher dendrites arborizations and higher spontaneous firing frequency. Importantly, only CGINs but not CINs have a pause response to the cortical burst stimulation, which might be an important mechanism for behavior flexibility.

The principle projections neurons (> 97 %) in the striatum are GABAergic MSNs that integrate glutamatergic inputs from the cortex and thalamus and send the GABAergic project to the GP and SNr (Surmeier et al., 2014). MSNs have a very negative resting membrane potential (-80 mV) and low input resistance due to the expression of inwardly rectifying potassium channels (Kirs) (Nisenbaum and Wilson, 1995). Also, depolarization of MSNs inactivates Kirs and activates the other types of potassium channels (e.g., fast- and slow-inactivating A-type and

persistent potassium channels) and this will contribute to a slow depolarization and delay of the first spike (Surmeier et al., 1989; Surmeier et al., 1991; Shen et al., 2004; Shen et al., 2005).

Back to 1980s, Wilson and Groves have found that the in vivo MSNs exhibited two different membrane potential: hyperpolarized potentials (-90 to -70 mV) and more depolarized potentials (-60 to -40 mV) (Wilson and Groves, 1981). Hyperpolarized potentials and relatively depolarized potentials are now termed as Down and Up states of MSNs (Wilson and Kawaguchi, 1996; Kreitzer, 2009). Down and Up states of MSNs might be due to the intrinsic membrane properties of MSNs and the timing of glutamatergic inputs from the cortex and thalamus (Wilson and Kawaguchi, 1996). High levels of Kir limit excitatory input-induced membrane depolarization and stabilize the MSNs membrane potentials at Down-state. However, sufficient glutamatergic inputs can generate enough depolarization on MSNs and block the Kirs, shifting MSNs from Down -state to Up-state (Blackwell et al., 2003). The duration and magnitude of Up-state are determined by the length of maintenance of sufficient excitatory inputs and activation of voltage-sensitive potassium channels, which are activated following MSNs depolarization and limit the extent of depolarization (Wilson and Kawaguchi, 1996). The switching between Down and Up-state also affects synaptic strength. For example, in the Down-state, excitatory postsynaptic potentials (EPSPs) are only mediated by AMPA receptors, whereas in the Up-state, the NMDA receptors can be depolarized and are able to contribute to the mediation of EPSPs. Additionally, Up-state also activates low-voltage-activated L-type calcium channels (Cav1.3), which contribute to the induction of long-term striatal depression (LTD) (Carter & Sabatini 2004, Choic & Lovinger 1997, Kreitzer & Malenka 2005).

MSNs are not a homogeneous population, based on the output target, the MSNs can be further classified into striatonigral (direct-pathway) and striatopallidal (indirect-pathway)

neurons. Striatonigral neurons mainly expressed DA D1 receptors (D1Rs) (also termed as D1-MSNs) and send projections to SNr and internal part of globus pallidus (GPi) (entopeduncular nucleus (EP) in rodents) (direct pathway), whereas the striatopallidal neurons mainly expressed DA D2 receptors (D2Rs) (also termed as D2-MSNs) and exclusively innervate the external part of GP (GPe) (indirect pathway), which then relays to the GPi and SNr (Smith et al., 1998; Gerfen and Surmeier, 2011; Maia and Frank, 2011; Durieux et al., 2012; Smith et al., 2013; Volkow et al., 2013; Sippy et al., 2015).

D1Rs and D2Rs are G protein-coupled receptors but have different kinetic property and control distinct downstream pathway and cause a distinct biological effect. In the striatum, D1Rs are mainly $G_{(olf)}$-coupled receptors and mediated excitatory downstream signaling pathway (Herve et al., 1993). Activation of D1Rs enhances cAMP and PKA activity and facilitates activation of the L-type Ca^{2+} channel and trafficking of AMPARs and NMDARs (Beaulieu and Gainetdinov, 2011). In contrast, D2Rs are Gi-coupled receptors and mediated inhibitory downstream signaling pathway. Activation of D2Rs triggers both Gi-signaling pathway and $G_{\beta\gamma}$-signaling pathway. As a result, the enhancement of Gi protein activity decreases the cAMP-mediated signaling pathway, and activation of $G_{\beta\gamma}$ protein increases K^+ efflux via GIRK channels as well as PP2B activity. The complex D2R-mediated signaling pathway leads to repolarization and inhibition of AMPAR and NMDAR trafficking. Besides the separate signaling pathway of D1Rs and D2Rs, they also show different kinetic feature. D1Rs are low-affinity DA receptor, while D2Rs are high-affinity DA receptor (Bromberg-Martin et al., 2010). As a result, phasic DA release mainly activates D1Rs and enhances direct-pathway activity, leading reinforcement and promotion of motor vigor, whereas tonic DA level change or phasic pause of DA release mainly

disinhibit D2Rs and enhances indirect-pathway activity, leading punishment and suppression of motor vigor (Bromberg-Martin et al., 2010; Durieux et al., 2012).

Besides distinct DA receptors expression, D1-MSNs also express muscarinic M4 receptors and synthesis dynorphin and substance P (Gerfen, 1992; Ince et al., 1997). In contrast, D2-MSNs exclusively express adenosine A2A receptors, synthesis enkephalin and neurotensin (Augood et al., 1996). Physiologically, D1- and D2-MSNs have similar properties, such as spine density, negative resting potential, and low firing rates. However, Kreitzer and Malenka found that D2-MSNs showed higher excitability than D1-MSNs. The difference of excitability between D1- and D2-MSNs may be due to that Kirs are more readily inactivated in D2-MSNs than D1-MSNs (Mermelstein et al., 1998). Besides the difference in Kir inactivation, M1 receptors in D2-MSNs produce more inhibition of Kir, which also contributes to the higher excitability on D2-MSNs.

The direct pathway and indirect pathway are thought to form a dynamic balance and oppositely coordinated motor vigor and motivational behavior. Excitation of the direct-pathway promotes voluntary motor behavior, such as locomotion activity, food intake, and drug-seeking behavior, whereas excitation of the indirect pathway suppresses these voluntary behaviors. An imbalance between the direct pathway and indirect pathway may cause many brain disorders, for example, Parkinson's disease, Huntington's disease, addiction, and compulsive disorder.

D1- and D2-MSNs have also been found to play a distinct role in drug addiction (Ferguson et al., 2011; Smith et al., 2013; Volkow et al., 2013; Creed et al., 2016). Using a pharmacological intervention method, Dry et al. found that systematic administration of a D1R antagonist, SCH-23390, impaired alcohol intake in the rat (1993). Later, the other two groups also found that the systematic administration of SCH-23390 impaired alcohol condition place

preference (CPP) in mice (Bahi and Dreyer, 2012; Pina and Cunningham, 2014). However, pharmacological intervention does not have any specificity to directly change the D1-MSN or D2-MSN activity. To circumvent this, more studies have combined conditional knockout or conditional expression with either optogenetic or chemogenetic to access D1- and D2-MSNs. Conditional knockout of DARPP-32 from D1-MSNs in the striatum induces a hypoactivity and reduces psychostimulant response, whereas conditional knockout of DARPP-32 from D2-MSNs in the striatum causes an opposite effect. Similarly, optogenetic or chemogenetic inhibition of D1-MSNs reduces sensitization of amphetamine and CPP, whereas optogenetic or chemogenetic activation of D2-MSNs enhances the sensitization of amphetamine and motivation of craving for cocaine (Hikida et al., 2010; Lobo et al., 2010; MacAskill et al., 2014).

1.6 Synaptic Plasticity and AUD

AUD, just like all other drug abuse, is considered to arise from abnormally enhanced learning and memory that is driven by alcohol or drug-mediated abnormal synaptic plasticity in distinct neural circuits (Hyman et al., 2006; Koob and Volkow, 2010; Luscher and Malenka, 2011). This drug-evoked plasticity has been found extensively in the striatum (Abrahao et al., 2017). The MSNs express two types of ionotropic glutamatergic receptors: AMPAR and NMDAR. AMPARs mediate fast excitatory synaptic transmission, and NMDARs are a calcium-permeable ion-channel, which are required for the induction of synaptic plasticity (Malenka and Nicoll, 1999; Martin et al., 2000). NMDARs are required for inducing LTP of AMPAR-mediated transmission in the striatum (Calabresi et al., 1992; Kerr and Wickens, 2001; Calabresi et al., 2007; Shen et al., 2008; Calabresi et al., 2014) and play key roles for learning and memory in the dorsal striatum. For example, microinjection of an NMDAR antagonist into the striatum causes memory deficiency in rats in a stimulus-response task (Packard and McGaugh, 1996).

The NMDAR has also been associated with many alcohol-related phenotypes. For example, inhibition of NMDAR activity impairs the development of alcohol tolerance (Khanna et al., 1993) and decreases alcohol intake (Holter et al., 2000). Also, NMDAR antagonists decreases the intensity of alcohol withdrawal symptoms (Bisaga et al., 2000). In addition, systematic administration of an NDMAR antagonist decreases relapse alcohol intake in the rat (Holter et al., 2000). The NMDAR contains two subunits: GluN1 and GluN2 (Sucher et al., 1996). In the striatum, the GluN2 subunit can be further divided into GluN2A and GluN2B subtypes (Wenzel et al., 1997). GluN2B has been long known that is very an important NMDAR subunit for learning and memory (Fox et al., 2006; Bartlett et al., 2007).

The NMDAR is a direct molecular target of alcohol (Ron, 2004). In 1989, Lovinger (1989) found that acute alcohol presentation inhibited NMDAR activity. However, recent studies found that repeated cycles of alcohol drinking and withdrawal-induced long-term facilitation of NMDAR activity in the dorsal striatum, particularly in the medial part of the dorsal striatum (DMS) (Wang et al., 2010; Wang et al., 2012). This NMDAR adaptation enhances LTP induction in the DMS (Wang et al., 2012). LTP, particularly NMDAR-dependent LTP, is thought to be a cellular mechanism of learning and memory, and this plasticity can be altered by and contributes to alcohol abuse (Silvers et al., 2003; Yin et al., 2007; McCool, 2011). Also, many studies have shown that prenatal and adult exposure to alcohol alters neuronal plasticity in the striatum (Yin et al., 2007; Rice et al., 2012; Wang et al., 2015). For example, acute adult alcohol exposure impairs LTP in the DMS by inhibiting NMDARs-mediate glutamatergic transmission (Yin et al., 2007), whereas chronic alcohol exposure facilitates LTP induction in the DMS, the BLA, and the hippocampus (McCool, 2011; Wang et al., 2012). In addition, prenatal alcohol exposure (PAE) facilitates dendritic branching and increase the dendritic length of MSNs. Also,

PAE increases glutamatergic transmission in the basolateral amygdala (Baculis and Valenzuela, 2015) and mPFC (Louth et al., 2016).

Despite these important findings of glutamatergic synaptic plasticity in regulating alcohol drinking and seeking behavior, much remains unknown about whether and how excessive alcohol intake alters synaptic transmission onto striatal D1- and D2-MSNs and how D1- and D2-MSNs gate alcohol-related behavior. In chapter II, I used whole-cell patch-clamp recording to examine both glutamatergic and GABAergic transmission in the DMS revealing that NMDAR was selectively potentiated in D1-MSNs and GABAergic activity was enhanced in D2-MSNs. Then, using chemogenetic intervention of the activity of D1- and D2-MSNs, I discovered that both D1- and D2-MSNs control alcohol consumptions in an opposite manner. Then, in chapter III, I paired optogenetic postsynaptic depolarization with a high-frequency presynaptic stimulation. This dual-channel optogenetic plasticity-inducing protocol produced a reliable NMDAR-dependent LTP mixed with an endocannabinoid (eCB)-dependent LTD. Note that in vivo delivery of the LTP protocol to the PFC-DMS synapses led to a long-lasting increase of alcohol-seeking behavior. In contrast, in vivo delivery of the LTD protocol produced a long time decrease in this behavior. Importantly, I confirmed that the plasticity protocol induced LTP and LTD selectively in D1-MSNs and that selective increase or decrease the alcohol-seeking behavior correspondingly. These findings contribute to establishing a causal link between corticostriatal synaptic plasticity and alcohol-seeking behavior. Finally, in chapter IV, I examined how prenatal alcohol exposure (PAE) affected glutamatergic transmission to DMS D1-MSNs. Like excessive adult drinking in the chapter II, PAE enhanced AMPA-mediated glutamatergic transmission onto D1-MSNs and increased the dendritic complexity of DMS D1-MSNs.

CHAPTER II

DISTINCT SYNAPTIC STRENGTHENING OF THE STRIATAL DIRECT AND INDIRECT PATHWAYS DRIVES ALCOHOL CONSUMPTION[*]

2.1 Overview

Repeated exposure to addictive drugs and alcohol triggers glutamatergic and GABAergic plasticity in many neuronal populations. The dorsomedial striatum (DMS), a brain region critically involved in addiction, contains medium spiny neurons (MSNs) expressing dopamine D1 or D2 receptors, which form direct and indirect pathways, respectively. It is unclear how alcohol-evoked plasticity in the DMS contributes to alcohol consumption in a cell type-specific manner. Mice were trained to consume alcohol using an intermittent-access two-bottle-choice drinking procedure. Slice electrophysiology was used to measure glutamatergic and GABAergic strength in DMS D1- and D2-MSNs of alcohol-drinking mice and their controls. *In vivo* chemogenetic and pharmacological approaches were employed to manipulate MSN activity, and their consequences on alcohol consumption were measured. Repeated cycles of alcohol consumption and withdrawal in mice strengthened glutamatergic transmission in D1-MSNs and GABAergic transmission in D2-MSNs. *In vivo* chemogenetic excitation of D1-MSNs, mimicking glutamatergic strengthening, promoted alcohol consumption; the same effect was induced by D2-MSN inhibition, mimicking GABAergic strengthening. Importantly, suppression of GABAergic transmission *via* D2 receptor-glycogen synthase kinase-3β (GSK3β) signaling dramatically reduced excessive alcohol consumption, as did selective inhibition of D1-MSNs or

[*] This chapter is re-printed with permission from "Distinct synaptic strengthening of the striatal direct and indirect pathways drives alcohol" by Cheng Y, Huang CCY, Ma T, Wei X, Wang X, Lu J, Wang J, 2017. *Biological Psychiatry*, 81, 918-929. Copyright [2018] by Elsevier.

excitation of D2-MSNs. Our results suggest that repeated cycles of excessive alcohol intake and withdrawal potentiates glutamatergic strength exclusively in D1-MSNs and GABAergic strength specifically in D2-MSNs of the DMS, which concurrently contribute to alcohol consumption. These results provide insight into the synaptic and cell type-specific mechanisms underlying alcohol addiction and identify targets for the development of new therapeutic approaches to alcohol abuse.

2.2 Introduction

Addiction is considered to arise from maladaptive learning and memory processes, involving various forms of aberrant synaptic plasticity in different populations of neurons within unique neural circuits (Hyman et al., 2006; Koob and Volkow, 2010; Luscher and Malenka, 2011). The striatum, a major area of the basal ganglia, is essential for drug and alcohol addiction (Hyman et al., 2006; Koob and Volkow, 2010; Luscher and Malenka, 2011). For instance, human imaging studies have indicated that the striatum is linked to cocaine and alcohol addiction (Filbey et al., 2008; Volkow and Morales, 2015). Moreover, rodent studies revealed that striatal glutamatergic inhibition attenuated cocaine sensitization and alcohol intake (Wang et al., 2010; Brown et al., 2011). Similarly, striatal knockdown of GABA receptors or inhibition of GABAergic transmission also reduces alcohol consumption (Hyytia and Koob, 1995; Nie et al., 2011). These studies indicate that both excitatory glutamatergic and inhibitory GABAergic activities in the striatum positively control alcohol consumption, although the underlying mechanisms are poorly characterized.

Increasing evidence suggests that the dorsal part of the striatum is essential for drug and alcohol addiction (Wang et al., 2007; Everitt and Robbins, 2013; Volkow and Morales, 2015). The dorsal striatum can be subdivided into the dorsolateral striatum, which is involved in habit

formation (Balleine and O'Doherty, 2010; Everitt and Robbins, 2013), and the dorsomedial striatum (DMS), which mediates goal-directed behaviors (Balleine and O'Doherty, 2010; Everitt and Robbins, 2013). The DMS has been strongly implicated in drug and alcohol abuse (Volkow et al., 2006; Wang et al., 2010; Wang et al., 2012; Nam et al., 2013; Wang et al., 2015). The principal cells of the striatum are medium spiny neurons (MSNs). MSNs expressing dopamine D1 receptors (D1-MSNs) project directly to the substantia nigra pars reticulata (SNr); this constitutes the direct pathway, which mediates "Go" actions in rewarding behaviors (Gerfen and Surmeier, 2011; Maia and Frank, 2011; Sippy et al., 2015). In contrast, D2-MSNs express dopamine D2 receptors (D2Rs) and connect indirectly to the SNr; this indirect pathway regulates "NoGo" behaviors (Gerfen and Surmeier, 2011; Maia and Frank, 2011). In MSNs, there are two major neurotransmissions: glutamatergic and GABAergic (Kreitzer, 2009). They are known to be regulated by alcohol in the DMS and other brain regions (Lovinger et al., 1990; Roberto et al., 2004; Wang et al., 2010). However, it is unclear whether these two types of neurotransmissions are modulated by alcohol in a cell type-specific manner, and it is not known how D1- and D2-MSNs distinctly influence alcohol consumption.

In this study, we measured both glutamatergic and GABAergic activity in D1-MSNs and D2-MSNs and found that NMDA receptor (NMDAR) activity in D1-MSNs and GABAergic activity in D2-MSNs were selectively potentiated following cycles of alcohol consumption and withdrawal. Using a chemogenetic approach employing designer receptors exclusively activated by designer drugs (DREADDs), which allowed selective manipulation of D1- or D2-MSN activity (Urban and Roth, 2015), we discovered that both of these cell types were not only necessary, but also sufficient, to drive alcohol consumption. Furthermore, we observed that D2R-glycogen synthase kinase-3β (GSK3β signaling regulated GABAergic activity and thus, alcohol

consumption. The findings of this study provide detailed mechanistic information indicating how different forms of neuroplasticity in distinct neuronal populations of the striatal direct and indirect pathways drive alcohol consumption.

2.3 Results

2.3.1. Selective Potentiation of Excitatory Transmission in DMS D1-MSNs Following Repeated Cycles of Excessive Alcohol Consumption and Withdrawal

The NMDAR is one of the major targets of alcohol (Lovinger et al., 1990; Holmes et al., 2013). However, it was unclear whether NMDAR-mediated excitatory transmission in D1- or D2-MSNs was altered by alcohol consumption and withdrawal. To measure NMDAR activity in these two sub-populations of striatal neurons, we generated new lines of mice to visualize fluorescently labeled D1- and D2-MSNs. These new mice were crossed by *drd1a*-Cre (D1-Cre) and *drd2*-Cre (D2-Cre) mice with Cre reporter lines (Gong et al., 2007). We confirmed that D1-MSNs projected to the internal part of the globus pallidus (GPi) and the SNr in the D1-Cre;Ai14 mice (Figure 2.1A) (Madisen et al., 2010), whereas D2-MSNs mainly projected to the external part of the globus pallidus (GPe) in the new D2-Cre;Ai14 mice (Figure 2.1B) (Gerfen and Surmeier, 2011). Importantly, our transgenic mouse model suggests less than 5% overlap of DMS D1- and D2-MSNs (Supplementary Figure 1), which is consistent with previous reports (Bertran-Gonzalez et al., 2008; Valjent et al., 2009). The animals were trained for 8 weeks to consume 20% alcohol using the widely used intermittent-access two-bottle-choice drinking procedure (Hwa et al., 2011; Becker and Ron, 2014; Wang et al., 2015). They consumed ~18-20 g/kg/24 hr of alcohol (Supplementary Figures. 2A, 3A), which was considered as excessive alcohol intake in C57BL/6 mice (Anacker et al., 2011; Hwa et al., 2011; Darcq et al., 2015). Twenty-four hr after the last alcohol-drinking session, whole-cell recording was conducted to

measure NMDAR activity in D1- and D2-MSNs of the DMS. We found that the amplitude of NMDA-induced currents in D1-MSNs was dramatically greater in alcohol-drinking mice than their water controls (Figure 2.1C; Supplementary Figure 2B). Surprisingly, the NMDA current in D2-MSNs was significantly smaller in the alcohol-drinking group than in the water-drinking group (Figure 2.1D). Since the NMDA-elicited current reflects both synaptic and extrasynaptic NMDAR activity (Carpenter-Hyland et al., 2004), these alcohol-related effects may result from changes in the synaptic and/or extrasynaptic NMDARs. To examine the synaptic NMDARs, we measured the input-output relationship for NMDAR-mediated excitatory postsynaptic currents (EPSCs) in D1- and D2-MSNs from alcohol- and water-treated mice. As shown in Figure 2.1E and 1F, the EPSC amplitudes were significantly higher in D1-MSNs from the alcohol group than in those from the water group, whereas the EPSC amplitudes in D2-MSNs were identical in these two groups. Furthermore, we observed that the NMDA/AMPA ratio was also increased selectively in D1- but not in D2-MSNs following alcohol consumption (Supplementary Figure 2C-F). These results suggest that repeated cycles of alcohol consumption and withdrawal selectively potentiated synaptic NMDAR activity in D1-MSNs, but not in D2-MSNs, within the DMS.

The NMDAR is composed of GluN1 and GluN2 (A-D) subunits (Paoletti et al., 2013). The activity of GluN2B-containing NMDARs was reported to increase after cycles of excessive alcohol consumption and withdrawal (Kash et al., 2009; Wang et al., 2010). Therefore, we examined whether the GluN2B activity was selectively altered in D1- or D2-MSNs of the DMS following excessive alcohol consumption and withdrawal. We observed that the GluN2B/NMDA ratio in D1-MSNs was significantly higher in the alcohol group than in the water group (Figure 2.1G). However, this effect was not observed in D2-MSNs (Figure 2.1H). Collectively, these

results suggest that alcohol-induced strengthening of the synaptic NMDAR-mediated glutamatergic input onto D1-MSNs of the DMS resulted, at least in part, from facilitation of GluN2B-NMDAR activity.

2.3.2. Selective Potentiation of Inhibitory Transmission in DMS D2-MSNs Following Repeated Cycles of Excessive Alcohol Consumption and Withdrawal

GABAergic changes have been found in many brain regions, including the striatum, following alcohol exposure (Weiner and Valenzuela, 2006; Nie et al., 2011). However, it was unclear whether prolonged excessive alcohol consumption and withdrawal changed GABAergic transmission selectively in D1- or D2-MSNs. Mice were trained and consumed comparable levels of alcohol as above (~20 g/kg/24 hr, Supplementary Figure 3A); GABAergic activity was measured in D1- and D2-MSNs of the DMS 24 hr after the last drinking session. We found that the amplitude of GABA-induced currents was moderately higher in D1-MSNs and dramatically elevated in D2-MSNs of alcohol-drinking mice, as compared with those of their water controls (Figure. 2.2A). Since $GABA_A$Rs are located at synaptic and extrasynaptic sites in MSNs (Luo et al., 2013), we investigated whether the synaptic GABAergic transmission was affected after prolonged excessive alcohol consumption and withdrawal. Miniature inhibitory postsynaptic currents (mIPSCs) were measured in both populations of MSNs. We found that neither the amplitude nor the frequency of mIPSCs differed in D1-MSNs from the alcohol and water groups (Figure 2.2B-D). The cumulative probability distributions of mIPSC amplitudes and inter-event intervals were not affected by alcohol exposure (Figure 2.2C,D). Hence, the increased GABA-induced currents in D1-MSNs of the alcohol group (Figure 2.2A) may result from enhanced extrasynaptic $GABA_A$R activity. Indeed, we found that tonic extrasynaptic GABA currents were enhanced in D1-MSNs following excessive alcohol intake (Supplementary Figure 3B). In

contrast, both the amplitude and frequency of mIPSCs were significantly higher in D2-MSNs in alcohol-drinking mice than in their water controls (Figure 2.2E-G; Supplementary Figure 3C-E); this was confirmed by analysis of cumulative probability distributions of mIPSCs. The distribution of mIPSC amplitudes showed a right shift (Figure 2.2F), indicating an increase in amplitude. The distribution of mIPSC inter-event intervals shifted to the left in alcohol-drinking mice (Figure 2.2G), demonstrating a reduced duration of mIPSC events, and thus an increased mIPSC frequency. Collectively, these results indicate that inhibitory GABAergic transmission is potentiated selectively in DMS D2-MSNs, but not in D1-MSNs, following repeated cycles of excessive alcohol consumption and withdrawal.

2.3.3. *In vivo* Chemogenetic D1-MSN Excitation or D2-MSN Inhibition Promotes Alcohol Consumption

The identified potentiation of excitatory glutamatergic transmission in D1-MSNs and of inhibitory GABAergic transmission in D2-MSNs of the DMS following excessive alcohol intake would be predicted to excite D1-MSNs and inhibit D2-MSNs. Since D1-MSNs control "Go" and D2-MSNs control "NoGo" actions in rewarding behaviors (Gerfen and Surmeier, 2011; Maia and Frank, 2011), we reasoned that the resulting increase in "Go" and reduction of "NoGo" could both promote alcohol consumption. To test these hypotheses, we selectively manipulated D1- or D2-MSN activity using DREADDs (Urban and Roth, 2015). To confirm selective expression of a DREADD in the targeted neuronal population, e.g., D1-MSNs, a Cre-inducible adeno-associated virus (AAV) expressing the *hM3Dq* gene (Figure 2.3A) was bilaterally infused into the DMS region of D1-Cre mice (Figure 2.3B, left). Expression of *hM3Dq* in the DMS was indicated by a red fluorescent reporter, mCherry (Figure 2.3B, right), and was restricted selectively to D1-MSNs, as confirmed by their GPi and SNr projections in the direct pathway

(Figure 2.3C). We also confirmed selective expression of *hM4Di* in the DMS D2-MSNs as indicated by mCherry in the GPe of the indirect pathway (Supplementary Figure 4A).

The effects of DREADDs on MSN activity were confirmed by recording from GPe neurons in the indirect pathway (Figure 2.3D). We infused two viruses encoding a DREADD and channelrhodopsion-2 (ChR2) into the DMS of D2-Cre mice and confirmed their co-expression in D2-MSN fibers within the GPe (Figure 2.3D,E). Optical stimulation of ChR2-containing fibers elicited optogenetically-induced inhibitory postsynaptic currents (oIPSCs) in GPe neurons (Figure 2.3F, left). In DMS slices expressing *hM3Dq*, bath application of the DREADD agonist, clozapine-N-oxide (CNO), significantly increased the amplitude of oIPSCs by 42.4% (Figure 2.3F, right). In contrast, in DMS slices expressing *hM4Di* (Figure 2.3G; Supplementary Figure 4B), CNO significantly reduced the oIPSC amplitude by 51.9% (Figure 2.3H). We also confirmed the effect of hM4Di and hM3Dq activation in D1-MSNs (Supplementary Figure 5). These results confirmed that hM3Dq activation excited, or hM4Di activation suppressed the MSN output, respectively.

To test the hypothesis that excitation of D1-MSNs is sufficient to increase alcohol consumption, we infused a viral vector encoding the excitatory *hM3Dq* into the DMS of D1-Cre mice. The animals were trained to consume alcohol as described above (Hwa et al., 2011; Wang et al., 2015). CNO was administered systemically 30 min before the drinking session and alcohol consumption was measured at 1, 4, and 24 hr. We found that 1-hr alcohol consumption was significantly increased following CNO administration (Figure 2.3I). In addition, 1-hr alcohol preference was also enhanced (Figure 2.3J). The CNO effects on alcohol consumption and preference were time-dependent (Figure 2.3K; Supplementary Figure 6A,B). Interestingly,

systemic administration of CNO also significantly decreased 1-hr water intake (Figure 2.3L), but not in 4- or 24-hr intake (Supplementary Figure 6C).

To test the hypothesis that inhibition of D2-MSNs promotes alcohol consumption, we expressed the inhibitory *hM4Di* in DMS D2-MSNs of D2-Cre mice. The animals underwent the drinking procedure and CNO treatment described above. We observed that CNO administration caused a significant increase in 1-hr alcohol drinking (Figure 2.3M) and preference (Figure 2.3N) in D2-Cre mice. The CNO effects on alcohol drinking and preference were diminished over time (Figure 2.3O; Supplementary Figure 6D,E). Water intake was not altered by systemic administration of CNO (Figure 2.3P; Supplementary Figure 6F).

Taken together, these results suggest that alterations of D1- and D2-MSN activity in the DMS are sufficient to drive alcohol consumption, and that these exert opposite influences on this behavior.

2.3.4. Direct *In Vivo* Chemogenetic Inhibition of D1-MSNs or Excitation of D2-MSNs Attenuates Excessive Alcohol Consumption

Next, we examined whether direct manipulations of these two neuronal populations reduced excessive alcohol consumption. First, we asked whether *in vivo* chemogenetic inhibition of D1-MSNs, which presumably suppresses “Go” actions, decreased excessive alcohol consumption in mice. These mice were trained to consume alcohol using the same procedure as above. We discovered that high levels of 1-hr alcohol consumption (Figure 2.4A) and preference (Figure 2.4B) were dramatically attenuated by administration of CNO. The CNO effects on alcohol intake and preference exhibited a time-dependent manner (Figure 2.4C; Figure Supplementary Figure 7A,B). However, neither water intake (Figure 2.4D; Supplementary Figure 7C) nor saccharin intake (Figure 2.4E; Supplementary Figure 7D) was altered by

administration of CNO. These findings suggest that inhibition of the output of DMS D1-MSNs in the direct pathway selectively decreases alcohol consumption by suppressing the preference for alcohol intake.

Conversely, we assessed whether excitation of D2-MSNs, which presumably enhances "NoGo" actions, reduced excessive alcohol consumption. An *hM3Dq* vector was bilaterally infused into the DMS of D2-Cre mice. We found that both 1-hr alcohol consumption (Figure 2.4F) and preference (Figure 2.4G) were significantly suppressed by CNO administration. The inhibitory effect of CNO on alcohol-drinking behavior was time-dependent (Figure 2.4H; Supplementary Figure 7E,F). Intake of water (Figure 2.4I; Supplementary Figure 7G) or saccharin (Figure 2.4J; Supplementary Figure 7H) was not affected by CNO injection. These results indicate that excitation of DMS D2-MSNs in the indirect pathway specifically decreases alcohol consumption by suppressing the preference for alcohol intake. In addition, we found that D2-MSN excitation prevented expression of alcohol-induced conditioned place preference (Supplementary Figure 8), which provides furthur evidence that D2-MSNs play a negative role in alcohol-related behavior.

Collectively, these results suggest that DMS D1- and D2-MSN activities are necessary to drive alcohol consumption and again in an opposite way.

2.3.5. D2R Signaling via GSK3β in the DMS Suppresses GABAergic Transmission in D2-MSNs and Inhibits Excessive Alcohol Consumption

Lastly, we asked whether and how D1- and D2-signaling contribute to alcohol consumption. Previously, we found that pharmacological inhibition of D1 receptors attenuated excessive alcohol consumption (Wang et al., 2015). Here, we investigated whether pharmacological modulation of D2R signaling suppressed alcohol consumption. Since the D2R

agonist, quinpirole, was shown to suppress cortical GABAergic transmission (Li et al., 2011; Li et al., 2012) and GABAergic activity is increased preferentially in D2-MSNs by alcohol (Figure 2.2), this compound may inhibit GABAergic transmission in D2-MSNs and thus decrease alcohol consumption. To assess this possibility, electronically-induced IPSCs (eIPSCs) were recorded in D2-MSNs from alcohol-drinking D2-Cre;Ai14 mice. We found that bath application of quinpirole significantly reduced eIPSC amplitudes (Figure 2.5A,C). We next explored the potential downstream target of D2R activation that may mediate quinpirole-induced inhibition of GABAergic transmission. Thus, we treated DMS slices with a GSK3β inhibitor (SB216763) and observed that this completely abolished the inhibitory effect of quinpirole on eIPSCs (Figure 2.5B,C). These results suggest that activation of D2Rs in D2-MSNs of the DMS suppresses GABAergic transmission in a GSK3β-dependent manner.

Additionally, we observed that GSK3β phosphorylation on the serine 9 residue was increased without alternation of its protein levels following cycles of excessive alcohol intake and withdrawal (Figure 2.5D-G). Furthermore, protein levels of $GABA_AR$ β3 subunit, which predominantly contributes to $GABA_AR$ activity in D2- rather than D1-MSNs (Janssen et al., 2009; Janssen et al., 2011), was also significantly augmented in the same animal (Figure 2.5D,H). Given that GSK3β phosphorylation decreases the kinase activity (Beaulieu et al., 2009; Beurel et al., 2015), these data indicate that prolonged alcohol consumption and withdrawal suppresses GSK3β activity, which, in turn, enhances $GABA_AR$ expression.

To test whether activation of D2Rs reduced alcohol intake, we bilaterally infused quinpirole or vehicle into the DMS of alcohol-drinking C57BL/6 mice and measured alcohol consumption at 2, 4, and 24 hr. We measured alcohol intake starting at 2 hr post-infusion, but not at 1 hr as in chemogenetic experiments, because local agent infusion took a longer time than the

i.p. injection used in chemogenetic experiments, and because 2-hr alcohol intake post-infusion was stable (Wang et al., 2015). We found that 2-hr alcohol consumption was significantly reduced in the quinpirole-treated group, as compared with the vehicle group, without alternation of water consumption (Figure 2.2.5I; Supplementary Figure 9A). Moreover, infusion of both quinpirole and SB216763 into the DMS did not significantly affect 2-hr alcohol or water intake, as compared with vehicle infusion (Figure 2.5I; Supplementary Figure 9B), suggesting that GSK3β inhibition abolished the quinpirole effect on alcohol consumption. Infusion of SB216763 alone did not affect alcohol intake (Figure 2.5J). The inhibitory effect of quinpirole on alcohol consumption was also observed at 4-hr, but not at 24-hr (Figure 2.5K). These results suggest that activation of D2Rs in the DMS suppresses alcohol consumption in a GSK3β-dependent manner.

Furthermore, we assessed whether direct inhibition of GABAergic activity suppressed alcohol consumption. A $GABA_AR$ inhibitor, picrotoxin, was bilaterally infused into the DMS of alcohol-drinking mice. We found that picrotoxin infusion produced a significant reduction in 2-hr alcohol consumption, but not water intake (Figure 2.5L; Supplementary Figure 9C). This inhibitory effect of picrotoxin on alcohol consumption gradually diminished over time (Figure 2.5L).

Collectively, these findings indicate that D2R signaling *via* GSK3β suppresses GABAergic transmission in D2-MSNs of the DMS and inhibits excessive alcohol consumption.

2.4 Discussion

The present study found that repeated cycles of excessive alcohol intake and withdrawal selectively potentiated GluN2B-NMDAR activity in direct-pathway D1-MSNs and GABAergic transmission in indirect-pathway D2-MSNs of the DMS. These changes in synaptic strength serve to excite D1-MSNs and inhibit D2-MSNs and we discovered that D1-MSN excitation or

D2-MSN inhibition using an *in vivo* chemogenetic approach promotes alcohol consumption. Conversely, D1-MSN inhibition or D2-MSN excitation suppress alcohol consumption. These findings suggest that changing the activity of either type of MSNs is sufficient and necessary to regulate alcohol-drinking behavior. Importantly, we demonstrated that the potentiation of D2-MSN GABAergic transmission from alcohol-drinking mice was reduced by pharmacological activation of D2Rs and subsequent GSK3β signaling. D2R activation or local GABAergic inhibition in the DMS reduced alcohol consumption. This study elucidated the detailed mechanism involved in the modulation of alcohol-drinking behavior by alcohol-mediated changes in neurotransmission onto distinct neuronal populations in the same brain region, i.e., the DMS (Figure 2.6).

2.4.1. Potentiation of Excitatory and Inhibitory Transmission Separately in D1- and D2-MSNs by Excessive Alcohol Intake

One major finding of this research is that NMDAR-mediated transmission is potentiated selectively in D1-MSNs, while GABAergic transmission is potentiated exclusively in D2-MSNs, following cycles of excessive alcohol consumption and withdrawal. We further observed that the NMDA/AMPA ratio was increased in D1- but not D2-MSNs. Given that both the AMPAR (Wang et al., 2015) and NMDAR activities are potentiated in D1-neurons following alcohol consumption, the increased NMDA/AMPA ratio suggests that cycles of alcohol consumption and withdrawal causes greater potentiation of NMDAR activity than of AMPAR activity. This conclusion is line with previous findings that the NMDAR, rather than the AMPAR, is the primary and direct target of alcohol (Lovinger et al., 1989; Wang et al., 2012) and that a similar change at the corticostriatal synapses in D1-MSNs was induced following chronic cocaine exposure (Pascoli et al., 2014). Since NMDAR activity is known to be facilitated by dopamine

activation of D1 receptors (Beaulieu and Gainetdinov, 2011; Gerfen and Surmeier, 2011), this selective change of NMDARs in D1-MSNs may result from alcohol-induced elevation of striatal dopamine levels (Sulzer, 2011). The increased NMDAR activity is consistent with drug-induced "silent" synapses (Huang et al., 2009). In contrast, a decrease in the NMDA-induced current was observed in D2-MSNs, which may reflect NMDAR inhibition by dopamine activation of D2Rs (Li et al., 2009). One mediator of the downstream signaling of D2R activation is GSK3β. This kinase, however, seems less likely involved in the reduction of NMDA currents in D2-MSNs since cycles of alcohol intake and withdrawal inhibit the kinase activity (as shown herein) (Neasta et al., 2011; Liu et al., 2016) and GSK3β inhibition has been reported to enhance NMDA currents (Xi et al., 2011). Additionally, we measured GABAergic activity in these two types of striatal neurons. In D1 neurons, an increased GABA-induced current without mIPSC alteration suggests that extrasynaptic $GABA_AR$ activity is enhanced following repeated cycles of alcohol exposure and withdrawal and confirmed by the increased GABAergic tonic current. Importantly, we observed enhancement of the mIPSC frequency in D2-MSNs, indicating a potential increase in GABAergic inputs onto this neuronal population. This concept is in agreement with a previous study indicating that withdrawal from repeated exposure to alcohol caused an allostatic state including dopaminergic deficiency in the striatum (Koob and Le Moal, 2008; Barak et al., 2011); this deficiency was reported to increase GABAergic interneuron connectivity onto D2-MSNs (Gittis et al., 2011).

2.4.2. D2Rs Regulate GABAergic Transmission via GSK3β Contributing to Excessive Alcohol Consumption

The second major finding is that D2R activation suppresses D2-MSN GABAergic transmission and alcohol intake in a GSK3β-dependent manner, indicating that D2R-GSK3β

signaling regulates alcohol intake (Figure 2.6). Chronic alcohol consumption has been reported to decrease protein levels of D2Rs and GSK3β activity in the striatum (Neasta et al., 2011; Volkow and Morales, 2015). Since GSK3β negatively regulates $GABA_AR$ trafficking and thereby GABAergic transmission (Li et al., 2012; Rui et al., 2013; Tyagarajan and Fritschy, 2014), excessive alcohol consumption leads to downregulation of D2R-GSK3β signaling and thereby increases GABAergic activity. Consistent with this notion, we observed an enhanced GSK3β phosphorylation and β3-containing $GABA_AR$ expression following excessive alcohol intake, suggesting that alcohol exposure and withdrawal downregulates GSK3β activity and consequently enhances $GABA_AR$ expression. The β3-containing $GABA_AR$, like the δ-containing one (Nie et al., 2011), mediates tonic inhibition (Janssen et al., 2009; Janssen et al., 2011) and are activated by ambient GABA that are likely released from tonically active GABAergic interneurons (Brickley and Mody, 2012). This indicates an important role of GABAergic interneurons in alcohol-drinking behavior and it would be of interest to examine the exact role in the future. These results also explain, in part, our observation that the GABA-induced currents and the mIPSC amplitudes in D2-MSNs were potentiated following excessive alcohol intake. Conversely, we found that D2R activation and signaling *via* GSK3β reduced GABAergic activity in D2-MSNs in alcohol-drinking animals. The D2R-GSK3β-mediated reduction of GABAergic transmission in the DMS inhibited alcohol consumption but not water intake, a finding that is supported by other reports indicating that GABAergic inhibition or GABA receptor knockdown in the striatum reduced alcohol intake (Hyytia and Koob, 1995; Nie et al., 2011).

2.4.3. Contrasting Roles of D1- and D2-MSNs in Alcohol Consumption

The third major finding of this research is that bidirectional chemogenetic manipulations of two different subtypes of MSNs produced distinct changes in alcohol-drinking behavior,

revealing the opposing roles of D1- and D2-MSNs in alcohol consumption and preference in mice.

Specifically, chemogenetic excitation of D1-MSNs promoted alcohol consumption, whereas inhibition of their activity attenuated alcohol consumption. This indicated a positive role of D1-MSNs in regulation of alcohol consumption. Our results are supported by pharmacological and genetic studies (Hodge et al., 1997; El-Ghundi et al., 1998; D'Souza, 2003; Wang et al., 2015). Importantly, our study on D2-MSNs advances the understanding of their negative role in alcohol consumption , which has not been seen in previous pharmacological studies using D2R agonists/antagonists (Dyr et al., 1993; Hodge et al., 1997; Phillips et al., 1998; Thanos et al., 2001; Wang et al., 2015), due to complex expression pattern of strital D2Rs (Beaulieu and Gainetdinov, 2011).

In summary, we found that repeated cycles of alcohol consumption and withdrawal potentiate excitatory glutamatergic strength in D1-MSNs and inhibitory GABAergic strength in D2-MSNs of the DMS. The excitatory potentiation may occur at the corticostriatal input, which has been reported in other drugs of abuse (Pascoli et al., 2014), and the inhibitory strengthening may result from GABAergic interneurons. Since the DMS is part of the cortico-striato-thalamo-cortex circuit, which is known to control action-outcome learning and goal-directed behavior (Gunaydin and Kreitzer, 2016), these glutamatergic and GABAergic changes presumably enhance process of goal-direct information in this circuit. Consequently, these changes increase D1-MSN-mediated “Go” and decrease D2-MSN-mediated “NoGo” actions controlling alcohol-associated behaviors (Figure 2.6). Both of these effects serve to reinforce alcohol consumption, leading to pathological excessive use of alcohol. This study provides an insight into the detailed mechanisms underlying the control of alcohol consumption, and perhaps the intake of other

drugs, by excitatory and inhibitory neurotransmission onto striatal neuronal subpopulations, identifying both synaptic and neuronal therapeutic targets for the development of new approaches to the treatment of alcohol abuse.

2.5 Materials and Methods

2.5.1. Reagents

CNO was obtained from the NIH through the NIMH Chemical Synthesis and Drug Supply Program. Quinpirole, Ro 25-6981, and tetrodotoxin (TTX) were obtained from Tocris. DNQX (6,7-dinitroquinoxaline-2,3-dione), CPP (3-[2-carboxypiperazin-4-yl]propyl-1-phosphonic acid), and SB216763 were purchased from Abcam. NBQX (2,3-dihydroxy-6-nitro-7-sulfonyl-benzo[F]quinoxaline) was obtained from R&D systems**.** Picrotoxin, bicuculline methiodide (BMI) and all other chemicals were purchased from Sigma. Cre-inducible AAV8-hSyn-DIO-hM4Di-mCherry (8×10^{12} vg/ml), AAV8-hSyn-DIO-hM3Dq-mCherry (4.7×10^{12} vg/ml), and AAV5-EF1α-DIO-ChR2-eYFP (5×10^{12} vg/ml) and AAV8-Syn-ChR90(Chronos)-GFP (5.8×10^{12} vg/ml) viruses were purchased from the University of North Carolina Vector Core. Monoclonal anti-GSK3β (Cat. #9315) and anti phospho-GSK3β (Ser9) (Cat. #9323) antibodies were purchased from Cell Signaling Technology. Anti-$GABA_AR$ β3 antibody were purchased from Novusbio Biologicals (Cat. #NB300-199). Anti-β-actin antibody was purchased from Sigma (Cat. #A5316). Preoxidase anti-Rabbit IgG (H+L) (Cat. #PI-1000) and preoxidase anti-mouse IgG (H+L) (Cat. #PI-2000) were purchased from Vector Laboratories. The BCA protein assay kit was purchased from Pierce Chemicals. The western lighting plus-ECL kit was purchased from Perkin-Elmer.

2.5.2. Animals

Drd1a-Cre (D1-Cre) and *Drd2*-Cre (D2-Cre) mice were obtained from the Mutant Mouse Regional Resource Center. DsRed, Ai14, Snap25, and C57BL/6J mice were purchased from the Jackson Laboratory. All mice were back-crossed onto a C57Bl/6 background. Hemizygous DsRed mice were bred with C57BL/6J mice. D1-Cre or D2-Cre mice were crossed with DsRed (Figure 2.1 and 2.2 only) or Ai14 to generate D1-Cre;DsRed, D1-Cre;Ai14, D2-Cre;DsRed, and D2-Cre;Ai14 mice for electrophysiology studies. Mouse genotypes were determined by PCR analysis of Cre or the fluorescent protein in tail DNA (Cre for D1-Cre and D2-Cre mice; DsRed for DsRed mice; tdTomato for Ai14 mice). Since we did not observe a significant difference in electrophysiology data obtained in D1-Cre;DsRed and D1-Cre;Ai14 mice, or in D2-Cre;DsRed and D2-Cre;Ai14 mice, we pooled the data from DsRed and Ai14 mice.

Mice were housed individually at 23°C under a 12-hr light: dark cycle, with lights on at 11:00 P.M. Food and water were provided *ad libitum*. All mice were bred onto the C57BL/6J genetic background. Twelve-week old male mice were used in this study. All animal care and experimental procedures were approved by the Texas A&M University Institutional Animal Care and Use Committee and were conducted in agreement with the National Research Council *Guide for the Care and Use of Laboratory Animals*.

2.5.3. Intermittent-access to 20% alcohol 2-bottle-choice drinking procedure

To establish a high level of alcohol consumption in mice, we employed the intermittent-access two-bottle choice drinking procedure (Hwa et al., 2011; Wang et al., 2015). Male mice were given 24-hr concurrent access to one bottle of 20% alcohol in water (vol/vol) and one bottle of water starting at 1:30 P.M. on every other day, with 24-hr periods of alcohol deprivation between the alcohol-drinking sessions. The water and alcohol bottles were weighed after the 24-

hr access period, unless stated otherwise. Control animals were treated in the same manner, except that they were presented with water only. This procedure was followed for 8 weeks.

2.5.4. Preparation of acute striatal slices and electrophysiology recordings

Twenty-four hr after the last alcohol-drinking session, animals were sacrificed and 200-μm coronal sections containing the DMS (Figures. 2.1, 2.2, 2.4) or sagittal sections containing the GPe (Figure. 2.3) in the same thickness were prepared. The brain slices were prepared using a vibratome (VT1200S, Leica) in an ice-cold cutting solution. The cutting solution contained the following (in mM): 40 NaCl, 148.5 sucrose, 4 KCl, 1.25 NaH_2PO_4, 25 $NaHCO_3$, 0.5 $CaCl_2$, 7 $MgCl_2$, 10 glucose, 1 sodium ascorbate, 3 sodium pyruvate, and 3 myo-inositol, saturated with 95% O_2 and 5% CO_2. Slices were then incubated in a 1:1 mixture of cutting solution and external solution at 32°C for 45 min. Slices were then maintained in external solution at room temperature until use.

Slices were placed in the recording chamber and perfused with the external solution at a flow rate of 3-4 ml/min. Neurons were visualized using an epifluorescent microscope (Examiner A1, Zeiss). D1- and D2-MSNs were identified by the fluorescence of GFP (D1-Cre;DsRed or D2-Cre;DsRed mice) or tdTomato (D1-Cre;Ai14 or D2-Cre;Ai14 mice). Neurons were clamped at -70 mV. NMDAR activity was measured in fluorescently-labeled D1- and D2-MSNs of the DMS. To measure NMDA-induced currents, NMDA (10 μM) was bath-applied for 30 sec with 0.05 mM external Mg^{2+}, in the presence of NBQX (10 μM) and picrotoxin (100 μM) to block AMPA receptor-mediated synaptic transmission and inhibitory synaptic currents, respectively. Holding currents were measured every 5 sec. To generate input-output curves for NMDAR-mediated excitatory postsynaptic currents (EPSCs), varying intensities of electrical stimulation (10-30 μA, with an increment of 5 μA) were delivered through bipolar electrodes that were

placed within the DMS. GluN2B/NMDA ratios were measured using a GluN2B-NMDAR antagonist, Ro 25-6981 (0.5 µM).

For measuring GABAergic activity and transmission, recordings were conducted at 32°C., DNQX (20 µM) and CPP (10 µM) were added to the external solution to block AMPA receptors and NMDARs, respectively. To record GABA-induced currents, GABA (100 µM) was bath-applied for 30 sec and holding currents were measured every 5 sec (Quintana et al., 2012). Miniature inhibitory postsynaptic currents (mIPSCs) were recorded in TTX (1 µM) for 3 min and analyzed. For tonic current measurements, GABA (5 µM) was bah-applied and the current magnitudes were obtained from the mean baseline currents before and during BMI (25 µM) application. To record optogenetically-induced inhibitory postsynaptic currents (oIPSCs) in GPe neurons, blue LED light (470 nm for 2 ms; 0.15-2.8 mW) was delivered through the objective lens to slices every 30 sec to trigger ChR2-mediated GABA release from D2-MSNs. CNO (10 µM) was bath-applied for 10 min. To record electronically-induced IPSCs (eIPSCs), bipolar stimulating electrodes were positioned 150-200 µm away from the recorded neurons. The eIPSCs were elicited every 20 sec. Recordings with more than 20% changes in access resistance were excluded from the analysis.

2.5.5. Stereotaxic viral infusion and cannula implantation

Viruses were bilaterally infused (500 nl at 75 nl/min) into the DMS of D1-Cre and D2-Cre mice. In order to increase viral expression areas within the DMS, the viruses were infused at two sites per hemisphere (Site 1: anterior-posterior, +1.18; medial-lateral, ±1.3; dorsal-ventral, -2.9 from Bregma. Site 2: anterior-posterior, +0.38; medial-lateral, ±1.55; dorsal-ventral, -2.88, from Bregma). For cannula implantation, dual guide cannulae (C235G-3.0, 26 gauge; Plastic

one) were placed to target the DMS at the following coordinates: anterior-posterior, +0.5; medial-lateral, ±1.5; dorsal-ventral, -2.0 from Bregma. For more details, see (Wang et al., 2015).

2.5.6. Intermittent-access to saccharin 2-bottle-choice drinking procedure

When the alcohol consumption experiments had been completed, the same cohort of mice were trained to drink 0.033% saccharin (Nam et al., 2013) using a similar procedure, except that alcohol was replaced by a saccharin solution (0.033%, w/v).

2.5.7. *In vivo* chemogenetic manipulation

Six weeks after infusion of the *hM4Di* or *hM3Dq* viruses in the DMS of D1-Cre and D2-Cre mice, when a stable baseline of alcohol intake was achieved, the animals were intraperitoneally injected with vehicle (5% DMSO in saline vol/vol) for 3 consecutive sessions. To manipulate mouse drinking behavior, 3 or 5 mg/kg of CNO (1 mg/ml in vehicle) was administered intraperitoneally 30 min prior to the start of the drinking sessions, and alcohol or saccharine intake was measured at 1, 4, and 24 hr.

2.5.8. Intra-DMS drug infusion

This procedure was conducted as described previously (Wang et al., 2015). Cannulae were implanted in male C57BL/6 mice trained to drink 20% alcohol, as described above. After a stable baseline of alcohol intake was achieved, mice were infused with 0.5 µl of vehicle (5% DMSO in saline), the D2 agonist quinpirole (6 µg), the GSK3β□ inhibitor, SB216763 (20 ng) (Xu et al., 2011), a cocktail of quinpirole (6 µg) and SB216763 (20 ng), or the $GABA_A$ receptor inhibitor picrotoxin (2 µg) (Salado-Castillo et al., 1996) 10 min before the start of drinking sessions. The injectors extended 1 mm below the tip of the cannula. Alcohol intake was measured at 2, 4, and 24 hr.

2.5.9. Conditioned Place Preference (CPP)

The CPP procedure was adapted from previously report (Cunningham et al., 2006; Logrip et al., 2009; Gibb et al., 2011; Bahi and Dreyer, 2012; Pina et al., 2015). Two groups of D2-Cre male mice were infused with AAV-DIO-hM3Dq into the DMS. Five weeks after infusion, place preference training was conducted in a Hamilton-Kinder open-field apparatus (16 inch x 16 inch x 15 inch, 16 beams per side per box), which was customized into two rectangle compartments (6.8 inch x 7.9 inch x 7.9 inch) that are connected via a hall (2.4 inch length, 3.1 inch width). Time spent in each compartment was detected by infrared beam crosses. Different visual and tactile cues distinguish the two compartments: black/white stripes with a “rod” flooring in the first compartment, and black/white dots with a metal plateflooring with holes in the second compartment. Each experiment consisted of three phases. During the first phase (day 1, preconditioning), each mouse was placed in the neutral hall and was given access to both compartments for 30 min. The time that the animal spent in each compartment was recorded. During the second phase (days 2 to 9, conditioning), the mice were administered 20% alcohol (2 g/kg) and immediately placed into one of the given compartments and confined for 5 min on days 3, 5, 7, and 9. On alternate days (conditioning days 2, 4, 6, and 8), mice were administered saline and immediately placed into the opposite compartment and confined for 5 min. During the last phase (day 10, post-conditioning test), mice in the experimental group were administered CNO (1 mg/kg) and mice in the control group were administered vehicle (5% vol/vol DMSO in saline). Thirty min after injection, mice were placed into the central of neutral hall and allowed free access to both compartments for 30 min. The total time spent in each compartments were recorded.

2.5.10. Western Blot Analysis

Male C57BL/6 mice were trained for 8 weeks to consume 20% alcohol using the intermittent-access 2-bottle choice drinking procedure. Control mice underwent the same treatment without alcohol provided. One day after the last alcohol session, both groups of mice were perfused intracardially with HEPES buffer containing sucrose (Li et al., 2012). The dorsal striatum were immediately collected on ice and homogenized with a sonicator in a radioimmunoprecipitation assay (RIPA) buffer containing 50 mM Tris-hydrochloride (HCl) pH 7.6, 150 mM sodium chloride, 1% vol/vol Nonidet P-40, 0.1% (weight/vol) sodium dodecyl sulfate (SDS), 0.5% (weight/vol) sodium deoxycholate, 2 mM ethylenediaminetetraacetic acid (EDTA) as well as protease and phosphatase inhibitors. The homogenates were centrifuged at 13,000 rmp for 5 min at 4˚C. The protein concentrations were determined by BCA protein assay kit. Samples (30 □g protein) were resolved on a 10% SDS-PAGE gel and transferred to a nitrocellulose membrane. Membranes were blocked for 1 hour in TBST containing 5% non-fat milk powder at room temperature. The membranes were incubated with monoclonal phospho-GSK3β (Ser9) at a dilution 1:1000 overnight in 4˚C. After rinsing 10 min with TBST for 3 times, the membranes were incubated in HRP-conjugated anti-rabbit IgG (H+L) at 1:1000 for 1 h followed by detection with Western Lightning Plus-ECL kit. The membranes were then stripped in a stripping buffer containing 62.5 mM Tris-HCl (pH6.8), 2% (w/v) SDS and 0.7% (v/v) -mercaptoethanol in a 50˚C water bath for 30 min, followed by washing with TBST for 5 x 20min. After re-blocking in TBST containing 5% non-fat milk powder, membranes were re-probed with monoclonal GSK3β at 1:1000. Similarly, the membranes were stripped and re-probed with anti-$GABA_AR$ β3 subunits (1:1000) and then anti-β-actin antibodies (1:1000). Western blot images were quantitively analyzed by densitometry with NIH Image J software.

Densities of phospho-GSK3β were normalized to those of GSK3β□ and□β-actin. Results were expressed as a percentage of the control (water groups).

2.5.11. Histology

When all behavioral tests had been completed, mice were perfused intracardially with 4% paraformaldehyde (PFA) in phosphate-buffered saline (PBS). The brains were removed and post-fixed in 4% PFA overnight at 4°C followed by dehydration in 30% sucrose solution and cryostat frozen sectioning. For verification of cannula placement, the brain was cut into 50-μm coronal sections, which were examined under a light microscope (Wang et al., 2015). The brains from D1-Cre;Ai14 and D2-Cre;Ai14 mice, and those from virus-infused D1-Cre and D2-Cre mice, were sectioned coronally and sagittally. The sections were stained with NeuroTrace green (1:100). A confocal laser-scanning microscope (A1si, Nikon) was used to image these sections using a 594-nm laser for excitation of mCherry and tdTomato and a 488-nm laser for NeuroTrace green.

2.5.12. Statistical analysis

Electrophysiological data were analyzed using paired or unpaired *t* tests and two-way ANOVA with repeated measures (two-way RM ANOVA), followed by the Student-Newman-Keuls (SNK) *post hoc test*. All behavioral data were analyzed with one-way ANOVA with repeated measures (one-way RM ANOVA) followed by SNK test, unless stated otherwise. Statistical analysis was conducted by OriginLab and SigmaPlot programs. mIPSCs were analyzed using Mini analysis software (Synaptosoft Inc.). All data are expressed as the Mean ± SEM.

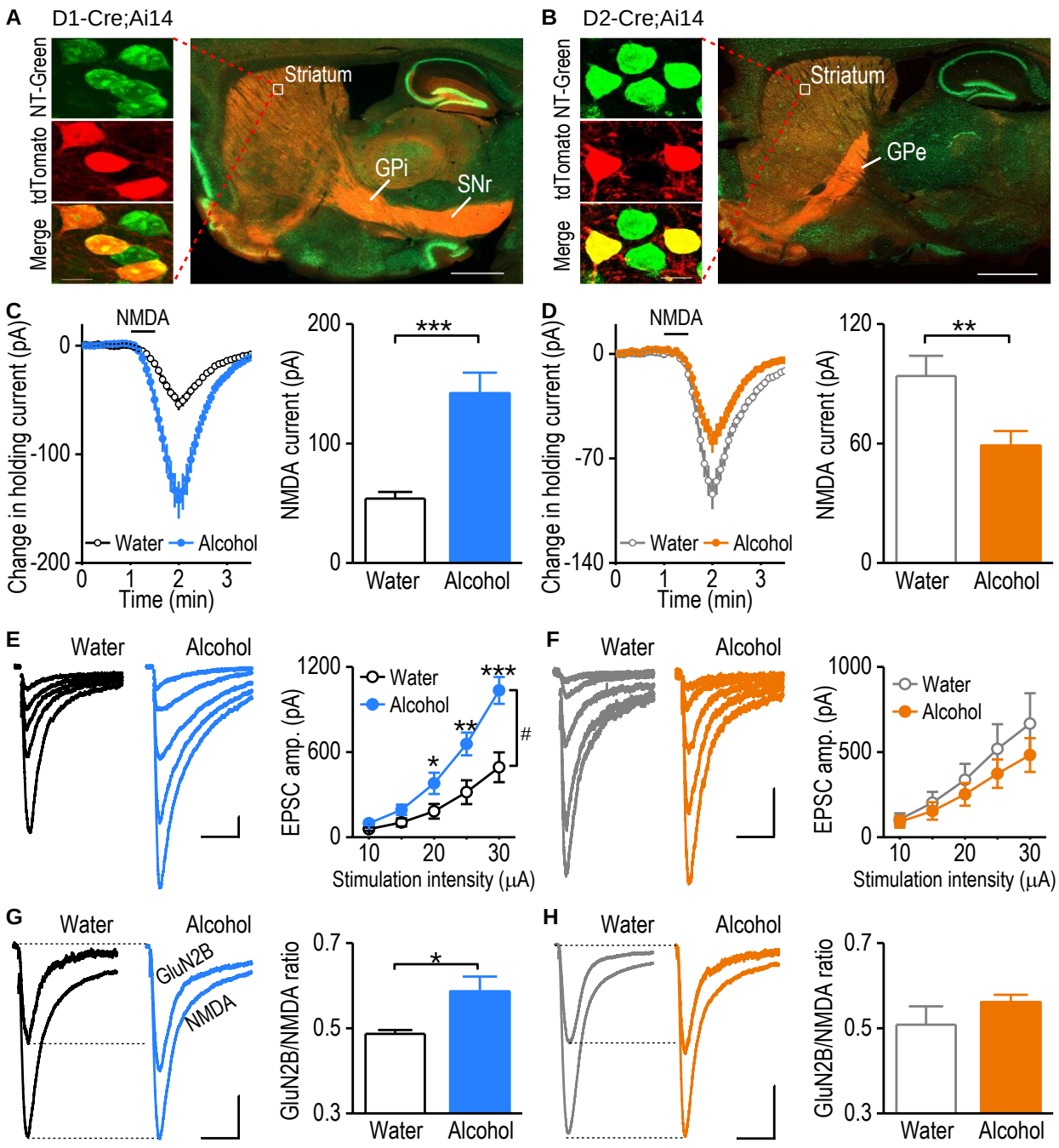

Figure 2.1. Selective potentiation of NMDAR activity in D1-MSNs following repeated cycles of excessive alcohol consumption and withdrawal.

(**A**) Verification of D1-MSNs from a D1-Cre;Ai14 mouse, based on their GPi and SNr projections in a sagittal section (right), counter-stained with NeuroTrace green (NT-green). Scale bar: 1 mm. Five striatal neurons from an indicated box are shown (left) stained with NT-green (top); three neurons expressed tdTomato (D1-MSNs, middle) and were yellow in the merged image (bottom). Scale bar: 10 μm. (**B**) Verification of D2-MSNs from a D2-Cre;Ai14 mouse based on the GPe projections. Four NT-green-stained striatal neurons are shown (left), two of which expressed tdTomato (D2-MSNs, middle). (**C**) Cycles of excessive alcohol consumption and withdrawal significantly increased NMDA-induced currents in D1-MSNs. Changes in holding currents were measured after NMDA (10 μM, 30 s) was applied to the slices (left). The peak amplitudes observed in these study groups (14 neurons, 3 mice per group) were summarized (right). $t_{(26)} = 4.77$, $p < 0.001$, unpaired *t* test. (**D**) Cycles of excessive alcohol consumption and withdrawal reduced NMDA-induced currents in D2-MSNs. Changes in holding currents were measured after NMDA was bath-applied (left) and the peak amplitudes in D2-MSNs from the alcohol (15 neurons, 3 mice) and water (14 neurons, 3 mice) groups of mice were compared (right). $t_{(27)} = -2.8$, $p < 0.01$, unpaired *t* test. (**E**) Cycles of excessive alcohol consumption and withdrawal significantly increased the NMDAR-EPSC amplitude in D1-MSNs. Representative EPSC traces evoked by a range of stimulation intensities in slices from the alcohol (16 neurons, 8 mice) and water (12 neurons, 6 mice) groups (left), with the corresponding input-output curves (right). $F_{(1,26)} = 7.43$, $^{\#}p < 0.05$, two-way RM-ANOVA. Scale bars: 200 pA, 100 ms. (**F**) Cycles of excessive alcohol consumption and withdrawal did not alter NMDAR-EPSCs in D2-MSNs. Representative EPSC traces evoked by a range of stimulation intensities in slices from the indicated groups of mice (left), with the corresponding input-output curves from the alcohol (12 neurons, 7 mice) and water (11 neurons, 6 mice) groups (right). $F_{(1,21)} = 0.43$, $p > 0.05$, two-way RM-ANOVA. (**G**) Cycles of excessive alcohol drinking and withdrawal increased the GluN2B/NMDA ratio in D1-MSNs. Sample GluN2B- and NMDAR-EPSC traces in the indicated groups (left) and the GluN2B/NMDA ratios in D1-MSNs from the alcohol (10 neurons, 6 mice) and water (8 neurons, 4 mice) groups (*right*). $t_{(16)} = -2.52$, $p < 0.05$, unpaired *t* test. (**H**) Cycles of excessive alcohol consumption and withdrawal did not change the GluN2B/NMDA ratio in D2-MSNs. Sample traces in the indicated groups (left), with the GluN2B/NMDA ratios in D2-MSNs from the alcohol (8 neurons, 5 mice) and water (8 neurons, 6 mice) groups (right). $t_{(14)} = -1.22$, $p > 0.05$, unpaired *t* test. Scale bars (F-H): 100 pA, 100 ms. Statistical comparisons between Alcohol and Water groups at the same levels are indicated by * for $p < 0.05$ and ** for $p < 0.01$ and *** for $p < 0.001$, respectively.

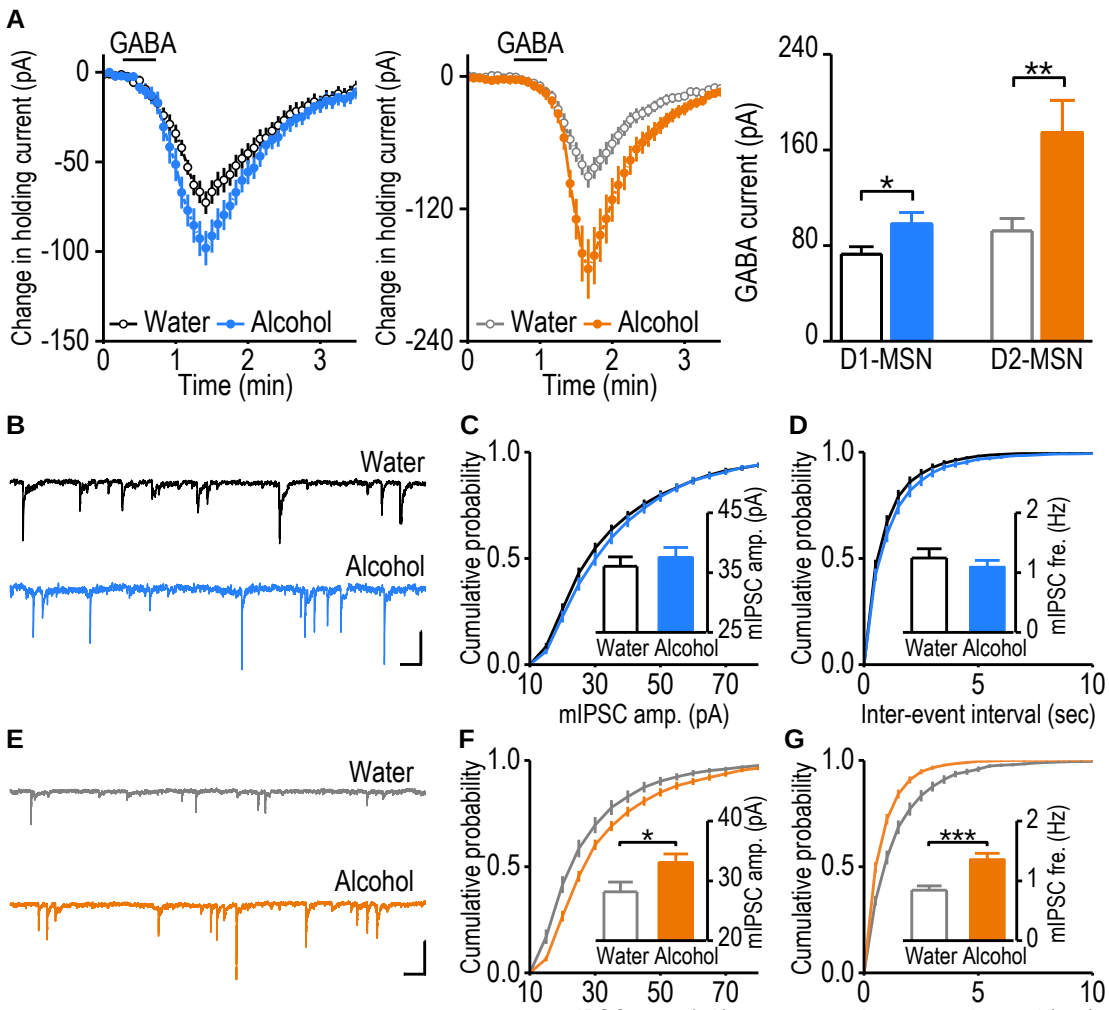

Figure 2.2. Selective potentiation of synaptic GABAergic activity in D2-MSNs after repeated cycles of excessive alcohol consumption and withdrawal.
GABAergic activity was measured in DMS D1- and D2-MSNs 24 hr after the last alcohol exposure. (**A**) GABA-induced currents in D1- and D2-MSNs in the indicated groups. Changes in holding currents recorded in D1-MSNs (left; 17 neurons from 5 mice for Water; 18 neurons from 6 mice for Alcohol) and D2-MSNs (middle; 19 neurons from 4 mice for Water; 20 neurons from 5 mice for Alcohol) after bath application of GABA (100 μM, 30 sec) to DMS slices and their peak amplitudes (right). $t_{(33)} = -2.28$, $p < 0.05$ (D1-MSNs); $t_{(37)} = 2.79$, $p < 0.01$ (D2-MSNs), unpaired *t* test. (**B**), Representative mIPSC traces in D1-MSNs from the indicated mice. (**C**,**D**) Cycles of excessive alcohol consumption and withdrawal did not alter mIPSCs in D1-MSNs. Cumulative probability plots for the distributions of mIPSC amplitudes (C) and inter-event intervals (D) in D1-MSNs from alcohol-drinking mice (27 neurons, 5 mice) and their water controls (19 neurons, 4 mice). Inset bar graphs summarize the respective average mIPSC amplitudes (C) and frequencies (D). $t_{(44)} = -0.6$, $p > 0.05$ for amplitude; $t_{(44)} = 0.8$, $p > 0.05$ for frequency, unpaired *t* test. (**E**), Representative mIPSC traces in D2-MSNs from the indicated mice. (**F**,**G**) Cycles of excessive alcohol drinking and withdrawal increased the amplitude and frequency of mIPSCs in D2-MSNs. Cumulative probability plots showing the distributions of mIPSC amplitudes (F) and inter-event intervals (G) in D2-MSNs from alcohol-drinking mice (17 neurons, 5 mice) and water controls (17 neurons, 4 mice). Inset bar graphs present the respective average mIPSC amplitudes (F) and frequencies (G). $t_{(32)} = -2.23$, $p < 0.05$ for amplitude; $t_{(32)} = -4.20$, $p < 0.001$ for frequency, unpaired *t* test. Scale bars: 30 pA, 0.5 sec (B, E). Statistical comparisons between Alcohol and Water groups are indicated by * for $p < 0.05$ and ** for $p < 0.01$ and *** for $p < 0.001$, respectively.

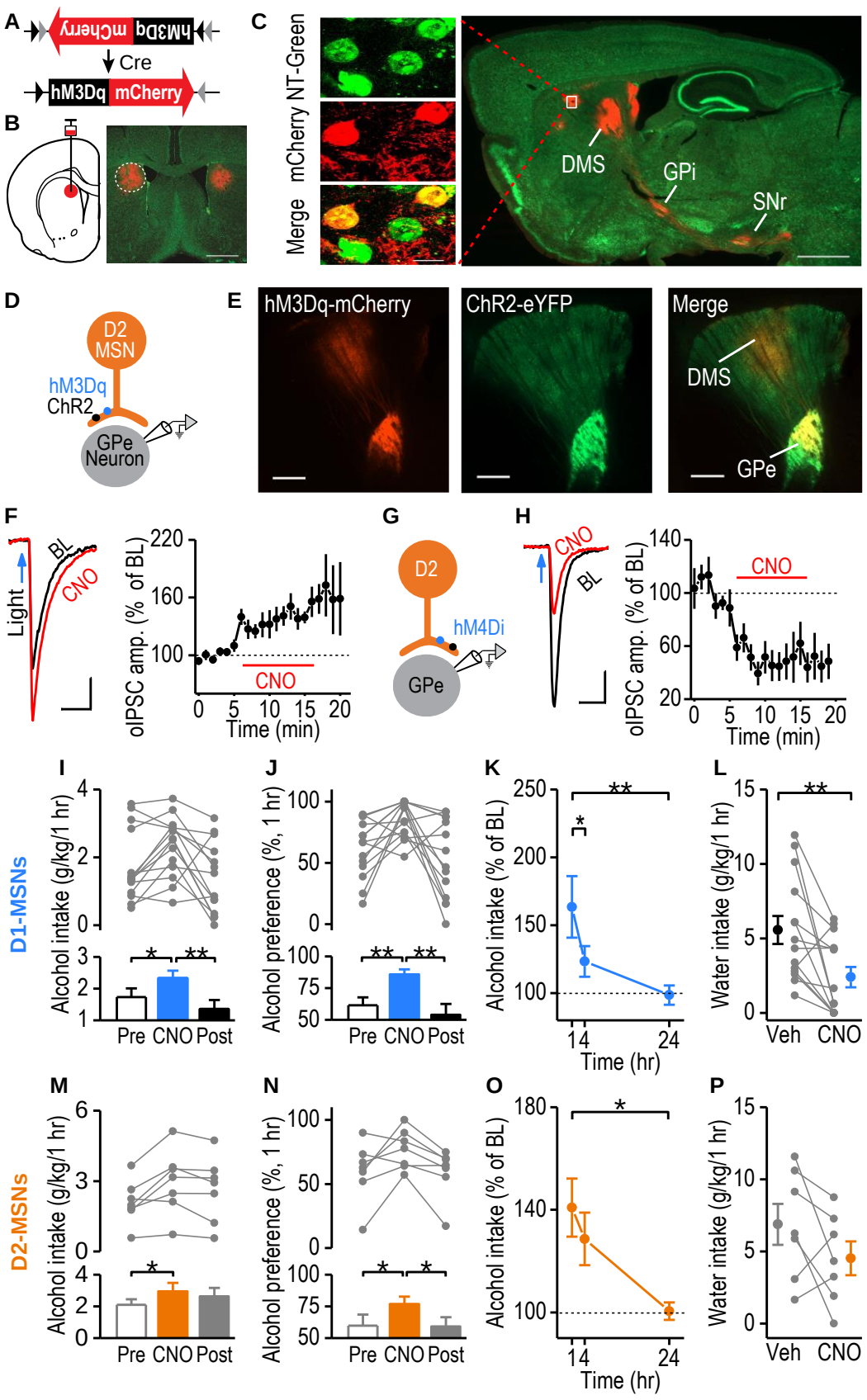

Figure 2.3. *In vivo* chemogenetic excitation of D1-MSNs in the direct pathway or inhibition of D2-MSNs in the indirect pathway promotes alcohol consumption in mice.

(**A**) Expression of the *hM3Dq* gene was driven by Cre recombinase. (**B**) Stereotaxic infusion of an AAV-DIO-hM3Dq-mCherry virus into the DMS region of D1-Cre mice (left) led to *hM3Dq-mCherry* expression, as indicated by the red mCherry fluorescence (right) in a section stained with NT-Green. Scale bar: 1 mm. (**C**) Verification of selective *hM3Dq* expression in D1-MSNs from a D1-Cre mouse infused with the virus (right). Note that *hM3Dq*-expressing D1-MSNs projected to the GPi and SNr. Scale bar: 1 mm. Inset, micrographs showing 4 striatal neurons from the indicated box (right) stained with NT-green (top); 2 of these expressed mCherry (middle) and were yellow in the merged image (bottom). Scale bar: 10 µm. (**D**) Schematic diagram illustrating *ex vivo* electrophysiology validation of hM3Dq enhancement of D2-MSN-mediated synaptic transmission in GPe neurons. A cocktail of AAV-DIO-hM3Dq-mCherry and AAV-DIO-ChR2-eYFP vectors was infused into the DMS of D2-Cre mice, and ChR2-mediated striatopallidal oIPSCs were recorded in GPe neurons. (**E**) Representative low- magnification sagittal view of mCherry and eYFP fluorescence in a brain slice from a D2-Cre mouse infused with the viral cocktail. Scale bar: 1 mm. (**F**) Bath application of CNO (10 µM) increased the amplitude of ChR2-mediated oIPSCs in GPe neurons from D2-Cre mice infused with the *hM3Dq* virus in the DMS. Left, sample traces of oIPSCs at baseline (BL) and during CNO application. Scale bars: 40 ms, 100 pA. Right, Time course of oIPSCs showing CNO significantly increased oIPSC amplitudes (8 neurons, 5 mice). $t_{(7)} = -4.3$, $p < 0.001$, paired *t* test. (**G**) Schematic showing *ex vivo* electrophysiology validation of hM4Di, as described for D. (**H**) CNO application to slices decreased the oIPSC amplitude in GPe neurons from D2-Cre mice infused with *hM4Di* and *ChR2* viruses in the DMS. Left, Sample traces of oIPSCs at baseline and during CNO application. Scale bars: 40 ms, 30 pA. Right, Time course of oIPSC amplitudes before, during, and after CNO application (6 neurons, 3 mice). $t_{(5)} = 4.01$, $p < 0.01$, paired *t* test. (**I**) Excitation of D1-MSNs by systemic administration of CNO (3 mg/kg) reversibly promoted 1-hr alcohol consumption in D1-Cre mice expressing *hM3Dq*. $F_{(2,13)} = 7.81$, $p < 0.01$. n = 14 mice. (**J**) CNO excitation of D1-MSNs reversibly increased 1-hr alcohol preference in D1-Cre expressing *hM3Dq*. $F_{(2,13)} = 8.45$, $p < 0.01$. n = 14 mice. (**K**) Time-dependency of the CNO-mediated enhancement of alcohol consumption in D1-Cre mice expressing *hM3Dq*. $F_{(2,13)} = 8.05$, $p < 0.01$. n = 14 mice. (**L**) CNO excitation of D1-MSNs reduced water intake in D1-Cre mice expressing *hM3Dq*. $t_{(13)} = 3.19$, $p < 0.01$, paired *t* test. n = 14 mice. (**M**) CNO inhibition of D2-MSNs reversibly increased 1-hr alcohol consumption in D2-Cre mice infused with the *hM4Di* virus. $F_{(2,6)} = 5.87$, $p < 0.05$. n = 7 mice. (**N**) CNO inhibition of D2-MSNs led to a reversible increase in the preference for alcohol in D2-Cre mice with *hM4Di* infusion. $F_{(2,6)} = 5.43$, $p < 0.05$. n = 7 mice. (**O**) Time-dependency of the CNO-mediated enhancement of alcohol consumption in D2-Cre mice with *hM4Di*. $F_{(2,6)} = 4.72$, $p < 0.05$. n = 7 mice**.** (**P**) CNO inhibition of D2-MSNs did not alter 1-hr water intake in D2-Cre mice expressing *hM4Di*. $t_{(6)} = 1.63$, $p > 0.05$, paired *t* test. n = 7 mice**.** Statistical comparisons within experimental groups are indicated by * for $p < 0.05$ and ** for $p < 0.01$, respectively.

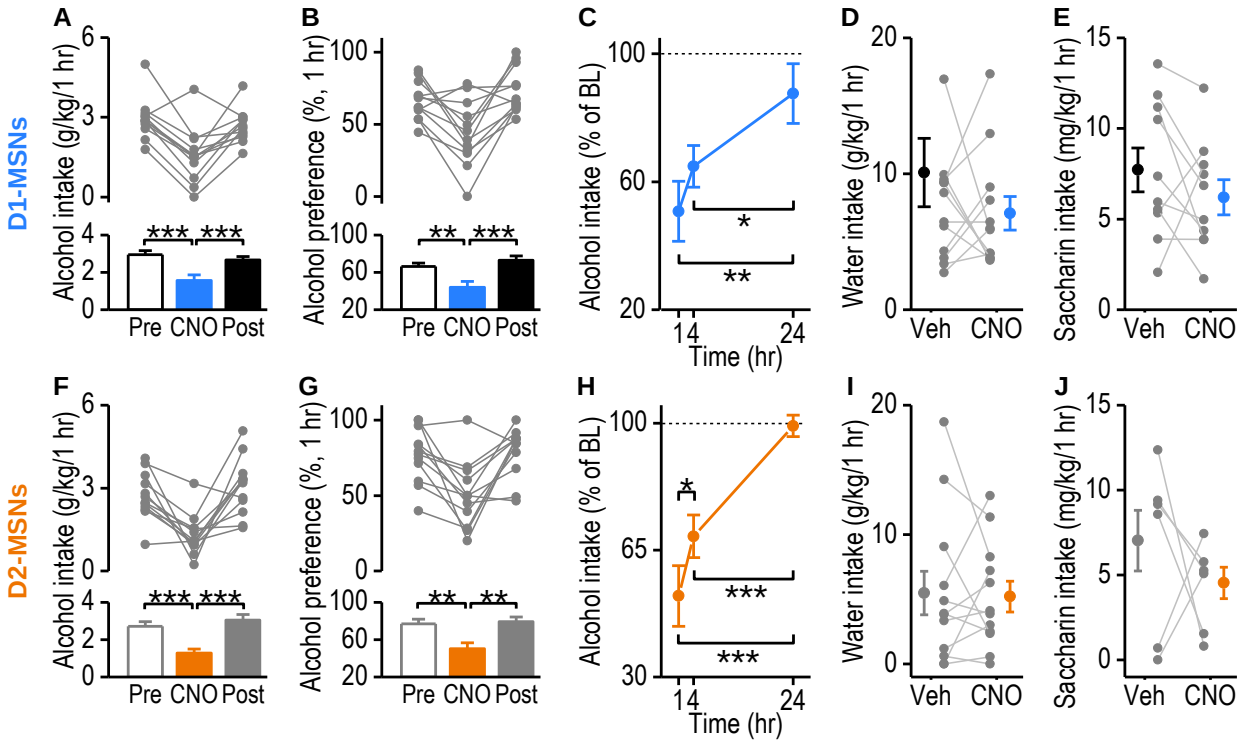

Figure 2.4. *In vivo* chemogenetic inhibition of D1-MSNs in the direct pathway or excitation of D2-MSNs in the indirect pathway reduces excessive alcohol consumption.
(**A**) Inhibition of D1-MSNs by administration of CNO (5 mg/kg) significantly and reversibly reduced 1-hr alcohol consumption in D1-Cre mice expressing *hM4Di*. $F_{(2,11)} = 14.07$, $p < 0.001$. n = 12 mice. (**B**) Inhibition of D1-MSNs by CNO administration reduced 1-hr alcohol preference in D1-Cre mice expressing *hM4Di*. $F_{(2,11)} = 12.68$, $p < 0.001$. n = 12 mice. (**C**) Time-dependent inhibition of alcohol consumption by CNO in D1-Cre mice expressing *hM4Di*. $F_{(2,11)} = 9.00$, $p < 0.01$. n = 12 mice. (**D**,**E**) Administration of CNO did not alter 1-hr water (D) or saccharin (0.033% w/v) (E) intake in D1-Cre mice expressing *hM4Di*. $t_{(11)} = 0.28$, $p > 0.05$ (D); $t_{(9)} = 1.23$, $p > 0.05$ (E), paired *t* test. n = 12 (D) and 10 (E) mice. (**F**) Excitation of D2-MSNs by administration of CNO significantly and reversibly reduced 1-hr alcohol consumption in D2-Cre mice expressing *hM3Dq*. $F_{(2,11)} = 16.33$, $p < 0.001$. n = 12 mice. (**G**) CNO excitation of D2-MSNs reversibly reduced 1-hr alcohol preference in D2-Cre mice expressing *hM3Dq*. $F_{(2,11)} = 9.42$, $p < 0.01$. n = 12 mice. (**H**) Inhibition of alcohol consumption by CNO excitation of D2-MSNs was time-dependent. $F_{(2,11)} = 27.91$, $p < 0.001$. n = 12 mice. (**I**,**J**) CNO excitation of D2-MSNs did not alter 1-hr water (I) or saccharin (J) intake in D2-Cre mice expressing *hM3Dq*. $t_{(11)} = 0.19$, $p > 0.05$ (I); $t_{(5)} = 0.82$, $p > 0.05$ (J), paired *t* test. n = 12 (I) and 6 (J) mice. Statistical comparisons within experimental groups are indicated by * for $p < 0.05$ and ** for $p < 0.01$ and *** for $p < 0.001$, respectively.

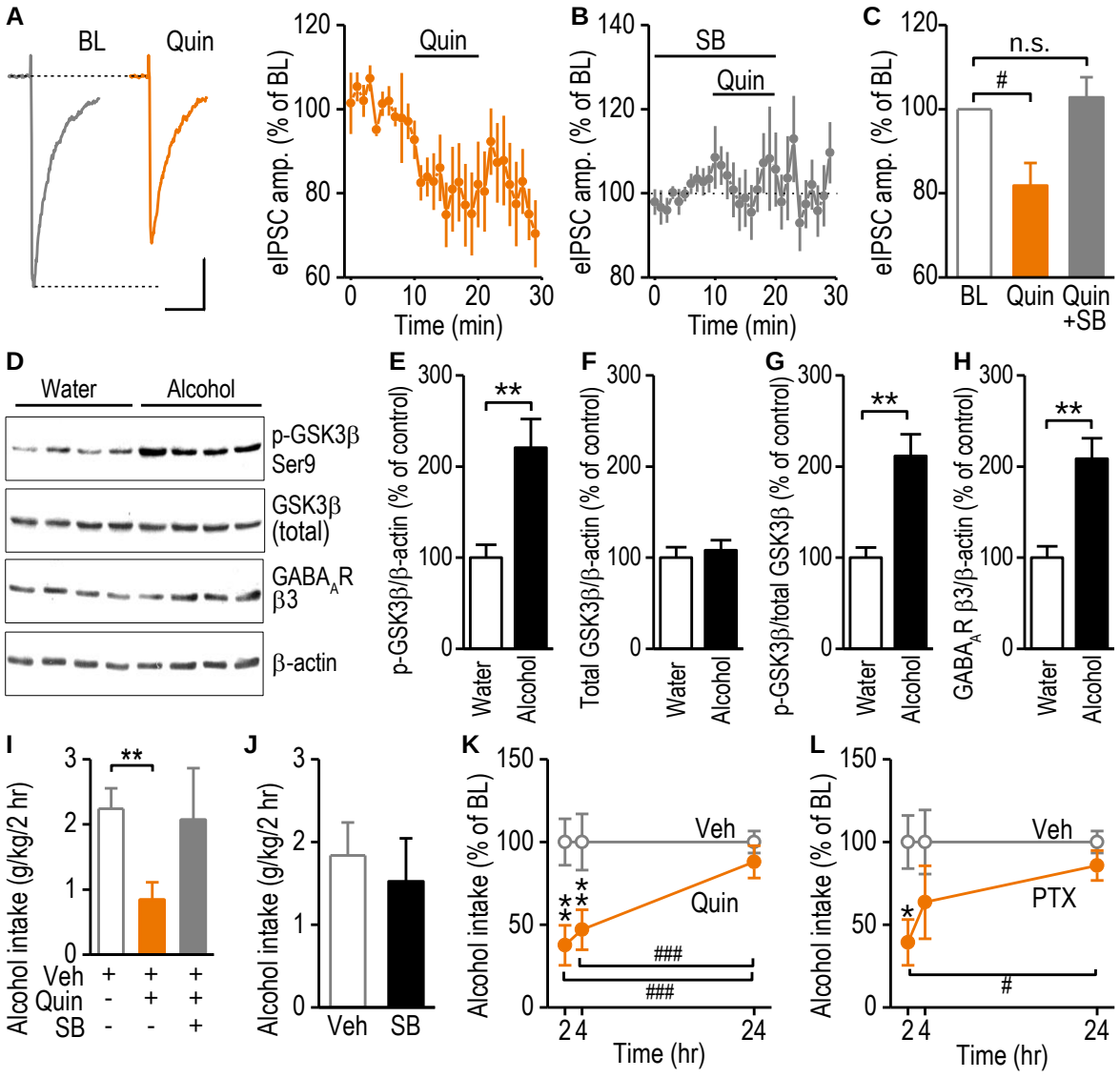

Figure 2.5. D2R signaling *via* GSK3β suppresses GABAergic transmission in D2-MSNs and attenuates excessive alcohol consumption.

(**A**) D2R activation reduced the eIPSC amplitude in D2-MSNs in alcohol-drinking mice. D2-Cre;Ai14 mice were trained to consume high levels of alcohol for 8 weeks, and eIPSCs were recorded in D2-MSNs 24 hr after the last drinking session. The D2R agonist, quinpirole (Quin; 10 μM), was bath-applied for 10 min. Left, Representative traces of eIPSCs at baseline (BL) and during quinpirole application. Scale bars: 100 pA, 100 ms. Right, Time course of eIPSC amplitudes before, during, and after quinpirole application (10 neurons, 8 mice). (**B**) Treatment of DMS slices with a GSK3β antagonist, SB216763 (SB; 10 μM), abolished quinpirole-mediated inhibition of eIPSCs in D2-MSNs. The slices were pre-treated for 25 min with SB216763, which was continuously applied as indicated during the recording period (10 neurons, 5 mice). (**C**) Bar graphs comparing the effects of quinpirole and quinpirole plus SB216763 on eIPSC amplitudes. The amplitudes were averaged from 0-10 min (baseline) and from 15-20 min (drug applications). $t_{(9)} = 2.59$, $p < 0.05$ for quinpirole vs vehicle, paired *t* test. $t_{(9)} = -0.68$, $p > 0.05$ for quinpirole plus SB216763 vs vehicle, paired *t* test. n.s., not significant. (**D**) Representative western-blots images showing the phosphorylation levels of GSK3β, protein levels of GSK3β, GABAAR, and □-actin. (**E-H**) Western blot quantification of the phosphorylation levels of GSK3β (p-GSK3β) (E), total protein levels of GSK3β (F), ratio of p-GSK/total GSK3β (G), and GABAAR (H). $t_{(16)} = -3.36$, $p < 0.01$ (E); $t_{(16)} = -0.52$ (F), $p > 0.05$; $t_{(16)} = -3.89$, $p < 0.01$ (G); $t_{(16)} = -3.93$, $p < 0.01$ (H), unpaired *t* test. n = 8 (Water) and 10 (Alcohol) mice. (**I**) Intra-DMS infusion of quinpirole (6 μg/0.5 μl in DMSO), but not of both quinpirole and SB216763 (40 ng/μl in DMSO), significantly reduced 2-hr alcohol consumption. $t_{(15)} = 3.33$, $p < 0.01$ for quinpirole vs vehicle; $t_{(16)} = 0.20$, $p > 0.05$ for quinpirole plus SB216763 vs vehicle, unpaired *t* test. n = 9 (Veh, DMSO), 8 (Quin), and 9 (Quin + SB) mice. (**J**) Intra-DMS infusion of SB216763 alone did not alter 2-hr alcohol drinking. $t_{(14)} = 0.23$, $p > 0.05$, unpaired *t* test. n = 8 mice per groups. (**K**) The inhibitory effect of quinpirole on alcohol consumption was time-dependent. $F_{(2,15)} = 15.19$, $p < 0.001$, two way RM-ANOVA. n = 9 (Veh) and 8 (Quin) mice. (**L**) Intra-DMS infusion of a GABAA receptor antagonist, picrotoxin (PTX; 1 μg/μl in DMSO) reduced alcohol drinking at 2 and 4 hr, but not at 24 hr. $F_{(2,11)} = 4.81$, $p < 0.05$, two way RM-ANOVA. n = 8 (Veh) and 5 (PTX) mice. Statistical comparisons between Treatment and Control groups are indicated by * for $p < 0.05$ and ** for $p < 0.01$, or comparisons within experimental groups are indicated by # for $p < 0.05$ and ### for $p < 0.001$, respectively.

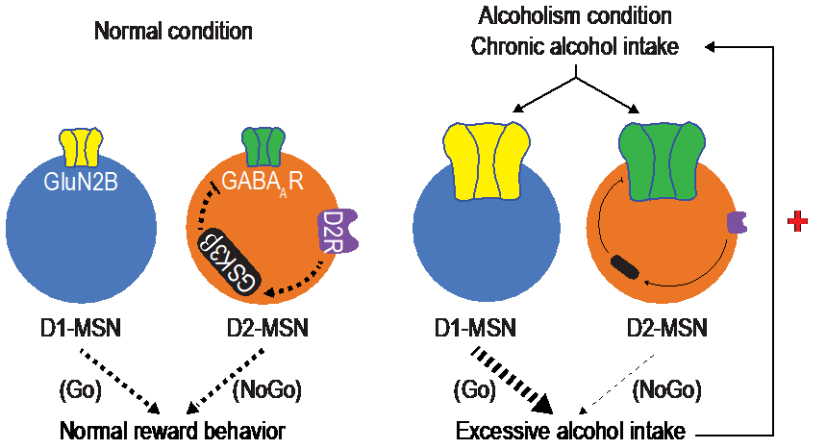

Figure 2.6. Hypothetical model of alcohol-Induced changes in glutamatergic and GABAergic strength in D1- and D2-MSNs of the DMS leading to excessive alcohol consumption.

Left, in the normal brain, D1-MSNs express GluN2B-NMDARs and D2-MSNs contain $GABA_AR$s, as well as D2Rs and GSK3β. D2R activation stimulates GSK3β signaling, which negatively regulates $GABA_AR$ activity. D1-MSN or D2-MSN excitation facilitates selection of "Go" or "NoGo" actions in reward behavior, respectively. Right, in the alcoholism brain, repeated cycles of alcohol intake and withdrawal increase GluN2B-NMDAR activity selectively in D1-MSNs, which facilitates selection of "Go" actions and consequently drives excessive alcohol consumption. Meanwhile, cycles of alcohol intake and withdrawal also enhance synaptic GABAergic activity in D2-MSNs by decreasing D2R-GSK3β signaling. This suppresses selection of "NoGo" actions. Together, the abnormally facilitated "Go" and suppressed "NoGo" actions reinforce excessive alcohol consumption. Note that the changes in activities of receptors, signaling, and behaviors are indicated by alterations of their sizes.

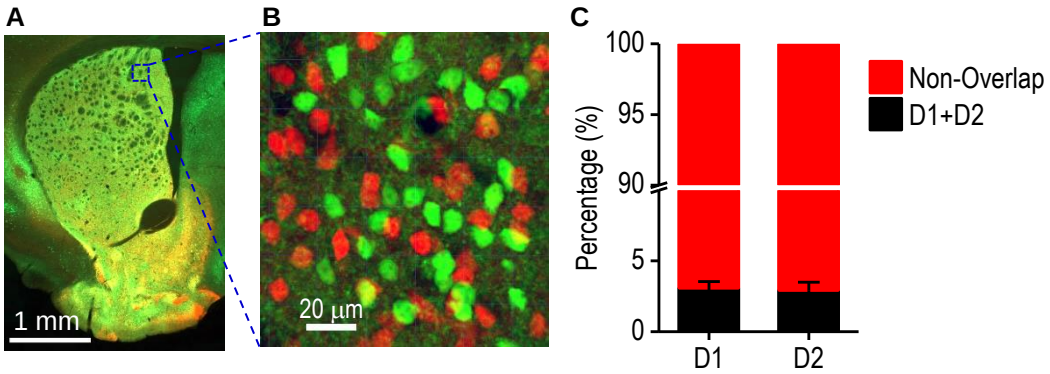

Figure 2.7. (Supplementary Figure 1 in Cheng et al., 2017) Separation of D1- and D2-MSNs in the DMS.

D1-tdTomato, D2-Cre, and Snap25 mice were bred into D1-tdTomato;D2-Cre;Snap25 mice. The Snap25 mice are a Cre reporter line which expresses eGFP in the presence of Cre (Madisen et al., 2015). (**A**) Coronal section from a D1-tdTomato;D2-Cre;Snap25 mouse displaying the tdTomato and eGFP fluorescence in the striatum. (**B**) Sample confocal image showing separation of D1-MSNs (red) and D2-MSNs (green) in the DMS (indicated box in A). (**C**) Bar graphs depicting percentage of overlap of D1- and D2-MSNs. n = 16 sections from 3 mice. Total 2947 D1-MSNs and 3050 D2R-MSNs were count; 96 neurons exhibit both green and red colors.

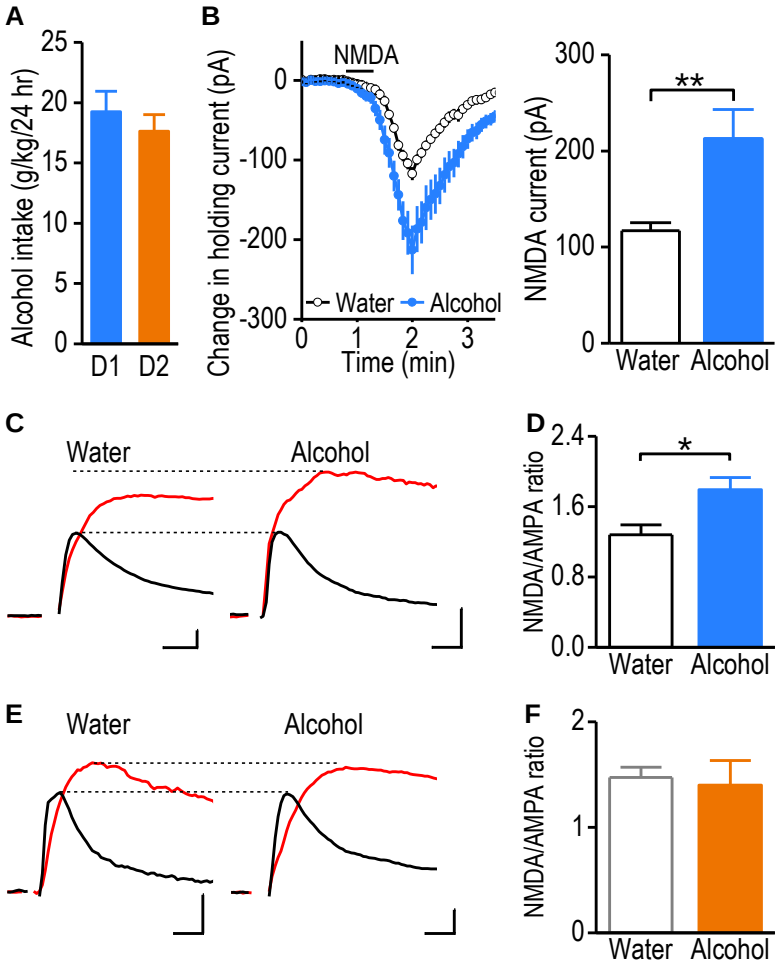

Figure 2.8. (Supplementary Figure 2 in Cheng et al., 2017) Selective enhancement of NMDAR activity in DMS D1-, but not D2-MSNs after repeated cycles of excessive alcohol intake and withdrawal.

(**A**) Identical alcohol-drinking levels of D1- and D2-labeling transgenic mice included in Figure 2.1. $p > 0.05$, unpaired *t* test. n = 8 (D1) and 7 (D2) mice. (**B**) Cycles of excessive alcohol consumption and withdrawal significantly increased NMDA-induced currents in D1-MSNs. D1-Cre;Ai14 mice were treated and D1-MSNs were recorded as in Figure 2.1C except that a different concentration of NMDA was used. Left, Changes in holding currents were measured after NMDA (15 μM) was applied to the slices. Right, bar graphs summarizing the peak amplitudes of NMDA currents in both water and alcohol groups. $^{**}p < 0.01$, unpaired *t* test. n = 17 neurons from 4 mice per group. (**C**) Sample traces of AMPAR-mediated (black) and NMDAR-mediated (red) EPSCs in D1-MSNs from the alcohol and water groups. (**D**) Bar graphs showing the NMDA/AMPA ratio was increased in the alcohol group (11 neurons, 7 mice) when compared to the water control (10 neurons, 7 mice). $^{*}p < 0.05$, unpaired *t* test. (**E**) Sample traces of AMPAR-mediated (black) and NMDAR-mediated (red) EPSCs in D2-MSNs from the alchol and water groups. (**F**) Bar graphs showing the NMDA/AMPA ratio did not differ between the alcohol (8 neurons, 6 mice) and water (9 neurons, 8 mice) groups. Scale bars (C and E): 50 pA, 10 ms.

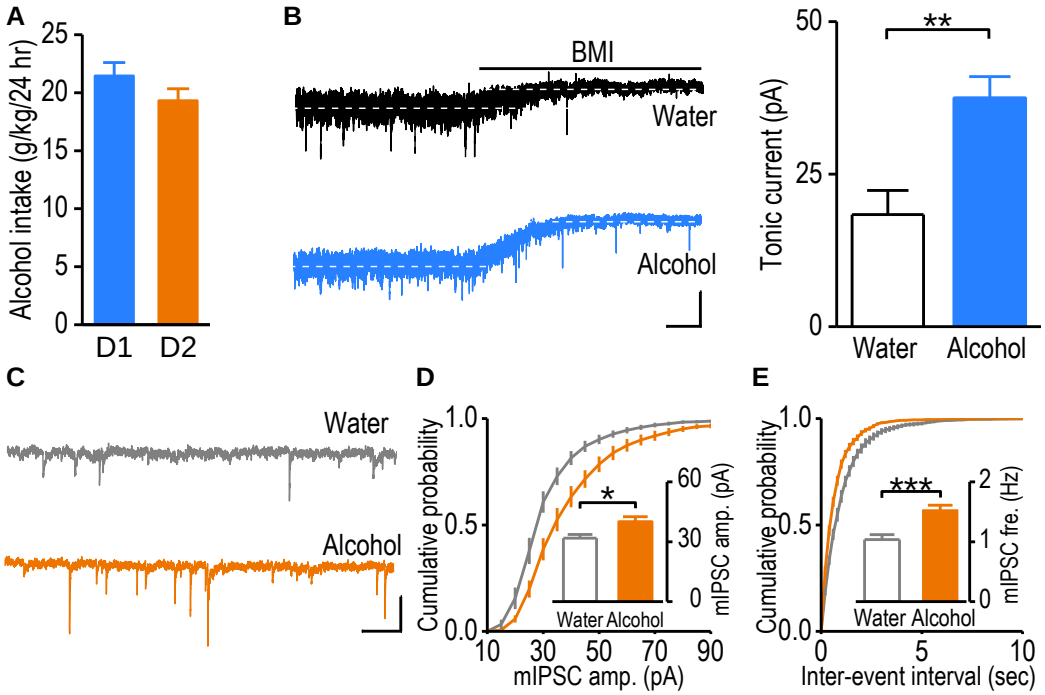

Figure 2.9. (Supplementary Figure 3 in Cheng et al., 2017) Enhancement of GABAergic activity in DMS neurons by repeated cycles of alcohol intake and withdrawal.
(**A**) Identical alcohol-drinking levels of D1- and D2-labeling transgenic mice included in Figure 2.2. $p > 0.05$ by unpaired *t* test. n = 6 (D1) and 5 (D2) mice. (**B**) Repeated cycles of excessive alcohol consumption and withdrawal significantly increased tonic GABA currents in DMS D1-MSNs. D1-Cre; Ai14 mice were treated and D1-MSNs were recorded as in Figure 2.2A. Slices were continuously perfused with GABA (5 μM) and followed by application of the $GABA_AR$ blocker, bicuculline methiodide (BMI, 25 μM) to obtain tonic GABA currents. Representative traces of tonic GABA currents in D1-MSNs from alcohol and water groups (left). The amplitudes of the tonic GABA currents observed in both groups (14 neurons from the alcohol group and 12 neurons from the water group, 4 mice per group) were summarized (right). $^{**}p < 0.01$, unpaired *t* test. Scale bar: 30 pA, 5 sec. (**C**-**E**) Repeated cycles of excessive alcohol drinking and withdrawal increased the mIPSC amplitudes and frequencies in non-fluorescent, putative D2-MSNs of the DMS from D1-Cre;Ai14 mice. Representative mIPSC traces (C) and cumulative probability plots showing the distributions of mIPSC amplitudes (D) and inter-event intervals (E) in putative D2-MSNs from alcohol-drinking mice (15 neurons, 4 mice) and water controls (16 neurons, 4 mice). Inset, bar graphs present the mean mIPSC amplitudes (D) and frequencies (E). Scale bar: 30 pA, 0.5 sec (C). $^{*}p < 0.05$, $^{***}p < 0.001$, unpaired *t* test.

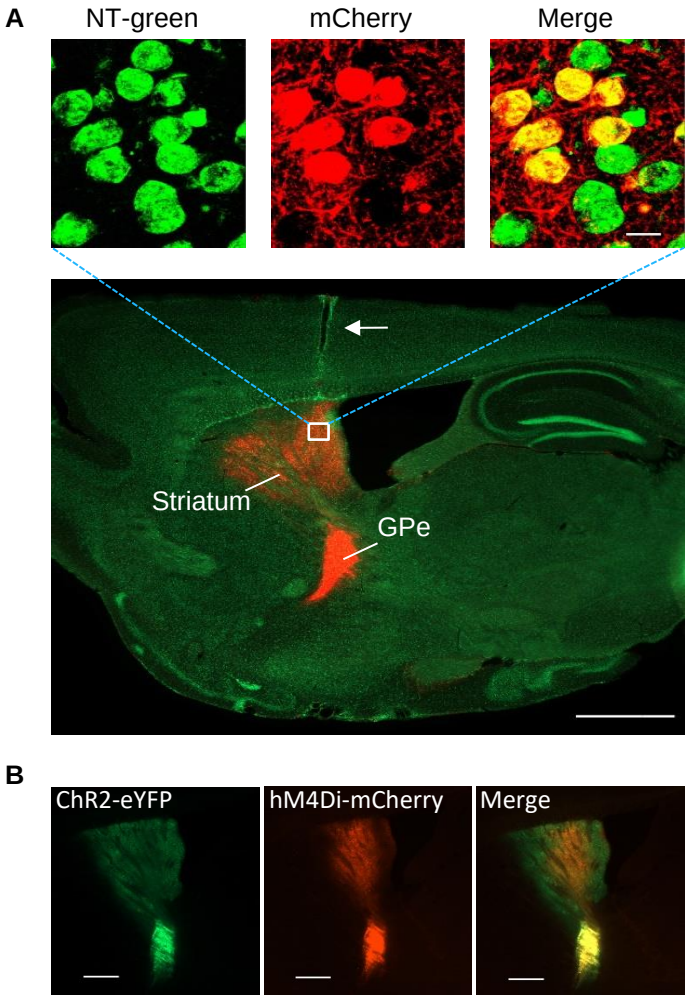

Figure 2.10. (Supplementary Figure 4 in Cheng et al., 2017) Verification of selective hM4Di and ChR2 expression in DMS D2-MSNs.
(**A**) AAV-DIO-hM4Di-mCherry was infused into the DMS of a D2-Cre mouse. hM4Di-expressing D2-MSNs projected to the GPe (bottom). Scale bar: 1 mm. The arrowhead indicates the injection track. The upper panels show micrographs of 12 striatal neurons from the indicated box (bottom), stained with NT-green (left). Six of these expressed mCherry (middle) and were yellow in the merged image (right). Scale bar: 10 µm. (**B**) Representative sagittal view of mCherry and eYFP fluorescence in a brain slice from a D2-Cre mouse infused with the viral cocktail expressing ChR2-eYFP and hM4Di-mCherry. Scale bar, 0.2 mm.

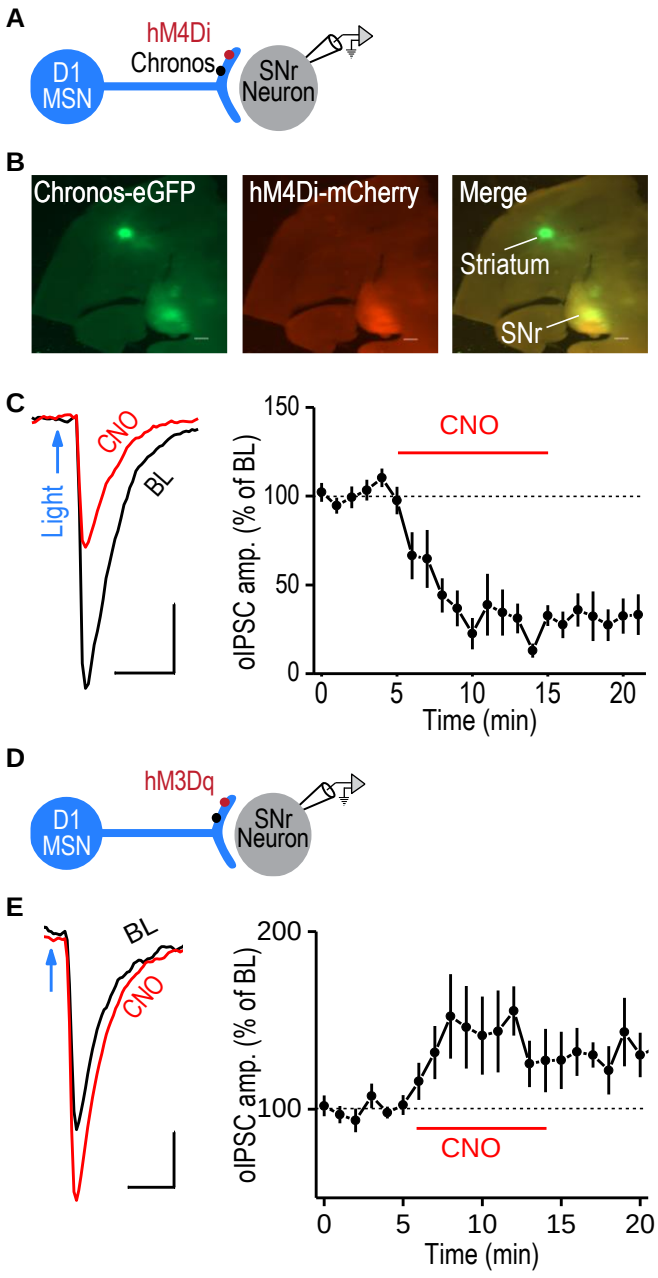

Figure 2.11. (Supplementary Figure 5 in Cheng et al., 2017) *Ex vivo* electrophysiology validation of DREADDs of D1-MSN-mediated synaptic transmission in SNr neurons.

(**A**) Schematic diagram of *ex vivo* electrophysiology validation. A cocktail of AAV-DIO-hM4Di-mCherry and AAV-Chronos-eGFP vectors was infused into the DMS of D1-Cre mice, and Chronos-mediated striatonigral oIPSCs were recorded in SNr neurons. (**B**) Representative low-magnification horizontal view of mCherry and eGFP fluorescence in a brain slice from a D1-Cre mouse infused with the viral cocktail. Scale bar, 0.2 mm. (**C**) CNO application to slices decreased the oIPSC amplitude in SNr neurons from D1-Cre mice infused with hM4Di and Chronos viruses in the DMS. Left, Sample traces of oIPSCs at baseline (BL) and during CNO application. Scale bars: 20 ms, 100 pA. Right, Time course of oIPSC amplitudes before, during, and after CNO application (5 neurons, 3 mice). (**D**) Schematic diagram of *ex vivo* electrophysiology validation of hM3Dq, as described for **A**. (**E**) Bath application of CNO increased the amplitude of Chronos-mediated oIPSCs in SNr neurons from D1-Cre mice infused with hM3Dq and Chronos viruses in the DMS. Left, Sample traces of oIPSCs at baseline (BL) and during CNO application. Scale bar: 20 ms, 200 pA. Right, Time course of oIPSCs before, during and after CNO application (7 neurons, 4 mice).

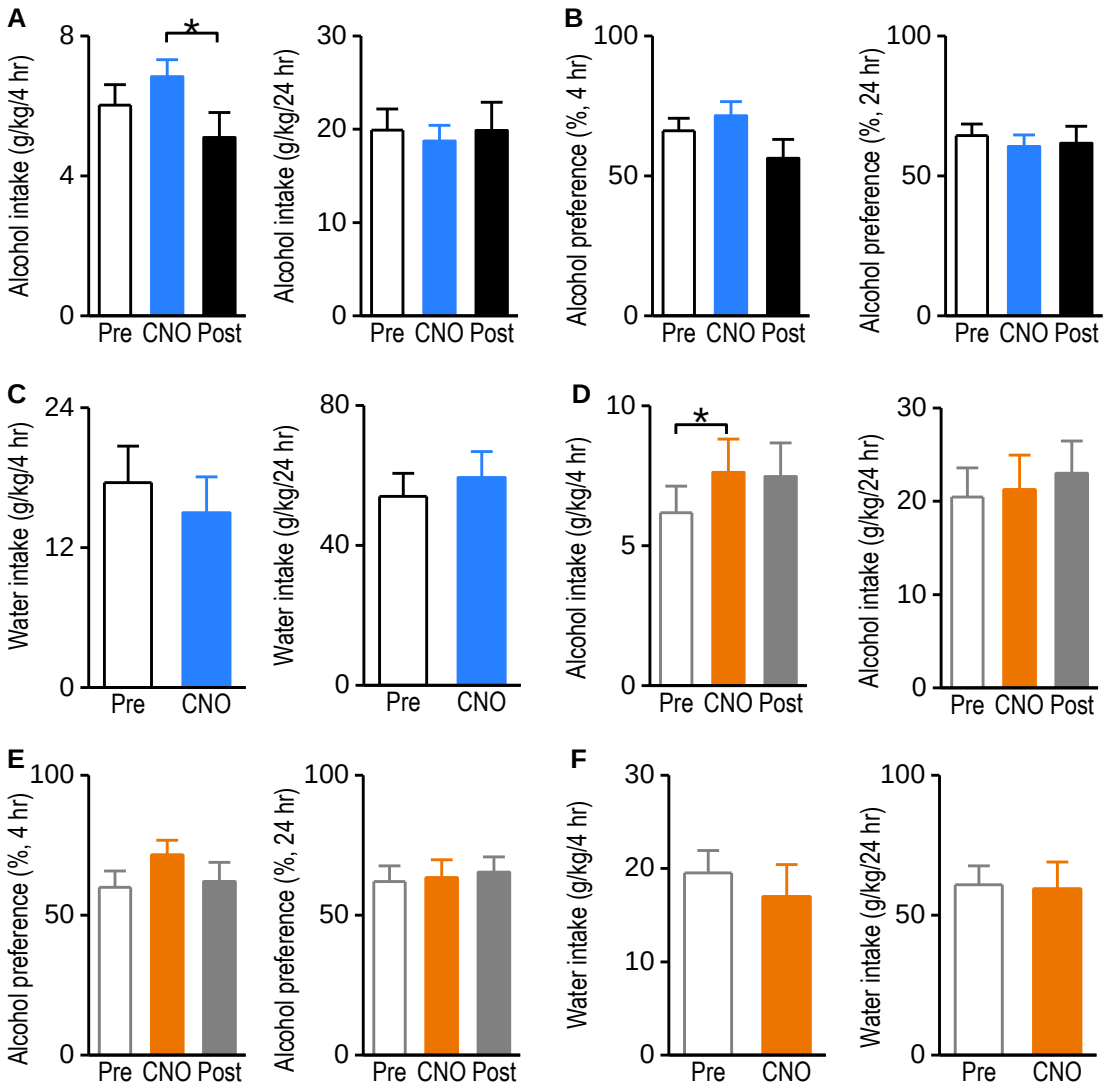

Figure 2.12. (Supplementary Figure 6 in Cheng et al., 2017) Effect of *in vivo* chemogenetic excitation of D1-MSNs or inhibition of D2-MSNs of the DMS on alcohol and water consumption at 4 and 24 hr. A Cre-inducible *hM3Dq* virus was infused into the DMS of D1-Cre mice and a Cre-inducible *hM4Di* virus was infused into the DMS of D2-Cre mice. (**A**) CNO administration (3 mg/kg) did not alter 4-hr (left) or 24-hr (right) alcohol intake in D1-Cre mice expressing *hM3Dq*. The 4-hr alcohol intake was reduced during post-CNO, as compared to during CNO. *$p < 0.05$. (**B**) CNO injection did not change 4-hr (left) or 24-hr (right) alcohol preference in D1-Cre mice expressing *hM3Dq*. (**C**) Administration of CNO did not change 4-hr (left) or 24-hr (right) water intake in D1-Cre mice expressing *hM3Dq*. (**D**) Systemic administration of CNO significantly increased in 4-ht (left) but not 24-hr (right) alcohol intake in D2-Cre mice expressing *hM4Di*. *$p < 0.05$. (**E**) CNO administration did not increase alcohol preference at 4-hr or 24-hr (right) in D2-Cre mice expressing *hM4Di*. (**F**) CNO injection did not alter 4-hr (left) or 24-hr (right) water intake in D2-Cre mice expressing *hM4Di*. n = 14 (A-C) and 7 (D-F) mice.

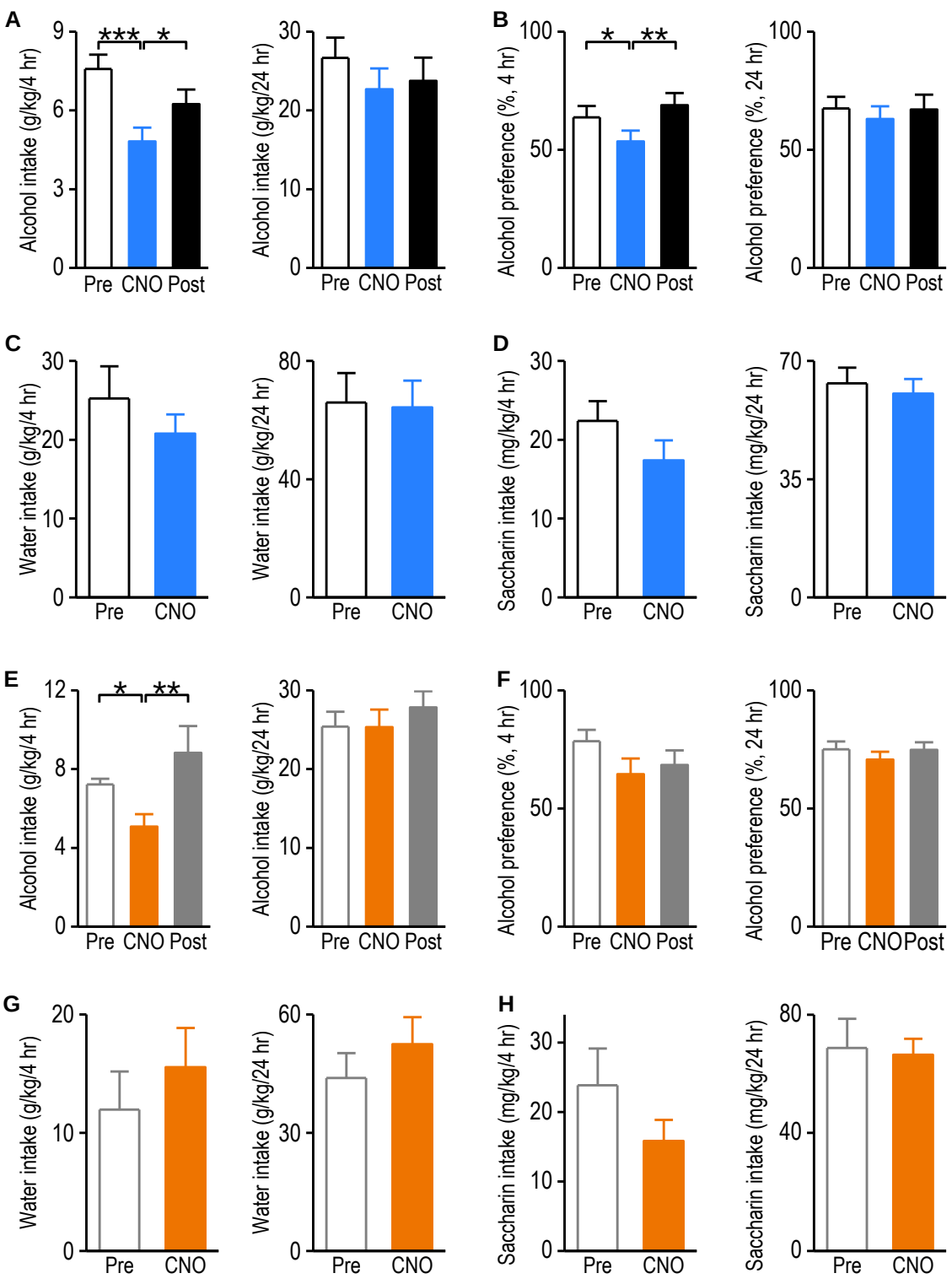

Figure 2.13. (Supplementary Figure 7 in Cheng et al., 2017) Effect of *in vivo* chemogenetic inhibition of D1-MSNs. (**A**-**D**) and excitation of D2-MSNs in the DMS on alcohol, water, and saccharin consumption (**E**-**H**). The cre-inducible hM4Di and hM3Dq viruses were infused into the DMS of D1-Cre and D2-Cre mice, respectively. (**A**,**B**) Systemic administration of CNO (5 mg/kg) reduced 4-hr (left), but not 24-hr (right) alcohol intake (A) and alcohol preference (**B**) in D1-Cre mice expressing *hM4Di*. *$p <$ 0.05, **$p < 0.01$, ***$p < 0.001$. (**C**,**D**) Systemic administration of CNO (5 mg/kg) did not change 4-hr (left) or 24-hr (right) water (**C**) or saccharin (**D**) intake in D1-Cre mice expressing *hM4Di*. (**E**) Systemic administration of CNO reduced 4-hr (left) but not 24-hr (right) alcohol intake in D2-Cre mice with *hM3Dq*. *$p < 0.05$, **$p < 0.01$. (**F**) CNO administration did not change 4-hr (left) or 24-hr (right) alcohol preference in D2-Cre mice expressing *hM3Dq*. (**G**,**H**) Systemic administration of CNO did not alter 4-hr (left) or 24-hr (right) water (**G**) and saccharin (**H**) intake in D2-Cre mice expressing *hM3Dq*. n = 12 (**A**-**D**) and 12 (**E**-**H**) mice.

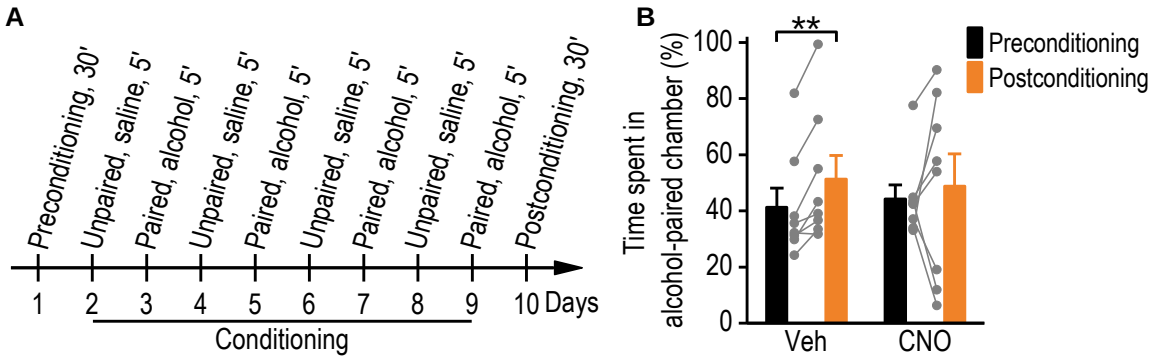

Figure 2.14. (Supplementary Figure 8 in Cheng et al., 2017) Chemogenetic excitation of DMS D2-MSNs prevented expression of alcohol-conditioned place preference.
(**A**) Diagram showing the schedule of the alcohol-conditioned place preference experiment. Two groups of D2-Cre mice were infused with AAV-hM3Dq in their DMS and then administered 20% alcohol (2 g/kg) and saline in paired and unpaired sessions, respectively. The experimental group received a CNO (1 mg/kg) injection and the control group received a vehicle injection 30 min before the postconditioning test. (**B**) CNO administration prevented the expression of alcohol-conditioned place preference. Alcohol-conditioned place preference was expressed as the ratio ± S.E.M. of the time spent in the alcohol-paired compartment divided by the time spent in all compartments. $^{**}p < 0.01$, paired *t* test. n = 8 mice per groups.

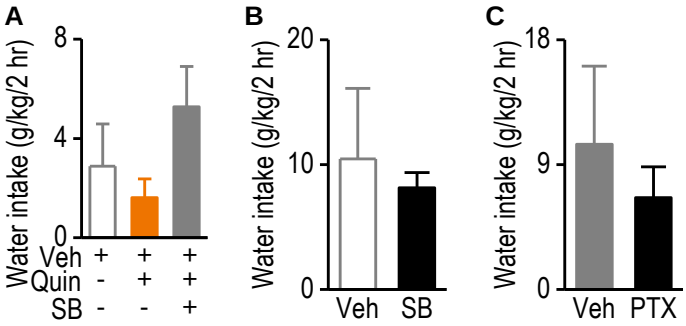

Figure 2.15. (Supplementary Figure 9 in Cheng et al., 2017) Manipulation of DMS D2R signaling *via* GSK3β did not change water intake.

(**A**) Intra-DMS infusion of vehicle (DMSO), quinpirole (6 µg/0.5 µl in DMSO), or a cocktail of quinpirole and SB216763 (40 ng/µl in DMSO) did not change 2-hr water consumption. Unpaired *t* test. n = 9 (Veh), 7 (Quin), and 9 (Quin + SB) mice. (**B**) Intra-DMS infusion of SB216763 alone did not alter 2-hr water drinking. Unpaired *t* test. n = 8 mice per groups. (**C**) Intra-DMS infusion of the $GABA_AR$ antagonist, picrotoxin (PTX, 1 µg/µl in DMSO) did not alter water drinking at 2 hr. Unpaired *t* test. n = 8 (Veh) and 5 (PTX) mice.

CHAPTER III

BIDIRECTIONAL AND LONG-LASTING CONTROL OF ALCOHOL-SEEKING BEHAVIOR BY CORTICOSTRIATAL LTP AND LTD[*]

3.1 Overview

Addiction is proposed to arise from alterations in synaptic strength via mechanisms of long-term potentiation (LTP) and depression (LTD). However, the causality between these synaptic processes and addictive behaviors is difficult to demonstrate. Here we report that LTP/LTD induction altered operant alcohol self-administration, a motivated drug-seeking behavior. We first induced LTP by pairing presynaptic glutamatergic stimulation with optogenetic postsynaptic depolarization in the dorsomedial striatum, a brain region known to control goal-directed behavior. Blockade of this LTP by NMDA receptor inhibition unmasked an endocannabinoid-dependent LTD. *In vivo* application of the LTP-inducing protocol caused a long-lasting increase in alcohol-seeking behavior, while the LTD protocol decreased this behavior. We further identified that optogenetic LTP/LTD induction at cortical inputs onto striatal dopamine D1 receptor-expressing neurons controlled these behavioral changes. Our results demonstrate a causal link between synaptic plasticity and alcohol-seeking behavior, and that modulation of this plasticity may inspire a therapeutic strategy for addiction.

3.2 Introduction

Drug addiction is a mental illness that is viewed as a transition from recreational use to compulsive drug-seeking and -taking (Koob and Volkow, 2010; Volkow and Morales, 2015;

[*] This chapter is re-printed with permission from "Bidirectional and long-lasting control of alcohol-seeking behavior by corticostriatal LTP and LTD" by Ma T, Cheng Y, Roltsch Hellard E, Wang X, Lu J, Gao X, Huang CCY, Wei XY, Ji JY, Wang J, 2018. *Nature Neuroscience*, 21, 373. Copyright [2018] by Springer Nature.

Everitt and Robbins, 2016). This behavioral transition is proposed to be controlled by "drug-evoked plasticity" (Koob and Volkow, 2010; Luscher and Malenka, 2011; Volkow and Morales, 2015; Everitt and Robbins, 2016). However, exactly how synaptic plasticity controls the adaptive changes in drug-seeking behavior remains unclear. The dorsomedial striatum (DMS), a brain region crucially involved in drug and alcohol addiction, receives glutamatergic inputs from several brain areas (Yin and Knowlton, 2006; Balleine and O'Doherty, 2010; Lovinger, 2010; Everitt and Robbins, 2016). In these neural circuits, the medial prefrontal cortex (mPFC) afferent into the DMS is essential for the control of goal-directed behaviors (Yin and Knowlton, 2006; Balleine and O'Doherty, 2010; Lovinger, 2010; Everitt and Robbins, 2016), and this connection is linked to drug or alcohol addiction (Yin and Knowlton, 2006; Everitt and Robbins, 2016; Ma et al., 2017). For example, exposure to drugs of abuse or alcohol potentiates AMPA receptor (AMPAR)- and NMDA receptor (NMDAR)-mediated glutamatergic transmission in the DMS (Wang et al., 2010; Wang et al., 2012; Corbit et al., 2014; Ma et al., 2017), while pharmacological inhibition of striatal glutamatergic transmission transiently suppresses operant alcohol self-administration and cocaine relapse (Wang et al., 2010; Wang et al., 2012; Ma et al., 2014; Pascoli et al., 2014). Although these studies indicate that drugs and alcohol evoke corticostriatal plasticity, which may, in turn, contribute to drug-seeking and -taking behaviors, there has been no direct demonstration that synaptic plasticity drives addictive behaviors.

The DMS contains two types of medium spiny neurons (MSNs): D1-MSNs express dopamine D1 receptors (D1Rs) and D2-MSNs contain D2Rs (Gerfen and Surmeier, 2011). Both neuronal types receive mPFC inputs(Pascoli et al., 2014). While synaptic plasticity, including long-term potentiation (LTP) and depression (LTD), was observed in both D1- and D2-MSNs (Shen et al., 2008), drug- or alcohol-induced plasticity was found predominantly in striatal D1-

MSNs (MacAskill et al., 2014; Pascoli et al., 2014; Cheng et al., 2017). Mimicking alcohol-evoked plasticity by inducing LTP, or reversing this plasticity by inducing LTD, will provide a new understanding of how this plasticity controls alcohol-seeking behavior. LTP/LTD induction at specific neuronal circuits requires simultaneous control of both pre- and post-synaptic neurons, which can be achieved using a recently developed dual-channel optogenetic technique (Fenno et al., 2011; Klapoetke et al., 2014).

In this study, we paired optogenetic postsynaptic depolarization (oPSD) with presynaptic glutamatergic stimulation; this greatly enhanced NMDAR-mediated transmission and induced a reliable NMDAR-dependent LTP, as well as an endocannabinoid (eCB)-dependent LTD. Importantly, *in vivo* optogenetic delivery of the LTP protocol to the corticostriatal synapses within the DMS produced a long-lasting increase in operant self-administration of alcohol. Conversely, delivery of the LTD protocol led to a long-lasting decrease in this behavior. Furthermore, we discovered that the *in vivo* LTP and LTD protocols preferentially induced plasticity in D1-MSNs and that selective induction of LTP/LTD in this neuronal type produced the corresponding changes in alcohol-seeking behavior. These findings demonstrate a causal link between DMS corticostriatal synaptic plasticity and alcohol-seeking behavior and indicate that the reversal of drug-evoked synaptic plasticity may provide a novel therapeutic strategy for the treatment of alcohol use disorder.

3.3 Results

3.3.1. oPSD facilitates induction of NMDAR-dependent LTP and eCB-LTD in the DMS

In dorsostriatal slices, LTD is the easiest form of synaptic plasticity to observe, while LTP is more difficult to detect (Surmeier et al., 2009; Lovinger, 2010). A D2R antagonist was thus included in the recording solution in order to prevent LTD (Shen et al., 2008) and favor the

induction of LTP. Field excitatory postsynaptic potentials/population spikes (fEPSP/PS) were evoked by electrical stimulation within the DMS (Figure 3.1A), but these were not potentiated by electrical high-frequency stimulation (eHFS) (Figure 3.1B and Supplementary Figure 1A**)**. This observation is consistent with previous reports (Kreitzer and Malenka, 2007; Lovinger, 2010). Previous studies also suggested that sufficient postsynaptic depolarization was necessary for reliable LTP induction (Surmeier et al., 2009). Therefore, we examined whether postsynaptic depolarization by somatic current injection (iPSD) facilitated LTP induction. Using whole-cell recording, we discovered that paired eHFS and iPSD produced little LTP (Supplementary Figure 1B). This is consistent with the notion that current injection-elicited action potentials do not back-propagate to the distal dendrites of striatal neurons (Surmeier et al., 2009); insufficient depolarization of this region means that no LTP is generated. In contrast, optogenetics can be used to depolarize any process of postsynaptic neurons, with no limitation of their distance to the soma, and in a non-invasive manner (Mattis et al., 2012). We observed that optogenetic postsynaptic depolarization (oPSD) induced a higher distal dendritic calcium transient than iPSD (Supplementary Figure 2), suggesting that oPSD produced more effective depolarization of this region.

Next, we assessed whether oPSD facilitates LTP induction. An adeno-associated virus (AAV) expressing a channelrhodopsin, C1V1 (Yizhar et al., 2011), was infused into the DMS, resulting in C1V1 expression in the soma and distal dendrites (Figure 3.1C). We found that pairing of eHFS with oPSD of DMS neurons induced a robust and reliable LTP, whereas oPSD alone did not (Figure 3.1D). Furthermore, paired presynaptic stimulation and oPSD enhanced synaptic NMDAR activity and consequently Ca^{2+} influx through this channel (Supplementary Figure 3). LTP was blocked by bath application of an NMDAR antagonist, APV (Figure 3.1E). In

addition, it was reported that dorsostriatal LTP induction also depended on D1R activation (Shen et al., 2008; Lovinger, 2010). We found that optogenetic LTP was inhibited by a D1R antagonist, SCH 23390, and was facilitated by D1R activation (Supplementary Figure 4). Collectively, these results suggest that paired presynaptic stimulation and oPSD produced effective distal dendrite depolarization and induced robust NMDAR-dependent LTP that is strongly regulated by D1R signaling.

Surprisingly, after blockade of optogenetic LTP by APV, LTD was observed (Figure 3.1E). This LTD was completely abolished by bath application of an eCB CB1 receptor (CB1R) antagonist, AM251 (Figure 3.1F). This was consistent with previous reports indicating that LTD in the dorsal striatum was mediated by the CB1R (Gerdeman et al., 2002; Mathur and Lovinger, 2012). Since this eCB-LTD only emerged after LTP was blocked, we reasoned that LTP and LTD were induced simultaneously, and that LTD was masked by LTP. To assess this possibility, we bath-applied AM251 throughout the recording period; this produced a significantly greater magnitude of LTP, as compared with that recorded in the absence of AM251 (Figure 3.1G). Collectively, these results suggest that both NMDAR-dependent LTP and eCB-LTD were induced simultaneously and that the LTP masked the LTD.

3.3.2. oPSD facilitates corticostriatal LTP in the DMS

Corticostriatal plasticity is critical for drug-seeking behaviors (Yin and Knowlton, 2006; Balleine and O'Doherty, 2010; Lovinger, 2010; Everitt and Robbins, 2016). We, therefore, examined whether oPSD facilitated LTP induction at specific corticostriatal afferents in the DMS. We expressed two channelrhodopsins simultaneously in order to selective stimulation of cortical inputs and oPSD of DMS neurons: Chronos (Klapoetke et al., 2014) was expressed in the mPFC and Chrimson (Klapoetke et al., 2014) was expressed in the DMS (Figure 3.2A,B).

Chronos-expressing mPFC neurons and their projections to the DMS were able to follow high-frequency (up to 50 Hz) light stimulation (Supplementary Figure 5). We thus used light stimulation of 50 Hz for 2 sec (oHFS), paired with oPSD of DMS neurons, to induce LTP. While oHFS of corticostriatal fibers or oPSD alone caused little potentiation (Figure 3.2C,D), a robust LTP was observed following paired oHFS and oPSD (Figure 3.2C). This corticostriatal LTP was abolished by APV or MK801, as expected (Figure 3.2E and Supplementary Figure 6A). Surprisingly, no LTD was observed after LTP was blocked (Figure 3.2E and Supplementary Figure 6B); this contrasted with the results produced by pairing eHFS and oPSD (Figure 2.1E). However, whole-cell recording detected a robust LTD in specific D1-MSNs (Supplementary Figure 6C). This was consistent with a recent report showing that selective optogenetic stimulation of cortical inputs induced LTD only in D1-MSNs (Wu et al., 2015). Collectively, these data suggest that paired oHFS and oPSD induces corticostriatal LTP, as well as LTD in D1-MSNs.

LTP stimulation has been demonstrated to induce expression of immediate early genes, contributing to drug addiction(Girault et al., 2007; Minatohara et al., 2015). We analyzed DMS slices and found that paired oHFS and oPSD, but not oHFS or oPSD alone, significantly increased mRNA levels of *Npas4 (neuronal PAS domain protein 4)* gene, which encodes the Npase4 protein (Figure 3.2F). This immediate early gene is associated with synaptic plasticity and positive valence experience (Sun and Lin, 2016; Ye et al., 2016).

3.3.3. *In vivo* optogenetic induction of corticostriatal LTP in the DMS produces a long-lasting increase in operant alcohol self-administration in rats

Our *ex vivo* findings revealed that paired oHFS and oPSD elicited LTP in the DMS. We thus asked whether *in vivo* delivery of this LTP-inducing protocol (oHFS+oPSD) altered alcohol-

seeking behavior. To test this possibility, rats were trained to self-administer alcohol in operant chambers. Chronos and Chrimson were expressed as described above, and optical fibers were implanted into the DMS (Figure 3.3A). We found that *in vivo* delivery of this optogenetic protocol produced significant increases in active lever presses, alcohol deliveries, and alcohol intake at 30 min, 2 days, and 4 days (Figure 3.3B and Supplementary Figure 7A). This increased alcohol intake resulted in elevated blood alcohol concentrations (Supplementary Figure 7B,C). In contrast, oHFS or oPSD alone did not alter alcohol-seeking behavior (Supplementary Figure 7D,E). Together, these data suggest that *in vivo* delivery of this LTP-inducing protocol is sufficient to cause long-lasting enhancement of alcohol-seeking behavior. However, systemic administration of antagonists of NMDARs (MK801) or D1Rs (SCH 23390) blocked this effect of the LTP-inducing protocol on alcohol-seeking behavior (Supplementary Figure 7F,G). Note that administration of SCH 23390 alone did not affect this behavior (Supplementary Figure 7H). These results suggest that both NMDARs and D1Rs are required for the enhancement of alcohol-seeking behavior by *in vivo* LTP induction.

Next, we asked whether the LTP-inducing protocol specifically enhanced alcohol-seeking behavior. Another cohort of rats was trained to self-administer sucrose prior to receiving the same LTP-inducing protocol as the alcohol group. We found that the LTP protocol did not alter the active lever presses, sucrose deliveries, or sucrose intake (Figure 3.3C and Supplementary Figure 7I). We then asked why the same LTP-inducing protocol specifically promoted alcohol-seeking, but not sucrose-seeking, in rats. On day 2 post-LTP induction, both AMPAR-mediated excitatory postsynaptic currents (EPSCs) and the AMPAR/NMDAR ratio were increased in the alcohol group (Figure 3.3D,E), but not in the sucrose group (Figure 3.3F,G). Interestingly, prior to *in vivo* LTP induction, operant alcohol or sucrose self-administration had increased the

AMPAR/NMDAR ratio, as compared with the water group without operant training (Supplementary Figure 8A). The increase was slightly lower in the alcohol-treated rats than in the sucrose controls, but the difference was not statistically significant (Q = 2.86, $P = 0.051$, SNK test). These data suggest that while operant-training produced plasticity in alcohol and sucrose groups, *in vivo* delivery of the LTP-inducing protocol caused further long-lasting synaptic potentiation selectively in the alcohol group. This difference may reflect the distinct effects of alcohol and sucrose on NMDAR activity (Rosenmund and Stevens, 1996; Wang et al., 2007; Kash et al., 2009; Lovinger, 2010). To investigate this, we measured NMDAR activity in the DMS of rats that self-administered alcohol or sucrose. We found that the amplitude of NMDAR-mediated EPSCs was significantly higher in the alcohol group than in the sucrose group (Supplementary Figure 8B,C). Furthermore, LTP was induced in DMS slices from the alcohol-treated rats, but not in those from the sucrose-drinking animals (Supplementary Figure 8D), suggesting that alcohol-mediated facilitation of NMDAR activity(McCool, 2011; Lovinger and Kash, 2015) promotes subsequent *ex vivo* and *in vivo* induction of LTP. In addition, the rectification index of AMPAR-EPSCs was significantly enhanced following *in vivo* LTP induction (Supplementary Figure 9), suggesting that this plasticity is mediated by an increase in calcium-permeable AMPARs.

Collectively, these results suggest that induction of corticostriatal LTP in the DMS produces a long-lasting and specific increase in operant alcohol self-administration in rats.

3.3.4. *In vivo* optogenetic delivery of an LTD-inducing protocol in the DMS produces a long-lasting decrease in alcohol-seeking behavior in rats

Having observed the link between LTP and alcohol-seeking behavior, we reasoned that reversal of alcohol-induced potentiation of corticostriatal inputs by LTD should reduce alcohol-

seeking behavior. To induce LTD *in vivo*, we systemically administered a cocktail of MK801 and a D2R antagonist, raclopride, 30 min before delivering oHFS and oPSD (Figure 3.4A). We used these two categories of antagonists because they were employed in the *ex vivo* LTD experiments described above (Figure 3.1E and Supplementary Figure 6C). Thirty minutes after oHFS and oPSD delivery, significant reductions in active lever presses, alcohol deliveries, and alcohol intake were observed; these reductions were maintained for at least 7 days (Figure 3.4B and Figure 3.5.18A). Note that neither the cocktail (MK801+raclopride) plus oHFS (Supplementary Figure 10B-D) nor the cocktail alone (Supplementary Figure 10E-G) affected alcohol-seeking behavior. Together with our finding that oHFS+oPSD+MK801 induced no changes in alcohol consumption (Supplementary Figure 7G), these data suggest that the *in vivo* LTD-inducing protocol (oHFS+oPSD+MK801+raclopride) produces a long-lasting reduction of alcohol-seeking behavior and that this induction requires D2R blockade.

Since the LTD induction is eCB-dependent (Figure 3.1E), we examined whether blockade of CB1Rs attenuated the effect of the LTD-inducing protocol on alcohol-seeking behavior. We found that systemic administration of additional AM251 completely abolished the LTD-induced reduction of active lever presses, alcohol deliveries, and alcohol intake (Figure 3.4C and Supplementary Figure 10H-I). In contrast, AM251 itself did not alter alcohol-seeking behavior (Supplementary Figure 10J-L). Lastly, our *ex vivo* results further ascertained that the paired-pulse ratio was significantly increased (Figure 3.4D) and that the frequency of spontaneous miniature EPSCs was decreased (Figure 3.4E) 2 days after delivery of the LTD protocol, confirming a presynaptically expressed striatal eCB-LTD. These data indicate that delivery of the *in vivo* LTD-inducing protocol at the corticostriatal synapses within the DMS produced a long-lasting suppression of alcohol-seeking behavior.

3.3.5. *In vivo* deliveries of LTP and LTD protocols cause plasticity preferentially in DMS D1-MSNs

The DMS contains D1- and D2-MSNs, which have been reported to exert opposite effects on drug and alcohol drinking behaviors (Lobo and Nestler, 2011; Cheng et al., 2017). We thus explored how LTP or LTD induction altered glutamatergic transmission in these two neuronal types.

First, to examine *ex vivo* LTP induction in D1- and D2-MSNs, we infused AAV-DIO-ChR2-mCherry into the DMS of *Drd1a*- and *Drd2*-*Cre* transgenic mice, to enable selective depolarization of D1- or D2-MSNs. Paired eHFS and oPSD induced significant LTP, which did not differ between D1- and D2-MSNs (Figure 3.5A,B). This promoted us to explore how synaptic transmission changed in these two neuronal populations following *in vivo* LTP induction. To achieve this, we infused Chronos into the mPFC and Chrimson into the DMS of adult rats, as described above (Figure 3.3A). D1-MSNs were labeled by retrograde beads infused into the substantia nigra pars reticulata (SNr) (Figure 3.5C, left), whereas D2-MSNs were labeled by infusion of AAV-D2SP-eYFP (Figure 3.5C, right). Two days after *in vivo* delivery of the LTP-inducing protocol, the AMPAR-EPSC amplitude and the AMPAR/NMDAR ratio were increased in D1-MSNs, but not in D2-MSNs (Figure 3.5D,E), as compared with slices from control rats that were not exposed to light stimulation. This cell type-specific LTP induction is likely attributable to the higher GluN2B/NMDA ratio in D1-MSNs than in D2-MSNs (Figure 3.5F), as alcohol-mediated enhancement of GluN2B promotes LTP induction (Wang et al., 2012; Wills et al., 2012). Collectively, these data indicate that the *in vivo* LTP protocol potentiated synaptic transmission selectively in D1-MSNs.

We next investigated whether LTD was also preferentially induced in D1-MSNs *ex vivo*

and *in vivo*. To induce oPSD selectively in rat D1-MSNs, we infused a retrograde AAV encoding Cre (AAV5-Cre) into the SNr and a Cre-inducible AAV expressing Chrimson (AAV-Flex-Chrimson-tdTomato) (Klapoetke et al., 2014) into the DMS. We found that in DMS slices from alcohol-naïve rats, a protocol (eHFS+oPSD+MK801+raclopride) that was similar to that used to successfully induce LTD (Figure 1E) caused a robust LTD in D1-MSNs; this LTD was abolished by AM251 (Figure 3.6A,B). To induce oPSD specifically in D2-MSNs, we infused AAV-D2SP-ChR2 (Zalocusky et al., 2016) into the DMS of alcohol-naïve rats. We found that the same protocol of eHFS+oPSD+MK801+raclopride did not produce any LTD in the D2-MSNs (Figure 3.6A,C), which was consistent with previous reports(Wang et al., 2006; Kreitzer and Malenka, 2007).

Lastly, to ascertain whether *in vivo* LTD induction caused glutamatergic depression in D1-MSNs, we measured corticostriatal EPSCs in DMS slices prepared two days after *in vivo* delivery of the LTD-inducing protocol. We found that the LTD protocol reduced the release probability, as indicated by the increased paired-pulse ratio, and reduced the mEPSC frequency in D1-, but not D2-, MSNs, as compared to neurons from control animals without LTD induction (Figure 3.6D-G). These results indicate that *in vivo* LTD induction leads to long-lasting depression of corticostriatal inputs selectively onto DMS D1-MSNs.

Taken together, our results suggest that *in vivo* delivery of optogenetic LTP and LTD protocols preferentially induced plasticity in DMS D1-MSNs.

3.3.6. Selective LTP and LTD induction in DMS D1-MSNs produces long-lasting changes in controls alcohol-seeking behavior

Finally, we examined whether *in vivo* induction of corticostriatal LTP or LTD directly in DMS D1-MSNs altered alcohol-seeking behavior. For oHFS, we infused AAV-Chronos into the

mPFC; for oPSD of D1-MSNs, we infused the retrograde AAV5-Cre into the SNr and AAV-Flex-Chrimson into the DMS (Figure 3.7A). These infusions led to Chronos expression at the mPFC inputs and selective Chrimson expression in DMS D1-MSNs (Figure 3.7B). *In vivo* LTP induction produced significant increases in active lever presses, alcohol deliveries, and alcohol intake at 30 min; this effect persisted for at least 2 days (Figure 3.7C and Supplementary Figure 11A). However, D1-MSN oPSD alone did not alter alcohol-seeking behavior (Figure 3.7D and Supplementary Figure 11B,C). These data suggest that *in vivo* corticostriatal LTP in DMS D1-MSNs caused a long-lasting potentiation of alcohol-seeking behavior.

In contrast, we found that delivery of the *in vivo* LTD-inducing protocol to the mPFC input onto D1-MSNs caused sustained decreases in active lever presses, alcohol deliveries, and alcohol intake at 30 min and 2 days (Figure 3.7E and Supplementary Figure 11D). This behavioral effect was abolished by systemic administration of AM251 (Figure 3.7F and Supplementary Figure 11E,F), which confirmed that eCB signaling regulated this inhibition of alcohol-seeking behavior. These data demonstrate that eCB-LTD in D1-MSNs is required for the long-lasting decrease in alcohol-seeking behavior.

3.4 Discussion

In this study, we provide evidence to suggest that alcohol intake induces glutamatergic plasticity, which can be further potentiated by *in vivo* LTP induction, and that this causes long-lasting enhancement of alcohol-seeking behavior (Figure 3.8A). In contrast, *in vivo* LTD induction suppresses this plasticity and produces a long-lasting reduction of this behavior. We report that pairing HFS of corticostriatal afferents with oPSD of DMS neurons induces a robust NMDAR-dependent LTP, which masks an eCB-LTD (Figure 3.8B). Furthermore, we discovered that LTP and LTD in D1-MSNs contributed to the alteration of alcohol-seeking behavior (Figure

3.8B,C). These results provide a direct causal link between long-term synaptic plasticity within a given neural circuit (mPFC → DMS D1-MSNs) and alcohol-seeking behavior. Our findings also demonstrate that induction of D1-MSN LTD might be a potential therapeutic strategy for alcohol use disorder.

3.4.1. oPSD facilitates LTP and LTD induction in the dorsal striatum

It has long been known that dorsostriatal LTP induction proves difficult, possibly due to insufficient depolarization of striatal neurons (Calabresi et al., 1992; Surmeier et al., 2009). In this study, oPSD was used to strongly depolarize the distal dendrites of these neurons, thus enhancing NMDAR channel opening and calcium influx, which is required for LTP induction (Calabresi et al., 1992; Surmeier et al., 2009) (Figure 3.8B). Interestingly, blockade of LTP by NMDAR antagonists leads to LTD; this is consistent with a study showing that LTP blockade by memantine shifted LTP to LTD (Mancini et al., 2016). However, APV or MK801 was found to shift the plasticity in the current research, but not in the study by Mancini et al. (Mancini et al., 2016). This discrepancy may reflect the fact that eCB-LTD was induced mainly by oPSD in the presence of a D2R antagonist in the current study, and by D2R activation in the previous research. In addition, we report that dopamine D1R signaling plays a critical modulatory role in optogenetic LTP. The observations that blockade of LTP unmasks eCB-LTD and that blockade of eCB-LTD enhances the LTP magnitude suggest that paired HFS and oPSD simultaneously induces NMDAR-dependent LTP and eCB-LTD.

The current oPSD also facilitated LTP in the specific corticostriatal input when we used dual-channel optogenetics. The precise control of both pre- and post-synaptic activity allowed us to reliably induce LTP for the first time. LTP induction is known to activate the expression of immediate early genes such as *Npas4*, which has recently been identified as an important factor

in brain plasticity (Sun and Lin, 2016). Expression of the *Npas4* gene requires Ca^{2+} influx and is associated with drug addiction (Ye et al., 2016). Indeed, the mRNA level *Npas4* gene is increased only after paired oHFS and oPSD, suggesting that oPSD predominantly facilitates LTP at corticostriatal synapses.

3.4.2. Optogenetic LTP induction promotes, and LTD induction suppresses, alcohol-seeking behavior

The corticostriatal circuit is believed to control goal-directed behaviors, including drug-seeking behavior (Yin and Knowlton, 2006; Balleine and O'Doherty, 2010; Lovinger, 2010; Everitt and Robbins, 2016). *In vivo* optogenetic induction of corticostriatal LTP enhances alcohol-seeking behavior, suggesting a link between this plasticity and the behavior. The selective effects of LTP on operant self-administration of alcohol versus sucrose may reflect the distinct activities of these two chemicals on the rats. Operant training with alcohol, but not with sucrose, enhanced NMDAR activity and facilitated subsequent *in vivo* and *ex vivo* induction of LTP. This finding is consistent with previous reports indicating that *ex vivo* or *in vivo* alcohol exposure caused long-term facilitation of NMDAR activity (Wang et al., 2007; Kash et al., 2009; Lovinger, 2010; Wang et al., 2010), which is required for LTP induction in the dorsal striatum (Lovinger, 2010) and for operant alcohol self-administration (Wang et al., 2010). Operant alcohol self-administration induced a smaller, but not significant, increase in AMPAR/NMDAR ratio than did operant sucrose training. This ratio difference might be attributable to the higher NMDAR activity in alcohol-treated rats than in sucrose controls.

How drug (e.g., cocaine)-evoked plasticity affects subsequent LTP induction is likely to depend on the degree of saturation of the plasticity. Our study reveals that operant alcohol self-administration using the FR3 schedule induced glutamatergic plasticity (increased

AMPAR/NMDAR ratio). This plasticity was not saturated because the AMPAR/NMDAR ratio was further potentiated by *in vivo* LTP induction, and LTP was induced in slices from alcohol-drinking animals. It is known that 1-2 day(s) withdrawal from cocaine exposure induces silent synapses that contain NMDARs but not AMPARs (Huang et al., 2009; Lee et al., 2013; Dong and Nestler, 2014; Ma et al., 2014); these can mature over time (e.g., at 45 days)(Lee et al., 2013; Ma et al., 2014; Ma et al., 2016) and potentially contribute to subsequent LTP occlusion (Creed et al., 2015; Creed et al., 2016). These studies suggest that short-term withdrawal from drug exposure induces unsaturated plasticity. Since we induced LTP 24 hours after the last alcohol exposure, it is not surprising that no occlusion was observed; this is consistent with previous reports (Wang et al., 2012; Wills et al., 2012).

Pharmacological inhibition of alcohol-evoked glutamatergic strengthening in the DMS attenuates alcohol consumption (Wang et al., 2012). However, this inhibition is transient and disappears as the inhibitory compounds are metabolized. Furthermore, structural plasticity, such as an increased density of mushroom spines, has been observed following alcohol consumption (Wang et al., 2015). In this study, *in vivo* eCB-LTD induction elicited a long-lasting decrease in alcohol-seeking behavior, indicating that this plasticity mediates more sustained behavior changes (Sidhpura and Parsons, 2011).

3.4.3. LTP and LTD in D1-MSNs affect alcohol-seeking behavior

While the present study and others (Shen et al., 2008; Surmeier et al., 2009) report that LTP can be induced in both D1- and D2-MSNs in slices from alcohol-naïve animals, *in vivo* delivery of our LTP-inducing protocol selectively causes long-lasting potentiation of corticostriatal transmission in D1-MSNs of alcohol-drinking rats. This selectivity may be attributed to the fact that alcohol consumption potentiates NMDAR activity in D1-, but not D2-,

MSNs (Cheng et al., 2017). The current study further identified that alcohol consumption specifically potentiated GluN2B-containing NMDAR activity at the mPFC input onto D1-MSNs. Alcohol-mediated potentiation of GluN2B-NMDARs was reported to facilitate LTP induction (Wang et al., 2012; Wills et al., 2012). Our *in vivo* LTD-inducing protocol also caused LTD in D1-, but not D2-, MSNs because we included a D2R antagonist, which blocks LTD induction in D2-MSNs (Kreitzer and Malenka, 2007; Shen et al., 2008) (Figure 3.8C,D). Our findings are in agreement with a recent report showing that eCB-LTD was induced at corticostriatal inputs to D1-, but not D2-, MSNs (Wu et al., 2015). Given that D1-MSNs positively control alcohol consumption (Cheng et al., 2017), it is not surprising that induction of D1-MSN LTP produces long-lasting enhancement of operant alcohol self-administration, while LTD induction in this neuronal type reduces the same behavior. The induction of LTP/LTD by inducing oPSD selectively in D1-MSNs confirmed that synaptic plasticity in this neuronal type is sufficient to control alcohol-seeking behavior in a bi-directional manner. Therefore, blockade of striatal LTP induction and promotion of eCB-LTD in D1-MSNs may inspire a therapeutic strategy to cause a long-lasting reduction of alcohol-seeking behavior. Although optogenetic intervention cannot be immediately translated to human use, deep brain stimulation (DBS) is an FDA-approved treatment that has the potential to cause LTP (Creed et al., 2015), and probably LTD. Thus, we believe that the combined use of DBS and antagonists of the NMDAR (e.g., memantine) and D2R may provide novel clinical treatments for alcohol use disorder.

In summary, we have demonstrated that optogenetic induction of bidirectional long-term synaptic plasticity at corticostriatal afferents within the DMS produced long-lasting increases or decreases in alcohol-seeking behavior. Importantly, we show that the plasticity of DMS D1-MSNs controls alcohol-seeking behavior. Our research establishes a causal link between

corticostriatal synaptic potentiation and alcohol-seeking behavior and provides an evidence base for therapeutic strategies to reduce excessive alcohol consumption.

3.5 Materials and Methods

3.5.1. Reagents

AAV5-CaMKIIa-C1V1(E122T/E162T)-eYFP (3×10^{12} vg/ml), AAV8-Syn-Chronos-GFP (5.6×10^{12} vg/ml), AAV8-Syn-Chrimson-tdTomato (5.5×10^{12} vg/ml), AAV8-Syn-Flex-Chrimson-tdTomato (4.1×10^{12} vg/ml) and AAV-EF1a-DIO-ChR2-mCherry (2×10^{12} vg/ml) were purchased from the University of North Carolina Vector Core. AAV5-CAG-GCaMP6s (2.2×10^{13} vg/ml) and AAV5-CMV-Cre-eGFP (4.9×10^{12} vg/ml) were obtained from the University of Pennsylvania Vector Core. AAV8-D2SP-eYFP (2.5×10^{12} vg/ml) and AAV8-D2SP-eChR2 (H134R)-eYFP (2.5×10^{12} vg/ml) were purchased from Gene Vector and Virus Core of Stanford University School of Medicine. NBQX and APV were purchased from R&D systems. Tetrodotoxin (TTX) was obtained from Tocris. Alexa Fluor 594 was purchased from Invitrogen. MK801, sulpiride, raclopride and the other reagents were obtained from Sigma.

3.5.2. Animals

Male Long-Evans rats (3 months old, Harlan Laboratories) and *Drd1a-Cre* (D1-Cre) and *Drd2-Cre* (D2-Cre) transgenic mice (C57BL/6 background, 3 months old, Mutant Mouse Regional Resource Centers) were used. Both rats (2/cages) and mice (5/cage) were group-housed. All animals were kept in a temperature- and humidity-controlled environment with a light: dark cycle of 12 h (lights on at 7:00 a.m.), and food and water available *ad libitum*. All behavior experiments were conducted in their light cycle, and animals had no history prior to the behavior reported in this paper. All animal care and experimental procedures were approved by the Texas A&M University Institutional Animal Care and Use Committee and were conducted in

agreement with the National Research Council *Guide for the Care and Use of Laboratory Animals*.

3.5.3. Stereotaxic virus infusion

The stereotaxic viral infusion was performed as described previously (Ma et al., 2017). Depending on experimental design, viruses or beads were infused into the mPFC (AP: +3.2 and +2.6 mm, ML: ±0.65 mm, DV: -4.0 mm from Bregma), the DMS (AP1: +1.2 mm, ML1: ±1.9 mm, DV1: -4.7 mm; AP2: +0.36 mm, ML2: ±2.3 mm, DV2: -4.7 mm), and the SNr (AP1: -4.92 mm, ML1: ±2.3 mm, DV1: -8.3 mm; AP2: -5.5 mm, ML2: ±2.0 mm, DV2: -8.6 mm) for rats. For mice, the viruses were infused into the DMS (AP1: +1.18 mm, ML1: ±1.3 mm, DV1: -2.9 mm; AP2: +0.38 mm, ML2: ±1.55 mm, DV2: -2.9 mm from Bregma). 0.5-1 µl of the virus was infused bilaterally at a rate of 0.08 µl/min. At the end of the infusion, the injectors remained at the site for 10 min to allow for virus diffusion. Animals infused for electrophysiology were maintained in their home cages for 6-8 weeks before recordings. For animals infused with viruses for behavioral experiments, we started training them to self-administer alcohol or sucrose one week after surgery.

3.5.4. Slice preparation

The procedure has been described previously (Huang et al., 2017; Ma et al., 2017; Wei et al., 2018). Briefly, coronal sections of the striatum (250 µm in thickness) were cut in an ice-cold solution containing the following (in mM): 40 NaCl, 143.5 sucrose, 4 KCl, 1.25 NaH_2PO_4, 26 $NaHCO_3$, 0.5 $CaCl_2$, 7 $MgCl_2$, 10 glucose, 1 sodium ascorbate, and 3 sodium pyruvate, saturated with 95% O_2 and 5% CO_2. Slices were then incubated in a 1:1 mixture of cutting solution and external solution at 32°C for 45 min. The external solution was composed of the following (in mM): 125 NaCl, 4.5 KCl, 2 $CaCl_2$, 1 $MgCl_2$, 1.25 NaH_2PO_4, 25 $NaHCO_3$, 15 sucrose and 15

glucose, saturated with 95% O_2 and 5% CO_2. Slices were maintained in external solution at room temperature until use.

3.5.5. Field potential recording

For LTP experiments, extracellular field recordings were conducted as previously described(Ma et al., 2017). Specifically, the recording used a patch pipette filled with 1 M NaCl and was placed within the DMS. DMS slices were visualized under an epifluorescent microscope (Examiner A1, Zeiss, Germany). Bipolar stimulating electrodes were positioned 100-150 μm away from the recording electrode. Field excitatory postsynaptic potentials/population spikes (fEPSP/PS)(Yin et al., 2007) were evoked by electrical stimuli through stimulating electrodes at 0.05 Hz. Picrotoxin (100 μM) was bath applied to block GABAergic transmission. The dopamine D2R antagonist, sulpiride (20 μM), was included externally for all experiments conducted in Figures 3.1, 3.5a, and Figure 3.9b, 4. Optical stimuli (2 ms, 405 nm) were delivered through the objective lens to elicit fEPSP/PS. fEPSP/PS were measured using a MultiClamp 700B amplifier with Clampex 10.4 software (Molecular Devices). After a stable baseline had been established for 10 min, high-frequency stimulation (HFS) was delivered through the stimulating electrodes or objective lens to induce LTP. HFS consists of 4 trains of stimuli repeated at an interval of 20 sec. Each train contains 100 pulses at 100 Hz (electrically HFS, eHFS) or 50 Hz (optogenetic HFS, oHFS). For pairing experiments, optogenetic postsynaptic depolarization (oPSD) was induced by light stimulation (590 nm, 1 sec for eHFS or 2 sec for oHFS) of DMS neurons through the objective lens.

3.5.6. Whole-cell recording

In Figures 3.9, 3.10, and 3.5.13b, we used a K^+-based intracellular solution, containing (in mM): 123 potassium gluconate, 10 HEPES, 0.2 EGTA, 8 NaCl, 2 MgATP, 0.3 NaGTP (pH

7.3). All other experiments utilized the Cs-based solution, containing (in mM): 119 $CsMeSO_4$, 8 TEA.Cl, 15 HEPES, 0.6 EGTA (10 BAPTA for Figure 3.11d,e), 0.3 Na_3GTP, 4 MgATP, 5 QX-314.Cl, 7 phosphocreatine, 0.05 Alexa Fluor 594 (Figure 3.11a-e), and 0.1 spermine (Figure 3.5.17). The pH was adjusted to 7.3 with CsOH. Neurons were clamped at -70 mV.

For measuring NMDAR-EPSPs in distal dendrites, Alexa Fluor 594 was infused through patch-pipettes into the recorded neurons to label their dendrites. Under the guidance of fluorescence, the stimulating electrodes were positioned close to the Alexa Fluor-labeled dendrites and were 100-150 μm away from the soma. AMPA receptor (AMPAR)-mediated EPSPs were recorded in 1.0 mM extracellular Mg^{2+}. NBQX (10 μM) was then bath applied to block AMPAR-EPSPs. Next, simultaneous presynaptic electrical stimulation and oPSD of striatal neurons induced a response that was mediated by a C1V1-induced depolarization (V_{c1v1}) plus an NMDAR response ($EPSP_{NMDA}$). Lastly, the $EPSP_{NMDA}$ component was blocked by bath application of APV (50 μM), and V_{c1v1} was isolated. The optogenetic-mediated $EPSP_{NMDA}$ was calculated by digital subtraction of V_{c1v1} from V_{c1v1} + $EPSP_{NMDA}$. The input-output relationships for AMPAR-mediated excitatory postsynaptic currents (EPSCs) were measured at 5 different stimulating laser powers. For measurement of the AMPAR/NMDAR ratio, the peak currents of AMPAR-mediated EPSCs were measured at a holding potential of -70 mV and the NMDAR-mediated EPSCs were estimated as the EPSCs at +40 mV at 30 ms after the peak AMPAR-EPSCs, when the contribution of the AMPAR component was minimal. The AMPA/NMDA ratio was calculated by dividing the NMDAR-EPSC by AMPAR-EPSC. To measure the GluN2B/NMDA ratio, NMDAR-EPSCs were recorded in the absence and presence of Ro 25-6981, and GluN2B-EPSCs were calculated by subtraction of these two responses. For measuring mEPSCs, we added TTX (1 μM) to the external solution to suppress action potential-driven

release. The paired-pulse ratio (PPR) was calculated by dividing the second light-evoked EPSC by the first with 100-ms intervals between the two. To measure above synaptic transmission in specific D1- and D2-MSNs (Figure 3.5, 3.6), we first patched bead-positive (D1-MSNs) or eYFP-positive neurons (D2-MSNs) within a DMS area containing strong green mPFC fibers (expressing Chronos-GFP) and red Chrimson-positive neurons. We then sequentially delivered 405-nm light to stimulate the mPFC inputs and 590-nm light to induce Chrimson-mediated oPSD. The synaptic inputs and oPSD were distinguished using 2- and 100-ms light stimulation, since the prolonged light stimulation increased the duration of oPSD, but not of synaptic transmission (Cruikshank et al., 2010). Only those neurons that received mPFC inputs and exhibited oPSD were selected for further experiments. At the end of the recording, NBQX was applied to confirm synaptic transmission induced by 405-nm light stimulation. To measure AMPAR rectification, AMPAR-EPSCs were recorded at three holding potentials of -70, 0, and +40 mV in the presence of APV (50 μM). Rectification index of the AMPAR-EPSC was calculated by plotting the EPSC magnitude at these potentials, and using the slope of the lines connecting the data between -70-0 mV and between 0-40 mV to calculate the ratio.

3.5.7. Calcium image

An AAV-C1V1 (Yizhar et al., 2011) and an AAV-GCaMP6s (Chen et al., 2013) were infused into the DMS. Whole-cell recordings were made in C1V1-expressing neurons. The GCaMP6s measures the calcium signal that is induced by current injection (iPSD), or optogenetic depolarization (oPSD) (Figure 3.10). In Figure 3.11f-g, fluorescent Ca^{2+} signals were elicited by eHFS or eHFS+oPSD without whole-cell recording. The distal dendrite (~120 μm from the soma) was chosen for analysis. Ca^{2+} signals were acquired and analyzed with the Zen program (Zeiss) and Origin software (Origin Lab Corporation, MA), and calculated as

previously described (Wang et al., 2004). The fluorescence signals were quantified by measuring the mean pixel intensities of the circular regions of interest (ROI). Fluorescence intensity is expressed as ΔF/F values vs. time, where F is the baseline fluorescence and ΔF is the baseline-subtracted fluorescence.

3.5.8. Operant self-administration of alcohol

After one week recovery from viral infusions, Long-Evans rats were trained to self-administer a 20% alcohol solution in operant self-administration chambers as described (June and Gilpin, 2010). Each chamber contains two levers; an active lever, in which presses result in a delivery of 0.1 ml of the alcohol solution, and an inactive lever, in which presses are recorded, but no programmed events occur. After 48-h of exposure to 20% alcohol in the home cage, and one overnight session in the chamber in which pressing the active lever delivers 0.1 ml of water in a fixed ratio 1 (FR1), operant sessions were conducted 5 days per week for two weeks in a FR1 schedule with an active lever press resulting in the delivery of 20% alcohol with sessions shortened from 3 h to 30 min. Following the first two weeks, operant sessions were run three days per week for one week, and the schedule requirement was increased to FR3. After one week of FR3 training, rats underwent surgery for optical fiber implantation. FR3 training was resumed one week after the surgery. Once a stable baseline of active lever presses was achieved, animals underwent *in vivo* LTP and LTD induction. Following the induction, some rats were continuously monitored with their operant behavior for 7-9 days, while other rats were euthanized at day 2 post-induction for electrophysiology recordings. To test drugs' effect without LTP/LTD induction, we systematically administered them 30 min before the operant behavior test. Simultaneously, we also measured inactive lever presses before and after treatment (Supplementary Figure 11).

3.5.9. Operant self-administration of sucrose

After a one-week recovery from viral infusions, Long-Evans rats were trained to self-administer a 2% sucrose in operant chambers using the same procedure as the alcohol group described above. Optical fiber implantation was also conducted in an identical manner to the alcohol group.

3.5.10. Optical fiber implantation

One-week following operant training with the FR3 schedule, animals were anesthetized with isoflurane and mounted in a stereotaxic frame. An incision was made, bilateral optical fiber implants (300-nm core fiber secured to a 2.5-mm ceramic ferrule with 5-mm fiber extending past the end of the ferrule) were lowered into the DMS (AP: +0.36 mm; ML: ±2.3 mm; DV: -4.6 mm from Bregma). Implants were secured to the skull with metal screws and dental cement (Henry Schein) and covered with denture acrylic (Lang Dental). The incision was closed around the head cap and the skin vet-bonded to the head cap. Rats were monitored for one week or until they resumed normal activity.

3.5.11. *In vivo* LTP and LTD induction and operant testing

Once a stable baseline of active lever presses was attained after optical fiber implantation, an LTP/LTD-inducing protocol was delivered 30 minutes before operant testing sessions in a neutral Plexiglass chamber, with no visual cues. LTP-induction consisting of paired oHFS+oPSD used the following protocol: 100 pulses at 50 Hz of 473-nm light (2 ms) with or without constant 590-nm light for 2 sec, repeated 4 times with 20-sec intervals. The protocol was repeated three times with 5-min intervals. LTD induction employed the following protocol: animals were injected with a cocktail of MK-801 (0.1 mg/kg) and raclopride (0.01 mg/kg) 15 minutes before delivery of oHFS and oPSD. The complete LTP/LTD-inducing procedure was performed once

and 30 min later animals were allowed to press levers for alcohol in a 30-min session. Operant sessions were repeated every 48 or 72 h until active lever presses returned to their levels prior to the induction.

3.5.12. Measurement of blood alcohol concentration (BAC)

To measure blood alcohol concentration, we used the same procedure as in Figure 3.3b to train two groups of rats. One week prior to LTP induction, we collected blood samples from the one side of the lateral saphenous vein (Carnicella et al., 2009) in both groups to measure baseline BAC. Thirty minutes after LTP induction, we collected blood samples from the other side of the lateral saphenous in one group of rats. Two days after the LTP induction, we collected blood samples from the other group of rats. BAC was measured using gas chromatography as previously described (Simms et al., 2010).

3.5.13. RNA extraction and quantitative PCR (qPCR) analysis

The rats were infused with AAV-Chronos-GFP in the mPFC and AAV-Chrimson-tdTomato in the DMS. Coronal striatal sections (250 μm) were prepared as described in Slice Preparation section above. A slice was placed in a recording chamber and perfused with the external solution at a flow rate of 3 mL/min. Optical stimuli were delivered through the objective lens to fluorescent DMS areas, which contained both GFP-expressing mPFC axons and tdTomato-expressing neurons using one of the following stimulation protocols: oHFS, oPSD, or oHFS+oPSD. All protocols were repeated three times with 5-min intervals, which is the same as the *in vivo* LTP-inducing protocol. Thirty minutes after completing the optogenetic stimulation, the DMS tissues from experimental and control groups were collected on ice. The RNA isolation, reverse transcription, and the qRT-PCR analyses were performed as described previously (Zhao et al., 2012). The mRNA level of *Npas4* was normalized against the GAPDH

mRNA level in the same sample and presented as fold changes over baseline using the delta-delta CT method. The following primers were used: *Npas4*, Forward: 5′-GAACCTCAAGGAACTGCTGC-3′, reverse: 5′- GTGCCTCCAGCAAAGAAGAC-3′; GAPDH, Forward: 5'- TGCCACTCAGAAGACTGTGG-3', reverse: 5'-TTCAGCTCTGGGATGACCTT-3'. For each experimental condition, two slices per rat were treated, and the averaged mRNA values were used.

3.5.14. Histology

Rats with viral and beads infusion were perfused intracardially with 4% paraformaldehyde (PFA) in phosphate-buffered saline (PBS). The brains were taken out and put into 4% PFA/PBS solution for post-fixation overnight at 4°C, followed by dehydration in 30% sucrose solution and cryostat frozen sectioning. The brains were cut into 50-μm coronal sections. A confocal laser-scanning microscope (Fluorview-1200, Olympus) was used to image these sections with a 470-nm laser to excite eYFP and GFP and with a 593-nm laser to excite Alexa Fluor 594 and tdTomato. All images were processed using Imaris 8.3.1 (Bitplane, Zurich, Switzerland).

3.5.15. Data acquisition and statistics

In electrophysiology experiments, we used 184 rats and 10 D1- and D2-Cre mice, with 10 rats excluded before data collection due to virus expression in the incorrect place or expression that was too weak. In behavioral tests, we used 156 rats, among which 28 were excluded due to lack of alcohol responding in the operant setting (< 10 active lever presses/ session), 6 were removed from data analysis due to death during surgery, and 21 were removed from the last experiments due to head cap loss. In the imaging experiments, we used 11 rats.

All data are expressed as mean ± SEM. Each experiment was replicated in 3–7 animals.

The data collection was randomized. Data were obtained and analyzed by experimenters who did not know the types of treatments of the animals except Figures. 3.3d-g, 3.4d,4e, 3.5d,5e, 3.6d-g. No data points were excluded unless specified, and the only exclusion standard was the health condition of the animal. Data from the repeated experiments for the same sub-study were pooled together for statistics. The sample size for each experiment was determined to be either at least 3 animals or 10 neurons. If animals in Figures. 3.3d-g, 3.4d,4e, 3.5d,5e, 3.6d-g were successfully induced *in vivo* changes, we measured responses *ex vivo* in enough neurons to evaluate the effect of light stimulation. The sample size was presented as "n = x, y", where "x" refers to the number of slices or neurons, and "y" refers to the number of animals. In electrophysiological experiments, 1-4 recordings were performed using slices from a single animal except for Figures. 3.3d, 3.3e, 3.4d,4e. Slice or neuron-based statistics were performed and reported for electrophysiology and animal-based statistics for behavioral data. Normal distribution was assumed and tested. Variance was estimated for most major results, and no significant difference was found between control and manipulation groups. Statistical significance was assessed in electrophysiological studies using the unpaired or paired *t* test, or two-way RM ANOVA followed by Student-Newman-Keuls (SNK) method. Behavioral studies were analyzed using the paired *t* test and one-way RM ANOVA followed by the SNK method. Two-tail tests were performed for all studies. Statistical significance was set at $P < 0.05$.

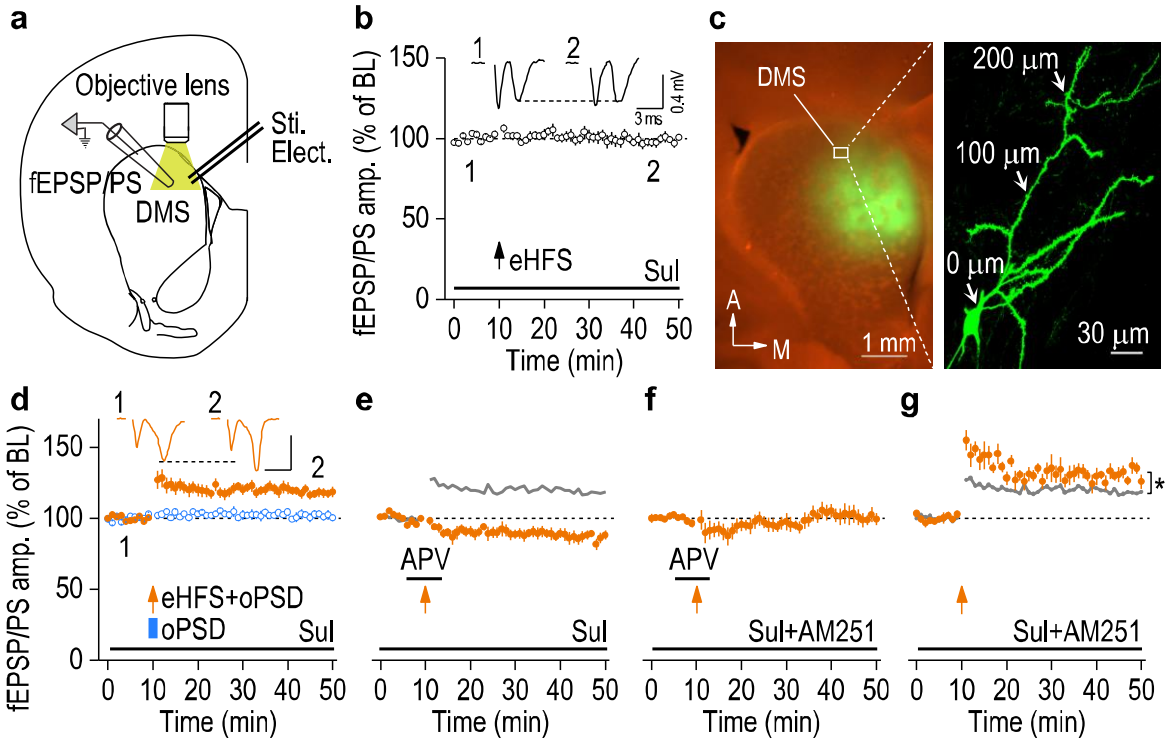

Figure 3.1. oPSD facilitated induction of NMDAR-dependent LTP and eCB-LTD in DMS slices.

(**A**) Schematic showing the bipolar stimulating electrodes (Sti. Elect.) used to evoke fEPSP/PS and the objective lens for optogenetic depolarization. (**B**) Presynaptic eHFS did not potentiate fEPSP/PS (98.59 ± 2.39% of baseline [BL], $t_{(7)} = 0.59$, $P = 0.57$; $n = 8$ slices, 6 rats). Inset, sample fEPSP/PS traces at time 1 and 2. Sulpiride (Sul; 20 µM) was bath-applied to prevent LTD and favor LTP induction in this and following recordings as indicated. (**C**) Representative fluorescent images showing C1V1-eYFP expression in the DMS (left) and in the full-length dendrites of a DMS neuron (right). The section was counter-stained with NeuroTrace (red). (**D**) Pairing of presynaptic eHFS and oPSD (1 sec), but not oPSD alone, induced robust LTP. eHFS+oPSD: 118.32 ± 2.96% of BL, $t_{(9)} = -6.18$, $P = 0.00016$; $n = 10$ slices, 6 rats; oPSD: 101.59 ± 2.26% of BL, $t_{(6)} = -0.70$, $P = 0.51$; $n = 7$ slices, 3 rats. Scale bars: 3 ms, 0.4 mV. (**E**) Optogenetic induction of LTP was abolished by APV (50 µM), leading to LTD (86.75 ± 3.06% of BL, $t_{(6)} = 4.33$, $P = 0.0049$; $n = 7$ slices, 6 rats). The grey line is the control LTP from d for reference. (**F**) LTD was completely abolished by the CB1R antagonist, AM251 (3 µM) (101.32 ± 4.71% of BL, $t_{(8)} = -0.28$, $P = 0.79$, $n = 9$ slices, 5 rats). (**G**) AM251 facilitated LTP induction (130.73 ± 2.89% of BL, $t_{(5)} = -10.62$, $P = 0.00013$; compared with the control LTP: $t_{(14)} = -2.79$, $^*P = 0.015$; $n = 6$ slices, 3 rats, unpaired t test). Two-sided paired t test for B and D-G, unless otherwise stated. Data are presented as mean ± s.e.m.

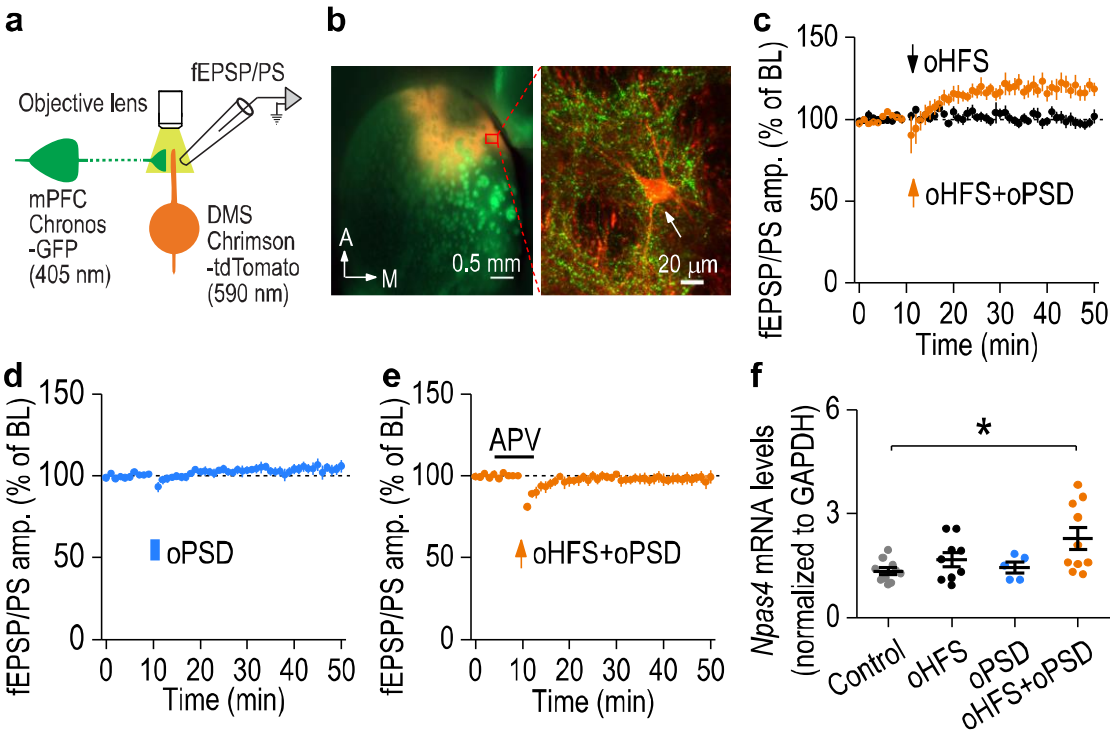

Figure 3.2. oPSD facilitated corticostriatal LTP induction in the DMS.
(**A**) Schematic illustration of selective pre- and post-synaptic stimulation of DMS corticostriatal synapses using dual-channel optogenetics. AAV-Chronos-GFP was infused into the mPFC and AAV-Chrimson-tdTomato into the DMS of rats. Chronos and Chrimson were activated by 405- and 590-nm light, respectively. (**B**) Confocal fluorescent images showing Chronos-GFP-expressing mPFC fibers (green) and Chrimson-tdTomato-expressing neurons (red) in the DMS. Images shown in b is representative of 3 experiments of 3 rats. (**C**) Pairing oHFS with oPSD produced robust LTP in the DMS (119.06 ± 4.69% of baseline [BL], $t_{(6)}$ = -4.07, P = 0.0066; n = 7 slices, 4 rats). oHFS alone did not alter fEPSP/PS (99.60 ± 3.12% of BL, $t_{(7)}$ = 0.13, P = 0.90; n = 8 slices, 5 rats). (**D**) oPSD alone did not induce LTP (104.55 ± 3.15% of BL, $t_{(6)}$ = -1.44, P = 0.20; n = 7 slices, 3 rats). (**E**) Dual-channel optogenetic induction of LTP was blocked by APV (98.06 ± 3.27% of BL; $t_{(8)}$ = 0.59, P = 0.57; n = 9 slices, 5 rats). (**F**) *Npas4* mRNA levels were significantly increased following paired oHFS+oPSD, but not after oHFS or oPSD only. $F_{(3,30)}$ = 3.86, P = 0.019; *P < 0.05; n = 10 (Control), 9 (oHFS), 5 (oPSD), and 10 (oHFS+oPSD) rats. Two-sided paired t test for C-E; one-way ANOVA followed by SNK test for F. Data are presented as mean ± s.e.m.

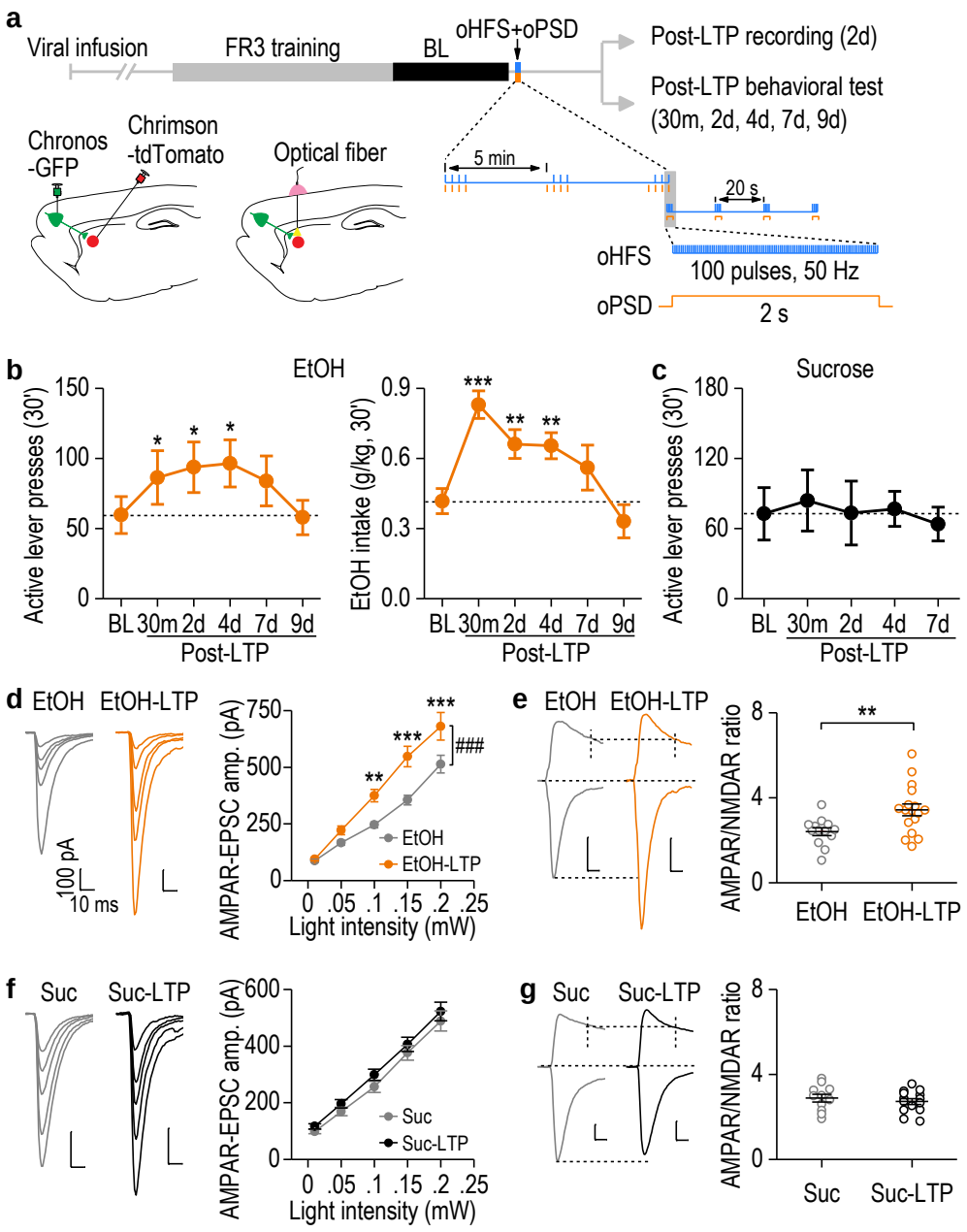

Figure 3.3. oPSD facilitated corticostriatal LTP induction in the DMS.

(**A**) Schematic illustration of selective pre- and post-synaptic stimulation of DMS corticostriatal synapses using dual-channel optogenetics. AAV-Chronos-GFP was infused into the mPFC and AAV-Chrimson-tdTomato into the DMS of rats. Chronos and Chrimson were activated by 405- and 590-nm light, respectively. (**B**) Confocal fluorescent images showing Chronos-GFP-expressing mPFC fibers (green) and Chrimson-tdTomato-expressing neurons (red) in the DMS. Images shown in b is representative of 3 experiments of 3 rats. (**C**) Pairing oHFS with oPSD produced robust LTP in the DMS (119.06 ± 4.69% of baseline [BL], $t_{(6)}$ = -4.07, P = 0.0066; n = 7 slices, 4 rats). oHFS alone did not alter fEPSP/PS (99.60 ± 3.12% of BL, $t_{(7)}$ = 0.13, P = 0.90; n = 8 slices, 5 rats). (**D**) oPSD alone did not induce LTP (104.55 ± 3.15% of BL, $t_{(6)}$ = -1.44, P = 0.20; n = 7 slices, 3 rats). (**E**) Dual-channel optogenetic induction of LTP was blocked by APV (98.06 ± 3.27% of BL; $t_{(8)}$ = 0.59, P = 0.57; n = 9 slices, 5 rats). (**F**) *Npas4* mRNA levels were significantly increased following paired oHFS+oPSD, but not after oHFS or oPSD only. $F_{(3,30)}$ = 3.86, P = 0.019; *P < 0.05; n = 10 (Control), 9 (oHFS), 5 (oPSD), and 10 (oHFS+oPSD) rats. Two-sided paired t test for C-E; one-way ANOVA followed by SNK test for F. Data are presented as mean ± s.e.m.

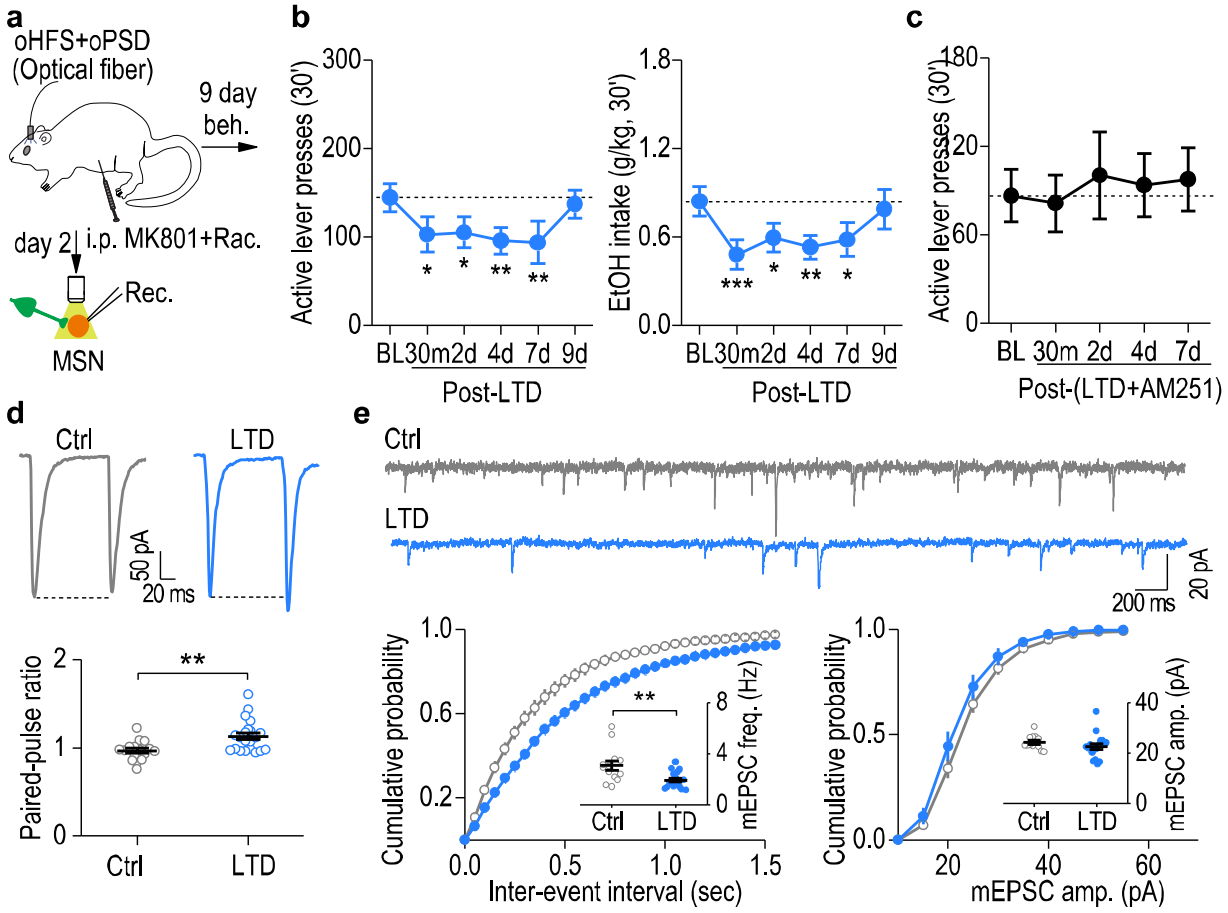

Figure 3.4. *In vivo* LTD induction caused a long-lasting reduction of alcohol-seeking behavior in an eCB-dependent manner.

(**A**) Schematic of the *in vivo* LTD-inducing protocol (oHFS+oPSD+MK801+raclopride) and *ex vivo* LTD measurement. MK801 (0.1 mg/kg) and raclopride (0.01 mg/kg) were systemically administered 15 min before the optogenetic stimulation. (**B**) Delivery of the *in vivo* LTD-inducing protocol in the DMS produced a long-lasting decrease in active lever presses (left, $F_{(5,38)} = 3.89$, $P = 0.006$) and alcohol intake (right, $F_{(5,35)} = 5.17$, $P = 0.0012$). $^{*}P < 0.05$, $^{**}P < 0.01$, $^{***}P < 0.001$ vs. baseline (BL); $n = 9$ rats. (**C**) Delivery of the *in vivo* LTD-inducing protocol in the presence of AM251 failed to alter active lever presses. $F_{(4,31)} = 0.40$, $P = 0.81$; $n = 9$ rats. (**D, E**) Delivery of the *in vivo* LTD-inducing protocol produced a long-lasting depression of glutamatergic transmission in the DMS on day 2 post-stimulation. (D) Top, sample traces showing paired-pulse ratios (100-ms inter-stimulus interval) measured in fluorescent neurons from LTD-induced rats and their controls (without light stimulation). Bottom, averaged data showing an increased paired-pulse ratio after LTD induction. $t_{(36)} = -3.31$, $P = 0.0021$; $n = 17$ neurons, 3 rats (Ctrl) and 21 neurons, 5 rats (LTD). (E) Top, representative traces of mEPSCs in fluorescent neurons in LTD-induced and control rats. Bottom, cumulative distributions of inter-event intervals and amplitudes of mEPSCs. Inset, reduced frequency (left), but not amplitude (right), of mEPSCs after *in vivo* LTD induction. $t_{(28)} = 2.97$, $P = 0.006$ for frequency; $t_{(28)} = 1.11$, $P = 0.28$ for amplitude; $n = 13$ neurons, 3 rats (Ctrl) and 17 neurons, 3 rats (LTD). One-way RM ANOVA for B, C; Two-sided unpaired *t* test for D, E. Data are presented as mean ± s.e.m.

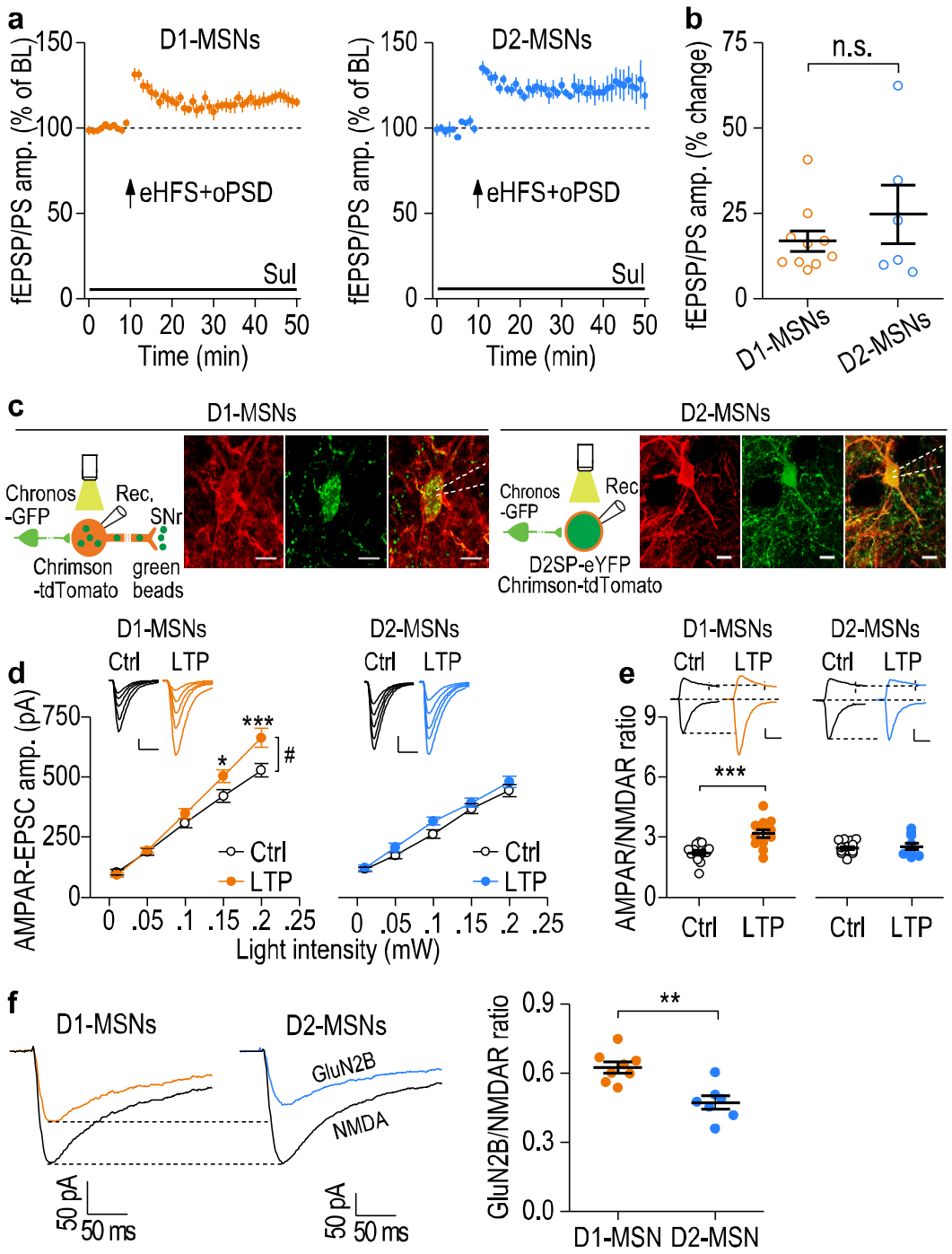

Figure 3.5. Corticostriatal LTP was preferentially induced in DMS D1-MSNs.
(A) AAV-DIO-ChR2-mCherry was infused into the DMS of D1-Cre and D2-Cre mice. Pairing of eHFS and oPSD induced LTP in both D1-MSNs (116.88 ± 3.07% of baseline [BL], $t_{(9)}$ = -5.49, P = 0.00038; n = 10 slices, 5 mice) and D2-MSNs (124.79 ± 8.58% of BL, $t_{(5)}$ = -2.89, P = 0.034; n = 6 slices, 5 mice). (**B**) There was no significant difference (n.s.) in D1- and D2-MSN LTP. $t_{(14)}$ = -1.04, P = 0.32. (**C**) Left, experimental design and sample images of retrograde bead labeling of a D1-MSN. AAV-Chronos-GFP, AAV-Chrimson-tdTomato, and green beads were infused into the mPFC, DMS, and SNr, respectively. Right, experimental design and sample images of labeling of a D2-MSNs with D2SP-eYFP. AAV-D2SP-eYFP was infused into the DMS. Scale bar: 10 µm. (**D**) Left, *In vivo* LTP induction resulted in higher AMPAR-EPSC amplitudes in D1- (left), but not D2- (right), MSNs from LTP-induced (LTP) rats, as compared with rats that were not exposed to light stimulation (Ctrl). Both groups of rats were trained to self-administer alcohol. D1-MSNs: $F_{(1,95)}$ = 4.72, P = 0.04; n = 13 neurons, 4 rats (Ctrl) and 13 neurons, 5 rats (LTP). D2-MSNs: $F_{(1,90)}$ = 2.11, P = 0.16; n = 14 neurons, 4 rats (Ctrl) and 11 neurons, 5 rats (LTP). Scale bars: 20 ms, 100 pA. (**E**) Left, the AMPAR/NMDAR ratio increased in D1- (Left), but not D2- (Right), MSNs after *in vivo* LTP induction. D1-MSNs: $t_{(25)}$ = -4.43, P = 0.00016; n = 15 neurons, 5 rats (Ctrl) and 12 neurons, 5 rats (LTP). D2-MSNs: $t_{(22)}$ = -0.52, P = 0.61; n = 14 neurons, 5 rats (Ctrl) and 10 neurons, 5 rats (LTP). Scale bars: 20 ms, 100 pA. (**F**) Operant alcohol self-administration resulted in a higher GluN2B/NMDA ratio in D1-MSNs than in D2-MSNs. Left and middle, sample trace of NMDAR-EPSCs in the absence or presence of Ro 25-6981 (0.5 µM). Right, summarized data of the ratios in D1-MSNs and D2-MSNs. $t_{(13)}$ = 4.16, P = 0.0011; n = 8 neurons, 5 rats (D1-MSNs), n = 7 neurons, 5 rats (D2-MSNs). Two-sided paired t test for A; Two-sided unpaired t test for B, E, F; two-way RM ANOVA for D. Data are presented as mean ± s.e.m.

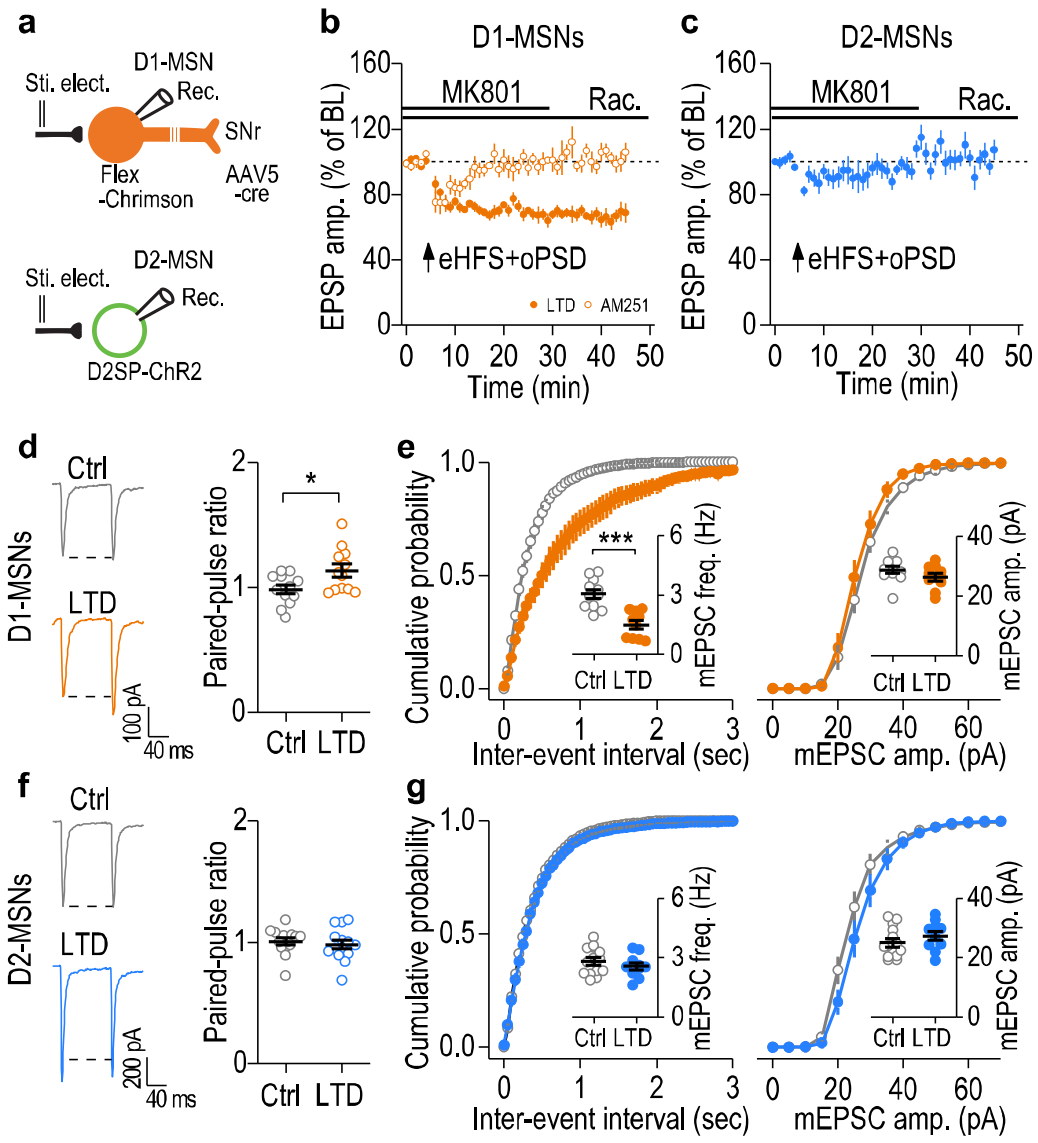

Figure 3.6. Corticostriatal LTD was preferentially induced in DMS D1-MSNs.
(**A**) Schematic of viral infusion and whole-cell recordings of rat D1- or D2-MSNs. (**B**) Paired eHFS and oPSD in the presence of NMDAR and D2R antagonists caused a robust LTD in DMS D1-MSNs (66.99 ± 4.56% of baseline [BL], $t_{(7)} = 7.23$, $P = 0.00017$; $n =$ 8 neurons, 5 rats), which was completely abolished by AM251 (3 μM) (102.82 ± 4.28% of BL, $t_{(6)} = -0.66$, $P = 0.53$; $n = 7$ neurons, 3 rats). (**C**) Paired eHFS and oPSD in the presence of NMDAR and D2R antagonists did not induce LTD in D2-MSNs (100.08 ± 5.15% of BL, $t_{(7)} = -0.02$, $P = 0.99$; $n = 8$ neurons, 3 rats). (**D**) Sample traces and averaged data showing an increased paired-pulse ratio in D1-MSNs 2 days after *in vivo* LTD induction. $t_{(22)} = -2.45$, $P = 0.023$; $n = 12$ neurons, 4 rats (Ctrl) and 12 neurons, 3 rats (LTD). (**E**) *In vivo* optogenetic LTD induction reduced the mEPSC frequency (left), but not the mEPSC amplitude (right) of DMS D1-MSNs. $t_{(19)} =$ 5.00, $P < 0.0001$ for frequency; $t_{(19)} = 1.30$, $P = 0.21$ for amplitude; $n = 11$ neurons, 4 rats (Ctrl) and 10 neurons, 3 rats (LTD). (**F**) *In vivo* LTD induction did not change paired-pulse ratios in D2-MSNs. $t_{(26)} = 0.59$, $P = 0.56$; $n = 14$ neurons, 4 rats (Ctrl) and 14 neurons, 3 rats (LTD). (**G**) *In vivo* LTD induction did not alter the mEPSC frequency (left, inset) or the mEPSC amplitude (right) in DMS D2-MSNs. $t_{(22)} = 0.95$, $P = 0.35$ for frequency; $t_{(22)} = -1.11$, $P = 0.28$ for amplitude; $n = 14$ neurons, 4 rats (Ctrl) and 10 neurons, 3 rats (LTD). Two-sided paired *t* test for B, C; Two-sided unpaired *t* test for D-G. Data are presented as mean ± s.e.m.

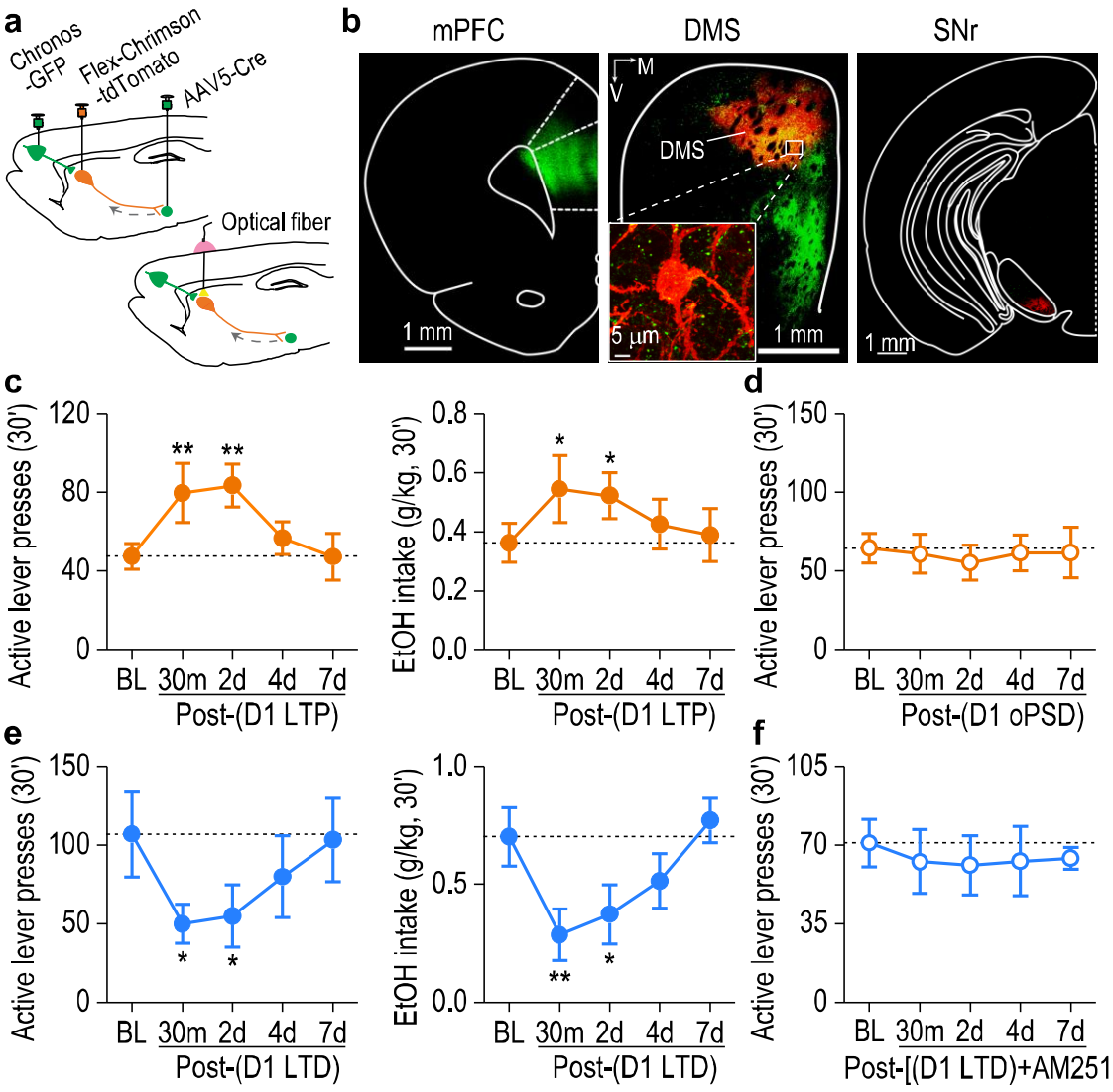

Figure 3.7. Selective *in vivo* LTP or LTD induction in D1-MSNs produced a long-lasting control of alcohol-seeking behavior. (**A**) Schematic showing viral infusion (top) and optical fiber implantation (bottom). (**B**) Representative fluorescent images showing that mPFC (left) and SNr infusions produced Chronos-expressing fibers (green) and Chrimson-tdTomato expression (red) in DMS D1-MSNs (middle), which project to the SNr (right). Images shown in b is representative of 3 experiments of 3 rats. (**C**) Paired oHFS of mPFC inputs and oPSD of D1-MSNs induced long-lasting increases in active lever presses (left, $F_{(4,24)} = 6.02$, $P = 0.0017$) and alcohol intake (right, $F_{(4,24)} = 3.74$, $P = 0.017$). $^{*}P < 0.05$, $^{**}P < 0.01$ vs. baseline (BL); $n = 8$ rats. (**D**) *In vivo* delivery of oPSD alone in DMS D1-MSNs did not alter active lever presses for alcohol. $F_{(4,18)} = 0.36$, $P = 0.83$; $n = 6$ rats. (**E**) Delivery of the *in vivo* LTD-inducing protocol to mPFC inputs onto DMS D1-MSNs produced a long-lasting attenuation in active lever presses (left, $F_{(4,23)} = 4.07$, $P < 0.0001$) and alcohol intake (right, $F_{(4,15)} = 6.67$, $P = 0.0027$). $^{*}P < 0.05$, $^{**}P < 0.01$ vs. BL; $n = 7$ rats for active lever presses and $n = 6$ rats for alcohol intake. (**F**) *In vivo* delivery of the LTD-inducing protocol in the presence of AM251 (oHFS+oPSD+MK801+raclopride+AM251) failed to alter active lever presses for alcohol. $F_{(4,22)} = 0.12$, $P = 0.97$, $n = 7$ rats. One-way RM ANOVA for C-F. Data are presented as mean ± s.e.m.

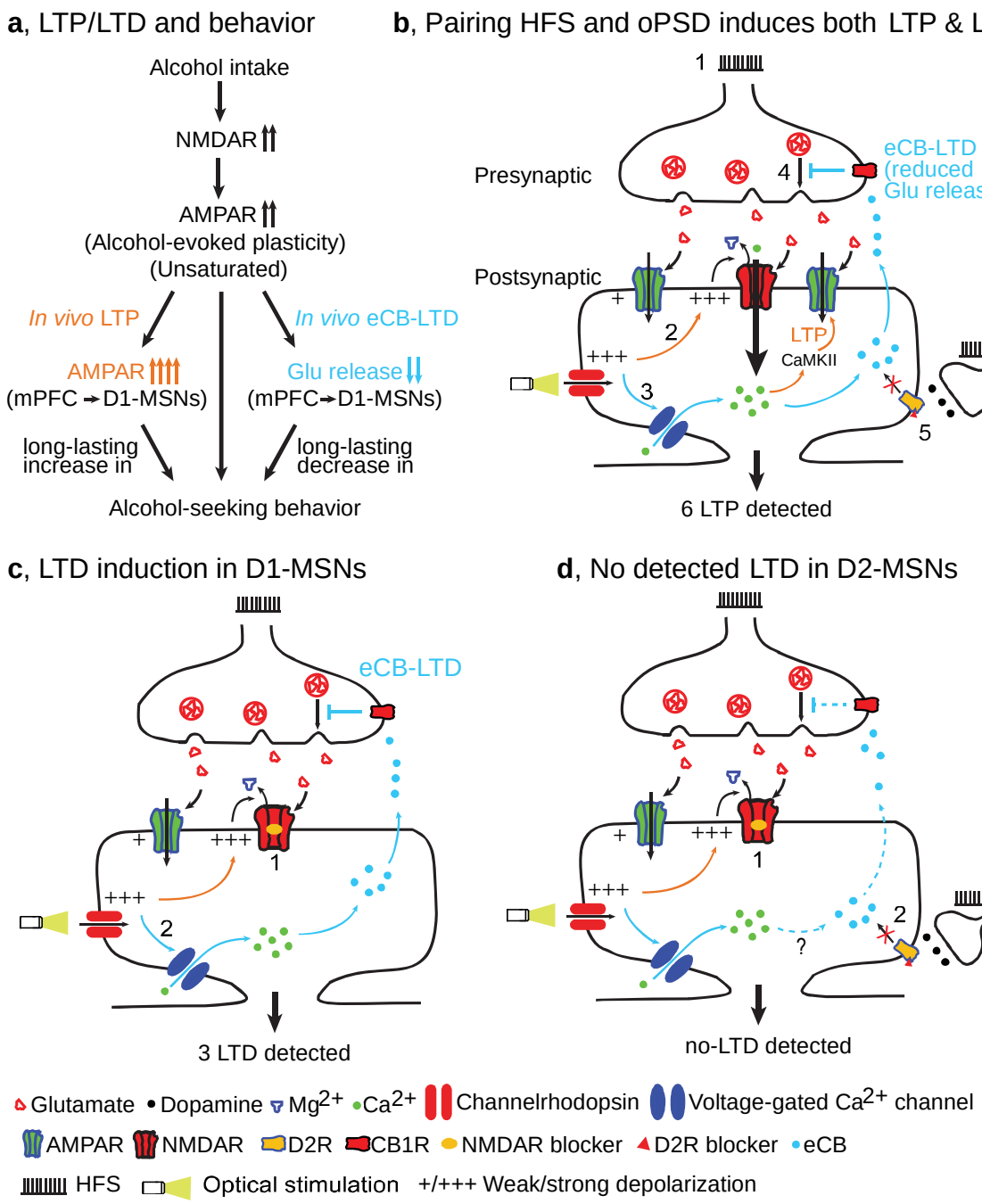

Figure 3.8. Model of bidirectional and long-lasting control of alcohol-seeking behavior by corticostriatal plasticity. (**A**) Alcohol intake facilitates NMDAR activity, leading to potentiation of AMPAR activity (unsaturated alcohol-evoked plasticity). This is further potentiated by *in vivo* LTP induction at mPFC inputs to DMS D1-MSNs, producing a long-lasting enhancement of alcohol-seeking behavior. Conversely, *in vivo* eCB-LTD induction at the same synapses elicited a long-lasting suppression of this behavior. (**B**) Paired HFS and oPSD induces both LTP and LTD, but only LTP is detected. 1, HFS causes presynaptic release of glutamate, which activates AMPARs. The resultant weak membrane depolarization is insufficient to remove the Mg^{2+} blockade of NMDARs and thus fails to induce LTP. 2, Optical stimulation of channelrhodopsin expressed on postsynaptic neurons causes strong membrane depolarization (oPSD). This is sufficient to remove Mg^{2+} blockade of NMDARs, leading to greater Ca^{2+} influx, activation of Ca^{2+}/calmodulin-dependent protein kinase II (CaMKII) signaling pathways, and consequently AMPAR insertion (LTP induction). 3, oPSD also opens voltage-gated Ca^{2+} channels, causing Ca^{2+} influx and production of endocannabinoids; these are retrogradely released into the synaptic cleft, where they activate presynaptic CB1Rs. 4, CB1R activation reduces glutamate release (eCB-LTD induction). 5, D2R antagonists are used to blocking D2R-mediated eCB-LTD, which may occur following eHFS *ex vivo* or oHFS *in vivo*. 6, Since the magnitude of LTP (~31%) is greater than that of LTD (~13%), only LTP is detected. (**C**) LTD induction and detection in D1-MSNs. Since LTP induction is blocked by NMDAR antagonists (1) and eCB-LTD is induced (2), only eCB-LTD is detected (3). (**D**) No LTD is detected in D2-MSNs because LTP is blocked by NMDAR antagonists (1) and eCB-LTD is blocked by D2R antagonists (2).

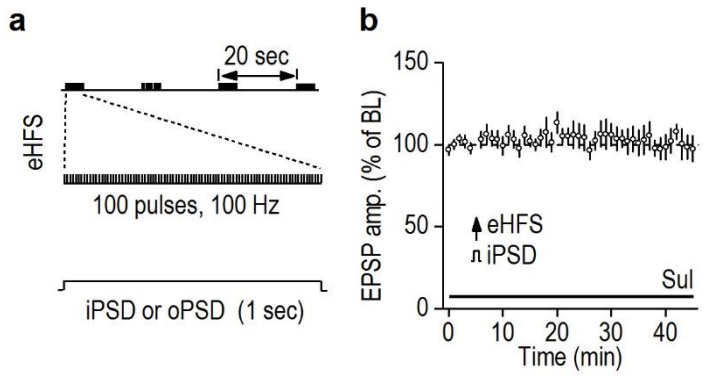

Figure 3.9. (Supplementary Figure 1 in Ma et al., 2018) Pairing of eHFS with somatic current injection-induced postsynaptic depolarization (iPSD) did not induce LTP in DMS slices of adult rats.
(**A**) Schematic illustration of LTP-inducing protocols. Presynaptic eHFS consists of 4 trains of stimuli at an interval of 20 sec, and each train contains 100 pulses at 100 Hz. eHFS was delivered alone or paired with somatic current injection-induced (iPSD) or optogenetically induced postsynaptic depolarization (oPSD). (**B**) Paired eHFS+iPSD did not induce LTP in DMS slices of adult rats (102.43 ± 6.47 % of baseline, $t_{(6)} = -0.38$, $P = 0.72$; paired *t* test. $n = 7$ slices from 5 rats). Whole-cell current-clamp recordings were conducted to measure excitatory postsynaptic potentials (EPSPs). Step currents (250 pA, 1 sec) were injected through the patch pipette during four trains of eHFS. Sulpiride was bath-applied to block LTD and favor LTP induction. Data are presented as mean ± s.e.m.

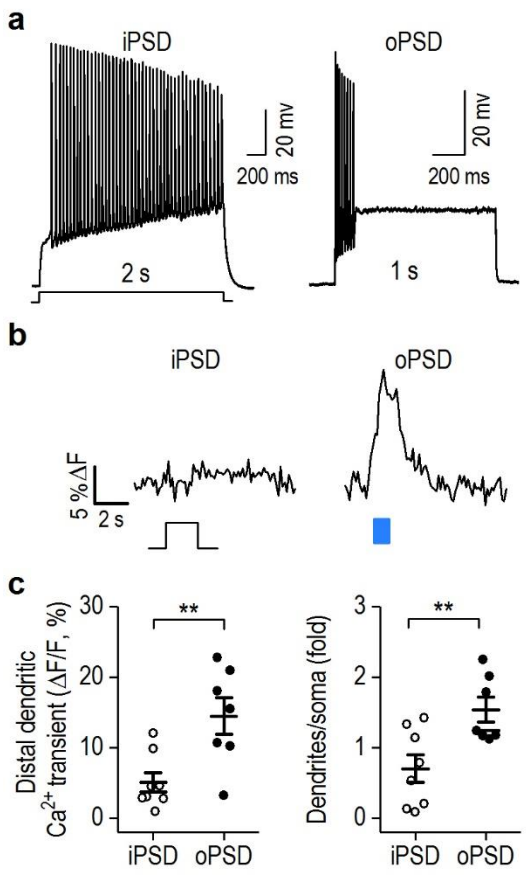

Figure 3.10. (Supplementary Figure 2 in Ma et al., 2018) oPSD induced greater Ca^{2+} transients in distal dendrites than iPSD. AAV-GCaMP6s and AAV-C1V1-eYFP were co-infused into the DMS, and whole-cell current-clamp recordings were conducted in C1V1-expressing neurons. A 2-sec step current was injected through the patch pipette, and 1-sec light stimulation (590 nm) was delivered through the objective lens. (**A**) Sample whole-cell recording showing action potentials elicited by iPSD or oPSD. Note that iPSD-induced a train of spikes, whereas oPSD induced a few spikes, which may be due to depolarization block(Kleinlogel et al., 2011). (**B**) Representative traces of dendritic Ca2+ transients induced by iPSD (left) or by oPSD (right). (**C**) oPSD induced significantly greater Ca2+ transients in the distal dendrites than did iPSD. Left, comparison of dendritic Ca2+ transients induced by iPSD and oPSD. t(13) = -3.34, **P = 0.0054. Right, comparison of normalized dendritic Ca2+ transients to the somatic ones. t(13) = -3.15, **P = 0.0077; Two-sided unpaired t test. n = 8 neurons, 5 rats (iPSD) and 7 neurons, 3 rats (oPSD). Data are presented as mean ± s.e.m.

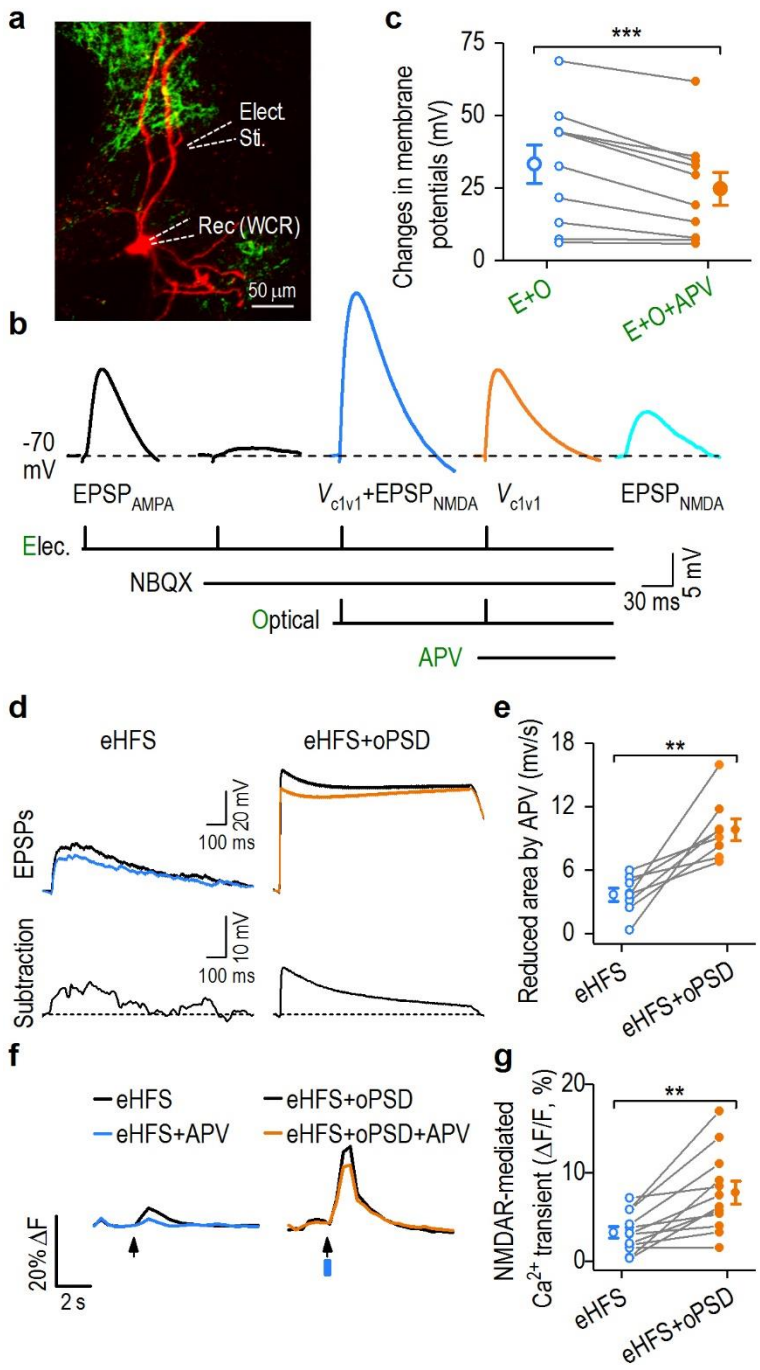

Figure 3.11. (Supplementary Figure 3 in Ma et al., 2018) oPSD enhanced NMDAR-mediated EPSPs (EPSP$_{NMDA}$) and Ca^{2+} influx.

AAV-C1V1-eYFP (a-e), AAV-Chrimson-tdTomato and AAV-GCaMP6s (f, g) were infused into the DMS. (**A**) Sample confocal image of an Alexa Fluor 594-filled C1V1-eYFP-expressing neuron showing the placement of stimulating (150 µm from the soma) and recording electrodes. (**B**) Representative traces depicting optogenetic-mediated EPSP in the distal dendrites in response to single synaptic stimulation. After blockade of the AMPAR-mediated EPSP (EPSP$_{AMPA}$) with NBQX (10 µM), simultaneous presynaptic stimulation and oPSD elicited a depolarization (C1V1-mediated response [V_{c1v1}] + EPSP$_{NMDA}$) that was reduced by bath application of APV (V_{c1v1}). The optogenetic-mediated EPSP$_{NMDA}$ was calculated by digital subtraction of V_{c1v1} from V_{c1v1} + EPSP$_{NMDA}$. (**C**) Comparison of the amplitudes of the electrically and optogenetically induced responses in the absence (E+O) and presence (E+O+APV) of APV. $t_{(9)}$ = 4.93, ***P = 0.00082; n = 10 neurons, 3 rats. (**D**) Top, sample EPSP traces in response to eHFS in the presence (color) and absence (black) of APV. Bottom, traces were generated by digital subtraction of the EPSP with APV from that without APV. (**E**) Paired eHFS+oPSD induced a greater area under EPSP$_{NMDA}$ than eHFS alone. $t_{(7)}$ = -4.50, **P = 0.0028; n = 8 neurons, 4 rats per group. (**F**) Representative traces of Ca^{2+} transients in distal dendrites in response to eHFS (left) and eHFS+oPSD (right) with and without APV application. (**G**) eHFS+oPSD induced greater NMDAR-mediated Ca^{2+} transients than that of eHFS. $t_{(11)}$ = 4.30, **P = 0.0012; n = 12 neurons, 3 rats per group. Two-sided paired t test for C, E, G. Data are presented as mean ± s.e.m.

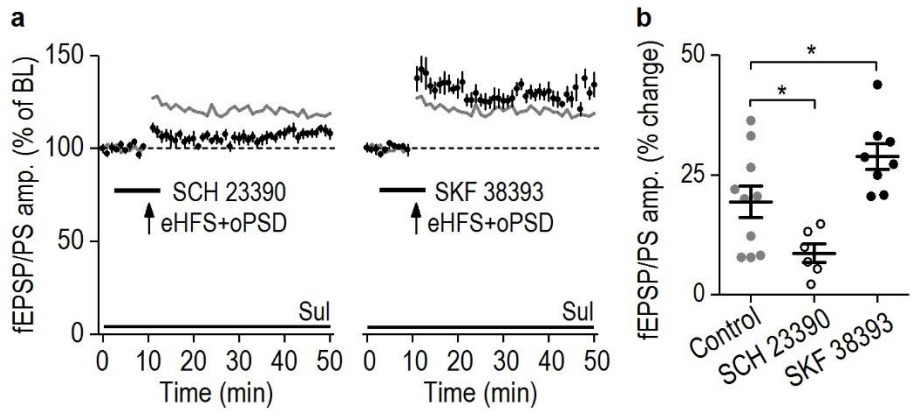

Figure 3.12. (Supplementary Figure 4 in Ma et al., 2018) Dopamine signaling regulated optogenetic LTP in DMS slices.
(**A**) Optogenetic induction of LTP in the presence of the dopamine D1R antagonist, SCH 23390 (10 μM, left), and agonist, SKF 38393 (20 μM, right) in DMS slices of rats. AAV-C1V1-eYFP was infused into the DMS. The grey lines are the control LTP from **Figure 3.1d** for reference. Left, suppression of LTP by SCH 23390 (108.65 ± 1.95% of baseline, $t_{(5)}$ = -4.44, P = 0.0068; n = 6 slices, 6 rats). Right, enhancement of LTP by SKF 38393 (128.84 ± 2.69% of baseline, $t_{(7)}$ = -10.70, P < 0.0001; n = 8 slices, 5 rats). Sulpiride was bath-applied to block LTD and favor LTP induction. (**B**) Comparison of the magnitudes of LTP in control and in the presence of SCH 23390 and of SKF 38393 in rats. The grey dots are from **Figure 3.1d** for comparison (SCH 23390 vs Control: $t_{(14)}$ = 2.33, *P = 0.035; SKF 38393 vs Control: $t_{(16)}$ = -2.56, *P = 0.021). n = 10 slices from 6 rats (Control), 6 slices from 6 rats (SCH 23390), and 8 slices from 5 rats (SKF 38393). Two-sided paired *t* test for A; two-sided unpaired *t* test for B. Data are presented as mean ± s.e.m.

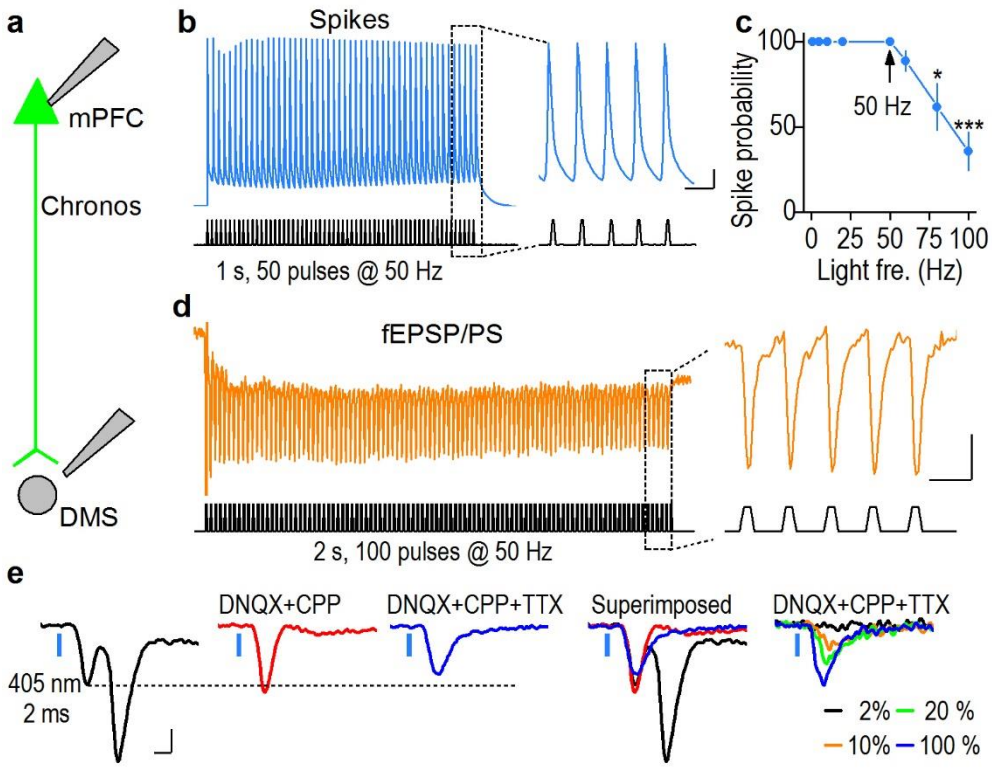

Figure 3.13. (Supplementary Figure 5 in Ma et al., 2018) Verification of the fidelity of spiking in mPFC neurons expressing Chronos and optical fEPSP/PS in DMS slices.

(**A**-**E**) AAV-Chronos-GFP was infused into the mPFC and coronal sections containing the mPFC or DMS were prepared eight weeks after infusion. (**A**) Schematic illustration of whole-cell recording in Chronos-expressing mPFC neurons and field recording in the DMS area containing the Chronos-expressing fibers in separated experiments. (**B**) Whole-cell recording showing that Chronos-expressing mPFC neurons can fire spikes in response to a train of light pulses (2 ms) at 50 Hz. Scale bars: 20 ms, 10 mV. (**C**) 405-nm light-driven spike probability over a range of frequencies. $F_{(3,12)} = 17.51$, $^{*}P < 0.05$, $^{***}P < 0.001$; $n = 6$ neurons, 2 rats. (**D**) Field recording demonstrating that Chronos-expressing mPFC fibers in the DMS can exert fEPSP/PS in response to 50-Hz train stimulation of light. Scale bars: 20 ms, 10 μV. (**E**) An example recording of a light-evoked fEPSP/PS, which was blocked by a mixture of AMPAR and NMDAR antagonists CNQX+CPP. Note that the remaining response in the presence of CNQX and CPP was partially blocked by TTX and completely by reducing light intensity to 2% of the original light intensity. Scale bars: 5 ms, 0.2 mV. One-way RM ANOVA for C. Data are presented as mean ± s.e.m.

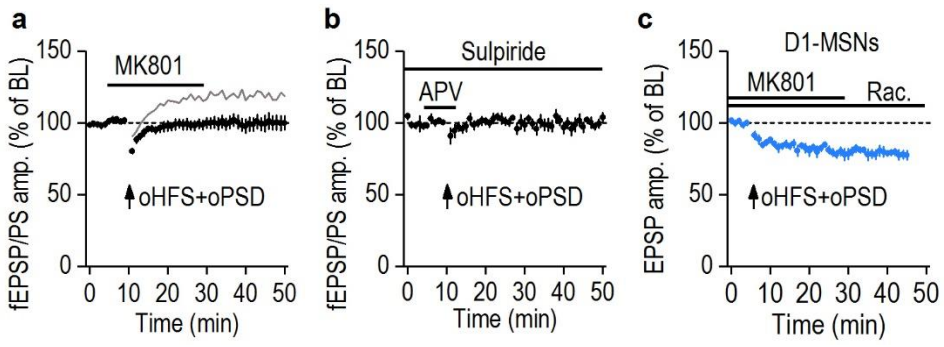

Figure 3.14. (Supplementary Figure 6 in Ma et al., 2018) LTD was not observed in field recording but in whole-cell recording of D1-MSNs.

(**A**) Paired oHFS+oPSD in the presence of MK801 (50 µM) failed to induce LTD in DMS slices (99.76 ± 4.99% of baseline, $t_{(7)}$ = 0.05, P = 0.96; n = 8 slices, 6 rats). The gray line is the averaged data from **Figure 3.2c** for comparison. (**B**) In presence of the D2R antagonist, sulpiride, and APV, paired oHFS+oPSD failed to induce LTD (99.49 ± 2.25% of baseline, $t_{(5)}$ = 0.22, P = 0.83; n = 6 slices, 3 rats). (**C**) Optogenetic induction of corticostriatal LTD in DMS D1-MSNs. AAV-Chronos-GFP was infused into the mPFC for selective stimulation of this input; the retrograde AAV5-Cre was infused into the SNr and AAV-Flex-Chrimson-tdTomato into the DMS for selective oPSD of D1-MSNs. Whole-cell recording was conducted in tdTomato-positive neurons to measure EPSPs before and after paired oHFS+oPSD. The pairing in the presence of MK801 and raclopride induced LTD in D1-MSNs (78.28 ± 2.60% of baseline, $t_{(6)}$ = 8.35, P = 0.00016; n = 7 neurons, 4 rats). Two-sided paired t test for A-C. Data are presented as mean ± s.e.m.

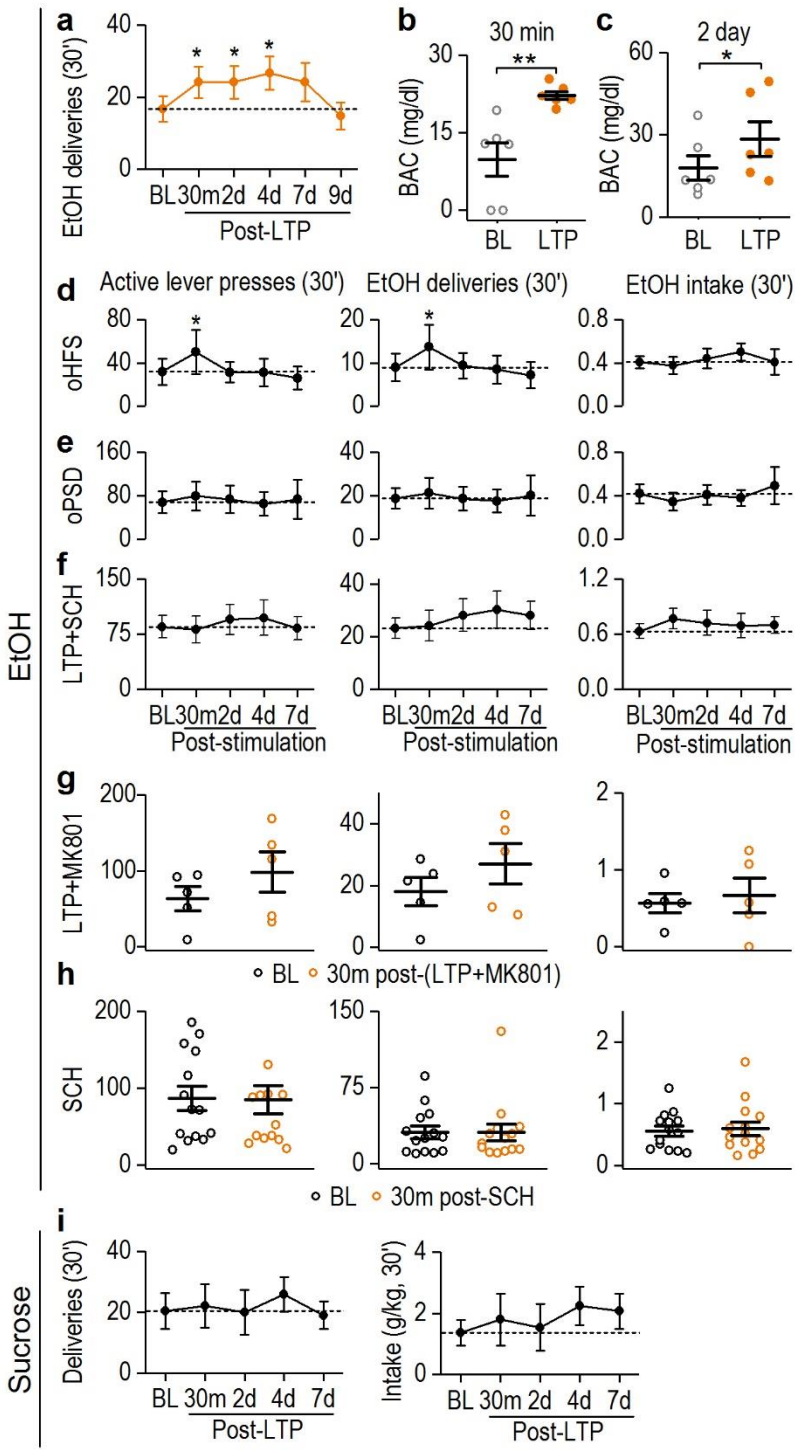

Figure 3.15. (Supplementary Figure 7 in Ma et al., 2018) *In vivo* delivery of the optogenetic LTP-inducing protocol facilitated alcohol-, but not sucrose-, seeking behavior.

(**A**) *In vivo* optogenetic LTP induction persistently increased alcohol deliveries. $F_{(5,54)} = 3.83$, $P = 0.0048$, $^*P < 0.05$ vs. baseline (BL). $n = 14$ rats. (**B,C**) *In vivo* LTP induction increased blood alcohol concentration (BAC) at 30 min (b) and 2 days (c) after induction. 30 min: $t_{(5)} = -4.25$, $P = 0.0081$, $n = 6$ rats; 2 days: $t_{(5)} = -3.36$, $P = 0.02$, $n = 6$ rats. $^*P < 0.05$ and $^{**}P < 0.01$ vs. baseline (BL). (**D**) *In vivo* oHFS stimulation alone did not persistently alter lever presses for alcohol (left; $F_{(4,17)} = 4.38$, $P = 0.013$, $n = 6$ rats), alcohol deliveries (middle; $F_{(4,17)} = 4.67$, $P = 0.01$, $n = 6$ rats), or alcohol intake (right; $F_{(4,17)} = 0.59$, $P = 0.67$, $n = 6$ rats). $^*P < 0.05$. (**E**) *In vivo* oPSD stimulation alone did not alter lever presses for alcohol (left; $F_{(4,26)} = 0.63$, $P = 0.65$, $n = 8$ rats), alcohol deliveries (middle; $F_{(4,26)} = 0.41$, $P = 0.80$, $n = 8$ rats), or alcohol intake (right; $F_{(4,26)} = 0.6$, $P = 0.66$, $n = 8$ rats). (**F**) *In vivo* LTP induction in the presence of a D1R antagonist, SCH 23390 (SCH, 0.01 mg/kg), failed to alter lever presses (left; $F_{(4,40)} = 0.66$, $P = 0.63$), alcohol deliveries (middle; $F_{(4,39)} = 1.26$, $P = 0.30$), or alcohol intake (right; $F_{(4,39)} = 0.58$, $P = 0.68$). $n = 12$ rats. (**G**) *In vivo* LTP induction in the presence of MK801 failed to alter lever presses (left; $t_{(4)} = -2.09$, $P = 0.11$), alcohol deliveries (middle; $t_{(4)} = -2.07$, $P = 0.11$), or alcohol intake (right; $t_{(4)} = -0.60$, $P = 0.58$). $n = 5$ rats. (**H**) Systematic administration of SCH 23309 did not alter lever presses (left; $t_{(13)} = 0.16$, $P = 0.87$), alcohol deliveries (middle; $t_{(13)} = 0.03$, $P = 0.98$), or alcohol intake (right; $t_{(13)} = -0.85$, $P = 0.41$), as compared to baseline (BL). $n = 14$ rats. (**I**) *In vivo* LTP induction did not alter sucrose deliveries (left) or intake (right). Deliveries: $F_{(4,19)} = 0.84$, $P = 0.51$; intake: $F_{(4,18)} = 1.94$, $P = 0.15$, $n = 6$ rats. One-way RM ANOVA for A,D-F,I; two-sided paired *t* test for B, C, G, and H. Data are presented as mean ± s.e.m.

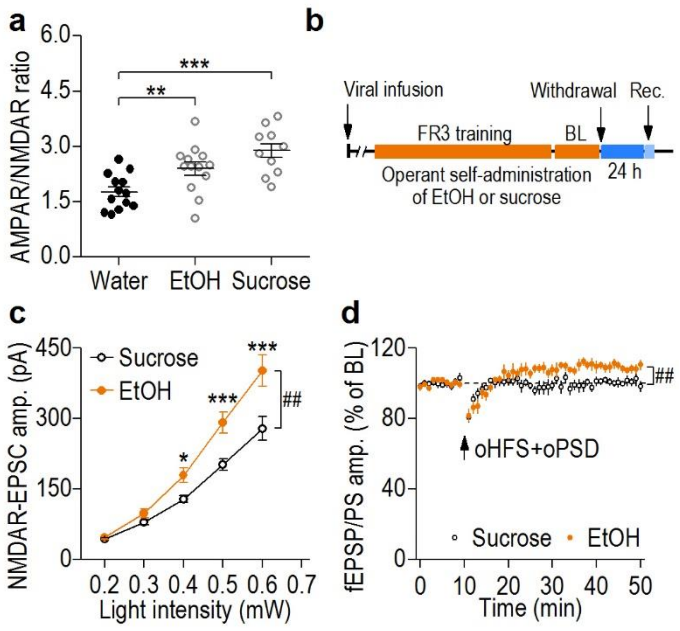

Figure 3.16. (Supplementary Figure 8 in Ma et al., 2018) Operant alcohol self-administration facilitated NMDAR activity and corticostriatal LTP induction in the DMS.

(**A**) Operant alcohol or sucrose self-administration increased the AMPAR/NMDAR ratio, as compared with age-matched water controls. Note that the data for the EtOH and sucrose groups (grey dots) are the same as in **Figure 3.3e** and **3.3g**, respectively. Rats in the water control group did not receive operant training. $F_{(2,34)}$ = 11.13, P = 0.00019; $^{**}P < 0.01$ and $^{***}P < 0.001$ versus Water; n = 13 neurons from 3 rats (Water), 13 neurons from 5 rats (EtOH), and 11 neurons from 5 rats (Sucrose). (**B**) Schematic illustration of the experimental procedure: After infusion of AAV-Chronos into the mPFC and AAV-Chrimson into the DMS as **Figure 3.3a**, rats underwent operant training but without *in vivo* light stimulation. Twenty-four hours after the last alcohol or sucrose exposure, DMS slices were prepared. (**C**) Operant alcohol self-administration caused higher NMDAR activity than did operant sucrose self-administration. Comparison of input-output relation for NMDAR-EPSCs between alcohol and sucrose groups. $F_{(1, 94)}$ = 9.62, $^{\#\#}P$ = 0.0049; n = 13 neurons from 4 rats (Sucrose) and 13 neurons from 5 rats (EtOH). (**D**) Paired oHFS+oPSD induced a LTP in DMS slices from alcohol-exposed [109.66 ± 1.92% of baseline (BL), $t_{(9)}$ = -5.02, P = 0.00072], but not from sucrose-exposed rats [100.81 ± 1.69% of BL, $t_{(6)}$ = -0.48, P = 0.65; Two-sided paired t test]. $^{\#\#}P$ = 0.0052; two-sided unpaired t test. n = 10 slices from 8 rats (EtOH) and 7 slices from 4 rats (Sucrose). One-way ANOVA followed by SNK test for A; two-way RM ANOVA followed by SNK test for C. Data are presented as mean ± s.e.m.

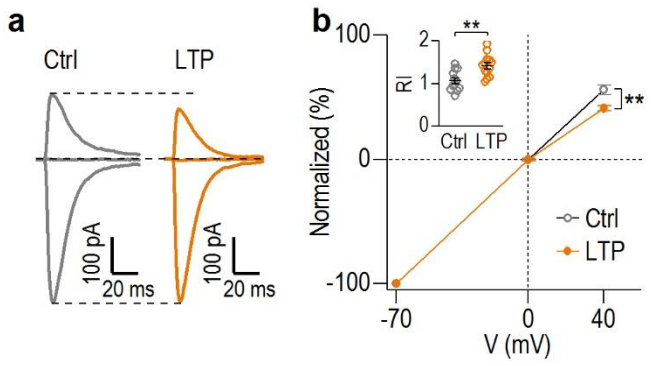

Figure 3.17. (Supplementary Figure 9 in Ma et al., 2018) *In vivo* LTP-inducing protocol increased AMPAR-EPSC rectification. (**A**) Representative traces recorded at -70, 0, and +40 mV in the control (Ctrl) and LTP groups. Control rats received training of operant alcohol self-administration, but without *in vivo* light stimulation. LTP rats received the same operant training and *in vivo* LTP induction two days before the recording. (**B**) I/V curves and rectification index (RI) of light-evoked AMPAR-EPSCs at -70, 0, and +40 mV show that *in vivo* LTP induction increased the RI of AMPAR-EPSCs. The curves were plotted by normalizing the EPSC amplitudes at +40 and 0 mV to the amplitude at -70 mV. $t_{(23)} = 3.54$, $^{**}P = 0.0018$ for difference in AMPAR-EPSCs at +40 mV; $t_{(23)} = -3.53$, $^{**}P = 0.0018$ for RI. $n = 12$ neurons from 3 rats (Ctrl) and 13 neurons from 3 rats (LTP). Two-sided unpaired *t* test. Data are presented as mean ± s.e.m.

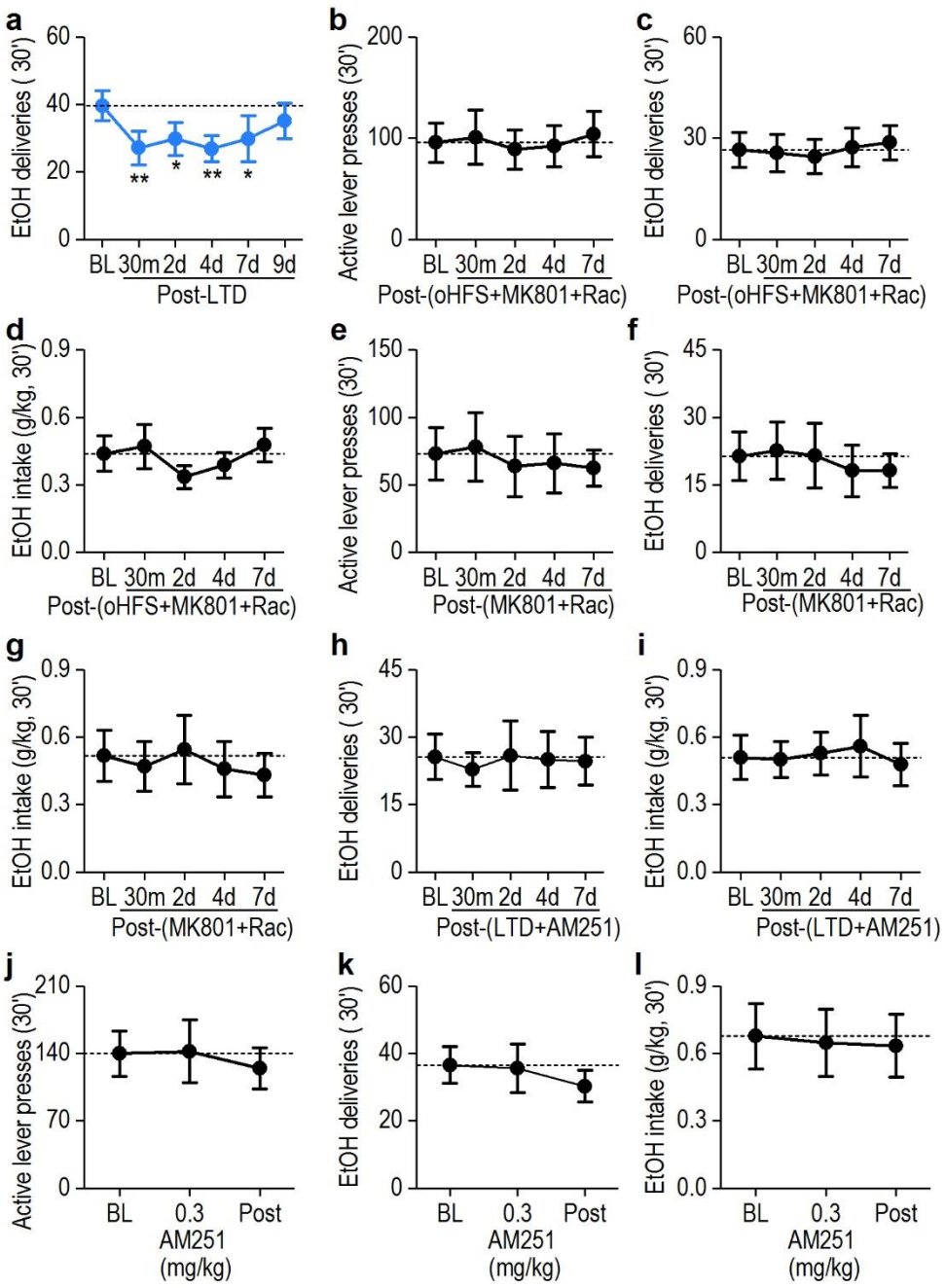

Figure 3.18. (Supplementary Figure 10 in Ma et al., 2018) *In vivo* delivery of the optogenetic LTD-inducing protocol reduced alcohol-seeking behavior in an endocannabinoid manner.

(**A**) *In vivo* delivery of LTD-inducing protocol (oHFS+oPSD+MK801+raclopride) in the DMS produced a long-lasting decrease in alcohol deliveries. $F_{(5,38)} = 4.27$, $P = 0.0035$. *$P < 0.05$, **$P < 0.01$ vs. baseline (BL). $n = 9$ rats. (**B-D**) *In vivo* oHFS stimulation in presence of the cocktail (MK801+raclopride) did not alter lever presses (B; $F_{(4,27)} = 0.50$, $P = 0.74$), alcohol deliveries (C; $F_{(4,27)} = 0.32$, $P = 0.86$), or alcohol intake (D; $F_{(4,27)} = 0.53$, $P = 0.72$). $n = 9$ rats. (**E-G**) Administration of the cocktail (MK801+raclopride) did not affect lever presses (E; $F_{(4,21)} = 2.12$, $P = 0.11$), alcohol deliveries (F; $F_{(4,21)} = 1.43$, $P = 0.26$), or alcohol intake (G; $F_{(4,21)} = 0.42$, $P = 0.79$). $n = 8$ rats. (**H-I**) *In vivo* optogenetic delivery of the LTD-inducing protocol (oHFS+oPSD+MK801+raclopride) in the presence of AM251 failed to alter alcohol deliveries (H; $F_{(4,31)} = 0.46$, $P = 0.76$), or alcohol intake (I; $F_{(4,32)} = 0.42$, $P = 0.79$). $n = 9$ rats. (**J-L**) Systemic administration of AM251 (0.3 mg/kg) did not affect lever presses (J; $F_{(2,17)} = 0.33$, $P = 0.73$), alcohol deliveries (K; $F_{(2,17)} = 1.05$, $P = 0.37$), or alcohol intake (L; $F_{(2,17)} = 2.31$, $P = 0.13$), as compared to before (baseline, BL) and after (Post) treatment. $n = 10$ rats. One-way RM ANOVA for all figures. Data are presented as mean ± s.e.m.

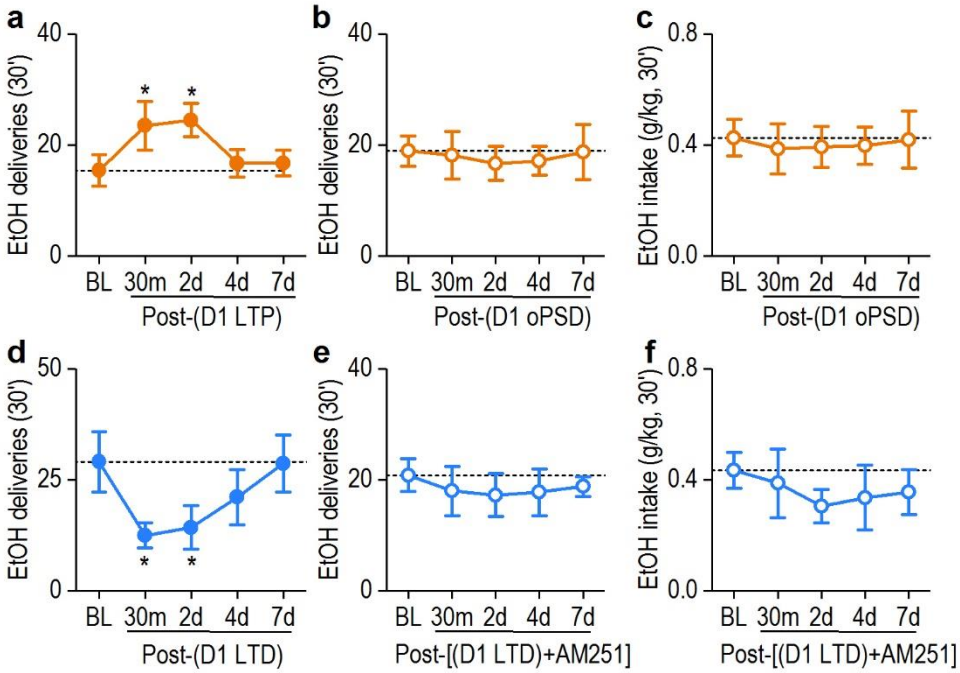

Figure 3.19. (Supplementary Figure 11 in Ma et al., 2018) *In vivo* delivery of the LTP- and LTD-inducing protocols to mPFC inputs onto D1-MSNs distinctly modulated alcohol seeking-behavior.

(**A**) *In vivo* delivery of the LTP-inducing protocol (oHFS+oPSD) to the mPFC input onto DMS D1-MSNs induced a persistent increase in alcohol-deliveries. **P* < 0.05 vs. baseline (BL). $F_{(4,23)}$ = 4.77, *P* = 0.0060; *n* = 8 rats. (**B**, **C**) *In vivo* oPSD of D1-MSNs alone did not alter alcohol deliveries (b; $F_{(4,18)}$ = 0.32, *P* = 0.86) or intake (c; $F_{(4,18)}$ = 0.76, *P* = 0.56; *n* = 6 rats). (**D**) *In vivo* delivery of LTD-inducing protocol (oHFS+oPSD+MK801+raclopride) to the mPFC input onto DMS D1-MSNs produced a long-lasting attenuation in alcohol deliveries. **P* < 0.05 vs. baseline (BL). $F_{(4,23)}$ = 4.99, *P* = 0.0048; *n* = 7 rats. (**E**,**F**) *In vivo* delivery of the LTD-inducing protocol in the presence of AM251 (oHFS+oPSD+MK801+raclopride+AM251) failed to alter alcohol deliveries (E; $F_{(4,20)}$ = 0.24, *P* = 0.91) or intake (F; $F_{(4,19)}$ = 1.67, *P* = 0.20; *n* = 7 rats). One-way RM ANOVA for all figures. Data are presented as mean ± s.e.m.

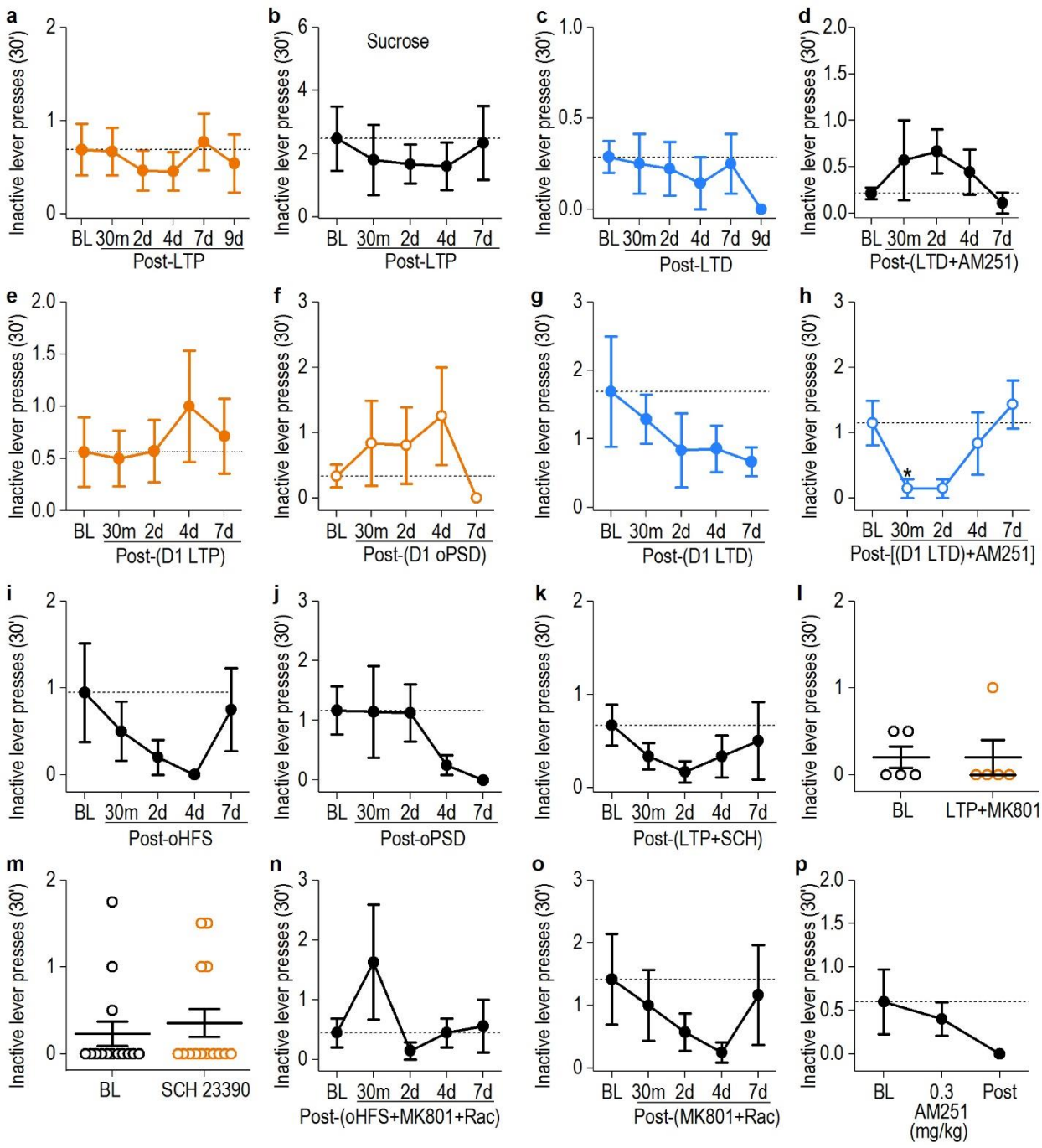

Figure 3.20. (Supplementary Figure 12 in Ma et al., 2018) *In vivo* delivery of the LTP- or LTD-inducing protocol did not alter inactive lever presses.

(**A**-**B**) *In vivo* delivery of the optogenetic LTP-inducing protocol did not change inactive lever presses for alcohol (A, $F_{(5,54)} = 0.41$, $P = 0.84$; $n = 14$ rats; related to Figure 3.3B) or for sucrose (B, $F_{(4,18)} = 0.31$, $P = 0.87$; $n = 6$ rats; related to Figure 3.3C). (**C**) *In vivo* delivery of the optogenetic LTD-inducing protocol did not change inactive lever presses for alcohol. $F_{(5,30)} = 1.05$, $P = 0.41$; $n = 9$ rats; related to Figure 3.4B. (**D**) *In vivo* delivery of the optogenetic LTD-inducing protocol in the presence of AM251 did not change inactive lever presses for alcohol. $F_{(4,30)} = 1.33$, $P = 0.28$; $n = 9$ rats; related to Figure 3.4C. (**E**-**F**) *In vivo* delivery of the LTP-inducing protocol (oHFS+oPSD) (E, $F_{(4,25)} = 0.53$, $P = 0.72$; $n = 8$ rats; related to Figure 3.7C) or oPSD (F, $F_{(4,16)} = 1.44$, $P = 0.27$; $n = 6$ rats; related to Figure 3.7D) to the mPFC input onto DMS D1-MSNs did not affect inactive lever presses for alcohol. (**G**) *In vivo* delivery of the LTD-inducing protocol to the mPFC input onto DMS D1-MSNs did not alter inactive lever presses for alcohol. $F_{(4,18)} = 1.59$, $P = 0.22$; $n = 6$ rats; related to Figure 3.7E. (**H**) *In vivo* delivery of the LTD-inducing protocol to the mPFC input onto DMS D1-MSNs in the presence of AM251 decreased inactive lever presses for alcohol only at 30 min, but not on day 2, 4, or 7. *$P < 0.05$ versus baseline (BL). $F_{(4,23)} = 5.04$, $P = 0.0046$; $n = 7$ rats; related to Figure 3.7F. (**I**-**J**) *In vivo* delivery of oHFS (I, $F_{(4,17)} = 1.86$, $P = 0.16$; $n = 6$ rats; related to Figure 3.5.14D) or oPSD (J, $F_{(4,25)} = 1.39$, $P = 0.26$; $n = 8$ rats; related to Figure 3.5.15E) did not cause any change on inactive lever presses for alcohol. (**K**-**L**) *In vivo* delivery of the LTP-inducing protocol in the presence of SCH 23390 (K, $F_{(4,43)} = 0.57$, $P = 0.69$; $n = 12$ rats; related to Figure 3.5.15F) or MK801 (L, $t_{(4)} = 0$, $P = 1$; $n = 5$ rats; related to Figure 3.5.15G) did not change the inactive lever presses for alcohol. (**M**) Systematic administration of SCH 23390 did not alter inactive lever presses at 30 min ($t_{(13)} = 0.16$, $P = 0.87$; $n = 13$ rats; related to Figure 3.5.15H). (**N**) *In vivo* delivery of oHFS with administration of MK801 and raclopride did not change inactive lever presses for alcohol. $F_{(4,28)} = 1.17$, $P = 0.34$; $n = 9$ rats; related to Figure 3.5.18B. (**O**) Systematic administration of a cocktail of MK801 and raclopride did not affect the inactive lever presses for alcohol. $F_{(4,24)} = 0.96$, $P = 0.45$; $n = 8$ rats; related to Figure 3.5.18E. (**P**) Systematic administration of AM251 (0.3 mg/kg) did not alter inactive lever presses for alcohol. $F_{(2,18)} = 2.04$, $P = 0.16$; $n = 10$ rats; related to Figure 3.10J. One-way RM ANOVA for Figures A-K and N-P; two-sided paired *t* test for Figures L and M. Data are presented as mean ± s.e.m.

CHAPTER IV

PRENATAL EXPOSURE TO ALCOHOL INDUCES FUNCTIONAL AND STRUCTURAL PLASTICITY IN DOPAMINE D1 RECEPTOR-EXPRESSING NEURONS OF THE DORSOMEDIAL STRIATUM[*]

4.1 Overview

Prenatal alcohol exposure (PAE) is a leading cause of hyperactivity in children. Excitation of dopamine D1 receptor-expressing medium spiny neurons (D1-MSNs) of the dorsomedial striatum (DMS), a brain region that controls voluntary behavior, is known to induce hyperactivity in mice. We therefore hypothesized that PAE-linked hyperactivity was due to persistently altered glutamatergic activity in DMS D1-MSNs. Female Ai14 tdTomato-reporter mice were given access to alcohol in an intermittent-access, 2-bottle choice paradigm before pregnancy, and following mating with male D1-Cre mice, through the pregnancy period, and until postnatal day (P) 10. Locomotor activity was tested in juvenile (P21) and adult (P133) offspring, and alcohol conditioned place preference (CPP) was measured in adult offspring. Glutamatergic activity in DMS D1-MSNs of adult PAE and control mice was measured by slice electrophysiology followed by measurements of dendritic morphology. Our voluntary maternal alcohol consumption model resulted in increased locomotor activity in juvenile PAE mice, and this hyperactivity was maintained into adulthood. Furthermore, PAE resulted in a higher alcohol-induced CPP in adult offspring. Glutamatergic activity onto DMS D1-MSNs was also enhanced by PAE. Finally, PAE increased dendritic complexity in DMS D1-MSNs in adult offspring. Our

[*] This chapter is re-printed with permission from "Prenatal exposure to alcohol induces functional and structural plasticity in dopamine D1 receptor-expressing neurons of the dorsomedial striatum" by Cheng Y, Wang X, Wei X, Xie X, Melo S, Miranda RC, Wang J, 2018. *Alcoholism: Clinical and Experimental Research*, 42, 1493-1502. Copyright [2018] by Wiley-Blackwell.

model of PAE does result in persistent hyperactivity in offspring. In adult PAE offspring, hyperactivity is accompanied by potentiated glutamatergic strength and afferent connectivity in DMS D1-MSNs, an outcome that is also consistent with the observed increase in alcohol preference in PAE offspring. Consequently, a PAE-sensitive circuit, centered within the D1-MSN may be linked to behavioral outcomes of PAE.

4.2 Introduction

Prenatal alcohol exposure (PAE) can result in a cluster of neurobehavioral and other developmental disabilities that are collectively termed fetal alcohol spectrum disorders (FASD)(Mattson et al., 2011; Riley et al., 2011). FASD is common and its worldwide prevalence in the general population is estimated at ~2.3% with a high of 11.3% in South Africa (Roozen et al., 2016). A recent Texas study reported that 8.4% of proportionately sampled newborns had biochemical evidence for PAE (Bakhireva et al., 2017), and in the US, FASD may account for between 1% and 5% of school-aged children (May et al., 2018). Attention deficit-hyperactivity disorder (ADHD) was found to be a very common co-morbid disorder in children with FASD (Lange et al., 2018), and hyperactivity has also been reported in animal models of PAE (Hausknecht et al., 2005; Shea et al., 2012; Idrus et al., 2014). Though ADHD and FASD exhibit overlap in behavioral indices (Infante et al., 2015), medications commonly used for ADHD are less effective in managing hyperactivity in FASD children (Frankel et al., 2006), and FASD children exhibit somewhat different patterns of cerebral cortical activation in response-inhibition tasks compared to ADHD children (Kodali et al., 2017) suggesting that neural mechanisms mediating loss of impulse control and hyperactivity due to PAE may differ from those mediating other forms of ADHD.

A few studies have suggested that ADHD-like hyperactivity following PAE is associated

with abnormal synaptic plasticity within the cerebral cortex and the striatum (Robbins, 2002; Emond et al., 2009; Sonuga-Barke et al., 2016). The striatum is the major nucleus of the basal ganglia and gates all the cortical inputs to the basal ganglia (Gunaydin and Kreitzer, 2016). The dorsomedial part of the striatum (DMS) controls voluntary behavior and has been strongly implicated in neurobiology of alcohol and substance use disorders (Wang et al., 2007; Gittis and Kreitzer, 2012; Volkow and Morales, 2015). Prenatal and adult exposure to alcohol has been shown to alter plasticity in DMS neurons (Yin et al., 2007; Rice et al., 2012; Wang et al., 2015; Cheng et al., 2017; Ma et al., 2018), though the cellular substrate for PAE in the DMS is unclear. The principal cells of the DMS, the medium spiny neurons (MSNs), can be divided into two neuronal populations with little overlap: D1 and D2-MSNs (Santana et al., 2009; Gerfen and Surmeier, 2011; Maia and Frank, 2011; Sippy et al., 2015). D1-MSNs are known to mediate "Go" actions (Gerfen and Surmeier, 2011; Maia and Frank, 2011; Sippy et al., 2015; Cheng et al., 2017) and overactivation of D1-MSNs in the dorsal striatum results in a hyperactivity in mice (Kravitz et al., 2010; Kravitz et al., 2012; Freeze et al., 2013). Previous studies have shown that PAE results in increased glutamatergic transmission in the basolateral amygdala (Baculis and Valenzuela, 2015) and medial prefrontal cortex (Louth et al., 2016), supporting the hypothesis that PAE facilitates excitatory neurotransmission in the DMS as well. Our previous studies found that excessive alcohol consumption in adult rodents selectively increased the activity of glutamatergic inputs onto D1-MSNs and altered the morphology of the D1-MSNs in the DMS (Wang et al., 2015; Cheng et al., 2017). We also found that interfering with the activity of D1-MSNs in the adult DMS resulted in altered alcohol intake and preference (Wang et al., 2015; Cheng et al., 2017; Ma et al., 2018). Thus, we hypothesized that PAE would cause glutamatergic and morphological plasticity in DMS D1-MSNs.

Collectively, our data show that in a voluntary consumption model, prenatal alcohol exposure results in increased alcohol preference, and as predicted, hyperactivity in affected offspring. Moreover, PAE resulted in increased glutamatergic activity and significant augmentation of dendritic complexity in D1-MSNs of the DMS, a group of neurons that have been implicated previously in both locomotor and alcohol seeking behaviors in the adult.

4.3 Results

4.3.1. Characterization of maternal volunteer alcohol drinking using the two-bottle choice paradigm

To model a natural human drinking pattern and establish high drinking level in mice, we initially trained adult female mice to drink 20% alcohol using the intermittent access two-bottle choice procedure for over 6 weeks (Ron and Barak, 2016; Cheng et al., 2017; Ma et al., 2018) (Figure 4.1A). Alcohol was not available during mating to prevent interruption of mating (Figure 4.1A). During pregnancy, the alcohol concentration was decreased to 10% to avoid premature pregnancy termination, and alcohol was available until P10 (Kleiber et al., 2011) (Figure 4.1A). During the drinking session, both water and alcohol bottles were available. To assess whether adult female mice achieved a high level of alcohol drinking in the pre-pregnancy period, alcohol intake was measured at the end of the drinking session in last two weeks of the training period (week 5 and 6). We found that the alcohol consumption was maintained at a high level (~20 g/kg/24 h) (Ron and Barak, 2016; Cheng et al., 2017), and did not change across weeks 5 and 6 (Figure 4.1B; $t_{(3)} = -0.94$, $p = 0.42$). Importantly, alcohol preference of pre-pregnant mice was more than 60%, and did not change across weeks 5 and 6 (Figure 4.1C; $t_{(3)} = 1.45$, $p = 0.24$). To examine whether mice underwent dehydration or malnutrition during the training, which could also impact the development of the offspring, water intake and body weight were also measured

in weeks 5 and 6. We did not find any significant change in their water intake nor body weight (Figure 4.1D and 1E; for 1D: $t_{(3)} = -1.82$, $p = 0.17$; for 1E: $t_{(3)} = -2.14$, $p = 0.12$). These results demonstrate that excessive alcohol drinking using intermittent access to alcohol two-bottle choice establishes high alcohol intake and preference in adult female mice without causing dehydration or malnutrition.

4.3.2. Prenatal exposure to alcohol elevates locomotor activity in childhood mice

To examine hyperactivity in juvenile (P21) PAE mice, we measured locomotor activity in the open field for 30 min (Sanchez Vega et al., 2013). Compared to the age-matched water control, PAE mice exhibited a longer overall traveled distance (Figure 4.2A; main effect of time: $F_{(5,90)} = 2.65$, $p = 0.028$; main effect of prenatal treatment: $F_{(1,18)} = 8.06$, $p = 0.011$; time X prenatal treatment interaction: $F_{(5,90)} = 2.97$, $p = 0.016$). For the first 10 min and the last 5 min, we observed a significant increase of travel distance in the PAE group than the age-matched control group (Figure 4.2A; 5 min: $q = 6.3$, $p = 0.00015$; 10 min: $q = 3.13$, $p = 0.031$; 30 min: $q = 3.13$, $p = 0.031$). Also, the total 30-min traveled distance was significantly higher in the PAE group compared to the age-matched water group (Figure 4.2B; $t_{(18)} = -2.84$, $p = 0.011$). Interestingly, the velocity of movement was lower in PAE mice than in their age-matched water controls (Figure 4.2C; $t_{(18)} = 2.22$, $p = 0.04$). However, PAE mice moved for a longer time period than their age-matched water controls (Figure 4.2D; $t_{(18)} = -3.18$, $p = 0.0052$). We also measured anxiety-liked behavior and found that PAE mice presented the periphery area of the open-field arena for significantly less time than control mice (Figure 4.2E; $t_{(18)} = 3.79$, $p = 0.0013$). Taken together, these results suggest that prenatal exposure to alcohol causes hyperactivity in juvenile (P21) mice, but with decreased movement velocity and lower anxiety.

4.3.3. PAE mice exhibit higher alcohol conditional place preference and preserve hyper-locomotor activity in adult age

It has been reported that prenatal exposure to cocaine induces CPP to cocaine in adult mice (Malanga et al., 2007). To assess whether prenatal exposure to alcohol can induce CPP to alcohol in adulthood, we performed an alcohol CPP test in PAE adult mice (at P133), and compared performance to age-matched water control. Mice were tested in a customized CPP apparatus with a neutral chamber and two test chambers that have different visual and tactile cues (Figure 4.3A). All mice were permitted to freely explore all chambers in the CPP apparatus before the conditioning (pre-conditioning). Each mouse was then conditioned in the alcohol-associated chamber and the saline-associated chamber for 8 days (conditioning). On the last day, the time that each mouse spent in both alcohol- and saline-chamber was recorded (post-conditioning). The preferences for each chamber in both pre- and post-conditioning days were measured as the ratio of time in the alcohol- over the saline-chamber. We found that the PAE adult mice showed higher preference ratio than their age-matched water controls in post-conditioning day, but not in the pre-conditioning day (Figure 4.3B; $F_{(1,10)} = 5.93$, $p = 0.035$; for post-conditioning: $q = 4.12$, $p = 0.013$; for pre-conditioning: $q = 1.96$, $p = 0.19$). Additionally, the PAE adult mice presented higher preference ratio in their post- than pre-conditioning day ($q = 4.35$, $p = 0.012$). Next, we tested whether the PAE mice continued to exhibit hyper-locomotor activity in adulthood (P133). We found that the PAE mice exhibited higher overall total traveled distance than their water controls (Figure 4.3C; $t_{(10)} = -3.26$, $p = 0.0086$). Additionally, the moving time of adult PAE mice is slightly longer than that of their age-matched water controls, but this difference is not significant (Figure 4.3D; $t_{(10)} = -1.52$, $p = 0.18$). In summary, our results

suggest that prenatal exposure to alcohol produces a higher alcohol CPP and that hyperactivity is still preserved in adult age PAE mice.

4.3.4. Prenatal exposure to alcohol produces an increase in AMPAR-mediated glutamatergic transmission in D1-MSNs

Our recent study reveals that high alcohol preference in adult, non-PAE mice was strongly associated with enhancement of the glutamatergic activity selectively on DMS D1-MSNs (Wang et al., 2015; Cheng et al., 2017). Also, excitation of D1-MSNs induced hyperactivity (Kravitz et al., 2010; Kravitz et al., 2012; Freeze et al., 2013). Thus, we reasoned that the alcohol CPP and hyperactivity observed in adult PAE mice is driven by the enhancement of glutamatergic activity on D1-MSNs.

To investigate this possibility, we prepared brain slices from adult PAE and control D1-Cre;Ai14 mice and performed whole-cell electrophysiology. We first measured AMPA-receptor (AMPAR) activity in D1-MSNs and found that bath application of AMPA (5 μM) induced a significantly larger current in D1-MSNs of PAE mice than their age-matched water controls (Figure 4.4A and B; for 4B: $t_{(15)} = -3.28$, $p = 0.0051$). Next, to examine whether the glutamatergic synaptic transmission was affected by PAE, we measured miniature excitatory postsynaptic currents (mEPSCs). The mPESCs recorded from PAE mice showed significantly higher frequency and amplitude than those in age-matched control mice (Figure 4.4C). This was demonstrated by a rightward shift of the cumulative probability distributions of mEPSC amplitudes recorded from PAE mice (Figure 4.4D), and a significant increase in the mean amplitude of mPESCs (Figure 4.4D, inset; $t_{(30)} = -2.07$, $p = 0.047$). We also observed a leftward shift of cumulative probability distributions of mEPSC inter-event intervals (Figure 4.4E), and a significant increase in the mean frequency of mEPSCs from D1-MSNs of PAE mice compared to

age-matched controls (Figure 4.4E, inset; $t_{(30)}$ = -3.11, p = 0.0041). Taken together, these results suggest that PAE causes a long-term increase in glutamatergic afferents onto D1-MSNs.

4.3.5. Prenatal exposure to alcohol increases dendritic complexity of D1-MSNs of the DMS

Given that AMPAR-mediated glutamatergic plasticity has been associated with morphological changes in neurons (Kasai et al., 2010), we examined whether the complexity of dendritic arborization was altered by PAE in the DMS D1-MSNs. To visualize the overall dendritic branches and the soma of the D1-MSNs from above recording, the neuronal tracer biocytin was applied through the patching pipette into a patched D1-MSN, and biocytin-labeled D1-MSNs were imaged using confocal microscopy (Figure 4.5A). The number of dendritic processes was measured by Sholl analysis in concentric spheres centered on the soma (Wang et al., 2015). As shown in Figure 4.5B, dendrites that were 10-100 μm from the soma exhibited more intersections in DMS D1-MSNs from PAE mice than that in their age-matched water controls (Figure 4.5B; $F_{(16,231)}$ = 3.79, p = 0.000003). Furthermore, the total length of DMS D1-MSNs was significantly higher in PAE mice compared to their age-matched water controls (Figure 4.5C; $t_{(16)}$ = -3.16, p = 0.0061). We also observed the total number of dendritic branches of D1-MSNs was significantly increased in the PAE mice than that in their age-matched water controls (Figure 4.5D; $t_{(16)}$ = -3.67, p = 0.0021). Taken together, our findings reveal that prenatal exposure to alcohol changes the dendritic complexity in the DMS D1-MSNs.

4.5 Discussion

The present study confirmed that adult female mice voluntarily and stably consume high levels of alcohol in a two-bottle choice paradigm and exhibit preference for alcohol. Thus, the two-bottle choice paradigm in mice can be used to model voluntary alcohol consumption during pregnancy in human populations. Using this paradigm, we show that, as reported by others (Shea

et al., 2012; Kim et al., 2013; Idrus et al., 2014), PAE results in hyperactivity in exposed offspring during the juvenile period, and that hyperactivity persists into adulthood. Adult PAE mice also exhibited higher conditioned place preference to alcohol, compared to non-PAE controls. Importantly, we discovered that PAE increased AMPAR activity in DMS D1-MSNs in adult offspring. Furthermore, we found that prenatal exposure to alcohol increased total length and number of branches of DMS D1-MSNs in adult offspring. Our findings suggest that PAE triggers a long-term functional and structural plasticity in DMS D1-MSNs, potentially contributing to hyperactivity in both juvenile and adult offspring.

Hyperactivity is often a co-morbid condition in individuals diagnosed with a FASD (Lange et al., 2018). Consistent with data from human populations as well as with the results reported in a number of preclinical studies (Mantha et al., 2013; Sanchez Vega et al., 2013; Patten et al., 2014), we also observed an increase in locomotor activity in juvenile PAE offspring. Interestingly, despite the overall increase in the traveled distance, we also found that PAE juveniles exhibit decreased movement velocity. The latter data are consistent with preclinical evidence that PAE also disturbs musculoskeletal development and motor control circuits (Sylvain et al., 2010; Kleiber et al., 2011), and with clinical evidence for gait disturbances in FASD children (Taggart et al., 2017). More importantly, we found that PAE mice moved for a longer time, as compared with their water controls; this may account for the increased travel distance of PAE mice, despite their decreased speed of movement. An increase in the percentage of time spent moving by PAE juveniles is consistent with the hyperactivity component of ADHD. Although we observed a reduction of traveled distance over time in PAE group, habituation and fatigue in these mice could explain the data. In contrast, there was little decrement in distance traveled in the control mice, indicating that, as a group, control mice did

not exhibit significant habituation or fatigue during the test period. In our study, PAE offspring appeared to show less anxiety, since they spent less time in the periphery of the open-field arena compared to control offspring. Our data are in contrast to a few studies which showed that prenatal exposure to alcohol increased anxiety-like behavior (Hausknecht et al., 2005; Hellemans et al., 2008; Kleiber et al., 2011). However, other studies have reported that PAE for more restricted 1st and 2nd trimester-equivalent exposure periods (Mantha et al., 2013; Fish et al., 2016) result in increased exploratory behavior in the central zone of the open field arena. Moreover, PAE reportedly impairs the development of serotonin neurons in fetal mice (Zhou et al., 2001), which contributes to the facilitation of anxiety-like behavior. The inconsistency in data between different research groups may be due in part, to the timing and dose of alcohol exposure. Other differences in outcome may be partly explained by contextual components of experimental design. For example, Hellemans and colleagues (2008) pre-exposed PAE mice to a stress paradigm, before evaluating anxiety behaviors. However, reduced anxiety may also be due to other developmental consequences of PAE. For example, children with FASD exhibit deficits in sensory processing (Franklin et al., 2008), which may impair adaptation to anxiogenic environments.

It has been reported that the maternal 10% alcohol exposure procedure during pregnancy period can alter the epigenotype and the phenotype of offspring (Kaminen-Ahola et al., 2010). More importantly, this report indicated that this epigenotype change could be preserved in adult age. In line with this study, we found that the PAE adult offspring continued to exhibit indices of hyperactivity. We also found that adult PAE offspring demonstrated higher alcohol-induced CPP than their age-matched water controls. This finding is in line with previous reports which state

that prenatal exposure to cocaine results in a higher conditioned place preference (Malanga et al., 2007; Pautassi et al., 2012).

Previously, we reported that excessive alcohol drinking increases AMPAR and NMDAR activity in adult mice (Wang et al., 2015; Cheng et al., 2017). Here, we found that PAE enhanced the AMPAR-mEPSC amplitude in DMS D1-MSNs of adult offspring. In line with our results, others have also reported that PAE enhances AMPAR function in other basal forebrain regions as well (Hsiao and Frye, 2003). Moreover, another study reported that high-frequency stimulation induced an abnormal AMPAR-mediated LTP in the dorsal striatum of PAE adult mice and could be blocked by the application of D1R antagonist (Zhou et al., 2012). In our study, we also found that PAE resulted in an increase of the frequency of AMPAR-mediated mEPSCs in D1-MSNs in the DMS of adult offspring. These data suggest that PAE may result in increased glutamatergic release from presynaptic terminals onto D1-MSNs, and are consistent with previous research showing that, in alternate contexts, i.e., neurogenesis, PAE preferentially facilitates glutamatergic activity to facilitate an imbalance in excitatory signaling (Kim et al., 2010).

Enhancement of mEPSC frequency may attribute to the increased complexity of dendritic branching, where glutamatergic synapses are located (Kerchner and Nicoll, 2008). Cycles of alcohol consumption and withdrawal increase arborizations, the total number, and the total length of dendrites of D1-MSNs (Wang et al., 2015). In this study, we found an increase of dendritic arborizations, as well as the total number and the total length of dendritic branches of D1-MSNs in PAE adult mice, which is likely to account for the enhanced mEPSC frequency in D1-MSNs in response to prenatal exposure to alcohol. It should be noted that another study which was not able to document changes in morphology of striatal MSNs (Rice et al., 2012),

achieved lower levels of PAE and did not discriminate between D1 and D2 sub-populations of MSNs. Additionally, Rice et al used a male rat model of PAE instead of our mixed-sex mouse model, and the blood alcohol concentration may have been lower in rats than in the mice. Further studies will be needed to define thresholds for PAE activation of D1-MSNs. Interestingly methylphenidate, the psychostimulant commonly used to treat ADHD has been shown to increase spine density on D1-MSNs (Kim et al., 2009), suggesting that PAE may developmentally program the excitability of a brain circuit important for controlling activity and attention, and perhaps, explain the decreased efficacy of anti-ADHD medications in managing FASD. Lastly, we note that one limitation of the current study is that while we used a mixed-sex study model, our study was not statistically powered to assess sex differences due to PAE.

In summary, our results suggest that prenatal exposure to alcohol induced hyperactivity in both juvenile and adult offspring, and alcohol preference in adult offspring. More importantly, the PAE-induced hyperactivity and alcohol preference in adult offspring may be linked to functional and morphological change in D1-MSNs in the DMS.

4.6 Methods and Materials

4.6.1. Reagents

α-amino-3-hydroxy-5-methyl-4-isoxazolepropionic acid (AMPA) was obtained from Sigma (Saint Louis, MO). Cyclothiazide and Tetrodotoxin (TTX) were purchased from Tocris Bioscience (Minneapolis, MN). Alexa Fluor 594-conjugated streptavidin was purchased from Invitrogen (Carlsbad, CA). All other reagents were obtained from Sigma.

4.6.2. Animals

Drd1a-Cre (D1-Cre) mice were obtained from the Mutant Mouse Regional Resource Center. Ai14 mice were purchased from the Jackson Laboratory. Mouse genotypes were

determined by PCR analysis of tail DNA (Cheng et al., 2017; Wei et al., 2018). Before breeding, mice were housed in the same-sex colonies under a 12 h light/dark cycle with lights on at 11:00 P.M. and food and water available ad libitum. The light/dark cycle we used for all behavioral tests was the same as that of the breeding conditions. All behavioral tests were conducted during the dark phase of the light/dark cycle. All animal procedures in this study were approved by Texas A&M University Institutional Animal Care and Use Committee. All the procedures were conducted in agreement with the Guide for the Care and Use of Laboratory Animals, National Research Council, 1996.

4.6.3. Intermittent-Access to Alcohol 2-Bottle-Choice Drinking Procedure and Breeding

Individually housed, ~8-week old female Ai14 mice were randomly assigned and counterbalanced based on weight, to one of two drinking groups: a control group with free access to tap water only, or an alcohol drinking group with free access to both water and a 20% alcohol solution (vol/vol in tap water). The alcohol group was housed in the same room with controls.

To establish high levels of alcohol consumption in alcohol group mice, we employed an intermittent alcohol access, two-bottle choice drinking procedure as described previously (Wang et al., 2015; Cheng et al., 2017; Wei et al., 2018). Briefly, female mice were given 24-h concurrent access to one bottle of 20% alcohol in water (vol/vol) and one bottle of water starting at 1:30 P.M. on every other day, with 24-hr periods of alcohol deprivation between the alcohol-drinking sessions. Alcohol solutions were prepared by mixing alcohol (190 proof pure alcohol, KOPTEC) with tap water. The placement (left or right) of the bottles was alternated between each session to prevent side preference. The weight of water and alcohol bottles was measured 24 h after the start of each drinking session. This paradigm has been reported by others to induce

high levels of alcohol intake, up to 30 g/kg/day at 20% vol/vol in female mice (Hwa et al., 2011), reaching peak blood alcohol concentrations above 100 mg/dl.

Following the 6-week excessive alcohol drinking and withdrawal period, female Ai14 mice were mated overnight with 8-12-week-old D1-Cre males. During mating, only water was available to prevent males from consuming alcohol. Females were examined for the presence of a vaginal plug at the end of the mating period, indicating gestational day 0, and males were removed. If no vaginal plug was found in the cage, we allowed the females a maximum of 2 additional overnight mating sessions to ensure the pregnancy. For other experiments in this study, we did not assess estrous cycle stages of female mice. Successfully impregnated females were re-exposed to 10% alcohol (commonly used during pregnancy) in the two-bottle choice paradigm outlined above to decrease the potential toxicity to the infants (Kleiber et al., 2011; Sanchez Vega et al., 2013; Patten et al., 2014), through gestation and into the early postpartum period, corresponding to the 3rd trimester equivalent period of human fetal development, to postnatal day (P) 10 of pup development. After P10, alcohol was removed, and only water was provided to the female. Pups were weaned at P21 and housed with a maximum of five same-sex littermates for the duration of testing.

4.6.4. Locomotor activity

All pups were tested for locomotor activity in an open field box (16 inches x 16 inches x 15 inches, Hamilton Kinder) (Cheng et al., 2017). The traveled distance was detected as infrared beam crosses (16 beams per side per box) using activity monitors (Hamilton Kinder). Locomotion was tested for 30 min. At the end of testing, the mouse was removed and returned to its home cage. The surface and walls of the open field box were wiped clean with water and 30% isopropanol. Female and male mice were tested in different open field boxes.

4.6.5. Conditioned Place Preference

The conditioned place preference method was reported in our previous study (Cheng et al., 2017). Briefly, different visual and tactile cues distinguish the two chambers: black/white stripes with a “rod” flooring in the first chamber, and black/white dots with a metal plate flooring with holes in the second chamber. Each experiment consisted of three steps. For the first step (day 1, preconditioning), each mouse was placed in the neutral hall and was permitted to explore both chambers for 30 min. For the second step (days 2 to 9, conditioning), the mice were administered 20% alcohol (i.p.,2 g/kg) and immediately placed into one of the given chambers and confined for 5 min on days 3, 5, 7, and 9. On alternate days (conditioning days 2, 4, 6, and 8), mice were administered saline and immediately placed into the opposite chamber and confined for 5 min. For the third step (day 10, post-conditioning test), mice were placed in the center of the neutral hall and allowed free access to both chambers for 30 min. The total time spent in each chamber and the locomotion activity was recorded.

4.6.6. Preparation of Acute Striatal Slices and Electrophysiology Recordings

Slice preparation. Slice preparation was described previously (Wang et al., 2015; Cheng et al., 2017; Ma et al., 2018). For the present study, we usually prepared slices from two mouse brains per day, one in the late morning and the other one in the late afternoon. Briefly, coronal sections of the striatum (250 μm) were sliced using a vibratome (VT1200s, Leica) in an ice-cold cutting solution containing the following (in mM): 40 NaCl, 143.5 sucrose, 4 KCl, 1.25 NaH_2PO_4, 26 $NaHCO_3$, 0.5 $CaCl_2$, 7 $MgCl_2$, 10 glucose, 1 sodium ascorbate, and 3 sodium pyruvate, saturated with 95% O_2 and 5% CO_2. Slices were then incubated in a 1:1 mixture of cutting solution and an external solution at 32°C for 45 min before being transferred to a chamber that contained the external solution. The external solution was composed of the

following (in mM): 125 NaCl, 2.5 KCl, 2.5 $CaCl_2$, 1.3 $MgCl_2$, 1.25 NaH_2PO_4, 25 $NaHCO_3$, and 10 glucose, saturated with 95% O_2 and 5% CO_2. Slices were stored in the external solution at room temperature until use.

Whole-cell recording. Individual slices were placed in a recording chamber, and cells in the DMS were visualized using epifluorescence microscopy (Examiner A1; Zeiss). Whole-cell recordings were made using a Multiclamp 700A amplifier (Molecular Devices). Electrodes (4-6 MΩ) contained the following (in mM): 115 cesium methanesulfonate, 15 HEPES, 0.6 EGTA, 8 TEA-Cl, 4 MgATP, 0.3 NaGTP, 7 Na_2CrPO_4, Ph 7.2–7.3, and 0.5% biocytin with an osmolarity of 270–280 mOsm. AMPA induced currents and AMPAR-mediated mEPSCs were measured as described previously (Wang et al., 2010b, 2012). Specifically, AMPA (5 μM) was bath-applied for 30 s. mEPSCs were recorded in the presence of 1 μM TTX, 100□μM picrotoxin, and 1.3 mM external Mg^{2+} with neurons clamped at -70 mV.

4.6.7. Histology

Post-recording biocytin-staining and confocal imaging have been described previously (Wang et al., 2015). Briefly, immediately after electrophysiology recording, DMS sections containing biocytin-filled neurons were fixed in 4% paraformaldehyde at 4°C overnight. Sections were then incubated with Alexa Fluor 594-conjugated streptavidin for 72 h. Micrographs of overall dendritic branches and the soma of biocytin-filled neurons were acquired with a 40 X oil immersion objective at the vertical interval of 1 μm. A confocal microscope (Fluorview-1200, Olympus) was used to image fluorescent sections. EGFP was excited by the 470 nm laser.

4.6.8. Morphological Analysis

Biocytin-filled neurons were traced using Simple Neurite Tracer module in ImageJ (Fiji) (Longair et al., 2011; Ferreira et al., 2014). Dendritic branches were quantified with Sholl

analysis (Sholl, 1953). The center of each concentric spheres was defined as the center of the soma. The starting radius was 10 μm, and the ending radius was 160 μm from the center with an interval of 10 μm between radii.

4.6.9. Statistical Analysis

Data from male and female mice were combined for analysis and not assessed for sex differences. All data were analyzed using unpaired *t* tests and two-way ANOVA with repeated measures (two-way RM ANOVA), followed by the Student-Newman-Keuls (SNK) *post hoc test*. Statistical analysis was conducted by OriginLab and SigmaPlot programs. mIPSCs were analyzed using Mini Analysis software (Synaptosoft Inc.). All data were expressed as the Mean ± SEM.

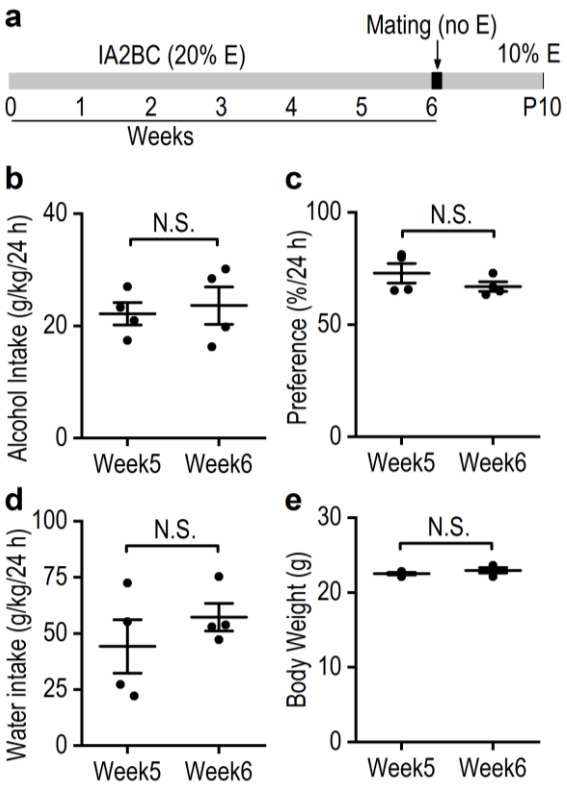

Figure 4.1. A voluntary, intermittent access alcohol-drinking paradigm established a high level of alcohol consumption and preference.

(**A**) Schematic of experimental design. Female Ai14 mice were trained to establish a high level of alcohol drinking with the intermittent access to 20% alcohol (20% E) two-bottle choice paradigm (IA2BC). To avoid fetal effects due to paternal alcohol consumption, no alcohol (no E) was available during the mating period. After that, IA2BC was reinstated, with 10% alcohol (10% E) through the period of pregnancy and into the post-partum period, until postnatal day 10 (P10). (**B**, **C**) Female mice achieved a high level of alcohol intake (B) and preference (C) in 24 h, which were remained at the same level in the last two weeks, week 5 and 6. Not significant (N.S.), $p > 0.05$, unpaired t test. (**D**, **E**) Water intake and the body weight of female mice did not change in the last 2 weeks, i.e., week 5 and 6 of the IA2BC paradigm. Not significant (N.S.), $p > 0.05$, unpaired t test. n = 4 female mice for B-E.

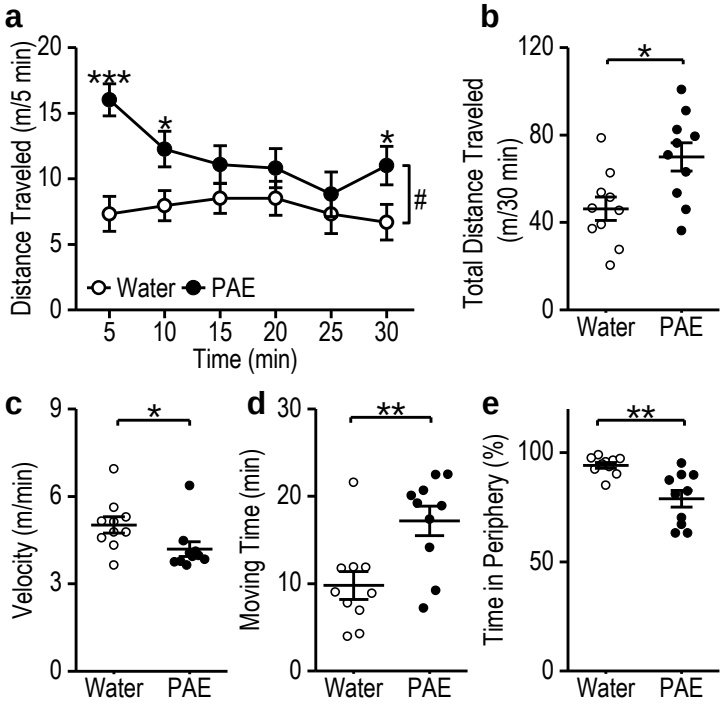

Figure 4.2. Prenatal exposure to alcohol increases locomotor activity.
(**A**) Time course of locomotor activity demonstrated that prenatal alcohol exposure (PAE) mice traveled more distance than their age-matched water controls at 5, 10 and 30 min. $^{\#}p < 0.05$, two-way RM ANOVA; $^{*}p < 0.05$ and $^{***}p < 0.001$ versus the water group at the same time points, post-hoc SNK test. (**B**) The cumulative distance traveled during the 30 min period was higher in PAE mice compared to water controls. $^{*}p < 0.05$ by unpaired *t* test. (**C**) PAE mice demonstrated a decreased velocity of movement compared to age-matched water controls. $^{*}p < 0.05$, unpaired *t* test. (**D**) PAE mice demonstrated a greater moving time than age-matched water controls. $^{**}p < 0.01$, unpaired *t* test. (**E**) PAE mice spent less time at the periphery of the open field arena than their age-matched water controls. $^{**}p < 0.01$, unpaired *t* test. n = 10 mice (7 males and 3 females) from 3 litters (Water); 10 mice (8 males and 2 females) from 4 litters (PAE) in **A**-**E**.

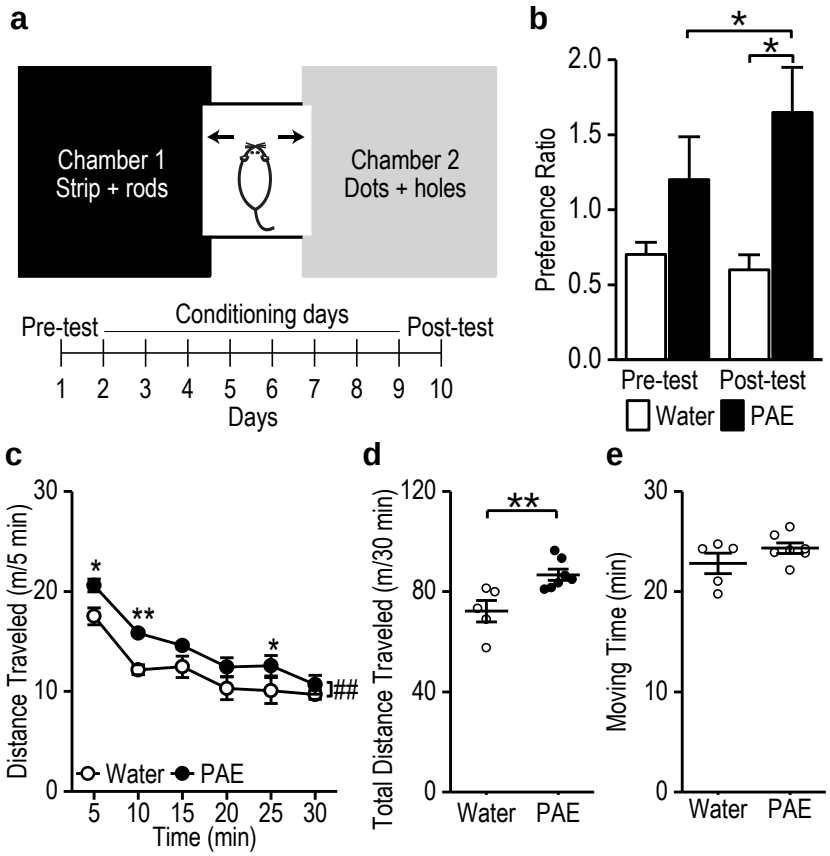

Figure 4.3. Prenatal alcohol exposure results in conditioned place preference for alcohol, and increased locomotor activity in adult (P133) offspring.

(**A**) Schematic of experimental procedures. The diagram illustrates the design of the customized CPP chambers and the timeline for the CPP experimental protocol. (**B**) Adult PAE mice exhibited a higher preference ratio on the post-conditioning test, compared to the pre-conditioning test. PAE mice also demonstrated a higher preference ratio on the post-conditioning test compared to age-matched water controls. Preference ratio = time spent in alcohol chamber/time spent in the saline chamber. *$p < 0.05$, two-way RM ANOVA; *$p < 0.05$, post-hoc SNK test. (**C**) Adult PAE mice showed a higher cumulative distance traveled in a 30-min testing session compared to their age-matched water controls. **$p < 0.01$, unpaired *t* test. (**D**) Adult PAE mice showed a slightly (but not significant) higher moving time, as compared with their age-matched water controls. $p > 0.05$, unpaired t test. n = 5 mice (3 males and 2 females) from 3 litters (Water); 7 mice (5 males and 2 females) from 4 litters (PAE) in B-D.

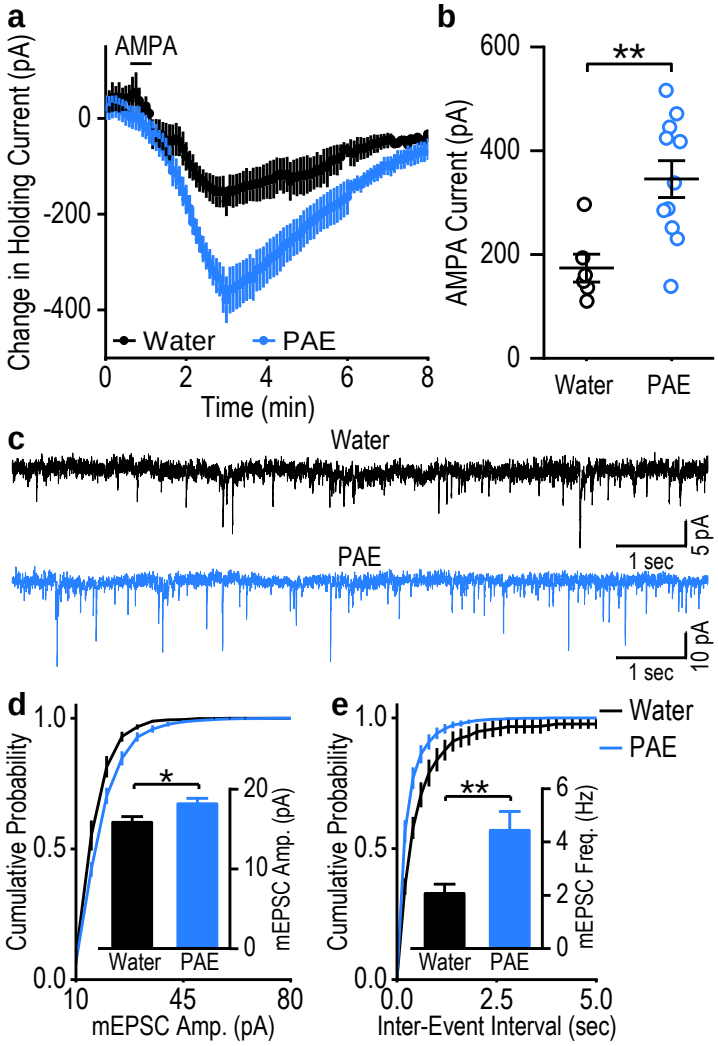

Figure 4.4. Prenatal exposure to alcohol increases AMPAR-mediated glutamatergic transmission in DMS D1-MSNs of adult offspring.

(**A**) PAE produced a long-lasting increase in the peak amplitude of the AMPA-induced current. AMPA (5 μm) was bath-applied. (**B**) The peak amplitude of AMPA-induced current was higher in PAE groups compared to age-matched controls. $^{**}p < 0.01$, unpaired *t* test. n = 6 neurons from 5 mice (4 males and 1 female) that were derived from 3 litters (Water); 11 neurons from 7 mice (6 males and 1 female) that were derived from 4 litters (PAE) in **A** and **B.** (**C**) Representative mEPSC traces of D1-MSNs from water and PAE groups. (**D**) PAE increased the amplitude of mPESCs as shown in cumulative probability plots for the mEPSC inter-event interval from water and PAE mice. Inset, bar graph represents the mean mEPSC amplitude in control and PAE groups. $^{*}p < 0.01$, unpaired *t* test. (**E**) Prenatal exposure to alcohol increased the frequency of mEPSCs as shown in the cumulative probability plots for mEPSC amplitude from control and PAE mice. Inset, bar graph represents the mean mEPSC frequency in control and PAE groups. $^{**}p < 0.01$, unpaired *t* test. n = 11 neurons from 5 mice (2 males and 3 females) that were derived from 3 litters (Water); 21 neurons from 7 mice (5 males and 2 females) that were derived from 4 litters (PAE) in **D-E**.

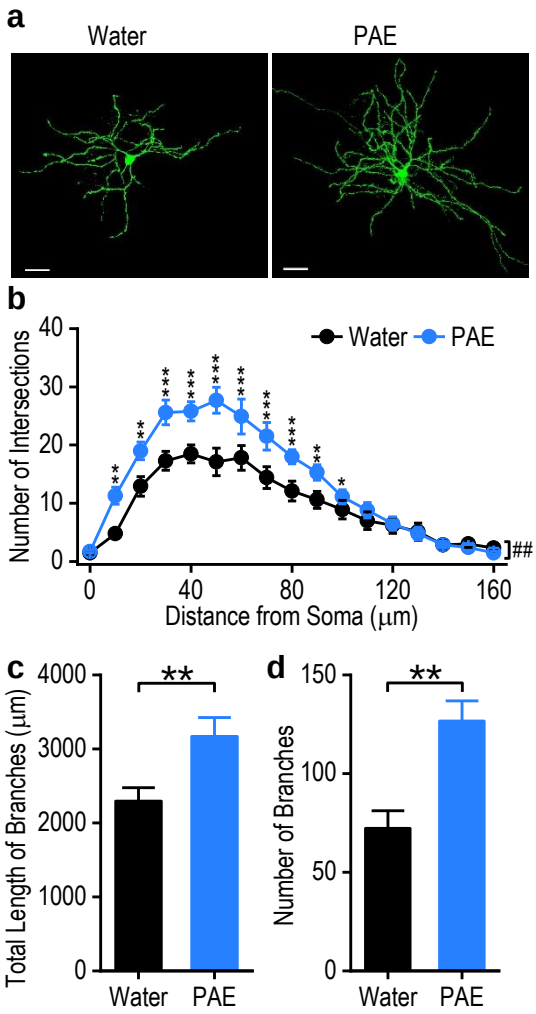

Figure 4.5. Prenatal exposure to alcohol results in increased dendritic length and branching in DMS D1-MSNs of adult offspring.

(**A**) Representative confocal images illustrate dendritic branches and soma of D1-MSNs from PAE mice and their water controls. Scale bar: 30 μm. (**B**) A three-dimensional Sholl analysis revealed significantly more intersections of the dendritic process at 10 - 100 μm from soma of D1-MSNs in PAE mice, compared to their age-matched controls. $^{\#\#}p < 0.01$, two-way RM ANOVA; $^{*}p < 0.05$, $^{**}p < 0.01$, $^{***}p < 0.001$, SNK test. (**C**) D1-MSNs from PAE mice exhibited increased lengths of dendritic branches compared to controls. $^{**}p < 0.01$, unpaired *t* test. (**D**) The total number of branches was increased in D1-MSNs of PAE mice compared to water controls. $^{**}p < 0.01$, unpaired *t* test. n = 8 neurons from 5 mice (3 males and 2 females) that were derived from 3 litters (Water); 10 neurons from 7 mice (6 males and 1 female) that were derived from 4 litters (PAE) (B-D).

CHAPTER V

CONCLUSION AND FUTURE STUDY

In this chapter, I list some conclusions that result from chapters II, III, and IV. I also propose potential future experiments to further test these conclusions.

One major finding of chapters II is that synaptic NMDAR-mediated transmission is enhanced selectively in D1-MSNs, while the synaptic GABAergic transmission is enhanced exclusively in D2-MSNs, after repeated alcohol consumption and withdrawal. It has been reported that both the AMPAR (Wang et al., 2015) and NMDAR activities are increased in D1-neurons following alcohol consumption and withdrawal. In chapter II, I observed an increased NMDA/AMPA ratio, which suggests a greater potentiation of NMDAR activity than of AMPAR activity following cycles of alcohol consumption and withdrawal. This finding could due to that the NMDAR, rather than the AMPAR, is the direct target of alcohol (Lovinger et al., 1989; Wang et al., 2012). Similarly, chronic cocaine exposure also causes an increase of NMDA/AMPA ratio at the corticostriatal synapses in D1-MSNs (Pascoli et al., 2014). The increased NMDAR activity may also suggest that repeated cycles of alcohol exposure and withdrawal induce silent synapses (only contain NMDARs but not AMPARs) on D1-MSNs (Huang et al., 2009). Given that activation of D1Rs can enhance NMDAR activity (Beaulieu and Gainetdinov, 2011; Gerfen and Surmeier, 2011), this selective potentiation of NMDARs in D1-MSNs may result from on-set of alcohol-induced phasic striatal dopamine release (Sulzer, 2011). This on-set alcohol-induced dopamine phasic release activates D2Rs that may result in a decrease of NMDAR activity in D2-MSNs (Li et al., 2009). A previous study showed that withdrawal from repeated exposure (off-set alcohol) decreased the basal level of dopamine (allostatic state) in the striatum (Koob and Le Moal, 2008; Barak et al., 2011; George et al.,

2012), and this hypodopaminergic basal level of dopamine was reported to increase synaptic strengthen of GABAergic interneuron onto D2-MSNs (Gittis et al., 2011). Alcohol-induced potentiation of GABAergic on D2-MSNs could result from the alternation of D2Rs signaling. One mediator of the downstream signaling of D2Rs is GSK3β. The protein levels of D2Rs and GSK3β activity in the striatum is decreased following chronic alcohol consumption (Neasta et al., 2011; Volkow and Morales, 2015). Given that GSK3β inhibit $GABA_AR$ trafficking and thereby GABAergic transmission (Li et al., 2012; Rui et al., 2013; Tyagarajan and Fritschy, 2014), alcohol-mediated decreased D2R-GSK3β signaling causes an enhancement of GABAergic activity. Consistent with this notion, in chapter II, I found that excessive alcohol drinking and withdrawal suppress GSK3β activity and consequently enhances β3-containing $GABA_AR$ expression. The β3-containing $GABA_AR$ regulates tonic inhibition (Janssen et al., 2009; Janssen et al., 2011) and the tonic GABA is likely released from GABAergic interneurons (Brickley and Mody, 2012). Thus, a future investigation on the role of GABAergic interneurons in alcohol-drinking behavior is needed. Others have reported that GABAergic inhibition or GABA receptor knockdown in the striatum reduced alcohol intake (Hyytia and Koob, 1995; Nie et al., 2011). Another major finding of chapter II is that bidirectional chemogenetic manipulation of D1- and D2-MSNs produced distinct changes in alcohol-drinking behavior, suggesting the opposing roles of D1- and D2-MSNs in alcohol consumption and preference in mice. Specifically, chemogenetic activation of D1-MSNs promoted alcohol consumption and preference, whereas inhibition of their activity attenuated alcohol consumption and preference. This indicated a positive role of D1-MSNs in controlling alcohol consumption and expression of alcohol preference. These results are in line with previous pharmacological and genetic studies (Hodge et al., 1997; El-Ghundi et al., 1998; D'Souza, 2003; Wang et al., 2015). Importantly, our

findings in chapter II also advance understanding of D2-MSNs negative gating alcohol consumption and alcohol preference. However, due to complex expression pattern of striatal D2Rs (Beaulieu and Gainetdinov, 2011), previous pharmacological studies using D2R agonists/antagonists reveals different effect on alcohol consumption and preference (Dyr et al., 1993; Hodge et al., 1997; Phillips et al., 1998; Thanos et al., 2001; Wang et al., 2015).

In chapter III, we developed in vivo optogenetic induction protocol and provided a direct causal link between long-term synaptic plasticity within mPFC-DMS D1-MSNs and alcohol-seeking behavior. It has long been known that the difficulty of induction of dorsostriatal LTP is probably due to insufficient depolarization of striatal neurons (Calabresi et al., 1992; Surmeier et al., 2009). In chapter III, I optogenetically depolarize the distal dendrites of MSNs thereby enhancing NMDAR channel opening and calcium influx, which could facilitate dorsostriatal LTP induction (Calabresi et al., 1992; Surmeier et al., 2009). Similar to other reports, blockade of LTP by NMDAR antagonists (memantine) leads to LTD (Mancini et al., 2016). However, APV or MK801 that we used to induce LTD were not found to shift the plasticity in a study by Mancini et al. (Mancini et al., 2016). This discrepancy may be due to the fact that optogenetic postsynaptic depolarization induces eCB-LTD in the presence of a D2R antagonist in chapter III. The precise control of the presynaptic release of glutamate and depolarization of postsynaptic MSNs allowed us to reliably induce LTP and LTD in the dorsostriatum for the first time. The expression of an immediate early gene, *Npas4*, which has been associated with drug addiction, also support the successful LTP induction in the dorsostriatum (Sun and Lin, 2016; Ye et al., 2016). The mPFC-DMS circuit is believed to control goal-directed behaviors and associated with drug-seeking behavior (Yin and Knowlton, 2006; Balleine and O'Doherty, 2010; Lovinger, 2010; Everitt and Robbins, 2016). In chapter III, I found that operant self-administration of alcohol, but

not sucrose, enhanced NMDAR activity and facilitate ex vivo and in vivo induction of LTP on mPFC-DMS. This finding is in line with previous reports that *ex vivo* or *in vivo* alcohol exposure caused long-term facilitation of NMDAR activity (Wang et al., 2007; Kash et al., 2009; Lovinger, 2010; Wang et al., 2010), which is essential for LTP induction in the dorsal striatum (Lovinger, 2010). The extent of in vivo LTP induction likely depends on the degree of saturation of the drug-evoked plasticity. Chapter III reveals that operant alcohol self-administration using the FR3 schedule-induced unsaturated glutamatergic plasticity (indicated by AMPAR/NMDAR ratio) because the AMPAR/NMDAR ratio was further potentiated by *in vivo* LTP induction. Previous studies have shown that 1-2 day(s) withdrawal from cocaine exposure induces silent synapses (Huang et al., 2009; Lee et al., 2013; Dong and Nestler, 2014; Ma et al., 2014) and can mature over time (e.g., at 45 days) (Lee et al., 2013; Ma et al., 2014; Ma et al., 2016), which potentially occlude subsequent LTP (Creed et al., 2015; Creed et al., 2016). Taken together, this evidence suggests that short-term withdrawal from alcohol exposure induces unsaturated plasticity and allow us to further induce plasticity in vivo (Wang et al., 2012; Wills et al., 2012).

In chapter II, I used pharmacological and chemogenetic intervention to inhibit alcohol-evoked glutamatergic strengthening in the DMS, which attenuates alcohol consumption (Wang et al., 2012). However, this inhibitory effect is transient and disappears normally in 24 hrs. In chapter III, I induced *in vivo* eCB-LTD, and this LTD resulted in a long-term decrease (last for > 7d) in alcohol-seeking behavior, indicating that this eCB-LTD may mediate more sustained behavior changes (Sidhpura and Parsons, 2011). Although in chapter III and many other studies demonstrated that LTP could be induced in both D1- and D2-MSNs in slices (Shen et al., 2008; Surmeier et al., 2009), delivery of our LTP-inducing protocol *in vivo* selectively causes LTP of mPFC glutamatergic transmission in D1-MSNs of alcohol-drinking rats. This specificity of

induction may be attributed to the finding in chapter II that excessive alcohol consumption facilitates NMDAR activity in D1-, but not D2-, MSNs (Cheng et al., 2017). The chapter III further identified that operant self-administration of alcohol specifically increased GluN2B-containing NMDAR activity at the mPFC input onto D1-MSNs. This potentiation was reported to facilitate LTP induction (Wang et al., 2012; Wills et al., 2012). Similar to LTP induction protocol, our *in vivo* LTD-inducing protocol also exclusively produced LTD in D1-MSNs because I included a D2R antagonist during the induction, which blocks LTD induction in D2-MSNs (Kreitzer and Malenka, 2007; Shen et al., 2008). This selectivity has also been shown in Wu et al. (2015) that eCB-LTD was induced at corticostriatal inputs to D1-, but not D2-, MSNs. Since in chapter II, I found that D1-MSNs positively control alcohol consumption (Cheng et al., 2017), thus inducing LTP on D1-MSNs produces long-lasting enhancement of alcohol-seeking behavior, while inducing LTD on D1-MSNs reduces the same behavior. Although optogenetic stimulation cannot be immediately applied in clinical treatment, deep brain stimulation (DBS), an FDA-approved treatment, has the potential to induce in vivo LTP (Creed et al., 2015), and probably also LTD. Thus, it would be of great interest to explore the possibility to DBS together with a cocktail of antagonists of NMDAR (e.g., memantine) and D2R as a novel clinical treatment for alcohol use disorder.

In chapter IV, I confirmed that prenatal alcohol exposure (PAE), as reported by others (Shea et al., 2012; Kim et al., 2013; Idrus et al., 2014), results in hyperactivity in the PAE offspring during the juvenile period, and this hyperactivity persists into adulthood. Hyperactivity is diagnosed together with an FASD (Lange et al., 2018), which is consistent with data from human populations and the results reported in a number of preclinical studies (Mantha et al., 2013; Sanchez Vega et al., 2013; Patten et al., 2014). In chapter IV, I also observed hyperactivity

in juvenile PAE offspring. Interestingly, although the total traveled distance is increased, the movement velocity was decreased in PAE juveniles. The decrease of movement velocity may due to that PAE cause deficiency of musculoskeletal development and motor control circuits (Sylvain et al., 2010; Kleiber et al., 2011), and in line with clinical evidence for gait disturbance in FASD children (Taggart et al., 2017). Thus, one explanation of increased travel distance in PAE mice may be attributed to the increased travel time of PAE mice as I found in chapter IV. Another possibility of the decreased travel distance could be habituation or fatigue in these mice. Less time in the periphery of the open-field arena indicates PAE offspring express less anxiety. In contrast, other studies showed that PAE increased anxiety-like behavior (Hausknecht et al., 2005; Hellemans et al., 2008; Kleiber et al., 2011). Also, it has been reported that PAE impairs the development of serotonin neurons in fetal mice (Zhou et al., 2001), which could also contribute to the facilitation of anxiety-like behavior. This discrepancy could be attributed to that these studies restrict alcohol exposure to 1st and 2nd trimester of pregnancy and use a lower dose of alcohol before and after pregnancy (Mantha et al., 2013; Fish et al., 2016).

It has been reported that PAE can alter the epigenotype in the offspring (Kaminen-Ahola et al., 2010), which could be preserved in adult age. This probably can explain that the PAE adult offsprings continue to exhibit indices of hyperactivity. In addition, I found that adult PAE offspring exhibited higher alcohol CPP than water controls, which is in line with previous reports that prenatal exposure to cocaine results in a higher conditioned place preference (Malanga et al., 2007; Pautassi et al., 2012).

In chapter II and our previous study showed that excessive alcohol intake and withdrawal increases AMPAR and NMDAR activity in adult mice (Wang et al., 2015; Cheng et al., 2017). Similarly, in chapter IV, I found that PAE also enhanced the AMPAR-mediated glutamatergic

transmission in D1-MSNs of adult offspring. In line with our results, others have also reported that PAE enhances AMPAR function in other basal forebrain regions as well (Hsiao and Frye, 2003; Zhou et al., 2012). I further found that PAE resulted in an increase of the frequency of AMPAR-mediated mEPSCs in D1-MSNs of adult offspring, which suggest that an increased presynaptic glutamate release, and are consistent with previous findings that PAE preferentially facilitates glutamatergic release (Kim et al., 2010). This enhancement of mEPSC frequency may result from the increased arborization of dendritic (Kerchner and Nicoll, 2008). Our previous study found that repeated alcohol exposure and withdrawal increase arborizations of dendrites of D1-MSNs (Wang et al., 2015). In chapter IV, I found a similar result, which is in line with the enhanced mEPSC frequency in D1-MSNs after PAE. Although Rice et al. (2012) was not able to observe the same changes in morphology of striatal MSNs, this could be due to serval reasons: 1, they did not discriminate between D1 and D2 sub-populations of MSNs; 2, they used a male rat model of PAE instead of our mixed-sex mouse model; 3, the blood alcohol concentration may have been lower in rats than in the mice . Further studies are needed to define maternal blood alcohol concentration thresholds for PAE activation of D1-MSNs.

In summary, I found that excessive alcohol drinking in adults potentiated glutamatergic activity in D1-MSNs and GABAergic activity in D2-MSNs of the DMS (Figure 5.1). Consequently, alcohol-induced changes increased D1-MSN-mediated selection of “Go” actions and decreased D2-MSN-mediated selection of “NoGo” actions, controlling alcohol-related behaviors (Figure 5.1). This potentiation of glutamatergic inputs may occur at the corticostriatal synapses in the DMS, which has been reported that in other drugs of abuse (Pascoli et al., 2014). Then, we established causality between corticostriatal plasticity in the DMS and alcohol-seeking and -taking behaviors. I demonstrated that the plasticity of mPFC→D1-MSNs in the DMS

controlled alcohol-seeking and -taking behavior (Figure 5.1). Furthermore, alcohol-evoked glutamatergic plasticity of DMS D1-MSNs was found not only in adult alcohol-drinking animals but also in PAE-induced offspring (Figure 5.1). The PAE-induced increased D1-MSN activity potentially contributes to the formation of hyperactivity in the offspring (Figure 5.1). Because the DMS is part of the cortico-striato-thalamo-cortex circuit, which is known to control the acquisition of action-outcome association and goal-directed behavior. Thus, adult and prenatal alcohol exposure-evoked synaptic plasticity presumably enhances the process of goal-direct information. In adult alcohol-drinking animal, the alcohol-mediated enhancement of goal-direct behavior may facilitate the reinforcement of alcohol, leading to the pathological chronic use of alcohol. In PAE offspring, this enhancement of goal-direct process may contribute to the maladaptive behavior observed in PAE offspring (Pautassi et al., 2012). My research provides an insight into the detailed mechanisms underlying the control of alcohol consumption, establishes a causal link between corticostriatal synaptic potentiation and alcohol-seeking behavior, and also linked the activity of DMS D1-MSNs to the PAE-induced hyperactivity. These findings provide an evidence base for therapeutic strategies to reduce excessive alcohol consumption and PAE-induced hyperactivity.

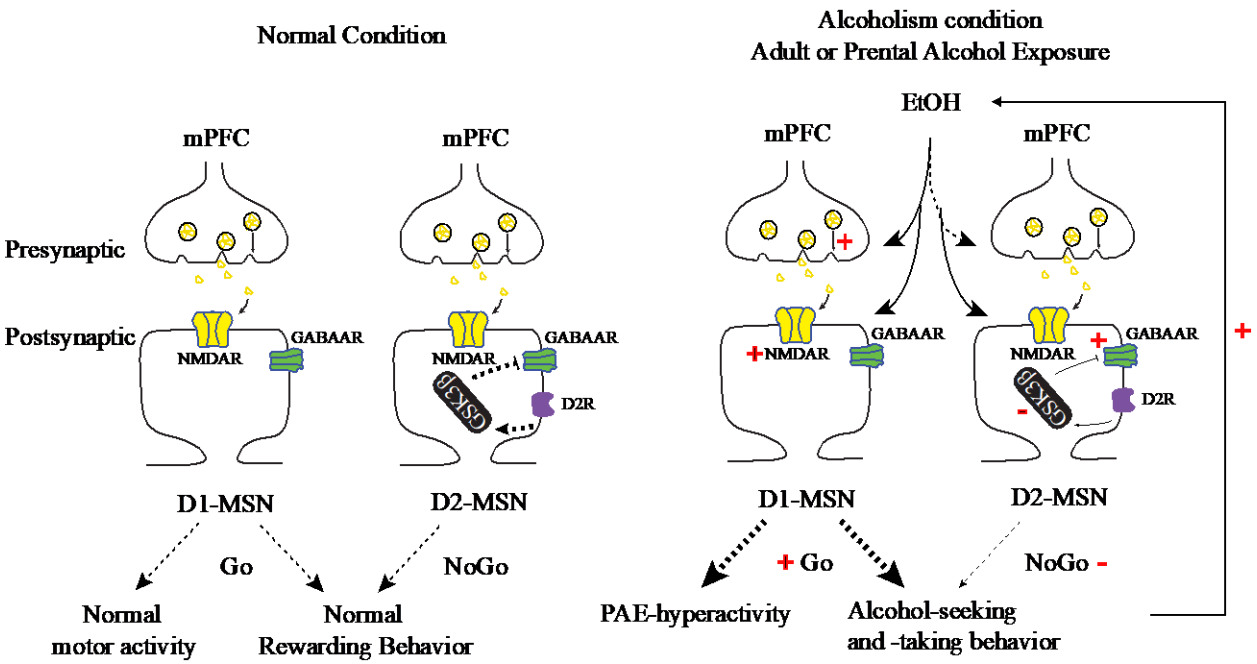

Figure 5.1 Hypothetical model of alcohol-induced changes in glutamatergic and gamma-aminobutyric acidergic (GABAergic) strength in D1- and D2-medium spiny neurons (MSNs) of the dorsomedial striatum leading to pathological alcohol-related behaviors. (Left) In a normal brain, both D1-MSNs and D2-MSNs receives presynaptic glutamatergic inputs from a critical brain region, the medial prefrontal cortex (mPFC). The yellow dots represent releasing of glutamate from presynaptic terminal. At the postsynaptic site, D1-MSN and D2-MSN express glutamatergic NMDARs and $GABA_AR$s. In addition to these two receptors, D2-MSN also express dopamine D2Rs and glycogen synthase kinase-3β (GSK3β). D2R activation stimulates GSK3β signaling, which negatively regulates $GABA_AR$ activity. D1-MSN and D2-MSN excitation respectively facilitate selection of "Go" and "NoGo" actions in normal rewarding behavior and normal motor activity. (Right) In the alcoholism condition, adult or prenatal alcohol exposure (PAE) enhances glutamatergic release. Specifically, adult alcohol drinking enhances glutamatergic release from mPFC terminals onto D1-MSNs, which results in enhanced D1-MSN activity. In addition, adult alcohol exposure selectively enhances NMDAR activity in D1-MSN, which facilitates "Go" action towards alcohol-seeking and -taking behavior. In contrast, adult alcohol drinking increases $GABA_AR$ activity in D2-MSN by decreasing D2R-GSK3β signaling. This suppression of "NoGo" actions also contribute to alcohol drinking behavior. Note that PAE-mediated facilitation of D1-MSN activity may contribute to the hyperactivity induced by PAE. Changes in activities of receptors, signaling, and behaviors are indicated by "+" or "-" symbols as well as alterations of their sizes.

REFERENCES

Aalto S, Ingman K, Alakurtti K, Kaasinen V, Virkkala J, Nagren K, Rinne JO, Scheinin H (2015) Intravenous ethanol increases dopamine release in the ventral striatum in humans: PET study using bolus-plus-infusion administration of [(11)C]raclopride. Journal of Cerebral Blood Flow and Metabolism 35:424-431.

Abrahao KP, Salinas AG, Lovinger DM (2017) Alcohol and the brain: neuronal molecular targets, synapses, and circuits. Neuron 96:1223-1238.

Adermark L, Lovinger DM (2007) Combined activation of L-type Ca2+ channels and synaptic transmission is sufficient to induce striatal long-term depression. Journal of Neuroscience 27:6781-6787.

Adrover MF, Shin JH, Alvarez VA (2014) Glutamate and dopamine transmission from midbrain dopamine neurons share similar release properties but are differentially affected by cocaine. Journal of Neuroscience 34:3183-3192.

Ahlenius S, Carlsson A, Engel J, Svensson T (1973) Antagonism by alpha methyltyrosine of the ethanol‐induced stimulation and euphoria in man. Clinical Pharmacology and Therapeutics 14:586-591.

Anacker AM, Loftis JM, Kaur S, Ryabinin AE (2011) Prairie voles as a novel model of socially facilitated excessive drinking. Addiction Biology 16:92-107.

Anderson P, Baumberg B (2006) Alcohol in europe: a public health persepctive. A report for the European commission. London, UK: Institute of Alcohol Studies.

Arevalo E, Shanmugasundararaj S, Wilkemeyer MF, Dou X, Chen S, Charness ME, Miller KW (2008) An alcohol binding site on the neural cell adhesion molecule L1. Proceedings of the National Academy of Sciences 105:371-375.

Aryal P, Dvir H, Choe S, Slesinger PA (2009) A discrete alcohol pocket involved in GIRK channel activation. Nature Neuroscience 12:988-995.

Augood S, Westmore K, Emson P (1996) Phenotypic characterization of neurotensin messenger RNA-expressing cells in the neuroleptic-treated rat striatum: a detailed cellular co-expression study. Neuroscience 76:763-774.

Baculis BC, Valenzuela CF (2015) Ethanol exposure during the third trimester equivalent does not affect GABAA or AMPA receptor-mediated spontaneous synaptic transmission in rat CA3 pyramidal neurons. Journal of Negative Results in Biomedicine 14:19.

Badanich KA, Mulholland PJ, Beckley JT, Trantham-Davidson H, Woodward JJ (2013) Ethanol reduces neuronal excitability of lateral orbitofrontal cortex neurons via a glycine receptor dependent mechanism. Neuropsychopharmacology 38:1176-1188.

Bahi A, Dreyer JL (2012) Involvement of nucleus accumbens dopamine D1 receptors in ethanol drinking, ethanol-induced conditioned place preference, and ethanol-induced psychomotor sensitization in mice. Psychopharmacology 222:141-153.

Bailey CPOC, M.J.; Croft, A.P.; Manley, S.J.; Little, H.J. (2001) Alterations in mesolimbic dopamine function during the abstinence period following chronic ethanol consumption. Neuropharmacology 41:989-999.

Bakhireva LN, Sharkis J, Shrestha S, Miranda‐Sohrabji TJ, Williams S, Miranda RC (2017) Prevalence of prenatal alcohol exposure in the state of Texas as assessed by phosphatidylethanol in newborn dried blood spot specimens. Alcoholism: Clinical and Experimental Research 41:1004-1011.

Balleine BW, O'Doherty JP (2010) Human and rodent homologies in action control: corticostriatal determinants of goal-directed and habitual action. Neuropsychopharmacology 35:48-69.

Barak S, Carnicella S, Yowell QV, Ron D (2011) Glial cell line-derived neurotrophic factor reverses alcohol-induced allostasis of the mesolimbic dopaminergic system: implications for alcohol reward and seeking. Journal of Neuroscience 31:9885-9894.

Barker JM, Torregrossa MM, Taylor JR (2013) Bidirectional modulation of infralimbic dopamine D1 and D2 receptor activity regulates flexible reward seeking. Frontiers in Neuroscience 7:126.

Barrientos C, Knowland D, Wu MMJ, Lilascharoen V, Huang KW, Malenka RC, Lim BK (2018) Cocaine-induced structural plasticity in input regions to distinct cell types in nucleus accumbens. Biological Psychiatry [Epub ahead of print].

Bartlett TE, Bannister NJ, Collett VJ, Dargan SL, Massey PV, Bortolotto ZA, Fitzjohn SM, Bashir ZI, Collingridge GL, Lodge D (2007) Differential roles of NR2A and NR2B-containing NMDA receptors in LTP and LTD in the CA1 region of two-week old rat hippocampus. Neuropharmacology 52:60-70.

Bassareo V, De Luca MA, Aresu M, Aste A, Ariu T, Di Chiara G (2003) Differential adaptive properties of accumbens shell dopamine responses to ethanol as a drug and as a motivational stimulus. European Journal of Neuroscience 17:1465-1472.

Beaulieu JM, Gainetdinov RR (2011) The physiology, signaling, and pharmacology of dopamine receptors. Pharmacological Reviews 63:182-217.

Beaulieu JM, Gainetdinov RR, Caron MG (2009) Akt/GSK3 signaling in the action of psychotropic drugs. Annual Review of Pharmacology and Toxicology 49:327-347.

Becker HC, Ron D (2014) Animal models of excessive alcohol consumption: recent advances and future challenges. Alcohol 48:205-208.

Beier KT, Steinberg EE, DeLoach KE, Xie S, Miyamichi K, Schwarz L, Gao XJ, Kremer EJ, Malenka RC, Luo L (2015) Circuit architecture of VTA dopamine neurons revealed by systematic input-output mapping. Cell 162:622-634.

Belin D, Everitt BJ (2008) Cocaine seeking habits depend upon dopamine-dependent serial connectivity linking the ventral with the dorsal striatum. Neuron 57:432-441.

Bennett B, Bolam J (1994) Synaptic input and output of parvalbumin-immunoreactive neurons in the neostriatum of the rat. Neuroscience 62:707-719.

Bergson C, Mrzljak L, Smiley JF, Pappy M, Levenson R, Goldman-Rakic PS (1995) Regional, cellular, and subcellular variations in the distribution of D1 and D5 dopamine receptors in primate brain. Journal of Neuroscience 15:7821-7836.

Bertran-Gonzalez J, Bosch C, Maroteaux M, Matamales M, Herve D, Valjent E, Girault JA (2008) Opposing patterns of signaling activation in dopamine D1 and D2 receptor-expressing striatal neurons in response to cocaine and haloperidol. Journal of Neuroscience 28:5671-5685.

Betz H (1991) Glycine receptors: heterogeneous and widespread in the mammalian brain. Trends in Neurosciences 14:458-461.

Beurel E, Grieco SF, Jope RS (2015) Glycogen synthase kinase-3 (GSK3): regulation, actions, and diseases. Pharmacology and Therapeutics 148:114-131.

Bienkowski P, Koros E, Kostowski W, Danysz W (1999) Effects of N-methyl-D-aspartate receptor antagonists on reinforced and nonreinforced responding for ethanol in rats. Alcohol 18:131-137.

Blackwell KT, Czubayko U, Plenz D (2003) Quantitative estimate of synaptic inputs to striatal neurons during up and down states in vitro. Journal of Neuroscience 23:9123-9132.

Bock R, Shin JH, Kaplan AR, Dobi A, Markey E, Kramer PF, Gremel CM, Christensen CH, Adrover MF, Alvarez VA (2013) Strengthening the accumbal indirect pathway promotes resilience to compulsive cocaine use. Nature Neuroscience 16:632-638.

Bodhinathan K, Slesinger PA (2013) Molecular mechanism underlying ethanol activation of G-protein-gated inwardly rectifying potassium channels. Proceedings of the National Academy of Sciences 110:18309-18314.

Boehm SL, 2nd, Ponomarev I, Jennings AW, Whiting PJ, Rosahl TW, Garrett EM, Blednov YA, Harris RA (2004) gamma-Aminobutyric acid A receptor subunit mutant mice: new perspectives on alcohol actions. Biochemical Pharmacology 68:1581-1602.

Boileau I, Assaad JM, Pihl RO, Benkelfat C, Leyton M, Diksic M, Tremblay RE, Dagher A (2003) Alcohol promotes dopamine release in the human nucleus accumbens. Synapse 49:226-231.

Bonci A, Bernardi G, Grillner P, Mercuri NB (2003) The dopamine-containing neuron: maestro or simple musician in the orchestra of addiction? Trends in Pharmacological Sciences 24:172-177.

Bosron WF, Ehrig T, Li TK (1993) Genetic factors in alcohol metabolism and alcoholism. Seminars in Liver Disease 13:126-135.

Bossert JM, Adhikary S, St Laurent R, Marchant NJ, Wang HL, Morales M, Shaham Y (2016) Role of projections from ventral subiculum to nucleus accumbens shell in context-induced reinstatement of heroin seeking in rats. Psychopharmacology 233:1991-2004.

Bracci E, Centonze D, Bernardi G, Calabresi P (2002) Dopamine excites fast-spiking interneurons in the striatum. Journal of Neurophysiology 87:2190-2194.

Braunlich K, Seger C (2013) The basal ganglia. Wiley Interdisciplinary Reviews: Cognitive Science 4:135-148.

Brickley SG, Mody I (2012) Extrasynaptic GABA(A) receptors: their function in the CNS and implications for disease. Neuron 73:23-34.

Britt JP, Benaliouad F, McDevitt RA, Stuber GD, Wise RA, Bonci A (2012) Synaptic and behavioral profile of multiple glutamatergic inputs to the nucleus accumbens. Neuron 76:790-803.

Brodie MSASB (1998) The effects of ethanol on dopaminergic neurons of the ventral tegmental area studied with intracellular recording in brain slices Alcoholism: Clinical and Experimental Research 22:236-244.

Brodie MSP, C.; Appel, S. B. (1999) Ethanol directly excites dopaminergic ventral tegmental area reward neurons. Alcoholism: Clinical and Experimental Research 23:1848-1852.

Brodie MSSSDT (1990) Ethanol increases the firing rate of dopamine neurons of the rat ventral tegmental area in vitro. Brain Research 508:65-69.

Brodie MST, R. D.; Shefner S. (1994) Serotonin potentiates ethanol-induced excitation of ventral tegmental area neurons in brain slices from three different rat strains. The Journal of Pharmacology and Experimental Therapeutics 273:1139-1145.

Bromberg-Martin ES, Matsumoto M, Hikosaka O (2010) Dopamine in motivational control: rewarding, aversive, and alerting. Neuron 68:815-834.

Brown HD, Baker PM, Ragozzino ME (2010) The parafascicular thalamic nucleus concomitantly influences behavioral flexibility and dorsomedial striatal acetylcholine output in rats. Journal of Neuroscience 30:14390-14398.

Brown TE, Lee BR, Mu P, Ferguson D, Dietz D, Ohnishi YN, Lin Y, Suska A, Ishikawa M, Huang YH, Shen H, Kalivas PW, Sorg BA, Zukin RS, Nestler EJ, Dong Y, Schluter OM (2011) A silent synapse-based mechanism for cocaine-induced locomotor sensitization. Journal of Neuroscience 31:8163-8174.

Bukiya AN, Kuntamallappanavar G, Edwards J, Singh AK, Shivakumar B, Dopico AM (2014) An alcohol-sensing site in the calcium- and voltage-gated, large conductance potassium (BK) channel. Proceedings of the National Academy of Sciences 111:9313-9318.

Calabresi P, Pisani A, Mercuri N, Bernardi G (1992) Long‐term potentiation in the striatum is unmasked by removing the voltage‐dependent magnesium block of NMDA receptor channels. European Journal of Neuroscience 4:929-935.

Calabresi P, Picconi B, Tozzi A, Di Filippo M (2007) Dopamine-mediated regulation of corticostriatal synaptic plasticity. Trends in Neurosciences 30:211-219.

Calabresi P, Picconi B, Tozzi A, Ghiglieri V, Di Filippo M (2014) Direct and indirect pathways of basal ganglia: a critical reappraisal. Nature Neuroscience 17:1022-1030.

Carlson SL, Bohnsack JP, Morrow AL (2016) Ethanol regulation of synaptic GABAA α4 receptors is prevented by protein kinase A activation. Journal of Pharmacology and Experimental Therapeutics 357:10-16.

Carnicella S, Amamoto R, Ron D (2009) Excessive alcohol consumption is blocked by glial cell line-derived neurotrophic factor. Alcohol 43:35-43.

Carpenter-Hyland EP, Woodward JJ, Chandler LJ (2004) Chronic ethanol induces synaptic but not extrasynaptic targeting of NMDA receptors. Journal of Neuroscience 24:7859-7868.

Cederbaum AI (2012) Alcohol metabolism. Clinics in Liver Disease 16:667-685.

Center for Behavioral Health Statistics and Quality (2015) Behavioral health trends in the United States: Results from the 2014 National Survey on Drug Use and Health: HHS Publication.

Centonze D, Grande C, Usiello A, Gubellini P, Erbs E, Martin AB, Pisani A, Tognazzi N, Bernardi G, Moratalla R, Borrelli E, Calabresi P (2003) Receptor subtypes involved in the presynaptic and postsynaptic actions of dopamine on striatal interneurons. Journal of Neuroscience 23:6245-6254.

Chang CY, Esber GR, Marrero-Garcia Y, Yau HJ, Bonci A, Schoenbaum G (2016) Brief optogenetic inhibition of dopamine neurons mimics endogenous negative reward prediction errors. Nature Neuroscience 19:111-116.

Chen BT, Bowers MS, Martin M, Hopf FW, Guillory AM, Carelli RM, Chou JK, Bonci A (2008) Cocaine but not natural reward self-administration nor passive cocaine infusion produces persistent LTP in the VTA. Neuron 59:288-297.

Chen T-W, Wardill TJ, Sun Y, Pulver SR, Renninger SL, Baohan A, Schreiter ER, Kerr RA, Orger MB, Jayaraman V (2013) Ultrasensitive fluorescent proteins for imaging neuronal activity. Nature 499:295.

Chen YH, Lin BJ, Hsieh TH, Kuo TT, Miller J, Chou YC, Huang EY, Hoffer BJ (2018) Differences in nicotine encoding dopamine release between the striatum and shell portion of the nucleus accumbens. Cell Transplantation:963689718775382.

Cheng Y, Huang CCY, Ma T, Wei X, Wang X, Lu J, Wang J (2017) Distinct synaptic strengthening of the striatal direct and indirect pathways drives alcohol consumption. Biological Psychiatry 81:918-929.

Corbit LH, Muir JL, Balleine BW (2001) The role of the nucleus accumbens in instrumental conditioning: Evidence of a functional dissociation between accumbens core and shell. Journal of Neuroscience 21:3251-3260.

Corbit LH, Chieng BC, Balleine BW (2014) Effects of repeated cocaine exposure on habit learning and reversal by N-acetylcysteine. Neuropsychopharmacology 39:1893-1901.

Crabbe JC, Phillips TJ, Harris RA, Arends MA, Koob GF (2006) Alcohol-related genes: contributions from studies with genetically engineered mice. Addiction Biology 11:195-269.

Creed M, Pascoli VJ, Luscher C (2015) Addiction therapy. Refining deep brain stimulation to emulate optogenetic treatment of synaptic pathology. Science 347:659-664.

Creed M, Ntamati NR, Chandra R, Lobo MK, Luscher C (2016) Convergence of reinforcing and anhedonic cocaine effects in the ventral pallidum. Neuron 92:214-226.

Cruikshank SJ, Urabe H, Nurmikko AV, Connors BW (2010) Pathway-specific feedforward circuits between thalamus and neocortex revealed by selective optical stimulation of axons. Neuron 65:230-245.

Cunningham CL, Gremel CM, Groblewski PA (2006) Drug-induced conditioned place preference and aversion in mice. Nature Protocols 1:1662-1670.

D'Souza M (2003) Chronic D1 agonist and ethanol coadministration facilitate ethanol-mediated behaviors. Pharmacology Biochemistry and Behavior 76:335-342.

Darcq E, Warnault V, Phamluong K, Besserer GM, Liu F, Ron D (2015) MicroRNA-30a-5p in the prefrontal cortex controls the transition from moderate to excessive alcohol consumption. Molecular Psychiatry 20:1219-1231.

Dayas CV, Liu X, Simms JA, Weiss F (2007) Distinct patterns of neural activation associated with ethanol seeking: effects of naltrexone. Biological Psychiatry 61:979-989.

Diana M (2011) The dopamine hypothesis of drug addiction and its potential therapeutic value. Front Psychiatry 2:64.

Diaz MR, Vollmer CC, Zamudio-Bulcock PA, Vollmer W, Blomquist SL, Morton RA, Everett JC, Zurek AA, Yu J, Orser BA, Valenzuela CF (2014) Repeated intermittent alcohol exposure during the third trimester-equivalent increases expression of the GABA(A) receptor delta subunit in cerebellar granule neurons and delays motor development in rats. Neuropharmacology 79:262-274.

DiPadova C, Worner TM, Julkunen RJK, Lieber CS (1987) Effects of fasting and chronic alcohol consumption on the first-pass metabolism of ethanol. Gastroenterology 92:1169-1173.

Dong Y, Nestler EJ (2014) The neural rejuvenation hypothesis of cocaine addiction. Trends in Pharmacological Sciences 35:374-383.

Dopico AM, Bukiya AN, Martin GE (2014) Ethanol modulation of mammalian BK channels in excitable tissues: molecular targets and their possible contribution to alcohol-induced altered behavior. Frontiers in Physiology 5:466.

Doyon WM, York JL, Diaz LM, Samson HH, Czachowski CL, Gonzales RA (2003) Dopamine activity in the nucleus accumbens during consummatory phases of oral ethanol self-administration. Alcoholism: Clinical and Experimental Research 27:1573-1582.

Durieux PF, Schiffmann SN, de Kerchove d'Exaerde A (2012) Differential regulation of motor control and response to dopaminergic drugs by D1R and D2R neurons in distinct dorsal striatum subregions. The EMBO Journal 31:640-653.

Dyr W, McBride WJ, Lumeng L, Li TK, Murphy JM (1993) Effects of D1 and D2 dopamine receptor agents on ethanol consumption in the high-alcohol-drinking (HAD) line of rats. Alcohol 10:207-212.

El-Ghundi M, George SR, Drago J, Fletcher PJ, Fan T, Nguyen T, Liu C, Sibley DR, Westphal H, O'Dowd BF (1998) Disruption of dopamine D1 receptor gene expression attenuates alcohol-seeking behavior. European Journal of Pharmacology 353:149-158.

Emond V, Joyal C, Poissant H (2009) Structural and functional neuroanatomy of attention-deficit hyperactivity disorder (ADHD). Encephale 35:107-114.

Engel JAF, C.; Hulthe, P.; Hard, E.; Johannessen, K.; Snape, B.; Svensson, L. (1988) Biochemical and behavioral evidence for an interaction between ethanol and calcium channel antagonists. Journal of Neural Transmission 74:181-193.

Enoch M-A, Goldman D (2002) Problem drinking and alcoholism: diagnosis and treatment. American Family Physician 65:441-454.

Ericson M, Molander A, Löf E, Engel JA, Söderpalm B (2003) Ethanol elevates accumbal dopamine levels via indirect activation of ventral tegmental nicotinic acetylcholine receptors. European Journal of Pharmacology 467:85-93.

Everitt BJ, Robbins TW (2013) From the ventral to the dorsal striatum: devolving views of their roles in drug addiction. Neuroscience and Biobehavioral Reviews 37:1946-1954.

Everitt BJ, Robbins TW (2016) Drug Addiction: Updating Actions to Habits to Compulsions Ten Years On. Annual Review of Psychology 67:23-50.

Fadda FA, A.; Melis, M. R.; Serra, G.; Gessa, G. L. (1980) Differential effect of acute and chronic ethanol on dopamine metabolism in frontal cortex, caudate nucleus and substantia nigra. Life Sciences 27:979-986.

Fenno L, Yizhar O, Deisseroth K (2011) The development and application of optogenetics. Annual Review of Neuroscience 34.

Ferguson SM, Eskenazi D, Ishikawa M, Wanat MJ, Phillips PE, Dong Y, Roth BL, Neumaier JF (2011) Transient neuronal inhibition reveals opposing roles of indirect and direct pathways in sensitization. Nature Neuroscience 14:22-24.

Fernandez AM, Torres-Aleman I (2012) The many faces of insulin-like peptide signalling in the brain. Nature Reviews: Neuroscience 13:225-239.

Ferreira TA, Blackman AV, Oyrer J, Jayabal S, Chung AJ, Watt AJ, Sjostrom PJ, van Meyel DJ (2014) Neuronal morphometry directly from bitmap images. Nature Methods 11:982-984.

Filbey FM, Claus E, Audette AR, Niculescu M, Banich MT, Tanabe J, Du YP, Hutchison KE (2008) Exposure to the taste of alcohol elicits activation of the mesocorticolimbic neurocircuitry. Neuropsychopharmacology 33:1391-1401.

Fish E, Holloway H, Rumple A, Baker L, Wieczorek L, Moy S, Paniagua B, Parnell S (2016) Acute alcohol exposure during neurulation: Behavioral and brain structural consequences in adolescent C57BL/6J mice. Behavioural Brain Research 311:70-80.

Floresco SB, McLaughlin RJ, Haluk DM (2008) Opposing roles for the nucleus accumbens core and shell in cue-induced reinstatement of food-seeking behavior. Neuroscience 154:877-884.

Fox CJ, Russell KI, Wang YT, Christie BR (2006) Contribution of NR2A and NR2B NMDA subunits to bidirectional synaptic plasticity in the hippocampus in vivo. Hippocampus 16:907-915.

Frankel F, Paley B, Marquardt R, O'Connor M (2006) Stimulants, neuroleptics, and children's friendship training for children with fetal alcohol spectrum disorders. Journal of Child and Adolescent Psychopharmacology 16:777-789.

Franklin L, Deitz J, Jirikowic T, Astley S (2008) Children with fetal alcohol spectrum disorders: problem behaviors and sensory processing. The American Journal of Occupational Therapy 62:265.

Freeze BS, Kravitz AV, Hammack N, Berke JD, Kreitzer AC (2013) Control of basal ganglia output by direct and indirect pathway projection neurons. Journal of Neuroscience 33:18531-18539.

Fuchs RA, Branham RK, See RE (2006) Different neural substrates mediate cocaine seeking after abstinence versus extinction training: a critical role for the dorsolateral caudate-putamen. Journal of Neuroscience 26:3584-3588.

Garlsson AE, J.; Strombom, U.; Svensson, T. H.; Waldeck, B. (1974) Suppresion by dopamine-agonists of the ethanol-induced stimulation of locomotor activity and brain dopamine synthesis. Naunyn-Schmiedeberg's Arch Pharmacol 283:117-128.

George O, Le Moal M, Koob GF (2012) Allostasis and addiction: role of the dopamine and corticotropin-releasing factor systems. Physiology and Behavior 106:58-64.

Gerdeman GL, Ronesi J, Lovinger DM (2002) Postsynaptic endocannabinoid release is critical to long-term depression in the striatum. Nature Neuroscience 5:446.

Gerfen CR (1992) The neostriatal mosaic: multiple levels of compartmental organization in the basal ganglia. Annual Review of Neuroscience 15:285-320.

Gerfen CR, Surmeier DJ (2011) Modulation of striatal projection systems by dopamine. Annual Review of Neuroscience 34:441-466.

Gessa GLM, F.; Collu, M.; Vargui, L.; Mereu G. (1985) Low doses of ethanol activate dopaminergic neurons in the ventral tegmental area. Brain Research 348:201-203.

Gibb SL, Jeanblanc J, Barak S, Yowell QV, Yaka R, Ron D (2011) Lyn kinase regulates mesolimbic dopamine release: implication for alcohol reward. Journal of Neuroscience 31:2180-2187.

Girault J-A, Valjent E, Caboche J, Hervé D (2007) ERK2: a logical AND gate critical for drug-induced plasticity? Current Opinion in Pharmacology 7:77-85.

Giros BJ, M.; Jones, S. R.; Wightman, R. M.; Caron, M. G. (1996) Hyperlocomotion and indifference to cocaine and amphetamine in mice lacking the dopamine transporter. Nature 379:606-612.

Gittis AH, Kreitzer AC (2012) Striatal microcircuitry and movement disorders. Trends in Neurosciences 35:557-564.

Gittis AH, Hang GB, LaDow ES, Shoenfeld LR, Atallah BV, Finkbeiner S, Kreitzer AC (2011) Rapid target-specific remodeling of fast-spiking inhibitory circuits after loss of dopamine. Neuron 71:858-868.

Gittis AH, Berke JD, Bevan MD, Chan CS, Mallet N, Morrow MM, Schmidt R (2014) New roles for the external globus pallidus in basal ganglia circuits and behavior. Journal of Neuroscience 34:15178-15183.

Glaaser IW, Slesinger PA (2017) Dual activation of neuronal G protein-gated inwardly rectifying potassium (GIRK) channels by cholesterol and alcohol. Scientific Reports 7:4592.

Glantz MD et al. (2014) Alcohol abuse in developed and developing countries in the World Mental Health Surveys: Socially defined consequences or psychiatric disorder? American Journal on Addictions 23:145-155.

Golovko AI, Golovko SI, Leontieva LV, Zefirov SY (2002) The influence of ethanol on the functional status of GABA(A) receptors. Biochemistry (moscow) 67:719-729.

Gong S, Doughty M, Harbaugh CR, Cummins A, Hatten ME, Heintz N, Gerfen CR (2007) Targeting Cre recombinase to specific neuron populations with bacterial artificial chromosome constructs. Journal of Neuroscience 27:9817-9823.

Grace A, Bunney B (1983) Intracellular and extracellular electrophysiology of nigral dopaminergic neurons—1. Identification and characterization. Neuroscience 10:301-315.

Grace AA, Floresco SB, Goto Y, Lodge DJ (2007) Regulation of firing of dopaminergic neurons and control of goal-directed behaviors. Trends in Neurosciences 30:220-227.

Graybiel AM, Aosaki T, Flaherty AW, Kimura M (1994) The basal ganglia and adaptive motor control. Science 265:1826-1831.

Gremel CM, Costa RM (2013a) Premotor cortex is critical for goal-directed actions. Frontiers in Computational Neuroscience 7:110.

Gremel CM, Costa RM (2013b) Orbitofrontal and striatal circuits dynamically encode the shift between goal-directed and habitual actions. Nature Communications 4:2264.

Gremel CM, Chancey JH, Atwood BK, Luo G, Neve R, Ramakrishnan C, Deisseroth K, Lovinger DM, Costa RM (2016) Endocannabinoid modulation of orbitostriatal circuits gates habit formation. Neuron 90:1312-1324.

Groenewegen HJ, Wright CI, Beijer AV (1996) The nucleus accumbens: gateway for limbic structures to reach the motor system? Progress in Brain Research 107:485-511.

Gunaydin LA, Kreitzer AC (2016) Cortico-Basal Ganglia Circuit Function in Psychiatric Disease. Annual Review of Physiology 78:327-350.

Hart AS, Rutledge RB, Glimcher PW, Phillips PE (2014) Phasic dopamine release in the rat nucleus accumbens symmetrically encodes a reward prediction error term. Journal of Neuroscience 34:698-704.

Hausknecht KA, Acheson A, Farrar AM, Kieres AK, Shen RY, Richards JB, Sabol KE (2005) Prenatal alcohol exposure causes attention deficits in male rats. Behavioral Neuroscience 119:302-310.

Hayashi S, Watanabe J, Kawajiri K (1991) Genetic polymorphisms in the 5'-flanking region change transcriptional regulation of the human cytochrome P450IIE1 gene. Journal of Biochemistry 110:559-565.

Healey JC, Winder DG, Kash TL (2008) Chronic ethanol exposure leads to divergent control of dopaminergic synapses in distinct target regions. Alcohol 42:179-190.

Health USDo, Abuse HSS, Statistics MHSACfBH, Quality (2016) National survey on drug use and health, 2014. In: Inter-university Consortium for Political and Social Research [distributor].

Hellemans KG, Verma P, Yoon E, Yu W, Weinberg J (2008) Prenatal alcohol exposure increases vulnerability to stress and anxiety-like disorders in adulthood. Annals of the New York Academy of Sciences 1144:154-175.

Hernandez PJ, Sadeghian K, Kelley AE (2002) Early consolidation of instrumental learning requires protein synthesis in the nucleus accumbens. Nature Neuroscience 5:1327-1331.

Hersch SM, Gutekunst C-A, Rees H, Heilman CJ, Levey AI (1994) Distribution of m1-m4 muscarinic receptor proteins in the rat striatum: light and electron microscopic immunocytochemistry using subtype-specific antibodies. Journal of Neuroscience 14:3351-3363.

Herve D, Levi-Strauss M, Marey-Semper I, Verney C, Tassin J, Glowinski J, Girault J (1993) G (olf) and Gs in rat basal ganglia: possible involvement of G (olf) in the coupling of dopamine D1 receptor with adenylyl cyclase. Journal of Neuroscience 13:2237-2248.

Hikida T, Kimura K, Wada N, Funabiki K, Nakanishi S (2010) Distinct roles of synaptic transmission in direct and indirect striatal pathways to reward and aversive behavior. Neuron 66:896-907.

Hodge CW, Samson HH, Chappelle AM (1997) Alcohol self-administration: further examination of the role of dopamine receptors in the nucleus accumbens. Alcoholism: Clinical and Experimental Research 21:1083-1091.

Holmes A, Spanagel R, Krystal JH (2013) Glutamatergic targets for new alcohol medications. Psychopharmacology 229:539-554.

Hoover WB, Vertes RP (2011) Projections of the medial orbital and ventral orbital cortex in the rat. Journal of Comparative Neurology 519:3766-3801.

Hsiao SH, Frye GD (2003) AMPA receptors on developing medial septum/diagonal band neurons are sensitive to early postnatal binge-like ethanol exposure. Developmental Brain Research 142:89-99.

Huang CC, Ma T, Hellard EAR, Wang X, Selvamani A, Lu J, Sohrabji F, Wang J (2017) Stroke triggers nigrostriatal plasticity and increases alcohol consumption in rats. Scientific Reports 7:2501.

Huang YH, Lin Y, Mu P, Lee BR, Brown TE, Wayman G, Marie H, Liu W, Yan Z, Sorg BA, Schluter OM, Zukin RS, Dong Y (2009) In vivo cocaine experience generates silent synapses. Neuron 63:40-47.

Hwa LS, Chu A, Levinson SA, Kayyali TM, DeBold JF, Miczek KA (2011) Persistent escalation of alcohol drinking in C57BL/6J mice with intermittent access to 20% ethanol. Alcoholism: Clinical and Experimental Research 35:1938-1947.

Hyman SE, Malenka RC, Nestler EJ (2006) Neural mechanisms of addiction: the role of reward-related learning and memory. Annual Review of Neuroscience 29:565-598.

Hyytia P, Koob GF (1995) GABAA receptor antagonism in the extended amygdala decreases ethanol self-administration in rats. European Journal of Pharmacology 283:151-159.

Idrus NM, McGough NN, Riley EP, Thomas JD (2014) Administration of memantine during withdrawal mitigates overactivity and spatial learning impairments associated with neonatal alcohol exposure in rats. Alcoholism: Clinical and Experimental Research 38:529-537.

Ince E, Ciliax BJ, Levey AI (1997) Differential expression of D1 and D2 dopamine and m4 muscarinic acetylcholine receptor proteins in identified striatonigral neurons. Synapse 27:357-366.

Infante MA, Moore EM, Nguyen TT, Fourligas N, Mattson SN, Riley EP (2015) Objective assessment of ADHD core symptoms in children with heavy prenatal alcohol exposure. Physiology and Behavior 148:45-50.

Itier V, Bertrand D (2001) Neuronal nicotinic receptors: from protein structure to function. FEBS Letters 504:118-125.

Ito R, Robbins TW, Everitt BJ (2004) Differential control over cocaine-seeking behavior by nucleus accumbens core and shell. Nature Neuroscience 7:389-397.

Janssen MJ, Yasuda RP, Vicini S (2011) GABA(A) Receptor beta3 Subunit Expression Regulates Tonic Current in Developing Striatopallidal Medium Spiny Neurons. Frontiers in Cellular Neuroscience 5:15.

Janssen MJ, Ade KK, Fu Z, Vicini S (2009) Dopamine modulation of GABA tonic conductance in striatal output neurons. Journal of Neuroscience 29:5116-5126.

Jeanblanc J, He DY, Carnicella S, Kharazia V, Janak PH, Ron D (2009) Endogenous BDNF in the dorsolateral striatum gates alcohol drinking. Journal of Neuroscience 29:13494-13502.

Johnson SWN, R. A. (1992) Opioids excite dopamine neurons by hyperpolarization of local interneurons. Journal of Neuroscience 1992:2.

June HL, Gilpin NW (2010) Operant self‐administration models for testing the neuropharmacological basis of ethanol consumption in rats. Current Protocols in Neuroscience 51:9.12. 11-19.12. 26.

June HL, Sr., Foster KL, Eiler WJ, 2nd, Goergen J, Cook JB, Johnson N, Mensah-Zoe B, Simmons JO, June HL, Jr., Yin W, Cook JM, Homanics GE (2007) Dopamine and benzodiazepine-dependent mechanisms regulate the EtOH-enhanced locomotor stimulation in the GABAA alpha1 subunit null mutant mice. Neuropsychopharmacology 32:137-152.

Kahlig KM, Binda F, Khoshbouei H, Blakely RD, McMahon DG, Javitch JA, Galli A (2005) Amphetamine induces dopamine efflux through a dopamine transporter channel. Proceedings of the National Academy of Sciences 102:3495-3500.

Kalant H (1996) Pharmacokinetics of ethanol: absorption, distribution, and elimination. The pharmacology of alcohol and alcohol dependence:15-58.

Kaminen-Ahola N, Ahola A, Maga M, Mallitt KA, Fahey P, Cox TC, Whitelaw E, Chong S (2010) Maternal ethanol consumption alters the epigenotype and the phenotype of offspring in a mouse model. PLoS Genet 6:e1000811.

Kasai H, Fukuda M, Watanabe S, Hayashi-Takagi A, Noguchi J (2010) Structural dynamics of dendritic spines in memory and cognition. Trends in Neurosciences 33:121-129.

Kash TL, Baucum AJ, 2nd, Conrad KL, Colbran RJ, Winder DG (2009) Alcohol exposure alters NMDAR function in the bed nucleus of the stria terminalis. Neuropsychopharmacology 34:2420-2429.

Katner SNWF (1999) Ethanol-associated olfactory stimuli reinstate ethanol-seeking behavior after extinction and modify extracellular dopamine levels in the nucleus accumbens. Alcoholism: Clinical and Experimental Research 23:1751-1760.

Kerchner GA, Nicoll RA (2008) Silent synapses and the emergence of a postsynaptic mechanism for LTP. Nature Reviews Neuroscience 9:813-825.

Kerr JND, Wickens JR (2001) Dopamine D-1/D-5 receptor activation is required for long-term potentiation in the rat neostriatum in vitro. Journal of Neurophysiology 85:117-124.

Kim KC, Go HS, Bak HR, Choi CS, Choi I, Kim P, Han SH, Han SM, Shin CY, Ko KH (2010) Prenatal exposure of ethanol induces increased glutamatergic neuronal differentiation of neural progenitor cells. Journal of Biomedical Science 17:85.

Kim P, Park JH, Choi CS, Choi I, Joo SH, Kim MK, Kim SY, Kim KC, Park SH, Kwon KJ, Lee J, Han SH, Ryu JH, Cheong JH, Han JY, Ko KN, Shin CY (2013) Effects of ethanol

exposure during early pregnancy in hyperactive, inattentive and impulsive behaviors and MeCP2 expression in rodent offspring. Neurochemical Research 38:620-631.

Kim Y, Teylan MA, Baron M, Sands A, Nairn AC, Greengard P (2009) Methylphenidate-induced dendritic spine formation and ΔFosB expression in nucleus accumbens. Proceedings of the National Academy of Sciences:pnas-0813179106.

Klapoetke NC et al. (2014) Independent optical excitation of distinct neural populations. Nature Methods 11:338-346.

Kleiber ML, Wright E, Singh SM (2011) Maternal voluntary drinking in C57BL/6J mice: advancing a model for fetal alcohol spectrum disorders. Behavioural Brain Research 223:376-387.

Kleinlogel S, Feldbauer K, Dempski RE, Fotis H, Wood PG, Bamann C, Bamberg E (2011) Ultra light-sensitive and fast neuronal activation with the Ca(2)+-permeable channelrhodopsin CatCh. Nature Neuroscience 14:513-518.

Kobayashi T, Ikeda K, Kojima H, Niki H, Yano R, Yoshioka T, Kumanishi T (1999) Ethanol opens G-protein-activated inwardly rectifying K+ channels. Nature Neuroscience 2:1091.

Kodali VN, Jacobson JL, Lindinger NM, Dodge NC, Molteno CD, Meintjes EM, Jacobson SW (2017) Differential recruitment of brain regions during response inhibition in children prenatally exposed to alcohol. Alcoholism: Clinical and Experimental Research 41:334-344.

Koob GF (2013) Theoretical frameworks and mechanistic aspects of alcohol addiction: alcohol addiction as a reward deficit disorder. Current Topics in Behavioral Neurosciences 13:3-30.

Koob GF, Le Moal M (2008) Addiction and the brain antireward system. Annual Review of Psychology 59:29-53.

Koob GF, Volkow ND (2010) Neurocircuitry of addiction. Neuropsychopharmacology 35:217-238.

Koós T, Tepper JM (1999) Inhibitory control of neostriatal projection neurons by GABAergic interneurons. Nature Neuroscience 2:467.

Kravitz AV, Tye LD, Kreitzer AC (2012) Distinct roles for direct and indirect pathway striatal neurons in reinforcement. Nature Neuroscience 15:816-818.

Kravitz AV, Freeze BS, Parker PR, Kay K, Thwin MT, Deisseroth K, Kreitzer AC (2010) Regulation of parkinsonian motor behaviours by optogenetic control of basal ganglia circuitry. Nature 466:622-626.

Kreitzer AC (2009) Physiology and pharmacology of striatal neurons. Annual Review of Neuroscience 32:127-147.

Kreitzer AC, Malenka RC (2007) Endocannabinoid-mediated rescue of striatal LTD and motor deficits in Parkinson's disease models. Nature 445:643.

Kreitzer AC, Malenka RC (2008) Striatal plasticity and basal ganglia circuit function. Neuron 60:543-554.

Kroener S, Mulholland PJ, New NN, Gass JT, Becker HC, Chandler LJ (2012) Chronic alcohol exposure alters behavioral and synaptic plasticity of the rodent prefrontal cortex. PloS One 7:e37541.

Land BB, Narayanan NS, Liu RJ, Gianessi CA, Brayton CE, Grimaldi DM, Sarhan M, Guarnieri DJ, Deisseroth K, Aghajanian GK, DiLeone RJ (2014) Medial prefrontal D1 dopamine neurons control food intake. Nature Neuroscience 17:248-253.

Lange S, Rehm J, Anagnostou E, Popova S (2018) Prevalence of externalizing disorders and Autism Spectrum Disorders among children with Fetal Alcohol Spectrum Disorder: systematic review and meta-analysis. Biochemistry and Cell Biology 96:241-251.

Lapper S, Bolam J (1992) Input from the frontal cortex and the parafascicular nucleus to cholinergic interneurons in the dorsal striatum of the rat. Neuroscience 51:533-545.

Larsson A, Svensson L, Söderpalm B, Engel JA (2002) Role of different nicotinic acetylcholine receptors in mediating behavioral and neurochemical effects of ethanol in mice. Alcohol 28:157-167.

Larsson A, Edstrom L, Svensson L, Soderpalm B, Engel JA (2005) Voluntary ethanol intake increases extracellular acetylcholine levels in the ventral tegmental area in the rat. Alcohol and Alcoholism 40:349-358.

Lee BR, Ma Y-Y, Huang YH, Wang X, Otaka M, Ishikawa M, Neumann PA, Graziane NM, Brown TE, Suska A (2013) Maturation of silent synapses in amygdala-accumbens projection contributes to incubation of cocaine craving. Nature Neuroscience 16:1644.

Lee D (2008) Game theory and neural basis of social decision making. Nature Neuroscience 11:404-409.

Lerner TN, Shilyansky C, Davidson TJ, Evans KE, Beier KT, Zalocusky KA, Crow AK, Malenka RC, Luo L, Tomer R, Deisseroth K (2015) Intact-Brain Analyses Reveal Distinct Information Carried by SNc Dopamine Subcircuits. Cell 162:635-647.

Levey AI, Hersch SM, Rye DB, Sunahara RK, Niznik HB, Kitt CA, Price DL, Maggio R, Brann MR, Ciliax BJ (1993) Localization of D1 and D2 dopamine receptors in brain with subtype-specific antibodies. Proceedings of the National Academy of Sciences 90:8861-8865.

Lewohl JM, Wilson WR, Mayfield RD, Brozowski SJ, Morrisett RA, Harris RA (1999) G-protein-coupled inwardly rectifying potassium channels are targets of alcohol action. Nature Neuroscience 2:1084.

Li YC, Wang MJ, Gao WJ (2012) Hyperdopaminergic modulation of inhibitory transmission is dependent on GSK-3beta signaling-mediated trafficking of GABAA receptors. Journal of Neurochemistry 122:308-320.

Li YC, Xi D, Roman J, Huang YQ, Gao WJ (2009) Activation of glycogen synthase kinase-3 beta is required for hyperdopamine and D2 receptor-mediated inhibition of synaptic NMDA receptor function in the rat prefrontal cortex. Journal of Neuroscience 29:15551-15563.

Li YC, Kellendonk C, Simpson EH, Kandel ER, Gao WJ (2011) D2 receptor overexpression in the striatum leads to a deficit in inhibitory transmission and dopamine sensitivity in mouse prefrontal cortex. Proceedings of the National Academy of Sciences 108:12107-12112.

Lieber CS (1992) Medical and nutritional complications of alcoholism: mechanisms and management. New York: Plenum.

Lieber CS (2000) ALCOHOL: its metabolism and interaction with nutrients. Annual Review of Nutrition 20:395-430.

Lieber CS (2005) Metabolism of alcohol. Clinics in Liver Disease 9:1-35.

Lieber CS, DeCarli LM (1968) Ethanol oxidation by hepatic microsomes: adaptive increase after ethanol feeding. Science 162:917-918.

Liu F, Laguesse S, Legastelois R, Morisot N, Ben Hamida S, Ron D (2016) mTORC1-dependent translation of collapsin response mediator protein-2 drives neuroadaptations underlying excessive alcohol-drinking behaviors. Molecular Psychiatry 22:89.

Lobo MK, Nestler EJ (2011) The striatal balancing act in drug addiction: distinct roles of direct and indirect pathway medium spiny neurons. Frontiers in Neuroanatomy 5:41.

Lobo MK, Covington HE, 3rd, Chaudhury D, Friedman AK, Sun H, Damez-Werno D, Dietz DM, Zaman S, Koo JW, Kennedy PJ, Mouzon E, Mogri M, Neve RL, Deisseroth K, Han MH, Nestler EJ (2010) Cell type-specific loss of BDNF signaling mimics optogenetic control of cocaine reward. Science 330:385-390.

Logrip ML, Janak PH, Ron D (2009) Blockade of ethanol reward by the kappa opioid receptor agonist U50,488H. Alcohol 43:359-365.

Longair MH, Baker DA, Armstrong JD (2011) Simple neurite tracer: open source software for reconstruction, visualization and analysis of neuronal processes. Bioinformatics 27:2453-2454.

Louth EL, Bignell W, Taylor CL, Bailey CD (2016) Developmental ethanol exposure leads to long-term deficits in attention and its underlying prefrontal circuitry. Eneuro 3.

Lovinger DM (2010) Neurotransmitter roles in synaptic modulation, plasticity and learning in the dorsal striatum. Neuropharmacology 58:951-961.

Lovinger DM, Kash TL (2015) Mechanisms of neuroplasticity and ethanol's effects on plasticity in the striatum and bed nucleus of the stria terminalis. Alcohol Research: Current Reviews 37:109.

Lovinger DM, White G, Weight FF (1989) Ethanol inhibits NMDA-activated ion current in hippocampal neurons. Science 243:1721-1724.

Lovinger DM, White G, Weight FF (1990) NMDA receptor-mediated synaptic excitation selectively inhibited by ethanol in hippocampal slice from adult rat. Journal of Neuroscience 10:1372-1379.

Luo R, Partridge JG, Vicini S (2013) Distinct roles of synaptic and extrasynaptic GABAAreceptors in striatal inhibition dynamics. Front Neural Circuits 7:186.

Luscher C, Malenka RC (2011) Drug-evoked synaptic plasticity in addiction: from molecular changes to circuit remodeling. Neuron 69:650-663.

Ma T, Barbee B, Wang X, Wang J (2017) Alcohol induces input-specific aberrant synaptic plasticity in the rat dorsomedial striatum. Neuropharmacology 123:46-54.

Ma T, Cheng Y, Roltsch Hellard E, Wang X, Lu J, Gao X, Huang CCY, Wei XY, Ji JY, Wang J (2018) Bidirectional and long-lasting control of alcohol-seeking behavior by corticostriatal LTP and LTD. Nature Neuroscience 21.

Ma Y-Y, Wang X, Huang Y, Marie H, Nestler EJ, Schlüter OM, Dong Y (2016) Re-silencing of silent synapses unmasks anti-relapse effects of environmental enrichment. Proceedings of the National Academy of Sciences:201524739.

Ma Y-Y, Lee BR, Wang X, Guo C, Liu L, Cui R, Lan Y, Balcita-Pedicino JJ, Wolf ME, Sesack SR (2014) Bidirectional modulation of incubation of cocaine craving by silent synapse-based remodeling of prefrontal cortex to accumbens projections. Neuron 83:1453-1467.

MacAskill AF, Cassel JM, Carter AG (2014) Cocaine exposure reorganizes cell type- and input-specific connectivity in the nucleus accumbens. Nature Neuroscience 17:1198-1207.

Madisen L, Zwingman TA, Sunkin SM, Oh SW, Zariwala HA, Gu H, Ng LL, Palmiter RD, Hawrylycz MJ, Jones AR, Lein ES, Zeng H (2010) A robust and high-throughput Cre

reporting and characterization system for the whole mouse brain. Nature Neuroscience 13:133-140.

Madisen L et al. (2015) Transgenic mice for intersectional targeting of neural sensors and effectors with high specificity and performance. Neuron 85:942-958.

Maia TV, Frank MJ (2011) From reinforcement learning models to psychiatric and neurological disorders. Nature Neuroscience 14:154-162.

Malanga CJ, Pejchal M, Kosofsky BE (2007) Prenatal exposure to cocaine alters the development of conditioned place-preference to cocaine in adult mice. Pharmacology, Biochemistry and Behavior 87:462-471.

Mallet N, Le Moine C, Charpier S, Gonon F (2005) Feedforward inhibition of projection neurons by fast-spiking GABA interneurons in the rat striatum in vivo. Journal of Neuroscience 25:3857-3869.

Mallet N, Pogosyan A, Marton LF, Bolam JP, Brown P, Magill PJ (2008) Parkinsonian beta oscillations in the external globus pallidus and their relationship with subthalamic nucleus activity. Journal of Neuroscience 28:14245-14258.

Mallet N, Schmidt R, Leventhal D, Chen F, Amer N, Boraud T, Berke JD (2016) Arkypallidal cells send a stop signal to striatum. Neuron.

Mancini M, Ghiglieri V, Bagetta V, Pendolino V, Vannelli A, Cacace F, Mineo D, Calabresi P, Picconi B (2016) Memantine alters striatal plasticity inducing a shift of synaptic responses toward long-term depression. Neuropharmacology 101:341-350.

Maness PF, Schachner M (2007) Neural recognition molecules of the immunoglobulin superfamily: signaling transducers of axon guidance and neuronal migration. Nature Neuroscience 10:19-26.

Mantha K, Kleiber M, Singh S (2013) Neurodevelopmental timing of ethanol exposure may contribute to observed heterogeneity of behavioral deficits in a mouse model of fetal alcohol spectrum disorder (FASD). Journal of Behavioral and Brain Science 03:85-99.

Martinez D, Gil R, Slifstein M, Hwang DR, Huang Y, Perez A, Kegeles L, Talbot P, Evans S, Krystal J, Laruelle M, Abi-Dargham A (2005) Alcohol dependence is associated with blunted dopamine transmission in the ventral striatum. Biological Psychiatry 58:779-786.

Maskos U, Molles BE, Pons S, Besson M, Guiard BP, Guilloux JP, Evrard A, Cazala P, Cormier A, Mameli-Engvall M, Dufour N, Cloez-Tayarani I, Bemelmans AP, Mallet J, Gardier AM, David V, Faure P, Granon S, Changeux JP (2005) Nicotine reinforcement and cognition restored by targeted expression of nicotinic receptors. Nature 436:103-107.

Mathur BN, Lovinger DM (2012) Endocannabinoid–dopamine interactions in striatal synaptic plasticity. Frontiers in Pharmacology 3:66.

Mattis J, Tye KM, Ferenczi EA, Ramakrishnan C, O'shea DJ, Prakash R, Gunaydin LA, Hyun M, Fenno LE, Gradinaru V (2012) Principles for applying optogenetic tools derived from direct comparative analysis of microbial opsins. Nature Methods 9:159.

Mattson SN, Crocker N, Nguyen TT (2011) Fetal alcohol spectrum disorders: neuropsychological and behavioral features. Neuropsychology Review 21:81-101.

Matzopoulos RG, Truen S, Bowman B, Corrigall J (2014) The cost of harmful alcohol use in South Africa. South African Medical Journal 104:127-132.

May PA, Chambers CD, Kalberg WO, Zellner J, Feldman H, Buckley D, Kopald D, Hasken JM, Xu R, Honerkamp-Smith G (2018) Prevalence of fetal alcohol spectrum disorders in 4 US communities. JAMA 319:474-482.

McBride WJD, W.; Lumeng, L; Li, T. K. (1993) Densities of dopamine D2 receptors are reduced in CNS regions of alcohol-preferring P rats. Alcohol 10:387-390.

McCool BA (2011) Ethanol modulation of synaptic plasticity. Neuropharmacology 61:1097-1108.

McGough NN, He DY, Logrip ML, Jeanblanc J, Phamluong K, Luong K, Kharazia V, Janak PH, Ron D (2004) RACK1 and brain-derived neurotrophic factor: a homeostatic pathway that regulates alcohol addiction. Journal of Neuroscience 24:10542-10552.

McGuier NS, Padula AE, Lopez MF, Woodward JJ, Mulholland PJ (2015) Withdrawal from chronic intermittent alcohol exposure increases dendritic spine density in the lateral orbitofrontal cortex of mice. Alcohol 49:21-27.

Melendez RIR-H, Z. A., Engleman, E. A.; Li, T.; McBride, W. J.; Murphy J. M. (2002) Microdialysis of dopamine in the nucleus accumbens of alcohol-preferring (P) rats during anticipation and operant self-administration of ethanol. Alcoholism: Clinical and Experimental Research 26:318-325.

Mermelstein PG, Song W-J, Tkatch T, Yan Z, Surmeier DJ (1998) Inwardly rectifying potassium (IRK) currents are correlated with IRK subunit expression in rat nucleus accumbens medium spiny neurons. Journal of Neuroscience 18:6650-6661.

Mifsud JH, L; Hoebel, B. (1989) Nicotine infused into the nucleus accumbens increases synaptic dopamine as measured by in vivo microdialysis. Brain Research 478:365-367.

Mihalek RM, Bowers BJ, Wehner JM, Kralic JE, VanDoren MJ, Morrow AL, Homanics GE (2001) GABAA‐receptor δ subunit knockout mice have multiple defects in behavioral responses to ethanol. Alcoholism: Clinical and Experimental Research 25:1708-1718.

Minatohara K, Akiyoshi M, Okuno H (2015) Role of immediate-early genes in synaptic plasticity and neuronal ensembles underlying the memory trace. Front Mol Neurosci 8:78.

Molander A, Lof E, Stomberg R, Ericson M, Soderpalm B (2005) Involvement of accumbal glycine receptors in the regulation of voluntary ethanol intake in the rat. Alcoholism: Clinical and Experimental Research 29:38-45.

Mullikin-Kilpatrick D, Treistman SN (1994) Ethanol inhibition of L-type Ca2+ channels in PC12 cells: role of permeant ions. European Journal of Pharmacology: Environmental Toxicology and Pharmacology 270:17-25.

Munoz B, Fritz BM, Yin F, Atwood BK (2018) Alcohol exposure disrupts mu opioid receptor-mediated long-term depression at insular cortex inputs to dorsolateral striatum. Nature Communications 9:1318.

Nam HW, Hinton DJ, Kang NY, Kim T, Lee MR, Oliveros A, Adams C, Ruby CL, Choi DS (2013) Adenosine transporter ENT1 regulates the acquisition of goal-directed behavior and ethanol drinking through A2A receptor in the dorsomedial striatum. Journal of Neuroscience 33:4329-4338.

National Center for Health Statistics (2013) Health, United States, 2012: With special feature on emergency care. Hyattsville, MD.

National Drug Intelligence Center (2011) National drug threat assessment. Johnstown, PA.

Neasta J, Ben Hamida S, Yowell QV, Carnicella S, Ron D (2011) AKT signaling pathway in the nucleus accumbens mediates excessive alcohol drinking behaviors. Biological Psychiatry 70:575-582.

Nie H, Rewal M, Gill TM, Ron D, Janak PH (2011) Extrasynaptic delta-containing GABAA receptors in the nucleus accumbens dorsomedial shell contribute to alcohol intake. Proceedings of the National Academy of Sciences 108:4459-4464.

Nisenbaum ES, Wilson C (1995) Potassium currents responsible for inward and outward rectification in rat neostriatal spiny projection neurons. Journal of Neuroscience Methods 15:4449-4463.

Oh KH, Haney JJ, Wang X, Chuang CF, Richmond JE, Kim H (2017) ERG-28 controls BK channel trafficking in the ER to regulate synaptic function and alcohol response in C. elegans. Elife 6.

Ortiz J, Fitzgerald LW, Charlton M, Lane S, Trevisan L, Guitart X, Shoemaker W, Duman RS, Nestler EJ (1995) Biochemical actions of chronic ethanol exposure in the mesolimbic dopamine system. Synapse 21:289-298.

Packard MG, McGaugh JL (1996) Inactivation of hippocampus or caudate nucleus with lidocaine differentially affects expression of place and response learning. Neurobiology of Learning and Memory 65:65-72.

Paoletti P, Bellone C, Zhou Q (2013) NMDA receptor subunit diversity: impact on receptor properties, synaptic plasticity and disease. Nature Reviews: Neuroscience 14:383-400.

Parker PR, Lalive AL, Kreitzer AC (2016) Pathway-specific remodeling of thalamostriatal synapses in parkinsonian mice. Neuron 89:734-740.

Pascoli V, Terrier J, Espallergues J, Valjent E, O'Connor EC, Luscher C (2014) Contrasting forms of cocaine-evoked plasticity control components of relapse. Nature 509:459-464.

Patten AR, Fontaine CJ, Christie BR (2014) A comparison of the different animal models of fetal alcohol spectrum disorders and their use in studying complex behaviors. Frontiers in pediatrics 2:93.

Pautassi RM, Nizhnikov ME, Spear NE, Molina JC (2012) Prenatal ethanol exposure leads to greater ethanol-induced appetitive reinforcement. Alcohol 46:585-593.

Phillips TJ, Brown KJ, Burkhart-Kasch S, Wenger CD, Kelly MA, Rubinstein M, Grandy DK, Low MJ (1998) Alcohol preference and sensitivity are markedly reduced in mice lacking dopamine D2 receptors. Nature Neuroscience 1:610-615.

Pina MM, Cunningham CL (2014) Effects of dopamine receptor antagonists on the acquisition of ethanol-induced conditioned place preference in mice. Psychopharmacology 231:459-468.

Pina MM, Young EA, Ryabinin AE, Cunningham CL (2015) The bed nucleus of the stria terminalis regulates ethanol-seeking behavior in mice. Neuropharmacology 99:627-638.

Placzek MS, Zhao W, Wey HY, Morin TM, Hooker JM (2016) PET Neurochemical Imaging Modes. Seminars in Nuclear Medicine 46:20-27.

Quintana A, Sanz E, Wang W, Storey GP, Guler AD, Wanat MJ, Roller BA, La Torre A, Amieux PS, McKnight GS, Bamford NS, Palmiter RD (2012) Lack of GPR88 enhances medium spiny neuron activity and alters motor- and cue-dependent behaviors. Nature Neuroscience 15:1547-1555.

Ramanathan S, Hanley JJ, Deniau J-M, Bolam JP (2002) Synaptic convergence of motor and somatosensory cortical afferents onto GABAergic interneurons in the rat striatum. Journal of Neuroscience 22:8158-8169.

Rando K, Hong KI, Bhagwagar Z, Li CS, Bergquist K, Guarnaccia J, Sinha R (2011) Association of frontal and posterior cortical gray matter volume with time to alcohol relapse: a prospective study. American Journal of Psychiatry 168:183-192.

Resnicoff M, Rubini M, Baserga R, Rubin R (1994) Ethanol inhibits insulin-like growth factor-1-mediated signalling and proliferation of C6 rat glioblastoma cells. Laboratory investigation; a journal of technical methods and pathology 71:657-662.

Resnicoff M, Sell C, Ambrose D, Baserga R, Rubin R (1993) Ethanol inhibits the autophosphorylation of the insulin-like growth factor 1 (IGF-1) receptor and IGF-1-mediated proliferation of 3T3 cells. Journal of Biological Chemistry 268:21777-21782.

Rice JP, Suggs LE, Lusk AV, Parker MO, Candelaria-Cook FT, Akers KG, Savage DD, Hamilton DA (2012) Effects of exposure to moderate levels of ethanol during prenatal brain development on dendritic length, branching, and spine density in the nucleus accumbens and dorsal striatum of adult rats. Alcohol 46:577-584.

Riley EP, Infante MA, Warren KR (2011) Fetal alcohol spectrum disorders: an overview. Neuropsychology Review 21:73.

Robbins TW (2002) The 5-choice serial reaction time task: behavioural pharmacology and functional neurochemistry. Psychopharmacology 163:362-380.

Roberto M, Madamba SG, Stouffer DG, Parsons LH, Siggins GR (2004) Increased GABA release in the central amygdala of ethanol-dependent rats. Journal of Neuroscience 24:10159-10166.

Rock C, Zurita H, Wilson C, Apicella AJ (2016) An inhibitory corticostriatal pathway. Elife 5.

Ron D, Barak S (2016) Molecular mechanisms underlying alcohol-drinking behaviours. Nature Reviews: Neuroscience 17:576-591.

Roozen S, Peters GJY, Kok G, Townend D, Nijhuis J, Curfs L (2016) Worldwide prevalence of fetal alcohol spectrum disorders: A systematic literature review including meta‐analysis. Alcoholism: Clinical and Experimental Research 40:18-32.

Rosenmund C, Stevens CF (1996) Definition of the readily releasable pool of vesicles at hippocampal synapses. Neuron 16:1197-1207.

Rothblat DSR, E.; Schneider J.S. (2001) Effects of chronic alcohol ingestion on the mesostriatal dopamine system in the rat. Neuroscience Letters 300:63-66.

Rothwell PE, Hayton SJ, Sun GL, Fuccillo MV, Lim BK, Malenka RC (2015) Input- and output-specific regulation of serial order performance by corticostriatal circuits. Neuron 88:345-356.

Rui Y, Myers KR, Yu K, Wise A, De Blas AL, Hartzell HC, Zheng JQ (2013) Activity-dependent regulation of dendritic growth and maintenance by glycogen synthase kinase 3beta. Nature Communications 4:2628.

Rushworth MF, Behrens TE (2008) Choice, uncertainty and value in prefrontal and cingulate cortex. Nature Neuroscience 11:389-397.

Saal D, Dong Y, Bonci A, Malenka RC (2003) Drugs of abuse and stress trigger a common synaptic adaptation in dopamine neurons. Neuron 37:577-582.

Salado-Castillo R, Diaz del Guante MA, Alvarado R, Quirarte GL, Prado-Alcala RA (1996) Effects of regional GABAergic blockade of the striatum on memory consolidation. Neurobiology of Learning and Memory 66:102-108.

Salmela KS, Kessova IG, Tsyrlov IB, Lieber CS (1998) Respective roles of human cytochrome P-4502E1, 1A2, and 3A4 in the hepatic microsomal ethanol oxidizing system. Alcoholism: Clinical and Experimental Research 22:2125-2132.

Sanchez Vega MC, Chong S, Burne TH (2013) Early gestational exposure to moderate concentrations of ethanol alters adult behaviour in C57BL/6J mice. Behavioural Brain Research 252:326-333.

Santana N, Mengod G, Artigas F (2009) Quantitative analysis of the expression of dopamine D1 and D2 receptors in pyramidal and GABAergic neurons of the rat prefrontal cortex. Cerebral Cortex 19:849-860.

Saunders BT, Richard JM, Margolis EB, Janak PH (2018) Dopamine neurons create Pavlovian conditioned stimuli with circuit-defined motivational properties. Nature Neuroscience 21:1072-1083.

Schilman EA, Uylings HB, Galis-de Graaf Y, Joel D, Groenewegen HJ (2008) The orbital cortex in rats topographically projects to central parts of the caudate-putamen complex. Neuroscience Letters 432:40-45.

Schoenbaum G, Roesch MR, Stalnaker TA (2006) Orbitofrontal cortex, decision-making and drug addiction. Trends in Neurosciences 29:116-124.

Schultz W (2007) Multiple dopamine functions at different time courses. Annual Review of Neuroscience 30:259-288.

Schultz W, Dayan P, Montague PR (1997) A neural substrate of prediction and reward. Science 275:1593-1599.

Sebe JY, Eggers ED, Berger AJ (2003) Differential effects of ethanol on GABAA and glycine receptor-mediated synaptic currents in brain stem motoneurons. Journal of Neurophysiology 90:870-875.

See RE, Elliott JC, Feltenstein MW (2007) The role of dorsal vs ventral striatal pathways in cocaine-seeking behavior after prolonged abstinence in rats. Psychopharmacology 194:321-331.

Seiler AE, Henderson A, Rubin R (2000) Ethanol inhibits insulin receptor tyrosine kinase. Alcoholism: Clinical and Experimental Research 24:1869-1872.

Sesia T, Temel Y, Lim LW, Blokland A, Steinbusch HW, Visser-Vandewalle V (2008) Deep brain stimulation of the nucleus accumbens core and shell: opposite effects on impulsive action. Experimental Neurology 214:135-139.

Shea KM, Hewitt AJ, Olmstead MC, Brien JF, Reynolds JN (2012) Maternal ethanol consumption by pregnant guinea pigs causes neurobehavioral deficits and increases ethanol preference in offspring. Behavioural Pharmacology 23:105-112.

Shen RY (2003) Ethanol withdrawal reduces the number of spontaneously active ventral tegmental area dopamine neurons in conscious animals. Journal of Pharmacology and Experimental Therapeutics 307:566-572.

Shen RY, Choong KC, Thompson AC (2007) Long-term reduction in ventral tegmental area dopamine neuron population activity following repeated stimulant or ethanol treatment. Biological Psychiatry 61:93-100.

Shen W, Hamilton SE, Nathanson NM, Surmeier DJ (2005) Cholinergic suppression of KCNQ channel currents enhances excitability of striatal medium spiny neurons. Journal of Neuroscience 25:7449-7458.

Shen W, Flajolet M, Greengard P, Surmeier DJ (2008) Dichotomous dopaminergic control of striatal synaptic plasticity. Science 321:848-851.

Shen W, Hernandez-Lopez S, Tkatch T, Held JE, Surmeier DJ (2004) Kv1. 2-containing K+ channels regulate subthreshold excitability of striatal medium spiny neurons. Journal of Neurophysiology 91:1337-1349.

Sholl DA (1953) Dendritic organization in the neurons of the visual and motor cortices of the cat. Journal of Anatomy 87:387-406.

Siciliano CA, Locke JL, Mathews TA, Lopez MF, Becker HC, Jones SR (2017) Dopamine synthesis in alcohol drinking-prone and -resistant mouse strains. Alcohol 58:25-32.

Sidhpura N, Parsons LH (2011) Endocannabinoid-mediated synaptic plasticity and addiction-related behavior. Neuropharmacology 61:1070-1087.

Silvers JM, Tokunaga S, Berry RB, White AM, Matthews DB (2003) Impairments in spatial learning and memory: ethanol, allopregnanolone, and the hippocampus. Brain Research Reviews 43:275-284.

Simms JA, Bito-Onon JJ, Chatterjee S, Bartlett SE (2010) Long-Evans rats acquire operant self-administration of 20% ethanol without sucrose fading. Neuropsychopharmacology 35:1453-1463.

Sippy T, Lapray D, Crochet S, Petersen CC (2015) Cell-type-specific sensorimotor processing in striatal projection neurons during goal-directed behavior. Neuron 88:298-305.

Smith JB, Klug JR, Ross DL, Howard CD, Hollon NG, Ko VI, Hoffman H, Callaway EM, Gerfen CR, Jin X (2016) Genetic-based dissection unveils the inputs and outputs of striatal patch and matrix compartments. Neuron 91:1069-1084.

Smith RJ, Lobo MK, Spencer S, Kalivas PW (2013) Cocaine-induced adaptations in D1 and D2 accumbens projection neurons (a dichotomy not necessarily synonymous with direct and indirect pathways). Current Opinion in Neurobiology 23:546-552.

Smith Y, Bevan MD, Shink E, Bolam JP (1998) Microcircuitry of the direct and indirect pathways of the basal ganglia. Neuroscience 86:353-387.

Smothers CT, Jin C, Woodward JJ (2013) Deletion of the N-terminal domain alters the ethanol inhibition of N-methyl-D-aspartate receptors in a subunit-dependent manner. Alcoholism: Clinical and Experimental Research 37:1882-1890.

Smothers CT, Clayton R, Blevins T, Woodward JJ (2001) Ethanol sensitivity of recombinant human N-methyl-D-aspartate receptors. Neurochemistry International 38:333-340.

Sonuga-Barke EJ, Cortese S, Fairchild G, Stringaris A (2016) Annual research review: Transdiagnostic neuroscience of child and adolescent mental disorders--differentiating decision making in attention-deficit/hyperactivity disorder, conduct disorder, depression, and anxiety. Journal of Child Psychology and Psychiatry and Allied Disciplines 57:321-349.

Steinberg EE, Keiflin R, Boivin JR, Witten IB, Deisseroth K, Janak PH (2013) A causal link between prediction errors, dopamine neurons and learning. Nature Neuroscience 16:966-973.

Stephens EA, Taylor JA, Kaplan N, Yang CH, Hsieh LL, Lucier GW, Bell DA (1994) Ethnic variation in the CYP2E1 gene: polymorphism analysis of 695 African-Americans, European-Americans and Taiwanese. Pharmacogenetics 4:185-192.

Straub C, Saulnier JL, Begue A, Feng DD, Huang KW, Sabatini BL (2016) Principles of synaptic organization of GABAergic interneurons in the striatum. Neuron 92:84-92.

Stuber GD, Hopf FW, Hahn J, Cho SL, Guillory A, Bonci A (2008) Voluntary ethanol intake enhances excitatory synaptic strength in the ventral tegmental area. Alcoholism: Clinical and Experimental Research 32:1714-1720.

Sucher NJ, Awobuluyi M, Choi Y-B, Lipton SA (1996) NMDA receptors: from genes to channels. Trends in Pharmacological Sciences 17:348-355.

Sulzer D (2011) How addictive drugs disrupt presynaptic dopamine neurotransmission. Neuron 69:628-649.

Sun W, Rebec GV (2005) The role of prefrontal cortex D1-like and D2-like receptors in cocaine-seeking behavior in rats. Psychopharmacology 177:315-323.

Sun X, Lin Y (2016) Npas4: linking neuronal activity to memory. Trends in Neurosciences 39:264-275.

Sundstrom-Poromaa I, Smith DH, Gong QH, Sabado TN, Li X, Light A, Wiedmann M, Williams K, Smith SS (2002) Hormonally regulated alpha(4)beta(2)delta GABA(A) receptors are a target for alcohol. Nature Neuroscience 5:721-722.

Surmeier DJ, Bargas J, Kitai S (1989) Two types of A-current differing in voltage-dependence are expressed by neurons of the rat neostriatum. Neuroscience Letters 103:331-337.

Surmeier DJ, Plotkin J, Shen W (2009) Dopamine and synaptic plasticity in dorsal striatal circuits controlling action selection. Current Opinion in Neurobiology 19:621-628.

Surmeier DJ, Graves SM, Shen W (2014) Dopaminergic modulation of striatal networks in health and Parkinson's disease. Current Opinion in Neurobiology 29C:109-117.

Surmeier DJ, Stefani A, Foehring RC, Kitai S (1991) Developmental regulation of a slowly-inactivating potassium conductance in rat neostriatal neurons. Neuroscience Letters 122:41-46.

Sylvain NJ, Brewster DL, Ali DW (2010) Zebrafish embryos exposed to alcohol undergo abnormal development of motor neurons and muscle fibers. Neurotoxicology and Teratology 32:472-480.

Taggart TC, Simmons RW, Thomas JD, Riley EP (2017) Children with heavy prenatal alcohol exposure exhibit atypical gait characteristics. Alcoholism: Clinical and Experimental Research 41:1648-1655.

Tang N, He M, O'Riordan MA, Farkas C, Buck K, Lemmon V, Bearer CF (2006) Ethanol inhibits L1 cell adhesion molecule activation of mitogen-activated protein kinases. Journal of Neurochemistry 96:1480-1490.

Thanos PK, Volkow ND, Freimuth P, Umegaki H, Ikari H, Roth G, Ingram DK, Hitzemann R (2001) Overexpression of dopamine D2 receptors reduces alcohol self-administration. Journal of Neurochemistry 78:1094-1103.

Thomas TM, Smith Y, Levey AI, Hersch SM (2000) Cortical inputs to m2 ‐ immunoreactive striatal interneurons in rat and monkey. Synapse 37:252-261.

Tipps ME, Raybuck JD, Kozell LB, Lattal KM, Buck KJ (2016) G protein-gated inwardly rectifying potassium channel subunit 3 knock-out mice show enhanced ethanol reward. Alcoholism: Clinical and Experimental Research 40:857-864.

Tyagarajan SK, Fritschy JM (2014) Gephyrin: a master regulator of neuronal function? Nature Reviews Neuroscience 15:141-156.

U.S. Department of Health and Human Services (HHS) (2016) Facing addiction in America: the surgeon general’s report on alcohol, drugs, and health: Office of the Surgeon General.

Ungless MA, Whistler JL, Malenka RC, Bonci A (2001) Single cocaine exposure in vivo induces long-term potentiation in dopamine neurons. Nature 411:583-587.

Urban DJ, Roth BL (2015) DREADDs (Designer Receptors Exclusively Activated by Designer Drugs): Chemogenetic Tools with Therapeutic Utility. Annual Review of Pharmacology and Toxicology 55:399-417.

Urban NB, Kegeles LS, Slifstein M, Xu X, Martinez D, Sakr E, Castillo F, Moadel T, O'Malley SS, Krystal JH, Abi-Dargham A (2010) Sex differences in striatal dopamine release in young adults after oral alcohol challenge: a positron emission tomography imaging study with [(1)(1)C]raclopride. Biological Psychiatry 68:689-696.

Valjent E, Bertran-Gonzalez J, Herve D, Fisone G, Girault JA (2009) Looking BAC at striatal signaling: cell-specific analysis in new transgenic mice. Trends in Neurosciences 32:538-547.

Vengeliene V, Bilbao A, Molander A, Spanagel R (2008) Neuropharmacology of alcohol addiction. British Journal of Pharmacology 154:299-315.

Volkow ND, Morales M (2015) The Brain on drugs: from reward to dddiction. Cell 162:712-725.

Volkow ND, Wang GJ, Tomasi D, Baler RD (2013) Unbalanced neuronal circuits in addiction. Current Opinion in Neurobiology 23:639-648.

Volkow ND, Fowler JS, Wang GJ, Baler R, Telang F (2009) Imaging dopamine's role in drug abuse and addiction. Neuropharmacology 56 Suppl 1:3-8.

Volkow ND, Wang G-j, Fowler JS, Logan J, Hitzemann R, Ding Y-S, Pappas N, Shea Colleen, Piscanl K (1996) Decrease in dopamine receptors but not in dopamine transporters in alcoholics Alcoholism: Clinical and Experimental Research 20.

Volkow ND, Wang GJ, Telang F, Fowler JS, Logan J, Childress AR, Jayne M, Ma Y, Wong C (2006) Cocaine cues and dopamine in dorsal striatum: mechanism of craving in cocaine addiction. Journal of Neuroscience 26:6583-6588.

Volkow ND, Wang G-J, Fischman M, Foltin R, Fowler J, Abumrad N, Vitkun S, Logan J, Gatley S, Pappas N (1997) Relationship between subjective effects of cocaine and dopamine transporter occupancy. Nature 386:827.

Volkow ND, Wang G, Fischman MW, Foltin R, Fowler JS, Franceschi D, Franceschi M, Logan J, Gatley SJ, Wong C (2000) Effects of route of administration on cocaine induced dopamine transporter blockade in the human brain. Life Sciences 67:1507-1515.

Vollstadt-Klein S, Wichert S, Rabinstein J, Buhler M, Klein O, Ende G, Hermann D, Mann K (2010) Initial, habitual and compulsive alcohol use is characterized by a shift of cue processing from ventral to dorsal striatum. Addiction 105:1741-1749.

Voorn P, Vanderschuren LJ, Groenewegen HJ, Robbins TW, Pennartz CM (2004) Putting a spin on the dorsal-ventral divide of the striatum. Trends in Neurosciences 27:468-474.

Wall NR, De La Parra M, Callaway EM, Kreitzer AC (2013) Differential innervation of direct- and indirect-pathway striatal projection neurons. Neuron 79:347-360.

Wallner M, Hanchar H, Olsen R (2003) Ethanol enhances α4β3δ and α6β3δ γ-aminobutyric acid type A receptors at low concentrations known to affect humans. Proceedings of the National Academy of Sciences 100:15218-15223.

Wang J, Yeckel MF, Johnston D, Zucker RS (2004) Photolysis of postsynaptic caged Ca2+ can potentiate and depress mossy fiber synaptic responses in rat hippocampal CA3 pyramidal neurons. Journal of Neurophysiology 91:1596-1607.

Wang J, Lanfranco MF, Gibb SL, Yowell QV, Carnicella S, Ron D (2010) Long-lasting adaptations of the NR2B-containing NMDA receptors in the dorsomedial striatum play a crucial role in alcohol consumption and relapse. Journal of Neuroscience 30:10187-10198.

Wang J, Ben Hamida S, Darcq E, Zhu W, Gibb SL, Lanfranco MF, Carnicella S, Ron D (2012) Ethanol-mediated facilitation of AMPA receptor function in the dorsomedial striatum: implications for alcohol drinking behavior. Journal of Neuroscience 32:15124-15132.

Wang J, Cheng Y, Wang X, Roltsch Hellard E, Ma T, Gil H, Ben Hamida S, Ron D (2015) Alcohol elicits functional and structural plasticity selectively in dopamine D1 receptor-expressing neurons of the dorsomedial striatum. Journal of Neuroscience 35:11634-11643.

Wang J, Carnicella S, Phamluong K, Jeanblanc J, Ronesi JA, Chaudhri N, Janak PH, Lovinger DM, Ron D (2007) Ethanol induces long-term facilitation of NR2B-NMDA receptor activity in the dorsal striatum: implications for alcohol drinking behavior. Journal of Neuroscience 27:3593-3602.

Wang X, Wang G, Lemos JR, Treistman SN (1994) Ethanol directly modulates gating of a dihydropyridine-sensitive Ca2+ channel in neurohypophysial terminals. Journal of Neuroscience 14:5453-5460.

Wang Z, Kai L, Day M, Ronesi J, Yin HH, Ding J, Tkatch T, Lovinger DM, Surmeier DJ (2006) Dopaminergic control of corticostriatal long-term synaptic depression in medium spiny neurons is mediated by cholinergic interneurons. Neuron 50:443-452.

Warren GW, Alberg AJ, Kraft AS, Cummings KM (2014) The 2014 Surgeon General's report: "The health consequences of smoking--50 years of progress": a paradigm shift in cancer care. Cancer 120:1914-1916.

Wei X, Ma T, Cheng Y, Huang CCY, Wang X, Lu J, Wang J (2018) Dopamine D1 or D2 receptor-expressing neurons in the central nervous system. Addiction Biology 23:569-584.

Weiner JL, Valenzuela CF (2006) Ethanol modulation of GABAergic transmission: the view from the slice. Pharmacology and Therapeutics 111:533-554.

Weiss FL, M. T.; Bloom, F. E.; Koob, G. F. (1993) Oral alcohol self-administration stimulates dopamine release in the rat nucleus accumbens: genetic and motivational determinants. The Journal of Pharmacology and Experimental Therapeutics 267:250-258.

Wenzel A, Fritschy JM, Mohler H, Benke D (1997) NMDA receptor heterogeneity during postnatal development of the rat brain: differential expression of the NR2A, NR2B, and NR2C subunit proteins. Journal of Neurochemistry 68:469-478.

Whiteford HA, Degenhardt L, Rehm J, Baxter AJ, Ferrari AJ, Erskine HE, Charlson FJ, Norman RE, Flaxman AD, Johns N, Burstein R, Murray CJL, Vos T (2013) Global burden of disease attributable to mental and substance use disorders: findings from the Global Burden of Disease Study 2010. The Lancet 382:1575-1586.

Wilcox MV, Cuzon Carlson VC, Sherazee N, Sprow GM, Bock R, Thiele TE, Lovinger DM, Alvarez VA (2014) Repeated binge-like ethanol drinking alters ethanol drinking patterns and depresses striatal GABAergic transmission. Neuropsychopharmacology 39:579-594.

Wills TA, Klug JR, Silberman Y, Baucum AJ, Weitlauf C, Colbran RJ, Delpire E, Winder DG (2012) GluN2B subunit deletion reveals key role in acute and chronic ethanol sensitivity of glutamate synapses in bed nucleus of the stria terminalis. Proceedings of the National Academy of Sciences 109:E278-287.

Wilson CJ, Groves PM (1981) Spontaneous firing patterns of identified spiny neurons in the rat neostriatum. Brain Research 220:67-80.

Wilson CJ, Kawaguchi Y (1996) The origins of two-state spontaneous membrane potential fluctuations of neostriatal spiny neurons. Journal of Neuroscience 16:2397-2410.

Wise RA (2008) Dopamine and reward: the anhedonia hypothesis 30 years on. Neuroscience Research 14:169-183.

Wolf ME (2002) Addiction: making the connection between behavioral changes and neuronal plasticity in specific pathways. Molecular Interventions 2:146.

Wong DF et al. (2006) Increased occupancy of dopamine receptors in human striatum during cue-elicited cocaine craving. Neuropsychopharmacology 31:2716-2727.

World Health Organization (2014) Global status report on alcohol and health 2014. WHO Press:2-18.

Wu Y-W, Kim J-I, Tawfik VL, Lalchandani RR, Scherrer G, Ding JB (2015) Input-and cell-type-specific endocannabinoid-dependent LTD in the striatum. Cell Reports 10:75-87.

Xi D, Li YC, Snyder MA, Gao RY, Adelman AE, Zhang W, Shumsky JS, Gao WJ (2011) Group II metabotropic glutamate receptor agonist ameliorates MK801-induced dysfunction of NMDA receptors via the Akt/GSK-3beta pathway in adult rat prefrontal cortex. Neuropsychopharmacology 36:1260-1274.

Xu CM, Wang J, Wu P, Xue YX, Zhu WL, Li QQ, Zhai HF, Shi J, Lu L (2011) Glycogen synthase kinase 3beta in the nucleus accumbens core is critical for methamphetamine-induced behavioral sensitization. Journal of Neurochemistry 118:126-139.

Yamada H, Fujimoto K-i, Yoshida M (1995) Neuronal mechanism underlying dystonia induced by bicuculline injection into the putamen of the cat. Brain Research 677:333-336.

Ye JH, Tao L, Ren J, Schaefer R, Krnjević K, Liu PL, Schiller DA, McArdle JJ (2001) Ethanol potentiation of glycine-induced responses in dissociated neurons of rat ventral tegmental area. Journal of Pharmacology and Experimental Therapeutics 296:77-83.

Ye L, Allen WE, Thompson KR, Tian Q, Hsueh B, Ramakrishnan C, Wang AC, Jennings JH, Adhikari A, Halpern CH, Witten IB, Barth AL, Luo L, McNab JA, Deisseroth K (2016) Wiring and Molecular Features of Prefrontal Ensembles Representing Distinct Experiences. Cell 165:1776-1788.

Yin HH (2010) The sensorimotor striatum is necessary for serial order learning. Journal of Neuroscience 30:14719-14723.

Yin HH, Knowlton BJ (2006) The role of the basal ganglia in habit formation. Nature Reviews Neuroscience 7:464-476.

Yin HH, Knowlton BJ, Balleine BW (2005a) Blockade of NMDA receptors in the dorsomedial striatum prevents action-outcome learning in instrumental conditioning. European Journal of Neuroscience 22:505-512.

Yin HH, Ostlund SB, Knowlton BJ, Balleine BW (2005b) The role of the dorsomedial striatum in instrumental conditioning. European Journal of Neuroscience 22:513-523.

Yin HH, Park BS, Adermark L, Lovinger DM (2007) Ethanol reverses the direction of long-term synaptic plasticity in the dorsomedial striatum. European Journal of Neuroscience 25:3226-3232.

Yizhar O, Fenno LE, Prigge M, Schneider F, Davidson TJ, O'shea DJ, Sohal VS, Goshen I, Finkelstein J, Paz JT (2011) Neocortical excitation/inhibition balance in information processing and social dysfunction. Nature 477:171.

Yokoyama H, Baraona E, Lieber CS (1996) Molecular cloning and chromosomal localization of the ADH7 gene encoding human class IV (sigma) ADH. Genomics 31:243-245.

Yoshida M, Nagatsuka Y, Muramatsu S, Niijima K (1991) Differential roles of the caudate nucleus and putamen in motor behavior of the cat as investigated by local injection of GABA antagonists. Neuroscience Research 10:34-51.

Yoshimoto KM, W.J.; LUMENG, L.; Li, T.-K. (1991) Alcohol stimulates the release of dopamine and serotonin in the Nucleus Accumbens. Alcohol 9:17-22.

Yu D, Zhang L, Eisele J-L, Bertrand D, Changeux J-P, Weight FF (1996) Ethanol inhibition of nicotinic acetylcholine type alpha 7 receptors involves the amino-terminal domain of the receptor. Molecular Pharmacology 50:1010-1016.

Zalocusky KA, Ramakrishnan C, Lerner TN, Davidson TJ, Knutson B, Deisseroth K (2016) Nucleus accumbens D2R cells signal prior outcomes and control risky decision-making. Nature 531:642.

Zandy SL, Matthews DB, Tokunaga S, Miller A, Blaha CD, Mittleman G (2015) Reduced dopamine release in the nucleus accumbens core of adult rats following adolescent binge alcohol exposure: age and dose-dependent analysis. Psychopharmacology 232:777-784.

Zhang FX, Rubin R, Rooney TA (1998) Ethanol induces apoptosis in cerebellar granule neurons by inhibiting insulin‐like growth factor 1 signaling. Journal of Neurochemistry 71:196-204.

Zhao X, Feng D, Wang Q, Abdulla A, Xie X-J, Zhou J, Sun Y, Yang ES, Liu L-P, Vaitheesvaran B (2012) Regulation of lipogenesis by cyclin-dependent kinase 8–mediated control of SREBP-1. The Journal of Clinical Investigation 122:2417-2427.

Zhou FC, Sari Y, Zhang JK, Goodlett CR, Li T (2001) Prenatal alcohol exposure retards the migration and development of serotonin neurons in fetal C57BL mice. Brain Research: Developmental Brain Research 126:147-155.

Zhou FM, Wilson CJ, Dani JA (2002) Cholinergic interneuron characteristics and nicotinic properties in the striatum. Journal of Neurobiology 53:590-605.

Zhou R, Wang S, Zhu X (2012) Prenatal ethanol exposure alters synaptic plasticity in the dorsolateral striatum of rat offspring via changing the reactivity of dopamine receptor. PloS One 7:e42443.

Zhu Y, Wienecke CF, Nachtrab G, Chen X (2016) A thalamic input to the nucleus accumbens mediates opiate dependence. Nature 530:219-222.